Faculty of Science and Engineering
Department of Chemistry

Fundamental Studies into the Chemical and Physical Properties of Latent Fingermarks

Buddhika Niroshani Dorakumbura

This thesis is presented for the Degree of
Doctor of Philosophy
Of
Curtin University

December 2017

Declaration

To the best of my knowledge and belief, this thesis contains no material previously published by any other person except where due acknowledgement has been made.

This thesis contains no material which has been accepted for the award of any other degree or diploma in any university.

Human Ethics

The research presented and reported in this thesis was conducted in accordance with the National Health and Medical Research Council National Statement on Ethical Conduct in Human Research (2007) – updated March 2014. The proposed research study received human research ethics approval from the Curtin University Human Research Ethics Committee (EC00262), Approval Number RDSE-02-15.

Signature: 

Date: 12/12/2017

Abstract

Successful recovery of latent fingermarks at a crime scene holds great forensic significance as they can be used to place individuals at the scene. Fingermark detection techniques currently used in casework have limitations in their sensitivity, specificity, and applicability on challenging substrates, which emphasise the demand for further research. This research can be immensely benefited by a more comprehensive understanding of the fingermark residue itself and the transformations it undergoes over time as well as under different environmental conditions. This dissertation describes a series of investigations undertaken to generate fundamental knowledge on the chemical and physical properties of latent fingermarks on non-porous surfaces by using advanced analytical instrumentation.

The physical properties of fingermarks and their variation over time were investigated using a novel imaging mode of atomic force microscopy. The technique was effective in studying topography and adhesion of fingermark droplets without any significant sample damage. This enabled investigation of the same droplet over time. The adhesion between fresh eccrine droplets and hydrophilic cantilever tips was generally in the range of 5-17 nN while natural and sebaceous droplets were in the ranges of 2-7 nN and 0-2 nN respectively. The variation of topography and adhesion over time of eccrine and sebaceous droplets showed different broad trends. Propagation of a thin film of material from ridges to furrows was detected soon after deposition of a fingermark on a clean surface, which demonstrated the extremely dynamic nature of the residue on non-porous surfaces. The thickness of this thin layer was 0.2 nm after 2 h since deposition and then increased up to 1.0 nm in the next 21 h.

Spatial distribution of fingermark components was investigated at high-resolution using synchrotron-sourced Fourier transform infrared and confocal Raman microscopy to discern the inconclusive observations experienced with the physical properties. Chemical imaging of a number of droplets with different compositions from a range of donors showed that individual droplets can take a variety of configurations sometimes closely resembling droplets of emulsion depending on the eccrine to lipid ratio. These results further demonstrated the importance of consistent sampling of the fingermark residue when non-invasive analytical techniques are used in time-course experiments. The application of confocal Raman microscopy to probe the compositional variation of fingermark residue over time was also demonstrated.

Strategies to overcome challenges of studying fingermark compositional variation over time using chromatographic techniques caused by intra-donor variation was explored by means of quantifying squalene in fingermark deposits using gas chromatography-mass spectrometry. Fingermark residues obtained from three donors under four different sampling methods and analysed in triplicate revealed the difference in the amount of squalene deposited by both hands at a given time can be minimised by controlling the deposition pressure. Rubbing hands together followed by deposition of natural fingermarks by controlling deposition pressure resulted a percentage difference in the amount of squalene deposited by both hands of only 20%. This study allowed estimating the initial amount of squalene in every sample that was aged during the following study, hence compositional variation over time could be monitored despite the intra-donor variation.

Transformation of squalene in fingermarks over time under different storage conditions was examined against the initial composition through ultra-high-pressure liquid chromatography-high-resolution mass spectrometry. Squalene was detected in all fresh natural fingermarks and the amount ranged between 0.20-11.32 µg/5 fingertips. A notable difference in the transformation of squalene was observed with different storage conditions, where a dark aquatic environment accelerated degradation of squalene compared to dark but dry conditions. Squalene monohydroperoxide was extremely short-lived in natural deposits while the amount of squalene epoxide was still increasing relative to the initial amount, after ageing under dark and aquatic conditions for up to 7 days. Some oxidation by-products of cholesterol were tentatively identified, which exhibited a growth over time against their initial concentration under any storage condition.

These results advance the current understanding of the chemical and physical properties of fingermark residue, forming the basis for future research into improved fingermark detection.

Acknowledgements

I could spend a few hours in front of my computer thinking about many people who have made this PhD journey possible.

I would like to start by extending a huge thank to my primary supervisor, Professor Simon Lewis for taking me on-board as a PhD student in the first place. I feel extremely privileged to have had such an encouraging, flexible, even-tempered... (and the list goes on) supervisor who constantly believed in me over the past 3 ½ years. Huge thanks are also due to my co-supervisors, Dr. Thomas Becker and Dr. Frankie Busetti, without whom all my experimental results would not come to realise. Thanks to their excellent guidance, I managed to work with several analytical instrumentations without breaking any. An enormous amount of gratitude goes to Emeritus Professor Wilhelm van Bronswijk for casting his wisdom on my draft chapters. I would also like to thank Dr. Mark Hackett for his fruitful discussions on Raman data interpretation and reviewing my manuscripts.

A huge thank goes to my research group, the Forensic and Analytical Chemistry Research Group at Curtin where I found a bunch of *crazy* people who can turn any newcomer into one of them. Particular thanks go Drs. Holly Yu, Amanda Frick, Georgina Sauzier, and Patrick Fritz who helped me proofread my chapters. Your constant support deserves another Sri Lankan feast!

Peter Chapman, Geoff Chidlow, and Peter Hopper are also thanked for their technical expertise. Chappy never turned me down when I asked for technical support and Peter never said no to run more samples in his GCs.

Additional thanks are due to Dr. Danielle Martin and Dr. Mark Tobin from Australian Synchrotron for the invaluable guidance throughout the experiments carried out in their facility. Special thanks go to Matthias Kress from WITec GmbH, Germany who facilitated my unforgettable and first-ever adventure trip and also for taking me on a short tour to show the beauty of Germany. Dr. Andrea Richter, Dr. Thomas Dieing, and Dr. Stefan da Costa from WITec are also thanked for helping me with taking measurements using their state-of-the-art Raman microscopes and inspiring me to carry out more Raman analysis. Without such inspiration, one chapter of this thesis would not be possible.

All my fingermark donors are acknowledged for their cooperation, especially those who participated in multiple studies following my strict instructions just to touch a surface! I would also like to acknowledge my PhD scholarships from the Department of Chemistry, the

Australian Government Research Training Program, and the Curtin University. On that note, I would like to thank everyone from the Department of Chemistry, Curtin Library, and all those at Curtin University who helped me along the way.

Huge thanks go to the van der Pal family for taking care of me and treating me as family. Karin, thank you very much for reminding me to take enough breaks while writing this thesis. Mieke and Bill- thanks for reminding me that your doors are always open to me!

Of course my other tea group member, now-Dr. Jaime Cesar deserves special mention for his mutual understanding and passion to challenge my views on everything! I see myself lucky to share this extremely challenging life experience with both of you-Holly and Jaime! Dr. Charity Mundava, thank you very much for checking on me when Simon was on leave and making sure that I get things done on time. Jossie Bakri, Annushia Mallar, and Roshni Sha are thanked for their caring and welcoming hearts. Thanks to Kuldeep and Chandramalika for providing me with delicious food when I had no time to cook! Dr. Zuo Tong How and Emily Barker are also thanked for sharing their expertise on LC-MS and AFM.

My former mentor Dr. Sudarshana Somasiri and colleagues Vimarshi, Ruwani, and Thanuja at the Industrial Technology Institute, Sri Lanka are thanked for helping me to come up with ideas when I ran out of them. Asoka Dassanayake, my high school chemistry teacher is remembered with gratitude for moulding me to a *chemistry-obsessed* student which pushed me to come this far, pursuing a PhD in chemistry.

Last but definitely not least, I would like to pay my gratitude to my family for their everlasting love and encouragement. Special thanks to mum, dad, and my two aunties for their understanding. My elder sister is thanked for constantly entertaining me by sending videos of my two-year-old nephew.

I would like to dedicate this dissertation to all those who dedicated and sacrificed their lives defending my home country, Sri Lanka from terrorism and preserved its free will.

Publications

This dissertation contains work which has been published in the following peer reviewed journals:

Dorakumbura, B. N.; Boseley, R. E.; Becker, T.; Martin D. E.; Richter, A.; Tobin, M. J.; van Bronswijk, W.; Vongsvivut, J.; Hackett, M. J.; Lewis, S.W. Revealing the spatial distribution of chemical species within latent fingermarks using vibrational spectroscopy. *Analyst* **2018**.

DOI: 10.1039/C7AN01615H

Dorakumbura, B. N.; Becker, T.; Lewis, S.W. Nanomechanical mapping of latent fingermarks: a preliminary investigation into the changes in surface interactions and topography over time. *Forensic Science International* **2016,** *267*, 16-24.

DOI: https://doi.org/10.1016/j.forsciint.2016.07.024

In addition, the following peer reviewed article was published during the course of this dissertation:

Fritz, P.; van Bronswijk, W.; **Dorakumbura, B. N**.; Hackshaw, B.; Lewis, S. W. Evaluation of a solvent-free p-dimethylaminobenzaldehyde method for fingermark visualisation with a low cost light source suitable for remote locations. *Journal of Forensic Identification* **2015,** *65*(1), 67-90.

Conference Presentations

Selected aspects of the work contained within this thesis have been presented at the following conferences:

Oral Presentations

Studies into the chemical and physical properties of latent fingermarks, presented at the Royal Australian Chemical Institute Centenary Congress, 23rd-28th July 2017, Melbourne, Australia.

Chemical investigations into latent fingermark composition: Current challenges, presented at the 24th Annual Royal Australian Chemical Institute's Research and Development Topics Conference, 04th-07th December 2016, Sydney, Australia.

Investigations into the physical properties of latent fingermarks, presented at the 23rd Annual Royal Australian Chemical Institute's Research and Development Topics Conference, 06th-09th December 2015, Melbourne, Australia.

Fundamental studies into the chemical and physical properties of latent fingermarks, presented at the Inaugural Curtin University CUPSA Conference, 3rd September 2015, Perth, Australia.

Poster presentations

Probing the properties of latent fingermarks on the nanoscale with atomic force microscopy, presented at the 23rd International Symposium on the Forensic Sciences of the Australian and New Zealand Forensic Science Society (ANZFSS 2016), 18th-22nd September 2016, Auckland, New Zealand.

Fundamental studies into the chemical and physical properties of latent fingermarks, presented at the 22nd Annual Royal Australian Chemical Institute's Research and Development Topics Conference, 13th-15th December 2014, Adelaide, Australia.

- Awarded Runner-Up for the best poster presentation.

Table of Contents

List of Figures

List of Tables

List of Abbreviations

ACN	Acetonitrile
AERE	Atomic energy research establishment
AFM	Atomic force microscopy
ANOVA	Analysis of variance
ANSTO	Australian nuclear science and technology organisation
APCI	Atmospheric pressure chemical ionisation
ATR-FTIR	Attenuated total reflectance-Fourier transform infrared
ATR-IRE	Attenuated total reflectance-internal reflection element
AWRE	Atomic weapons research establishment
Da	Dalton
DCM	Dichloromethane
DFO	1,8-diazafluoren-9-one
DTGS	Deuterated triglycine sulphate
EI	Electron impact
ESI	Electrospray ionisation
F-d	Force distance
FTIR	Fourier transform infrared
FT-ICR	Fourier transform ion cyclotron resonance
GC-MS	Gas chromatography-mass spectrometry
IFRG	International fingerprint research group
LC-APCI/MS	Liquid chromatography-atmospheric chemical ionisation/ mass spectrometry
LC-CL	Liquid chromatography-chemiluminescence
LC-MS	Liquid chromatography-mass spectrometry
LOD	Limit of detection
LOQ	Limit of quantification
MALDI-MSI	Matrix-assisted laser desorption ionisation-mass spectral imaging
MCT	Mercury cadmium telluride
MMD	Multi metal deposition

MSI	Mass spectrometry imaging
MS^n	Multiple stage fragmentation
m/z	Mass-to-charge ratio
NA	Numerical aperture
NIST	National Institute of Standards and Technology
ORO	Oil red O
PCA	Principal component analysis
PD	Physical developer
PF QNM	PeakForce quantitative nanomechanical mapping
PMMA	Polymethyl methacrylate
PTFE	Polytetrafluoroethylene
PVC	Polyvinyl chloride
QIT	Quadrupole ion trap
QqQ	Triple quadrupole
Q-TOF	Quadrupole-time-of-flight
RH	Relative humidity
RP-HPLC	Reverse phase high-pressure liquid chromatography
RUVIS	Reflected ultraviolet imaging system
SMD	Single metal deposition
SEM	Scanning electron microscopy
SERS	Surface enhanced Raman spectroscopy
SPM	Scanning probe microscopy
SPR	Small particle reagent
SQ	Squalene
SQ-epoxide	Squalene epoxide
SQ-OOH	Squalene monohydroperoxide
$SQ\text{-}[OOH]_2$	Squalene dihydroperoxide
$SQ\text{-}[OOH]_5$	Squalene pentahydroperoxide
SRS	Stimulated Raman scattering microscopy
TICs	Total ion chromatograms

TOP	4,8,13,17,21-tetra-methyl-octadeca-4,8,12,16,20-pentaene-al
TOT	4,9,13,17-tetramethyl-octadeca-4,8,12,16-tetraeneal
TPs	Target products
TTT	5,9,13-trimethyl-tetradeca-4,8,12-triene-al
UHPLC-HRMS	Ultra-high-pressure liquid chromatography-high resolution mass spectrometry
UHPLC-HR Orbitrap™ MS	Liquid chromatography-high resolution Orbitrap™ MS
uPVC	Unplasticised polyvinyl chloride
UV	Ultraviolet
VMD	Vacuum metal deposition

Chapter 1: Introduction

1.1 Introduction

Scientific research carried out over more than a century has provided convincing evidence for the great variability of ridge patterns of human fingers, which established the use of fingerprints as a viable tool in forensic identification.[1-5] Fingermarks are distinct from fingerprints as they are those impressions left unintentionally upon the contact between individuals' fingers and the surfaces.[6-7] Latent or hidden fingermarks are one of the frequently encountered forms of physical evidence at crime scenes, which are subsequently used to provide proof of individual's contact with objects, persons, and places.[8-10]

As the name suggests, latent fingermarks are required to be detected and enhanced for subsequent comparison of their ridge patterns against databases. Detection of latent fingermarks is highly influenced by the chemical and physical properties of the deposits.[11-13] Typically, latent fingermarks are a complex mixture of skin secretions originating from eccrine and sebaceous glands of the skin, dead skin cells of the epidermis, and several exogenous contaminants.[14-15] Current understanding of these deposits is largely based on medical literature on bulk skin secretions,[16-17] however, recent advances in fingermark research have demonstrated that such findings do not necessarily represent the latent deposit.[17]

The majority of the first-generation fingermark visualisation techniques have been adapted from existing visualisation techniques of other fields (e. g. photography) based on empirical evidence. While they remain extremely effective in the current operational context from a fit-for-purpose perspective and practical realities, they do have limitations in their application. Regardless of the numerous options available, fingermark detection is still challenging, for example, detection of fingermarks on patterned substrates and aged deposits are rather complex.[12] This can be attributed to an incomplete understanding of the fingermark deposit itself and the transformation it experiences over time under diverse environmental conditions. These limitations emphasise the compelling demand for further improvements. In recent years, several studies have started addressing this issue by investigating the fingermark residue itself, primarily from a chemical perspective.[7, 14, 18-25]

In contrast, there is a paucity of studies into the physical characteristics of latent fingermarks, with only a few from over four decades ago and a limited number of recent ones.[26-33] While the chemical composition provides a wealth of information that is critical for fingermark detection and further developments, it does not offer a comprehensive knowledge of the deposit itself. Physical properties such as morphology, interactions with other surfaces, and

the distribution of components are critical parameters for the understanding of current or designing of novel detection techniques.[33]

This thesis depicts a series of investigations undertaken to fill in the gaps in the fundamental knowledge of latent fingermarks on non-porous surfaces by combining both their chemical and physical properties. This research lays the ground for more evidence-based approaches for future fingermark research.

1.2 Human skin

Skin is the largest organ of human body, which is composed of three anatomical layers: epidermis, dermis and hypodermis (Figure 1.1).[34] These layers together serve the body by performing several vital biological functions. The epidermis, the outermost layer of the skin, is a protective barrier to underlying tissues from hostile attacks, prevents evaporation of water, and acts as a receptor organ. It also constantly replaces the cells that are lost at its surface. The dermis cushions the body from stress, regulates the body temperature, and participates in sensory reception. The hypodermis lies below the dermis and contains a layer of fat that serves as an energy reserve.[34]

Several vital concepts of the fingerprint examination process rely on the anatomy and the physiology of the friction ridge skin (thick skin), which allows the gripping of objects by increasing friction.[34] The friction ridge skin is found exclusively on the soles of the feet, palms of the hands, and the surface lining the fingers and toes. Its epidermis is thicker than in other areas of the skin (Figure 1.1). The only skin appendage found in the friction ridge skin is eccrine sweat glands. These are one of the three main types of glands found in human skin, and distributed all over the skin surface although its density is highest in the friction ridge skin.[35] With the exception of friction ridge skin, sebaceous glands are found in all other areas of the body covered with thin skin, with the largest sebaceous glands found on the face and scalp.[35] The distribution of apocrine glands is restricted to areas such as underarms, genital, ears, and chest. Eccrine glands function predominantly in thermal regulation of the body while sebaceous glands produce oils to insulate and waterproof the skin.[35]

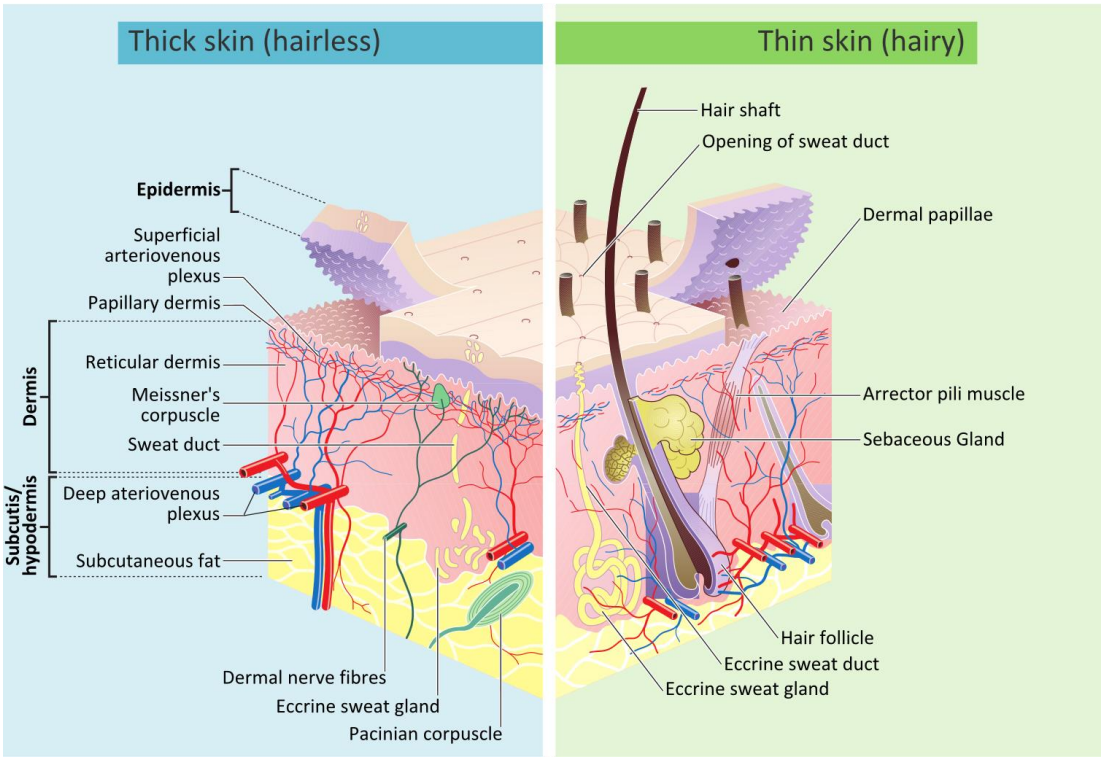

Figure 1.1 A schematic of layers of human thick skin and thin skin showing different appendages.[36]

1.3 Significance of fingermarks as forensic evidence

One of the core principles of forensic science is the exchange principle which was developed by Edmund Locard in early 1900s.[37-38] Although it is often erroneously paraphrased as "every contact leaves a trace", Locard's original expression stated that no individual can perform a crime with the intensity induced by criminal activities without leaving multiple traces at the scene.[37] Among several forms of such trace evidence, whose scientific examination is likely to offer robust and convincing investigative leads, fingermarks hold great potential. The first reported use of fingermarks as trace evidence in a criminal investigation was in 1892 by Juan Vucetich, based on the detailed systematic work reported by Francis Galton.[2, 39] Over the years, the use of fingermarks for personal identification purposes has been extensively challenged and enough scientific evidence has been put forward to establish its legitimacy based on two fundaments: permanency and uniqueness.[1, 3, 40-42]

The permanency of fingermarks is a result of the regenerative process of the skin. All cells of the outer layer of the skin (epidermis) are continuously generated at the inner protected basal layer and migrate outward to the epidermis, hence only damage to the inner basal layer can alter the ridge patterns at the epidermis. On the other hand, the process of formation of the characteristic ridge details is believed to be governed by a random process that is not yet completely understood.[8, 43] It is thought that inheritance, local physical conditions such as

pressure on the different parts of the finger of the foetus in the uterus are some of the influential factors in the development of the ridge structures.[39, 43] So far, with millions of fingerprint patterns identified, no two indistinguishable patterns have been identified, even in identical twins although they share the same genetic material and environment throughout gestation.[3, 40] DNA profiling in its current form is not specific enough in such cases.[44-45]

A well-developed image of the latent deposit is the key for the success of the following task, wherein the image is analysed, compared, evaluated, and verified for identification purposes.[8] As proposed by Ashbaugh, the information that can be recorded at this stage falls into three levels.[46] The first level details include overall pattern of the papillary ridge and are visible without further magnification.[8] Though they do not pose enough discriminatory power for identification, they are useful when only partially developed prints are available.[46] Both the second level (minutiæ details: changes in the major ridge path, Galton characteristics which include ridge endings, bifurcation, and dots) and third level details (alignment and shape of each ridge unit, pore shape, and relative pore positions) require magnification. Detection of these micron scale details is invaluable for an effective forensic identification.[8]

1.4 Detection of fingermarks

1.4.1 Detection techniques

Latent fingermarks are invisible or barely visible trace deposits that require some means of enhancement in order to visualise them.[47] Fingermark detection techniques exploit the chemical and/or physical properties of the residue components and their reactions or interactions with the substrate. A combination of techniques is frequently applied in sequence to maximise the amount of information that can be extracted from the latent deposit.[47-48] Selection of the detection technique(s) heavily depends upon the type of the substrate that the fingermarks are laid on and any knowledge of the composition of the deposit that may have been altered by the environment.[13, 47] Fingermark development techniques that are currently in operational use can be classified into five categories; (i) chemical reagents that react with known constituents, (ii) chemical or physical agents that are absorbed by or adhered to constituents, (iii) chemical reagents that rely on certain compounds that catalyse a chain reaction leading to a non-linear enhancement, (iv) chemical or physical agents that target known contaminants in the deposit and (v) optical techniques that interact with fingermark components by means of absorption,

scattering, polarisation or fluorescence.[13] However, the most general and simplest classification would be chemical techniques and other techniques including physical techniques.

Latent fingermarks on porous substrates are often visualised by chemical techniques, for example, those which react with water-soluble compounds of the deposit such as amino acids and those which react with water-insoluble lipids. Ninhydrin[49] and its analogues such as 1,8-diazafluoren-9-one (DFO)[50-51] and 1,2-indanedione[52-53] are some of the amino acid sensitive reagents that are frequently used in forensic laboratories.[13, 54] On reaction with amino acids including proteins and peptides, ninhydrin forms a non-fluorescent dark purple product called "Ruhemann's purple". DFO treatment results in a faint pink coloured product which fluoresces when viewed under an excitation source (525-550 nm) through a short-wave cut-off filter.[13] 1,2-indanedione reacts with α-amino acids to produce a pink colour product called "Joullié's pink".[52-53, 55-56] Developed exhibits are typically illuminated in the green/yellow region and viewed through orange/red filters.[13] Although ninhydrin treated fingermarks offer superior initial colour under white light, 1,2-indanedione treatment is more sensitive and yields improved contrast under luminescent conditions without further treatment.[54]

Most lipid sensitive reagents are lipophilic dyes that stain sebaceous compounds within the latent deposit. These include Sudan dyes, Oil red O (ORO), and Nile red. The dye molecules simply diffuse into the lipid fraction of the latent deposit during the enhancement by ORO and Nile red.[55, 57] Nile red offers superior sensitivity and applicability over a wide range of surfaces than the other methods due to its photo-luminescent properties.[55] Nile blue A, an alternative for Nile red has also been suggested which yields superior results in a similar fashion to Nile red.[58] In an aqueous solution, Nile blue A stains acidic components such as phospholipids and nucleic and fatty acids generating a dark blue colour.[58] A small amount of Nile blue A is hydrolysed to Nile red, which stains neutral lipids in pink or red colour.[58-60]

Development based upon deposition of colloidal metals onto the latent deposit is also routinely practised in forensic laboratories. Adapted from the photographic development process,[12] physical developer (PD) is a key technique that falls into this category.[55] The PD treatment involves reduction of silver ions in the working solution by a ferrous/ferric redox system, causing the precipitation of colloidal silver particles onto the fingermark deposit. Although the precise mechanism is unknown, it is believed that PD targets heavier fats and waxes within the latent deposit.[13, 55] Research has also suggested that it may target some water-soluble compounds such as amino acids and chloride ions trapped within the

sebaceous fraction.[13, 61-64] Even though the exact components are not identified, some studies have suggested that PD reacts with the "robust fraction" of fingermark lipids, which is not removed by solvents with low dielectric constant (hydrocarbon solvents) and is, therefore, able to visualise aged fingermarks on porous substrates.[57, 65-66]

Multi metal deposition (MMD) and single metal deposition (SMD) are also based on colloidal metal deposition on the fingermark. MMD involves deposition of two metals in sequence; gold and silver, while SMD deposits only gold particles.[55, 64] During the development with SMD, it is assumed that negatively charged colloidal gold particles bind to protonated amino acids, peptides, and proteins in the latent residue via electrostatic attraction.[67-68] It has also been shown that these two techniques can be applied on a variety of substrates ranging from porous to non-porous and on aged fingermarks.[69-70]

Regardless of all the techniques discussed above, the powdering method is perhaps the oldest, simplest, and most routinely practised enhancement technique on latent fingermarks, especially on non-porous surfaces.[47, 64] According to the UK Home Office, dusting of fingermarks accounts for 50% of the approximately 60,000 fingerprint identifications made in the UK per annum.[71] The powder method is essentially a physical process which involves the application of fine powder onto the fingermark and then removal of excess by tapping, brushing or blowing.[72] During this process, powder particles adhere to moisture and greasy substances of the deposit. Several powder formulations have been introduced so far, which can be broadly categorised into traditional, magnetic, luminescent, thermoplastic, nanotechnology, and anti-Stokes powders.[47]

Cyanoacrylate or superglue fuming has found its widespread use on non-porous surfaces.[73] During cyanoacrylate fuming, the glue is vaporised inside a chamber along with the piece of evidence so that the monomer of cyanoacrylate selectively polymerises on the fingermark.[74] This process forms white network-like structures on the residue, which is often then stained with dyes to enhance the contrast.[13, 75] The composition of the fingermark and the environmental conditions play a significant role in the development. Moisture is one such factor; high environmental humidity and moisture present in the fingermark yield better development. In addition, lactate ions present in the fingermark have been identified as the initiator of the polymerisation.[76]

Adapted from a commercial process for coating surfaces with thin films of metals, vacuum metal deposition (VMD) involves thermal evaporation of metals and their subsequent deposition onto the pieces of evidence, often non-porous surfaces, under vacuum.[13, 77] Gold

vapour is generated in the first stage of the development, and the resultant gold film forms nucleating sites for the subsequent deposition of zinc. Normally, zinc would deposit on the background, including furrows, rather than on the fingermark ridges as the nucleating layer of gold is buried within the ridges, resulting in a 'negative print'. The so-called 'reverse development' is the opposite of this process, where zinc deposits onto the ridges and not the background.[77] VMD is an extremely sensitive technique; in addition to reverse development, 'empty prints' (deposition of zinc on the general background but not on or between the ridges), has also been reported.[78]

1.4.2 Issues with current fingermark detection techniques

Hundreds of research papers can be found in the literature on novel chemical and/or physical treatments that claim to offer superior detection of latent fingermarks. Under realistic crime scene conditions, however, only about 15 basic techniques have frequently produced usable fingermarks for comparison purposes.[13] As discussed earlier, many fingermarks are still recovered at crime scenes with powdering technique as other operational techniques often require specialised laboratory facilities.[13] Regardless of all these existing techniques, a significant number of fingermarks left behind at crime scenes may remain undetected in casework.[79-80] This was demonstrated in a study where the performances of 1,2-indandione, DFO, and ninhydrin on a large number of used cheques was compared.[80] All of them were expected to bear latent fingermarks including depletion fingermarks. It was discovered that more than 50% of identifiable marks were left undetected by any of the techniques.[80]

Developing aged fingermarks, especially those exposed to severe environmental weathering, is challenging with most of the established techniques for casework. Evaporation of water and removal of volatile compounds from the deposit over time cause the fingermarks to be less susceptible to development by powder methods, cyanoacrylate, and iodine fuming.[13, 76] Exposure to high humidity or precipitation has a detrimental effect on amino acid sensitive reagents as this can wash away the water-soluble amino acids.[54, 71] VMD has shown better development over cyanoacrylate fuming, especially with aged fingermarks that were exposed to harsh environmental conditions.[77]

On the other hand, PD treatment can be effectively used in developing latent fingermarks on wetted porous substrates due to its sensitivity towards lipids.[55, 64] PD is also more sensitive to old marks than ORO and Nile red.[55, 57, 81] ORO has been found to develop fingermarks on wetted surfaces; however, many of these studies have used freshly deposited, groomed fingermarks, which are not representative of real-life cases.[71] Some of the techniques also

show undesirable affinity to substrates which can cause background staining. For example, PD and ORO treatments can give rise to severe background staining on certain types of paper which can obscure the fingermark and is undesirable for the evidence material.[57] In addition, implementing PD in operational laboratories is tedious due to its lengthy processing time, issues with the stability of working solution, and sensitivity towards glassware contamination.[55]

Dark, multi-coloured, and patterned surfaces are regarded as particularly challenging substrates for fingermark detection as white light illumination is not sufficient to enhance the contrast between the substrate and the developed mark. Techniques that yield fluorescence under certain excitation wavelengths such as 1,2-indanedione and fluorescent powders are preferred in this regard.

Health and safety concerns are other drawbacks associated with some techniques. These concerns include high flammability of solvents and toxicity by ingestion and inhalation. Iodine fuming is rarely used nowadays due to the corrosive and toxic nature of the iodine fumes.[13] Similarly, some powder formulations and chemical reagents that were previously in routine casework have now been replaced by much safer alternatives as they contained toxic heavy metals. Raised concerns regarding the use of nano-powders for improved sensitivity are also linked to this safety aspect.

The discussions made herein stress on some of the areas of fingermark research that need further investigation.

1.5 Latent fingermark composition

1.5.1 Initial composition

Secretions from the eccrine and sebaceous glands significantly contribute to the composition of latent fingermarks. For this reason, the current understanding of latent fingermark composition is largely based on the medical studies investigating the composition of these secretory glands.[11] Secretions from the apocrine glands are less likely to be found in latent fingermarks due to their anatomical location in the body.[10-11] Sebum, the oily mixture produced in the sebaceous glands is incorporated into the fingermark residue through habitual touching the areas of the body such as face and hair.[15] Epidermal lipids such as ceramides are less abundant in these areas, thus contributing less to fingermark composition. Sloughing of dead cells by the epidermis provides another key endogenous substance to the fingermark composition. It is hard to claim the exact number and the volume of endogenous species present in fingermarks as donor characteristics such as gender, age, diet, and health

largely influence the composition of the skin secretory glands.[11, 35] Apart from these endogenous components, residues of any substance that has been handled prior to deposition can be transferred onto the substrate upon contact. Some of these exogenous residues are food, cosmetics, dust, illicit drugs, and explosives and could be forensically significant depending on the case.

Nevertheless, the actual composition of the deposited fingermark may differ from the composition of the skin secretions of the skin surface due to the dynamics of deposition and substrate characteristics.[17, 82] These will be discussed later in this chapter. The complexity of fingermark composition is further escalated by factors such as variations in the deposition conditions (contact time, angle, and pressure) and the nature of the substrate (porous, semi-porous, and non-porous).

1.5.1.1 Compounds from eccrine and apocrine glands

Eccrine glands are the main source of the water-soluble (aqueous) portion of the fingermark composition (Table 1.1). They secrete predominantly water with other organic and inorganic compounds including proteins, amino acids, salts, and urea. The high water content of fingermarks (98% or more) cited in some literature[83-85] is based on the composition of eccrine glands, and not necessarily on the actual deposit. This figure was recently questioned by Kent in his review article and research into the actual deposit was recommended.[82] A few number of research has already suggested that the water content of fingermarks may not be as great as 99%.[29, 86] The major reason for this discrepancy is the evaporation/reabsorption of water from the surface of the friction ridge skin to regulating the body temperature.[82]

Table 1.1 Summary of main endogenous compounds/classes of compounds identified in latent fingermarks.[14, 18-19, 23, 33, 87-94]

Origin	Organic	Inorganic
Eccrine glands	Amino acids	Water
	Proteins	Chloride ions
	Polypeptides	Sodium ions
	Urea	Potassium ions
	Lactic acid	
Sebaceous glands	Free fatty acids	
	Wax esters	
	Mono, di, and triglycerides	
	Squalene and its oxidation products	
	Cholesterol and its esters	

Proteins and amino acids are found in fingermark deposits with serine being the most abundant amino acid (Figure 1.2).[18, 95] To a certain extent, these are one of the most vital classes of compounds for fingermark visualisation. More than 20 amino acids have been identified, though few proteins have been reliably detected in deposits.[15, 18] It should be noted here that quantitation of amino acids and proteins in fingermarks by chromatography may represent the total amino acids and protein content originating from both eccrine secretions and dead skin cells. Salts of sodium, potassium, and lactate ions are also widespread in fingermarks, with chloride and lactate ions are of interest for fingermark visualisation.

Free fatty acids and sterols have been identified in eccrine sweat that has been bulk sampled from the back and the chest areas of the body with minimal epidermal contamination. It was proposed that these lipids were incorporated from the secretory portion and the duct of the eccrine glands.[96-97] However, such presence of lipids in eccrine sweat rich fingermarks has not been reported so far while some antimicrobial molecules characteristic to sebaceous glands have been identified in such deposits.[98] Various other miscellaneous compounds such as creatinine and uric acid have been identified in eccrine sweat,[17, 99] but not necessarily in "real" fingermarks.

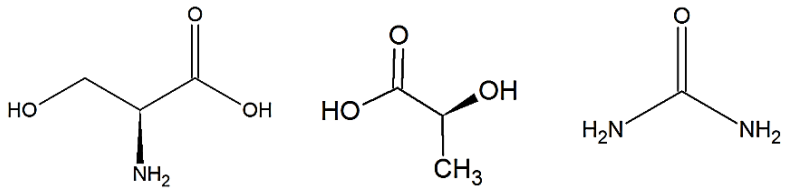

Figure 1.2 Some compounds from eccrine origin identified in fingermark residue.

Apocrine glands secrete water (>98%), proteins, carbohydrates, sterols, and iron, however, studies have not considered compounds emanating from apocrine glands in fingermarks due to their lower significance in fingermark composition. Generally, studies into apocrine gland secretions are challenging as secretions from eccrine and sebaceous glands can cause contamination.[17] They could, however, be significant in crimes of a sexual nature.[8]

1.5.1.2 Compounds from sebaceous glands

The sebaceous glands are primarily responsible for the water-insoluble portion of fingermarks. These compounds include glycerides, free fatty acids, wax esters, squalene, squalene oxidation products, cholesterol, and sterol esters (Table 1.1).[19, 87, 90-94] Squalene (Figure 1.3) is the most abundant single sebaceous compound identified through chromatographic analysis[19, 90, 92, 100] and is the principal unsaturated compound in fingermarks.[90]

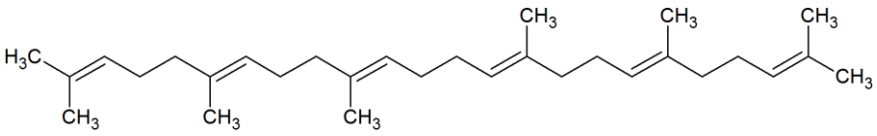

Figure 1.3 Molecular structure of squalene.

Long-chain saturated and monounsaturated free fatty acids (C_{12}-C_{18}) have also been readily identified, though the saturated fatty acids are more frequently detected than their unsaturated analogues.[92-93] Even-chain fatty acids are more common in fingermark composition than odd-chain fatty acids.[92-93] Palmitic acid (Figure 1.4) in particular, which is a long-even-chain saturated fatty acid, has been frequently identified as the most abundant fatty acid in fingermarks.[19, 87, 92, 100] In contrast to the claims regarding the widespread abundance of Δ9 hexadecenoic acid (palmitoleic acid) and Δ9 octadecenoic acid (oleic acid) in fingermarks,[19, 93-94] a recent study reported that the isomeric compounds, Δ6 hexadecenoic acid (sapienic acid) and Δ8 octadecenoic acids are the omnipresent acids in fingermark composition.[21] This claim was further supported by the fact that sapienic acid is an abundant fatty acid, unique to human sebum. Moreover, short-chain fatty acids are less commonly detected in fresh latent fingermarks, due to their high volatility.[19]

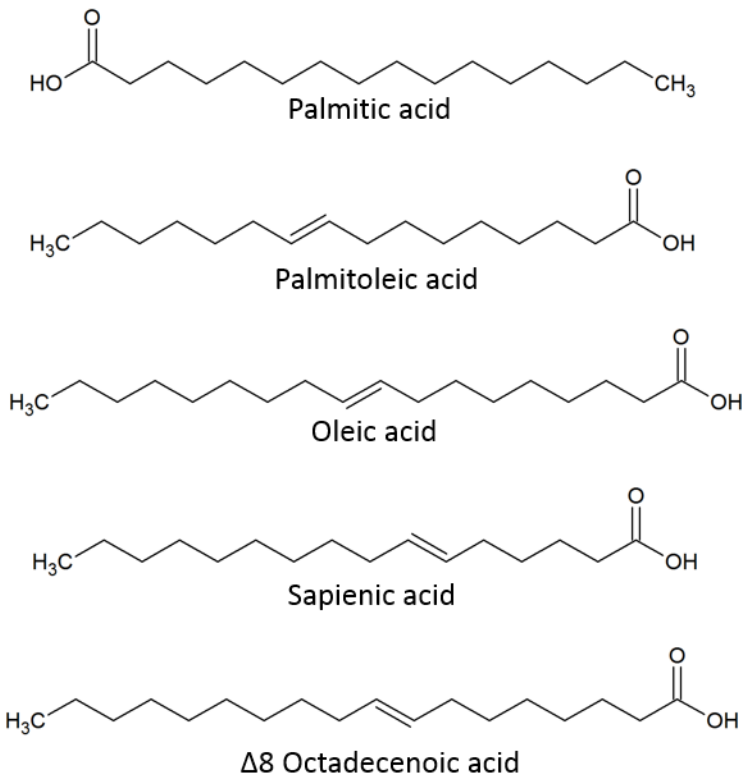

Figure 1.4 Some fatty acids identified in fingermark residue.

Cholesterol (Figure 1.5) is another sebaceous compound that has been repeatedly detected in fingermarks; however, its presence is not as abundant as squalene.[19, 92-93, 100] Wax esters (C_{28}-C_{37}) have also been identified in fingermark residue, with the most common including myristyl myristoleate, myristyl myristate, and myristyl palmitoleate (Figure 1.5).[91, 93, 101] Esters of benzoic acid and cholesterol and some oxidation by-products of squalene have been identified as endogenous sebaceous fingermark components.[91-93]

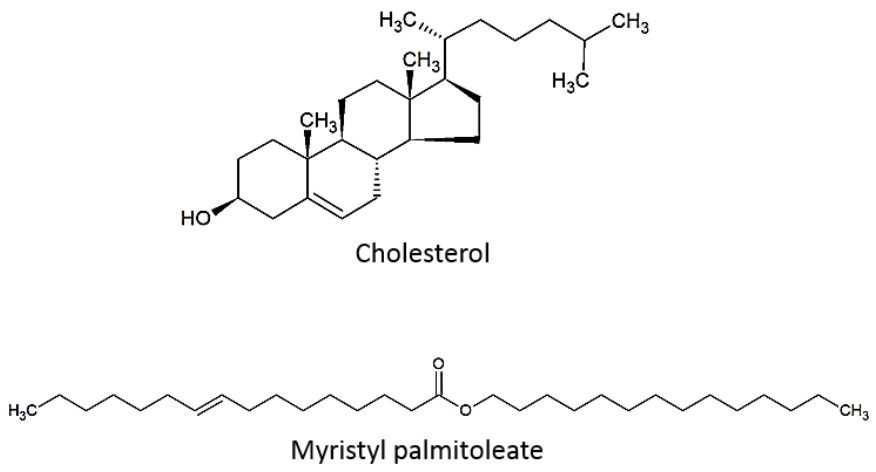

Figure 1.5 Molecular structures of cholesterol and myristyl palmitoleate.

1.5.1.3 Skin debris and other contaminants

Although skin debris (or dead skin cells) found in fingermarks are not currently targeted by fingermark detection techniques, they have been used to generate DNA profiles of individuals.[102] Sourced from the sloughing process of the epidermal skin, these dead cells are transferred onto substrates through skin secretions or by abrasion. The primary cell type of the epidermis is keratinocytes. They change their chemical composition upon reaching the skin surface; however, all keratinocytes can be distinguished by the presence of keratin intermediate filaments.[34] Keratin filaments of keratinocyte cells of the friction ridge skin display a more complex pattern than the thin skin to resist the greater level of stress that it experiences.[103]

Cosmetic products such as skin lotions, hair care products, and perfume residues are the key contaminants that have been often identified in the fingermark residue.[90, 92, 100] Free fatty acids, squalene, cholesterol, and wax esters are common ingredients of skin care products; thus they can cause overrepresentation of endogenous sebaceous compounds. Lipid compounds such as octyl methoxycinnamate and isopropyl myristate, hydrocarbons such as tetracosane and octacosane, and vitamin E are some of the compounds identified as originating from skin care products.[92, 100, 104]

Contaminants such as illicit drugs, nicotine, and explosive residues detected in fingermarks hold great forensic significance as they can reveal donor habits and materials handled by the donor before deposition.[105-109] It should be noted that detection of these compounds in fingermarks could be a result of active cross-contamination (handshaking), environmental exposure, and passive cross-contamination (contact with contaminated surfaces).[109] Research has shown that in the case of nicotine, these contaminations occurred at much lower levels than in direct smoking.[109]

1.5.2 Factors affecting the initial composition

1.5.2.1 Donor traits

Donor characteristics including age, gender, ethnicity, health, medication, psychological state, as well as personal habits such as smoking may alter the initial composition of fingermarks.[17, 78, 90, 93, 100, 109-110] The age of the donor significantly influences the composition of skin secretions, although no precise method is yet available to determine the donor's age by analysing the fingermark composition. Based on the observation that children's fingermarks disappear from surfaces more quickly than adults', studies have been conducted to investigate chemical differences of fingermarks between children's and adults'.[111] It was

reported that skin secretions of children mostly contain aqueous compounds (especially salts of lactic acid), volatile free fatty acids, and esters; while adults' secretions contain large amounts of less volatile long chain esters and fatty acids.[14, 22, 111] Moreover, the composition of children's fingermarks has been found to vary significantly across a population, where some fingermarks have shown increased levels of sebum similar to or even more than adults.[90] The production of sebum is stimulated by androgenic hormones, which are responsible for the enlargement of the sebaceous glands at the onset of puberty.[112] Testosterone in particular causes increased sebum production.[113-114] Therefore, these compositional variations of fingermarks amongst children were ascribed to changes in the hormone levels that occur with physical maturity.[90, 115] With regards to compounds of eccrine origin, the chloride content of fingermarks has been reported to decrease as the age of the donor increases.[116]

Research has also been led into gender discrimination through the analysis of fingermark components, both eccrine and sebaceous in origin.[89, 92, 98, 117] Cuthbertson *et al.* investigated the chloride concentration of fingermarks and found no correlation between the chloride content and the gender of the donor. Asano *et al.* analysed fingermark lipids for gender discrimination and found no significant differences between male and female deposits. Conversely, Buchanan *et al.* and Hartzell-Baguley *et al.* suggested two classes of compounds; steroids and urea respectively, as potential targets for gender discrimination.[104, 111] Recent investigations into the eccrine fraction of fingermarks; namely peptides, small proteins, and amino acids by using MALDI-MS and biocatalytic assay have shown promising results for the determination of gender.[98, 117]

As discussed in the previous section, contaminants identified in fingermarks can offer strong investigative leads. Traces of antibiotic and anti-inflammatory medications, which were administered orally, have been detected in the eccrine sweat of individuals,[118] which suggests detection of drug residues in fingermark secretions may reveal the donor's health status. In addition, dietary styles such as high/low calorie, seafood, dairy, and vegetarian have been shown to affect sweat composition[119] as well as the production of skin surface lipids.[120-123] Nonetheless, the influence of diet, donor ethnicity, and psychological state over the fingermark composition has not been reported so far in the open literature. It is accepted that contamination through immediate food consumption prior to deposition can directly affect the fingermark composition.[18]

1.5.2.2 Deposition conditions

Factors such as the pressure exerted by fingertips on the surface, the contact angle and duration, period within the day, the surface area of the finger that made contact with the surface, and any pre-treatments to hands are referred to as deposition conditions.[15, 124] Research has shown that the use of excessive pressure, contact duration, and induced sweating can result in smudged fingermarks.[124-125] However, one study recently reported that the deposition pressure was less influential on their 'lipid ageing parameters', which was a promising result for the development of fingermark dating methodologies.[101]

Some research has investigated the effect of the period within the day (morning and afternoon) on fingermark composition, which found no statistically significant correlation between the variables.[19, 92, 94] Similarly, research has found no significant correlation between the fingermark surface area and the amount of squalene and cholesterol detected in the residue.[100] One study observed the frequent use of dominant hand/finger(s) having a significant influence on the amount of chloride deposited and this influence was more pronounced on paper surfaces than on foil.[116] However, in another study, fingermarks obtained from left and right hands showed no statistical difference upon development with powders.[126]

1.5.2.3 Types of substrate

Substrates that are likely to bear fingermarks are broadly categorised according to the surface porosity of the substrate; porous, semi-porous and non-porous. Surface properties such as texture, physicochemical structure, temperature, surface tension, and electrostatic forces will further influence the interactions between fingermark residue and the substrate;[15, 127-128] however, these variations have not been studied yet in detail. Due to batch variations in raw materials and manufacturing processes, the same type of substrate (e. g. paper) may still display varying results in fingermark enhancement.[127, 129]

Porous substrates such as paper, cardboard, and wood rapidly absorb fingermark components,[130] with the eccrine sweat components more readily absorbed than the lipid components due to strong, stable hydrogen bonding of amino acids to the cellulose fibres.[128, 130] Amino acids in fingermarks, therefore, can be visualised by suitable reagents even after extended period of time.[64] Research into fingermarks on paper surfaces has shown that the chemical reaction used to visualise the fingermark occurs within the paper due to this penetration.[130] The depth of penetration depends upon the type of paper, where very smooth paper shows very little penetration. Lipids, on the other hand, are conjectured to

transfer onto surfaces via adhesive forces that are dependent upon the temperature and surface roughness.[128] As these forces are inversely proportional to temperature, lipids are easily transferred from fingertips to surfaces because the human body is often warmer than any surfaces.[128] Adhesive forces are directly proportional to the surface roughness, hence rough surfaces such as paper absorb more lipids than smooth surfaces.[128]

Both eccrine and lipid constituents penetrate semi-porous surfaces, but at a much slower pace. Non-water-soluble compounds stay over the surface for a significant period compared to the water-soluble fraction. Certain types of polymers, varnished wood, glossy papers, and waxy surfaces containing several layers fall into this category.[8] Comprehensive analysis of banknotes has revealed that the large variance observed in fingermark detectability on banknotes was related to the differences in their surface free energy, as one type of banknotes exhibited a behaviour similar to a smooth non-absorbent material caused by low surface energy.[127]

Materials such as metal, glass, porcelain, and some types of plastics are regarded as non-porous surfaces.[8, 128] Once deposited, both eccrine and lipid components remain on non-porous surfaces until the deposit is physically removed or degraded by chemical and biological processes.[15] Several studies have reported that the amount of material deposited on non-porous surfaces is little compared to the porous and semi-porous surfaces.[100-101, 116]

1.5.3 Aged composition

The composition of fingermarks discussed in preceding sections describes the initial composition that would alter over time (ageing). In real life, latent fingermarks are unlikely to be recovered from a crime scene immediately after deposition. There will generally be a time gap between the deposition and the recovery of the deposit, which can be a few hours, weeks or even several months. In recent years, ageing of latent fingermarks has been investigated with two broad objectives; to assist in the development of novel and/or improving existing fingermark detection techniques[14, 19-20, 23, 89, 92, 131-132] and to assist in development of fingermark dating methodologies.[21, 31, 86, 91, 93, 100-101, 133-137]

Most of the studies carried out with the first objective were based upon monitoring the changes of the deposit over time with an ultimate goal of identifying the compound(s) or properties which are robust against ageing or to compare the response of aged and fresh fingermarks to the method tested. On the other hand, dating of fingermarks has been approached by observing the physical features of either developed or undeveloped fingermarks through chemical or physical techniques,[31, 133-137] and systematic monitoring of

the interested chemical compound(s) at definite time intervals under certain environmental conditions.[19-20, 86, 93, 100-101, 138] Apart from time since deposition, there are other parameters which affect the aged fingermark composition; the initial composition itself, storage or environmental conditions, and the nature of the substrate on which traces are deposited.

1.5.3.1 Influence of the initial composition

Ageing of the fingermark residue starts soon after deposition and the inherent variability associated with the initial composition induces significant complexity in the aged composition (Figure 1.6). As the composition of deposits obtained from an individual, as well as from different individuals significantly varies due to the factors described in section 1.5.2, so far it has been challenging to estimate donor traits and time-since deposition using fingermark composition.[90-93, 100]

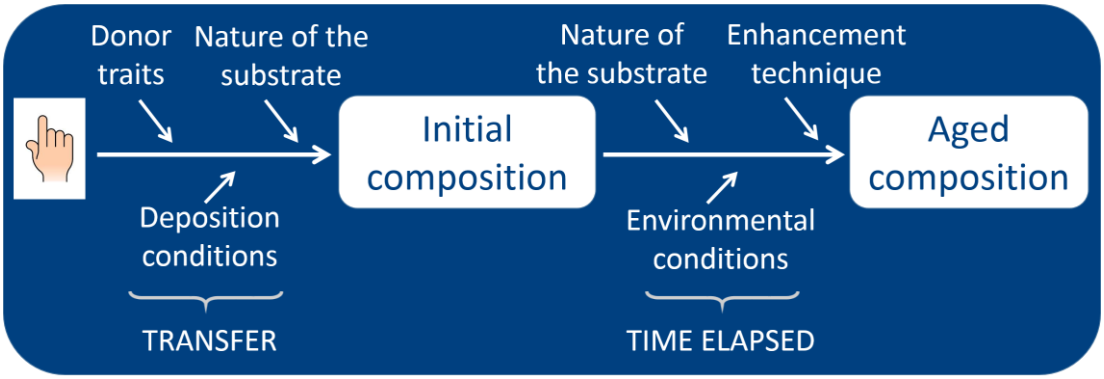

Figure 1.6 Schematic representation of the compositional variation of fingermarks induced by numerous influence factors occurring during two distinct and successive stages. Based on Girod *et al.*[15]

1.5.3.2 Influence of the storage conditions and nature of the substrate

The environmental conditions include, but not limited to, temperature, humidity, light exposure, air circulation, atmospheric contaminants, precipitation, condensation, friction (handling or other natural movements), and ultraviolet or other radiation.[139] Extensive examination of fingermark traces (20,000 examinations) on different substrates which were aged under different environments has suggested that age estimation of fingermarks could only be achieved when two conditions were achieved: (i) all the compositional changes occurring in the deposit over time are established and (ii) the environmental conditions under which the deposits were aged have been completely known.[30] This approach is unrealistic because knowing the exact environmental conditions existed at a crime scene is essentially impossible. Additionally, apart from the inherent chemical changes over time, there are also other factors that influence the fingermark's aged composition (i.e. variations in the initial composition). Although systematic monitoring of the ageing patterns of

compounds of the deposits stored under different environments may potentially lead to age estimation, these studies will be required to consider all possible factors influencing the composition.[101] Nonetheless, studying the influence of storage conditions and substrate on the fingermark composition may assist in developing detection techniques to enhance aged deposits and/or deposits exposed to harsh environments.

Many studies probing the influence of storage conditions have categorised light exposure as 'dark' and 'light' conditions, while air exposure has often been 'open-air' conditions. Room temperature, approximately 20 °C, seems to be the frequently used temperature under these conditions. De Paoli *et al.* investigated the induced photo- and thermal-degradation of compounds found in eccrine sweat using dilute solutions of the compounds instead of 'real' fingermarks.[25] It was found that while neither amino acids nor urea underwent photo-degradation when heated for 3 min, thermal degradation occurred at temperatures above 100 °C. In contrast, lactic acid showed significant photo-degradation after been exposed to an arc lamp source for approximately 8 min (equivalent to two days of sunlight exposure) and thermal degradation at 50 °C. Conversely, in a study focused on children's fingermarks, it was observed that the sodium salt of lactic acid was relatively stable at 70 °C over a period of 72 h.[22]

In terms of the sebaceous components, the environmental influence over squalene has been often studied as it is a key unsaturated compound in fingermarks.[19, 90, 93, 100-101, 132, 140] Light conditions have shown a detrimental effect on squalene as it was undetectable after ageing the deposits on paper under light for about 20 days,[19] while it was detectable after about a month when the deposits were aged under dark.[19, 90, 100, 132] However, the initial composition of the fingermark and subtle changes in the lighting conditions seem to affect the exact timespan and the extent of this reduction.[132]

In addition, squalene has shown to degrade extremely quickly on non-porous surfaces; however, the effect of light exposure is not clear when comparing its lifetime reported by different studies.[20, 100] Weyermann *et al.* could not detect squalene on glass approximately 2.5 days following deposition, when samples were stored in the dark with no air flow. In contrast, Mountfort *et al.* could detect squalene up to 5 days when stored in a light room.[20, 100] Both these studies deposited groomed fingermarks on glass substrates, but Weyermann *et al.* used four deposits per sample and detected through gas chromatography-mass spectrometry (GC-MS) while Mountfort *et al.* used five deposits per sample and detected using liquid chromatography-mass spectrometry (LC-MS). This could be one reason for this disparity. In the same study, Weyermann *et al.* also noticed that there was no

significant reduction in the amount of cholesterol in the deposits on paper over 30 days indicating longevity of cholesterol in fingermarks.[100] Moreover, the much slower rate of diminishing of cholesterol on the glass substrate was observed compared to squalene.[100]

In a recent study that combined degradation of fingermark lipids with principal component analysis (PCA), Girod *et al.* observed separation of fingermarks into two groups based on their age (younger or older than 3 days) when samples were stored at 15 and 20 °C.[101] However, samples stored at 25 °C did not show any separation based on the age due to the greater variability of the lipid composition at this temperature. It was thus demonstrated the significant influence of the storage conditions over degradation of lipids components.[101]

Regarding fatty acids, Archer *et al.* observed an initial increase of the amount of some saturated fatty acids followed by reduction back to the original levels in many of the samples on paper regardless of the light exposure.[19] A similar trend was observed with unsaturated fatty acids but it was not statistically significant in many samples. However, in Mong and co-workers' investigation, the level of saturated fatty acids appeared to be constant over the 60 days of the study period.[90] Similarly, Weyermann *et al.* observed the amount of fatty acids to be constant over the study period on both porous (30 days) and non-porous surfaces (2.5 days).[100] Pleik *et al.* investigated the ageing behaviour of unsaturated fatty acids in sebum-rich fingermarks deposited on aluminium foil that were stored under laboratory conditions exposing them to a diurnal cycle.[21] It was found that the unsaturated fatty acids studied during the study were no longer detectable after 14 days in most of the samples. Decanal was identified as a key degradation by-product of unsaturated fatty acids, thus, it was suggested as an important biomarker for the development of a reliable method for dating fingermarks.

Degradation of esters in children's fingermarks on non-porous surfaces was monitored by Williams *et al.* where rapid degradation was observed when the samples were exposed to elevated temperature (72 °C) for 72 h.[22] In Weyermann and co-workers' study where the samples were stored in dark with no air flow, wax esters were found to be relatively stable over time.[100]

1.6 The physical properties of fingermarks

Chemical studies into fingermark composition provide vital information of the fingermark residue itself, interactions it exhibits with substrates and development reagents, and its compositional variation over time. Nonetheless, all these phenomena encompass a physical aspect to a certain degree, which can be overlooked by investigating only the chemical

properties leading to a partial understanding of the deposit. As such, a series of studies into the physical properties of fingermarks was initiated in the 1970s by Thomas and his colleagues at the UK Home Office.[26-29, 141-142] However, such impetus was not consistently observed over the following years until very recently.[30-33, 135-137, 143-144] Physical properties such as morphology of the fingermark ridges, viscosity, resistivity, and adhesion of the secretions are important considerations in this regard.

1.6.1 Fresh deposits

The physical appearance of a fingermark deposit is highly influenced by its composition and the substrate on which it is deposited. The thickness, resistivity, refractive indices, and contact angles of fingermark secretions/droplets were measured during the early stage studies to improving the knowledge of existing detection techniques such as powdering and metal deposition.[27-29, 141-142] The diameter of droplets of a typical fingermark deposited on a glass slide have been reported to vary between approximately 1-50 µm and the maximum height of the droplets reported at about 2 µm.[28] In a later study, using fingermarks deposited on glass from four donors, the mean values of maximum thickness/height of the droplets were found to be within 0.6-0.8 µm, which demonstrates inter-donor variation discussed in previous sections.[29]

Thomas reported that eccrine-sweat rich deposits on glass generally take the form of isolated circular droplets, whereas sebum-rich deposits form ridges defined by continuous pools or by large, irregular shaped islands of material.[26] Further observations were made by Scruton *et al.*; eccrine-sweat material formed droplets on all types of surfaces while sebaceous material formed continuous films on low energy surfaces such as nylon, polyvinyl chloride (PVC) and polymethyl methacrylate (PMMA) except for polytetrafluoroethylene (PTFE).[142]

The contact angles for most of the droplets were within the range of 0-5° for silicone polished glass, PMMA and cellulose acetate substrates.[29] The authors suggested that this close similarity of contact angles indicates that the contact angle is not a characteristic of the substrate, but of a contamination layer produced by the retracting liquid as the droplets are formed. Moreover, they hypothesised that these measurements are largely receding angles rather than contact angles as the droplets are presumably formed after the rupture of the liquid film.[29] Observations made by Scruton *et al.* on the contact angles of droplets with different composition were somewhat conflicting with the typical behaviour of those compounds in solutions or in pure forms.[142] Generally, lipids form droplets on glass surfaces

with a high contact angle, but Scruton *et al.* observed that the contact angle of eccrine-sweat rich droplets (contain mostly an aqueous electrolytic solution) on high-energy surfaces (e.g. glass, aluminium, and mica) are larger in comparison to lipid-rich droplets.[142] The resistivity of skin secretions of donors, who were wearing polythene gloves for 30 min and then collected by scraping the surface of the fingers using a glass slide, have found to be in the order of 1-10 Ωm, representing a dilute electrolytic solution.[27] On the contrary, the refractive indices of fingermark droplets are reported to be within the range of 1.40-1.54 (reference to λ= 551 nm) which coincide with the range for most of the fatty acids found in fingermarks.[29] As the refractive index of water is outside of this range, they suggested that water is not present in the fingermark deposit to the extent that it is in sweat collected from fingers after stimulated perspiration. Four decades later, it was this idea that Kent reinforced in his recent review of the water content of fingermarks.[82]

Further investigations were carried out on the contamination layer produced during finger contact by using a metal evaporation process. This technique is sensitive to the presence of a contamination layer of an order of 3 nm.[28] Fingermarks were developed by cadmium condensation, which occurs only on furrows as the first thin film of gold is buried within the ridges, inhibiting condensation. To replicate fatty material of fingermarks, thin layers of fatty acids with varying thickness were deposited on glass slides. Then a gold layer (thickness 2 Å) followed by a cadmium layer (thickness 40 Å) were deposited over the fatty acid films by evaporation. It was found that a thin film of fatty acids with a thickness of 30 Å could inhibit cadmium condensation. Therefore, it was argued that the same inhibition mechanism is responsible for the prevention of cadmium condensation on the fingermark ridges. It was further suggested that a contamination layer of fatty material with a thickness of 30-100 Å is formed during finger to surface contact. The surface potential of a fingermark deposited on a clean gold surface was measured by Scruton *et al.*, who found that the surface potential increased when the electrostatic probe was moved from furrows to ridges.[141] The potential variation was in the order of 400 mV and the ridge spacing was generally greater than 300 μm.

True contact between a finger and a surface occurs only over a small region of the apparent ridge area due to the rough nature of friction ridges. This apparent contact area is load-dependent and an increase of the load from 0.5 to 10 N was able to increase the apparent area of contact from 55 to 80%.[142] The authors also noticed that cleaning fingers with acetone prior to deposition decreased the degree of coverage to only 40% or less although the width of contact area remained unchanged.

Recently, Moret *et al.* investigated the morphology of fingermarks deposited on different substrates such as glass, polyvinyl chloride (PVC), polyethene (PE), and polypropylene (PP) surfaces.[33] Examination of undeveloped and groomed fingermarks using a variety of microscopy techniques, this study found that the substrate has a remarkable influence on the morphology of the deposits as well as on the distribution of material. The ridges were observed to be thinner on PE than on PP while the majority of secretions was located in the middle of the ridges on thin PVC. On both PP and thick PVC, skin debris was embedded within the fingermark matrix, though skin debris appeared dry on thin PVC.

1.6.2 Aged deposits

As the chemical constituents of fingermarks alter with time, associated physical properties also display significant degradation. Thomas and Reynoldson noted that the topography of fingermark droplets became irregular upon ageing accompanied by an apparent increase in viscosity (viscosity measurements were not detailed).[29] A large initial reduction of the thickness was observed within the first 10 days in samples deposited on glass and stored in an open laboratory and on a rooftop (protected from rain) in contrast to the storage in constant relative humidity (RH) cabinets.[29] Conversely, a significant change was not observed in contact angles of fingermark droplets, regardless of the substrate.[29] Evaporation of water from the deposit was indicated by the increase in resistivity of secretions from 1-10 Ωm to 100-400 Ωm within the first 4 h followed by a plateau as residual fatty material has high resistivity and low vapour pressure.[27] This was further supported by the reduction of the surface potential of a fresh fingermark from 300 mV to 100 mV after two days since deposition.[141]

In contrast to early-stage studies, most of the recent physical studies were aimed at age estimation of fingermarks.[30-32, 135-137, 143-145] Upon ageing, typical physical alterations were the loss of continuity and narrowing of the fingerprint ridges and an increase in the pore size.[30-32, 144] Apart from these stages, research carried out in the Dactyloscopy Department of the main police headquarters in Poland identified further phases in the ageing process such as dustiness of the area between ridges and the response of the deposits to powder enhancement.[30] Moreover, it was reported that temperatures above 37 °C, low humidity (RH <30%), precipitation, light and air pollution accelerate ageing, while temperatures below 0 °C and high lipid content in fingermarks hinder this process.[30]

Similar physical observations were reported by Barros *et al.* where age estimation of fingermarks was approached by evaluating the morphology of palmprint ridges as a function of time.[31] As discussed in the chemical investigations, the major drawback of age estimation of fingermarks through chemical analysis is the difficulty of obtaining reproducible samples, regardless of the adoption of a grooming procedure.[19, 93, 100] Although such procedure offers unrealistic deposits, Barros *et al.* were able to overcome the reproducibility issue by using charged deposits.

Chromatic white light (CWL) image sensing, a non-invasive and high-resolution optical technique that captures physical features, has also been tested for fingermark age determination.[143-146] Several factors such as the type of secretion (eccrine and sebaceous), sensor settings (resolution and size of measured area), deposition conditions (contact time and pressure), type of substrate, environmental conditions and contamination (cosmetic use) were investigated during this series of studies, which can influence the ageing curves of the 'binary pixel feature'. This ageing parameter is mathematically generated by normalising a scanned fingermark image and binarising it using a threshold. Measuring the number of white background pixels in relation to the total number of pixels results in the binary pixel feature.[145] The 2D-intensity images displayed the strongest correlation to a specific ageing property than the 3D-topography due to the higher sensitivity of 3D-topography images to noise and droplet artefacts. It was able to determine whether a latent fingermark secured from an indoor crime scene is fresher than or older than 5 h based on 2D-intensity images from the CWL sensor.[144] Similar to chemical studies, intra- and inter-donor variations were found to have the highest impact on the ageing curves. Moreover, it was proposed to combine other non-invasive techniques such as spectroscopy and microscopy with CWL sensing to optimise the method suggested.

Alcaraz-Fossoul *et al.* recently published a series of reports on age estimation of fingermarks by visually investigating several physical degradation parameters, namely minutiæ count, colour contrast between ridges and furrows, and discontinuity index (a measure of occurrence of ridge discontinuities).[135-137] The minutiæ count of developed fingermarks was significantly reduced over time in eccrine deposits on the glass but the change was insignificant in sebaceous deposits.[135] Nevertheless, a significant reduction was displayed by both types of deposits on polystyrene substrate. Similar observations were made with regards to colour contrast between ridges and furrows, where both types of deposits on glass displayed slight change against environmental conditions compared to those deposited on polystyrene indicating the influence of the substrate over ageing of fingermarks.[136] Both the

chemical and physical investigations discussed so far suggest that the dark conditions are less effective in the ageing process of fingermarks. However, by investigating colour contrast and discontinuity index over time, Alcaraz-Fossoul *et al.* proposed that dark conditions do not always provide optimum conditions to preserve fingermark ridge details. Direct exposure to light was appeared to inhibit visual degradation under certain conditions.[136-137]

The phenomenon of fingermark ridge drift was first described by Alcaraz-Fossoul *et al.* using the same experimental approach mentioned above.[147] The modification of a single ridge (drift) was found to be independent of the type of deposit, substrate and environmental conditions while significant differences were noticed between different substrates. Moreover, the ridge drift was more frequently noticed on polystyrene substrate than on glass, although this was observed in a limited number of deposits. It was postulated that this phenomenon could be a result of either (i) microscopic diffusion (sliding) of the ridge on the non-porous surface over time; (ii) selective degradation that occurs only a certain location along the ridge; or (iii) influence of the sensitivity of the development technique (TiO_2 powder) towards components of secretions. They also emphasised the fact that this phenomenon can lead to misidentification and misattributions of fingermarks beyond human bias due to dissimilarities produced at the minutiæ level. Thus, these results indicate that issues with the ageing of fingermarks extend beyond the ability to detect them by chemical or physical means.

Overall, both these approaches, chemical and physical, have shown complying and robust evidence for crucial alterations of the fingermark residue that take place over time. Summarising the chemical and physical knowledge to date, rapid removal of water is the main effect of ageing on eccrine fraction which may play a role in the reduction of the thickness and hardening of the residue. The initial increase in the resistivity of the deposit is also associated with removal of water from the deposit. Amino acids and proteins have shown resilience over extended periods of time on paper substrates, provided that the moisture levels are not excessive. Significant degradation of sebaceous compounds over time has been noted resulting in new transformation by-products such as oxidised products. Transformation of unsaturated molecules to saturated analogues is also thought to be responsible for the hardening of the deposit. A considerable influence of environmental conditions over the degradation process has been demonstrated where light conditions have accelerated the ageing process in most cases. Migration of fingermark components on non-porous surfaces was reported recently which may challenge the use of fingermarks for identification purposes.

While the chemical studies have offered more detailed information of the changes occurring at the molecular level, the physical investigations have demonstrated the broad outcomes of those changes that may be overlooked by relying on just one approach.

1.7 Analytical techniques for the investigation of fundamental properties of latent fingermarks

As discussed in the previous section 1.4.2, there is a great demand for further research into improved fingermark detection and if possible, to extract extra information from the deposit (e. g. donor characteristics and the age of the deposit). While successful fingermark detection has been demonstrated through various chemical and physical treatments, there is yet a demand for more simple, accurate, cost-effective, and non-destructive universal methods.[148] Several instrumental approaches such as Fourier transform infrared (FTIR) spectroscopy,[23, 108, 131, 149] Raman spectroscopy,[150-151] and mass spectrometry imaging (MSI)[6, 152] have been employed in imaging fingermark deposits, however in their current forms, these advanced techniques are not the best portable instrumentation to be employed in the field. [148]

Despite various developments of chemical, physical, and advanced imaging techniques for fingermark detection, the demand for further research into the fundamental properties of fingermark residue was emphasised in a recent study, in order to address the issues with sensitivity and specificity of current detection techniques and cumbersome method optimisation.[33] Scientific evaluation of the properties of fingermarks was begun only in the late 1960s primarily by the Atomic Weapons Research Establishment (AWRE) and Atomic Energy Research Establishment (AERE), which were funded by the United Kingdom Home Office.[17, 116, 153] Significant advances have been achieved since then in both lines of research; chemical and physical, with the use of various analytical instrumentation which can be broadly categorised into microscopy, spectroscopy, and chromatography techniques. While microscopy techniques were frequently used in the physical investigations,[28-29, 31, 33] microscopy combined with FTIR[86, 89, 108, 140, 149] and Raman spectroscopy[105, 154-155] were utilised in many chemical investigations. In addition, the use of sophisticated microscopy techniques such as scanning electron microscopy (SEM)[33] and atomic force microscopy (AFM)[156] was also reported recently.

1.7.1 Microscopy techniques

1.7.1.1 Optical microscopy

Optical microscopy is one of the oldest techniques used for fingermark analysis. It is a simple yet very informative non-destructive technique and requires no sample preparation.[33] Early investigations into the physical properties have been carried out by interference microscopy, which provides intensity contrast images of phase changing specimens by means of optical interference phenomena.[28-29, 157] Recently, the performance of various forms of optical microscopy such as bright field, dark field, phase contrast, and cross-polarisation microscopy were evaluated for untreated fingermark analysis.[33] It was found that phase contrast microscopy was the most effective technique for extracting fine details of fingermarks and it could be occasionally complemented by other microscopy techniques.[33] Nonetheless, phase contrast optical microscopy requires transparent and non-textured substrates, which limits its application.[33]

1.7.1.2 Atomic force microscopy

Atomic force microscopy (AFM) belongs to the scanning probe microscopy (SPM) family which is used to study surface properties of samples such as topography at the nanometre to micrometre scale.[158-159] The key components of an AFM are the cantilever spring with an extremely sharp tip at the end and the piezo scanner (Figure 1.7).[158] The cantilever is mounted onto the piezo scanner which accurately controls the position of the cantilever, laterally (X-Y) and vertically (Z). Once the tip is brought in proximity to the sample, the tip experiences interactions with the sample surface as the scanner moves over the sample in a raster fashion. Forces acting between the tip and the sample cause the cantilever to deflect. These deflections are monitored by a laser beam deflection method.

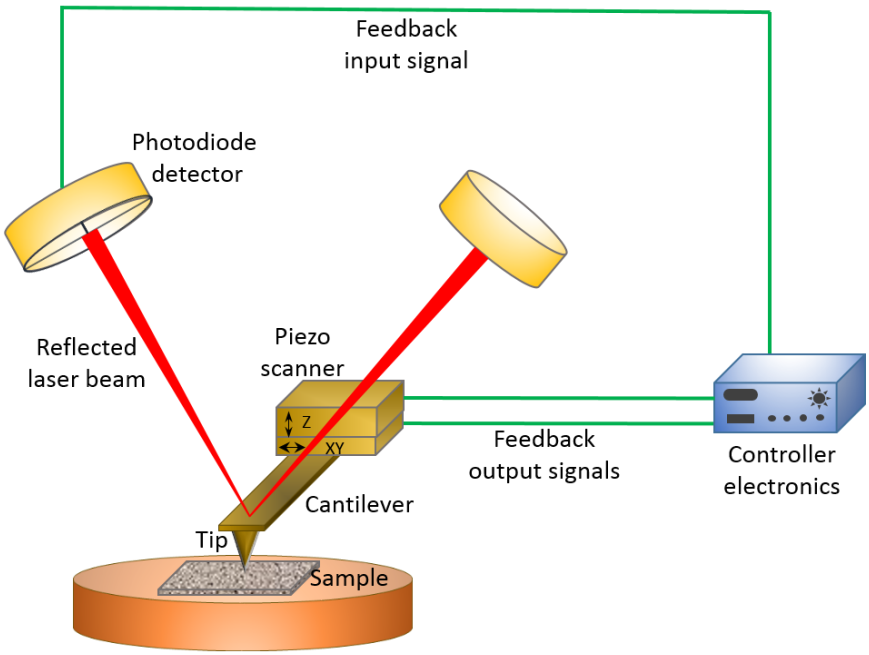

Figure 1.7 Schematic representation of a typical AFM setup illustrating key components; cantilever tip and scanner.

AFM uses a 'Z feedback loop' to ensure the tip accurately tracks the surface topography during scanning. This is essentially a mechanism which involves continuous comparison of the detector signal to a predetermined value known as the 'setpoint'.[159] If the setpoint and the detector signal are not equal, a voltage is applied to the scanner so that it moves towards or away from the sample to bring the error signal back to zero. The position of the Z-scanner at each imaging point is used to generate the 3D topography image.

AFM can be operated in the attractive regime or in the repulsive regime[160] as shown in Figure 1.8. Long-range attractive van der Waals forces and the short-range repulsive forces act between the tip and the sample.[160] As the tip is brought closer to the sample, atoms of both the tip and the sample attract each other (attractive regime). This attraction increases until they are sufficiently close that their electron clouds start repelling each other. The repulsion forces gradually weaken the attractive forces as the tip is brought closer to the surface. At a certain point, the net force becomes zero and then positive (repulsive regime).[159] The imaging modes of AFM can be categorised depending on the type of interaction probed (attractive or repulsive) and the state of the cantilever vibration.[160] There are three primary imaging modes; contact mode, non-contact mode, and intermittent tapping mode which is also known as Tapping Mode in Bruker AFM systems.

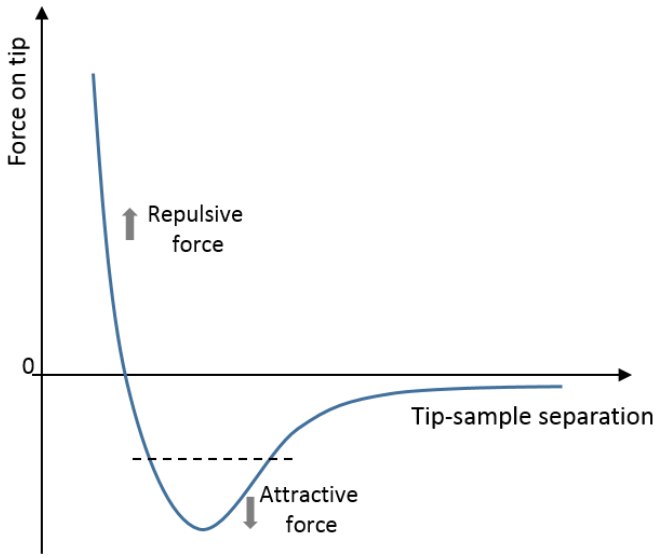

Figure 1.8 Qualitative behaviour of the force between the tip and the sample as a function of the tip-sample separation.[160]

In contact mode, the tip is in permanent contact with the sample and strong repulsive forces act between the tip and the sample which causing large lateral forces during scanning that can damage the sample.[160] In non-contact AFM, the tip never touches the sample and this mode is predominantly performed on very flat surfaces and under vacuum. In Tapping Mode, the cantilever is driven at or near its resonance frequency and the tip intermittently taps the sample surface, giving rise to strong tip-sample interactions.[160] The advantage of Tapping Mode over contact mode is that the lateral forces acting between the tip and the sample during scanning are eliminated allowing imaging of delicate and loosely held samples.[160] Several advanced imaging modes were introduced such as PeakForce Tapping Mode and PeakForce Quantitative nanomechanical mapping (PF QNM) in recent years which have shown superior imaging capabilities.[161-163]

1.7.2 Spectroscopy techniques

Spectroscopy techniques such as FTIR and Raman have the advantage of investigating fingermarks in a non-invasive manner while retaining the spatial integrity of the sample.[148-149, 164] They have thus been applied on both developed and undeveloped fingermarks to image ridge details,[23, 131, 149-150] as well as for the analysis of chemical composition on a variety of non-porous/semi-porous substrates.[86, 89, 108, 140] However, their ability to image ridge details seems to be the frequently researched aspect.

1.7.2.1 Fourier transform infrared (FTIR) spectroscopy

Upon interaction with the incident IR radiation, the resulting FTIR bands are characteristic to specific bonds in the molecules which can be used to determine the structure of the molecules present in the sample.[165] However, analysing complex mixtures using FTIR is challenging as peak assignment can be confusing and very difficult when multiple components are present in the sample.[166] This is likely why FTIR has been applied qualitatively rather than quantitatively in fingermark analysis.

Fingermarks consist of microstructures of material such as droplets of skin secretions, skin debris, and residual contaminants. Thus, FTIR microscopy has been shown to have great utility for examining only the targeted areas of the residue.[14, 22, 86, 89, 131, 140, 167] In FTIR microscopy, visible light is used to view a magnified image of the sample, then the IR beam is focused on the selected microscopic regions where IR analysis is to be performed.[168] Apart from improved sensitivity, some studies which compared ATR and reflection-absorption modes, have preferred reflection-absorption due to the convenience of sample collection and storage. It was noted that ATR yields less intense signals due to the inconsistent distribution of material across the deposit.[167]

Thermal detectors such as deuterated triglycine sulphate (DTGS) detectors are slow and yields noisy spectra, and hence are not suited for FTIR microscopy studies.[169] Conversely, quantum detectors such as mercury cadmium telluride (MCT) have been widely used in FTIR microscopic analysis of fingermarks as they reduce the spectral acquisition times and offer less noisy spectra from the minute quantities of material in fingermark residues. Many MCT detectors cut off their spectral range around 700 cm^{-1},[169] thus any fingermark component that absorbs beyond this level (>700 cm^{-1}) would not be detected.

1.7.2.2 Raman spectroscopy

Raman scattering occurs when the polarizability of the molecule changes with respect to its vibrational motion.[170] As a result of this interaction, the incident or the excitation radiation is inelastically scattered at the chemical bonds of a molecule, such that the energy of the scattered radiation is different from that of the incident light.[171] This shift in energy or frequency is characteristic of the scattering bond and is independent of the frequency of excitation.[171] The frequency scale of the Raman spectrum (X-axis) is expressed as the Raman shift with respect to the excitation radiation, thus Rayleigh scattering is at 0 cm^{-1}.

Fluorescence is a foremost problem in Raman spectroscopy. As Raman scattering is a weak effect, fluorescence can easily obscure the Raman signal if the sample fluoresces at the

excitation wavelength.[172] Although this can be overcome by selecting an excitation wavelength at which the sample does not fluoresce, this limits its application. Confocal Raman microscopes can dramatically reduce the fluorescence background signal as the volume viewed (sampling volume) is limited only to a thin layer.[172-173] In addition, confocal Raman microscopes suppress the out-of-focus planes resulting in improved resolution, high discriminatory power in the axial direction and the possibility for depth profiling, which could be lowered by exciting in the low wavenumber (red or near infrared) region.

The spatial resolution of a confocal Raman microscope is governed by the numerical aperture (NA) of the objective and the excitation wavelength. Considering the Rayleigh criterion, the diffraction limited lateral spatial resolution for a confocal Raman microscope with high NA is proportional to λ/NA, where λ is the excitation wavelength. For a given NA, shorter excitation wavelengths result in higher spatial resolution. However, shorter wavelengths are of high photon energy and can thus cause sample damage.

Raman spectra are not subject to interference by atmospheric moisture and carbon dioxide, unlike IR spectra, and the technique requires little to no sample preparation. Several forms of Raman spectroscopy including wide-field Raman microscopy, laser pointer-based Raman spectroscopy, surface enhanced Raman spectroscopy (SERS), and stimulated Raman scattering microscopy (SRS) have been utilised in the analysis/imaging of fingermarks.

1.7.3 Chromatography techniques

Unlike microscopy and spectroscopy techniques, chromatography techniques require the samples to be extracted to a suitable solvent system, which is destructive of the samples. In some instances, the analytes need to be derivatised.[21, 90, 174-176] These processes are time-consuming and can lead to sample contamination or loss. Nonetheless, they offer chemical information of samples at the molecular level with greater sensitivity and specificity. Therefore, they have become popular among chemical analysis of fingermarks.[16, 19, 21, 87, 90-91, 93, 100-101, 174, 177-178]

1.7.3.1 Gas chromatography-mass spectrometry (GC-MS)

GC-MS is one of the oldest and most prevalent analytical techniques used to investigate the endogenous chemical components of fingermark residue.[16, 19, 21, 87, 90-91, 93, 100-101, 174, 177-178] Since GC-MS is more efficient in analysing non-polar, volatile compounds that are stable upon heating,[179] this technique has been widely applied in studying the lipid fraction of fingermarks. The greater sensitivity and selectivity of modern GC-MS instrumentation have enabled identification of more than a hundred compounds present in fingermark

residue.[87, 91] Analysis of large, neutral lipids such as wax esters and glycerides, however, can cause issues due to their lower volatility and poor ionisation in the MS source.[180] This can be overcome by derivatisation of analytes with suitable derivatisation agents which forms the corresponding methyl or ethyl esters of fatty acids.[174-176] A sample concentration step was also frequently employed in the GC-MS analysis due to the small sample volume of fingermark residue.[19, 21, 87, 90-91, 93-94, 100-101, 174, 177, 181] This was achieved by evaporation of most of the extraction solvent(s) under a stream of an inert gas, followed by reconstitution to a small volume (20-150 µL).

Recent investigations have used a combination of methods for compound identification.[16, 91, 93, 100-101] These were (i) comparison of retention time and mass spectra with standard compounds; (ii) examination of mass spectra to reconstruct the molecules; and (iii) comparison with a computerised database (e. g. National Institute of Standards and Technology (NIST)). However, unsaturated lipid compounds of same aliphatic chain length but with different double bond positions (isomers) are not distinguishable by chromatographic separation coupled to mass spectrometry.[21, 91] For example, Δ8 octadecenoic acid and Δ9 octadecenoic acids are not differentiated by this approach. Derivatisation with MSTFA using iodotrimethylsilan as a catalyst, followed by analysis of degradation by-products using GC-triple quadrupole or -ion-trap MS, have facilitated the structure elucidation of these compounds.[21]

1.7.3.2 Liquid chromatography-mass spectrometry (LC-MS)

Although the analysis of amino acids in fingermarks by GC-MS was previously reported in the literature,[87, 181] studies suggest that LC-MS is more suitable in this regard because of the following reason: The affinity of amino acid molecules towards the stationary phases commonly used in GC-MS can be problematic, with or without derivatisation, due to their relatively high functionality and small size leading to an unexplainable lack in reproducibility of the developed methods.[95]

Pre-column derivatisation (derivatisation prior to chromatographic separation) coupled to reverse phase high-pressure liquid chromatography (RP-HPLC) has been frequently used for the analysis of amino acids in preference to post-column derivatisation, due to its rapid analysis time, sensitivity, and cost-effectiveness.[182] However, avoiding sample derivatisation is preferred to reduce sample handling and improve method simplicity, sensitivity and robustness while increasing the sample throughput.[183] Detection of amino acids without derivatisation has recently become more feasible due to increasing developments of chromatographic columns with improved performance and mass analysers.[183-184] One recent

study reported the use of a hydrophilic ethylene bridged hybrid amide column, which assisted in avoiding sample derivatisation and retention of polar compounds in the column that are too polar to retain by reverse phase chromatography.[24]

1.7.4 Sampling of fingermarks

1.7.4.1 Nature of the deposit

Latent fingermark deposits obtained for research purposes are of three types based on their composition; natural deposits (uncharged/ungroomed), eccrine deposits (eccrine-sweat rich), and sebaceous deposits (charged/groomed/greasy/sebum-rich).[98, 185-186] The term 'natural fingermark' is used to describe those deposits that are frequently encountered in real-life casework.[129] Deposition of these fingermarks in an experimental setup generally involves the donors touching the substrates without any prior treatments to the fingers. The deposits obtained without the donor touching any surfaces after washing hands are called eccrine deposits. These deposits are thought to have secretions from the eccrine glands only.[167]

Deposits obtained after rubbing fingertips against sebaceous rich areas of the body such as the nose, forehead, neck, and hair prior to deposition are referred to as charged deposits. The sole intention of these motions is to increase the amount of material deposited, especially sebum. Therefore, this approach is widely practised in studies into the lipid fraction of fingermarks.[16, 19-21, 91, 93, 100-101] The use of charged fingermarks is one of the most questioned practices not only in fingermark visualisation research but also in analytical studies into the fingermark residue itself.[87, 129] It was shown that the act of grooming significantly influences the analytical results quantitatively and to a lesser extent, qualitatively.[87] The use of 'artificial' fingermarks is another debated concept of fingermark research.[20, 25, 187-189] This approach was undertaken primarily to overcome the difficulties of obtaining reproducible fingermark samples.[187-189] While some studies have used solutions of individual compounds of interest,[20] others have used formulations that mimic eccrine sweat composition or sebaceous secretions in fingermarks.[25, 181, 187-189]

1.7.4.2 Deposition conditions

Controlling the deposition conditions has often been performed by researchers into latent fingermarks, to control the variability of fingermark composition between multiple samples.[31, 86, 93, 101] The International Fingerprint Research Group (IFRG) guidelines instruct researchers to provide clear descriptive deposition instructions to donors to ensure consistency across the sample set.[129] Some studies have provided descriptions regarding the

deposition conditions, for example, “touch the substrate with moderate pressure” or “the same pressure that would be used to grab an object”.[177] Some researchers employ assisted deposition where the researcher places the donor’s finger on the substrate to control the pressure exerted.[87] Employing more strict controls such as the use of a balance to control the force applied is also common in this regard.[31, 86, 93, 101] While employing substrates that are representative of real-life cases are preferred over the other substrates that are limited to research laboratories, limitations with analytical conditions often compromise such utility.

1.7.4.3 Number of donors

Appropriate considerations must be given when deciding the number of donors that are going to be employed in the study, as it has a considerable influence on the interpretation of analytical data. The number of donors in analytical studies largely depends on the key aim of the study and the availability of time and facilities. Therefore, there is little agreement on the number of donors used in published work. Some analytical studies have used only one donor where the possibility of employing a certain technique to study fingermarks was tested.[20, 33, 86] While studies into the initial properties of fingermarks and their variation over time have employed 3-30 donors,[19, 21, 23, 31, 87, 89, 93, 101, 132] most studies which attempted to infer donor traits have used much larger donor pools, typically between 20 to more than 100 donors.[22, 92, 94, 98] It is also notable that studies have used approximately equal numbers of male and female donors to maintain a balance between biological sexes.[31, 90, 94, 98]

1.8 Aims and overview

Despite significant ongoing research devoted to developing novel fingermark detection techniques, incomplete understanding of the fingermark itself impedes the efficacy of this process. The primary aim of this dissertation is to study the fundamental chemical and physical properties of latent fingermarks on non-porous surfaces by employing advanced analytical instrumentation, within the context of their detectability. This thesis combines two main streams of fingermark research; chemical and physical investigations towards generating a more comprehensive and evidence-based knowledge of the fingermark residue itself. Such knowledge is vital to improve current fingermark detection capabilities and to infer additional intelligence from the deposit.

Chapter 2 outlines the general approach utilised throughout the thesis to sampling of fingermarks and the different environmental conditions under which the deposits were aged. Chapter 3 investigates the physical properties of fingermarks and their variation over time in a novel approach using atomic force microscopy. Instead of studying only the morphometric

properties, other intrinsic properties such as adhesion were also measured. These measurements are invaluable to understand the interactions that fingermarks exhibit with other surfaces they come into contact with. Chapter 4 reveals the spatial distribution of chemical species within fingermark deposits using both conventional and synchrotron-sourced FTIR, as well as confocal Raman microscopy. Such knowledge at high-resolution was a significant gap in the current understanding which has confounded interpretation of both the chemical and physical measurements made on fingermarks.

Chapter 5 describes investigations into the appropriate methods of fingermark sampling for *ex-situ* time-course experiments by using GC-MS. Previous research has established the difficulty of obtaining reproducible samples as a significant impediment to monitoring the compositional variation of fingermarks over time. To this end, various sampling methods were tested and the impact of the proposed approach to data interpretation was demonstrated. Based on the results of Chapter 5, investigations carried out on the analysis of squalene and its transformation by-products in fingermarks formed during the storage under different environmental conditions are described in Chapter 6. Degradation products were separated and identified through UHPLC-HRMS and the products that showed relatively longer lifespans were suggested as promising biomarkers for the development of novel techniques for targeted visualisation of aged fingermarks.

Chapter 2: Fingermark sampling and storage

2.1 Introduction

As outlined in the previous chapter, sampling is a critical phase of fingermark research that needs significant attention during the designing of experiments. Currently, the approaches in fingermark research concerning fingermark composition have a minimal agreement with respect to their experimental design, causing inter-comparison of research findings more challenging. To this end, reasonable efforts were taken to maintain the sampling consistency throughout the thesis. This chapter outlines the general approach of fingermark sampling undertaken during this thesis and the environmental conditions used for storing them. More specific details are described in the relevant chapters. Furthermore, this chapter describes the ethics approval that was sought prior to any samples collection.

2.2 Experimental

2.2.1 Ethics approval

Although this research was not carried out directly on human participants, it has ethical dimensions as it involved samples obtained from humans and they could be used as proof of their identity. Application for the ethics approval of the sampling protocol was approved through the low-risk ethics approvals process by the Curtin University Human Research Ethics Committee (approval number RDSE-02-15) on the 29th of January 2015. Abiding by such approval ensures the donors' right to privacy, safety, and to request additional information and/or withdraw from the study if desired.

Donors involved in this study were provided with participant information sheets where the purpose of the research, participant rights and confidentiality were explained in written form. The same was explained verbally as well. The contact information of the researchers was also provided should they require further information or to withdraw from the study. Upon the donors' satisfaction with the information provided and willingness to volunteer in the study, signed consent forms were collected from them. Examples of the information sheet and the consent form are provided in Appendix 1. Each donor was assigned with an alphanumeric code which was used to label samples. All documents related to this process were stored separately where they were only accessible by the researcher.

2.2.2 Sample deposition

Demographics of the donors, type of the deposits obtained under each investigation, and donors' routine use of cosmetics are listed in Table 2.1.

Table 2.1 Details of the donors and types of deposits analysed throughout the thesis.

Donor	Study	Type of the deposit	Age (years)	Biological sex	Cosmetic use
D1F1	AFM, IR, Raman, GC-MS, LC-MS	Natural	33	Female	Regular use of moisturiser, cosmetics, hair oil and hand cream. Daily consumes fish oil as a nutritional supplement
	AFM, IR, Raman	Eccrine			
	AFM, GC-MS	Sebaceous			
D2M1	AFM, Raman, LC-MS	Natural	26	Male	Intermittent use of moisturiser and hair care products
	AFM, Raman	Eccrine			
	AFM	Sebaceous			
D3M2	AFM	Natural	48	Male	Intermittent use of moisturiser
	AFM, IR	Eccrine			
D4M3	IR	Natural	77	Male	None
D5M4	GC-MS	Natural	53	Male	Regular use of an oil blend on hands. Consumes fish oil as a nutritional supplement every two day
	GC-MS	Sebaceous			
D6F2	GC-MS	Natural	23	Female	Regular use of moisturiser and hand cream
	GC-MS	Sebaceous			
D7F3	Raman	Natural	32	Female	Regular use of moisturiser and cosmetics
D8F4	Raman	Natural	20	Female	Intermittent use of moisturiser and hand cream
	Raman	Sebaceous			
D9F5	Raman	Natural	23	Female	Regular use of moisturiser and cosmetics
D10M5	Raman	Natural	31	Male	Regular use of face cream
D11M6	LC-MS	Natural	32	Male	Regular use of hair care products
D12F6	LC-MS	Natural	25	Female	Intermittent use of moisturiser

Natural deposits were collected by instructing donors to wash their hands with liquid soap and warm water for about 2 min and allow them to air dry. Donors were then asked to engage in their regular activities for at least 30 min without washing their hands or handling any food or chemicals before deposition. Eccrine deposits were obtained 30 min after washing hands, without the donor touching any surfaces during this time. Sebaceous deposits were obtained by rubbing the fingers against the nose, forehead, and chin followed by deposition on the substrate. All male participants who provided sebaceous deposits in this thesis had no facial hair at the time of sampling. The sample collection protocol was based on the guidelines set by the IFRG and the purpose of obtaining different types of deposits was to study the influence of the fingermark composition (i. e. eccrine-rich, natural, and sebum-rich) on the measurements being made. The deposition time was 10 seconds in all cases. Where applicable, further details of sample deposition are provided in relevant chapters.

A range of non-porous substrates was used in this thesis which is listed in Table 2.2.

Table 2.2 Details of the substrates employed during the thesis.

Study	Substrates
AFM	Glass microscope slides (Mikro-Glass, Australia), Mica
IR	Glass microscope slides (Mikro-Glass, Australia), ZnSe slides and hemispheres (Crystran Ltd., UK), aluminium foil (heavy duty catering foil, Confoil, Australia)
Raman	Glass microscope slides (Deckgläser, Germany)
GC-MS and LC-MS	Aluminium foil (heavy duty catering foil, Confoil, Australia)

2.2.3 Sample storage

Storage conditions employed during the time-course experiments are given in Table 2.3. Since dust particles can be deposited on fingermark secretions during the exposure to open air, samples obtained for atomic force microscopy and confocal Raman microscopy investigations were placed inside plastic containers with limited air circulation.

Table 2.3 Different storage conditions used to store samples.

Study	Storage conditions
AFM	Sample slides were horizontally placed inside plastic containers with limited air circulation which were then stored away from light in a cabinet.
Raman	Sample slides were horizontally placed inside plastic containers with limited air circulation which were then stored in an office environment at room temperature (21-23 °C) as shown in Figure 2.1. The containers were exposed to diurnal light cycle.
LC-MS	Before storing samples under light or dark conditions, aluminium substrates were slightly rolled at one end and then inserted approximately 2 cm of that end into 20 mL glass vials (Gerresheimer, Germany).
	Storage under light conditions (**Figure 2.2):** Vials were stored vertically in an office environment at room temperature (21-23 °C) where samples were exposed to diurnal light cycle.
	Storage under dark conditions: Vials were placed vertically inside a cardboard box and covered with its lid such that samples were exposed to complete darkness.
	Storage underwater: Aluminium strips were submerged in a water bath filled with tap water. Clean glass slides were placed at the corners of strips without touching the fingermarks to prevent the strips floating on the surface. The water baths were covered completely from aluminium foil to prevent exposure light.

Figure 2.1 Storage of fingermarks deposited on glass slides inside plastic containers in an office environment.

Figure 2.2 Storage of fingermark samples in open vials under light conditions over a 7-day period.

Chapter 3: Studies into the physical properties of latent fingermarks on non-porous surfaces by atomic force microscopy (AFM)

Portions of this research have been published in the journal *Forensic Science International*:

Dorakumbura, B. N.; Becker, T.; Lewis, S.W. Nanomechanical mapping of latent fingermarks: a preliminary investigation into the changes in surface interactions and topography over time. *Forensic Science International* **2016,** *267*, 16-24.

DOI: https://doi.org/10.1016/j.forsciint.2016.07.024

3.1 Introduction

As highlighted in Chapter 1, understanding the physical properties of fingermarks is a keystone to generating more comprehensive knowledge of the deposit, its detection, and the ageing process. A key example of this is fingermark detection by powdering, which relies on properties such as the presence of moisture, greasy substances, and electrostatic charge distribution across the deposit.[26] However, the powder formulations and their methods of application have been developed in an improvised manner, without a firm understanding of the mechanism of powder adhesion.[26] It is thought that the powder particles adhere to water and greasy substances via a pressure deficit mechanism.[72] When the powder particle is wetted on the lower side by the fingermark droplet, it creates a curvature of the meniscus, leading to a pressure difference inside the droplet, thereby causing the particle to adhere. Thus, the presence of water and grease in the deposit promotes the mechanical adherence of particles by (i) wetting the particle surface; and (ii) interacting with the particles via capillary forces.[5] In a study into exploring adhesion of powder particles, the force required to detach aluminium powder particles (particle radius of 0.1-100 μm) from a deposit was reported to be in the range of 1×10^{-8} to 1×10^{-2} N.[26] The electrostatic attractions between the fingermark deposit and the dust powder particles are thought to play a minor role in powder adhesion.[26]

In recent years, there has been an increased interest towards the development of novel detection techniques that involve nanoparticles and their modified forms.[67, 69, 190-191] Some of these techniques utilise solution baths containing nanoparticles as the mode of application, while others apply nanoparticles as powders. These techniques, which are still in early development stage, are claimed to offer potentially superior outcomes across a wide range of substrates and on aged deposits.[67, 69, 190-191] However, there is as yet an incomplete understanding of the mechanisms of these techniques.[67, 192] For example, in the single metal deposition (SMD) technique, the deposition mechanism of colloidal gold nanoparticles onto the fingermark deposit is presumed to be via electrostatic attractions, although as yet this has not been confirmed.[67, 69] Similarly, despite its widespread application, the mechanism of physical developer (PD), which involves the deposition of silver nanoparticles, still remains inconclusive. In this context, exploring micro- and nanoscale features of fingermark deposits such as adhesion and topography is vital to generate an improved understanding of mechanisms of current and proposed techniques.

3.1.1 Atomic force microscopy in fingermark research

In 2007, Watson and Watson demonstrated potential applications of scanning probe microscopy (SPM) for the analysis of fingermark ridges.[193] During this study, the topographical and adhesive interactions of fingermark ridges deposited on glass were measured in ambient air as well as *in-situ* in water using contact mode. Moreover, two overlapping fingermarks deposited on glass were resolved by this approach.[193]

Surface characterisation of three smooth, non-porous plastic substrates by atomic force microscopy (AFM) was reported by Jones *et al.* where these characteristics were interpreted in relation to fingermark development by magnetic powder.[194] It was found that a single roughness parameter was not adequate to describe surface structures with respect to fingermark development. Despite the overall smoothness of Formica laminates, fingermark development was strongly influenced by sharp ridges on the surface (approximately 100 nm). However, this trend was less prominent on unplasticised polyvinyl chloride (uPVC) which had furrows instead of sharp ridges. Intriguingly, surface features such as parallel high ridges (5 µm) on polyethylene greatly contributed to perceived surface roughness but had little effect on development. On the other hand, magnetic powder particles were trapped within minor ridges, which were perpendicular to the general lay with furrows of 1-10 µm, and significantly degraded the developed print quality.[194]

Localised corrosion of brass substrates due to eccrine fingermarks was studied using AFM by Goddard *et al.* who proposed that the engraved negative topographical image could potentially be used to image the ridge details.[195] Storage of eccrine deposits at ambient temperature and high humidity followed by heating at 100 °C was less effective in changing the image appreciably. However, brief heating in the Bunsen flame (300 °C) drastically altered the topographical image, creating depression marks.[195]

The application of AFM for a detailed study of the intrinsic physical properties of fingermark microstructures (droplets) and their variation over time was first reported based on the work described herein by the author of this thesis.[196]

3.1.2 PeakForce quantitative nanomechanical mapping

PeakForce quantitative nanomechanical mapping (PF QNM) is a novel imaging mode proprietary to Bruker atomic force microscopes, which allows simultaneous acquisition of high-resolution topography images and co-localised measurements of nanomechanical sample properties such as adhesion, stiffness, elastic modulus and deformation. Although PeakForce Tapping and standard Tapping Mode function in a similar manner, PeakForce Tapping operates in a non-resonant mode where the probe is driven at a frequency well below its resonant frequency.[197] These improvements thus avoid filtering effects and the artefacts caused by dynamics of a resonating system.[197] PeakForce Tapping combines the benefits of both contact mode and Tapping Mode, offering direct force control and prevention of sample damage caused by lateral forces.[197] In PF QNM, the mechanical properties of the sample are derived in real-time, directly from the force-distance curves obtained at every interaction between the tip and the sample (Figure 3.1). When the AFM probe taps the sample, its velocity is minimal due to the sinusoidal motion of the piezo scanner, which makes this imaging mode ideal for soft samples.[161, 163, 197] This technique has been successfully applied to investigate interactions between the AFM tip and surface nanobubbles,[198] to study stiffness and evolution of interfacial micropancakes,[199] to observe assembly and disassembly process of hydrogels *in-situ*[162] and to probe topography and microscopic contact angles of hydrocarbon oil droplets on a polystyrene surface.[200]

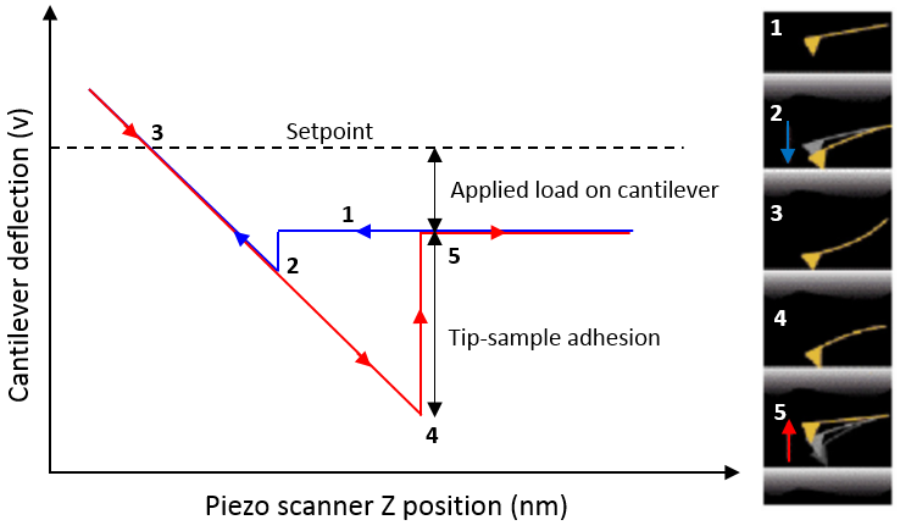

Figure 3.1 A typical force distance (F-d) curve showing the tip approach (blue) and withdraw (red). The total contact force is the sum of applied load and the tip-sample adhesion. Modified from Bruker application note.[197]

3.1.3 Aims

This chapter was aimed at exploring the physical properties of latent fingermarks on non-porous surfaces using atomic force microscopy. It was attempted to probe the interactions between fingermark secretions and dusting powder particles, as well as glass surfaces during the preliminary investigations. Variation of the topography and adhesion of fingermark droplets were then studied during storage under dark conditions over a period of one month. Eccrine, natural, and sebaceous deposits were analysed to investigate the influence of different secretions; primarily water-soluble (amino acids and proteins) and water-insoluble (lipids) components; over the physical properties. The area between ridges was probed to investigate possible contamination of the background.

3.2 Experimental

3.2.1 Sample collection and storage

Detailed information of the donors, sample deposition procedure and storage conditions is described in Chapter 2. The samples were analysed on the same day of deposition, then the same droplets were re-analysed after 7, 14, and 28 days. A detailed description of the approach undertaken for relocating the same droplet over time is given in Appendix 2. The eccrine deposit from the donor D3M2 was not re-analysed due to constraints of time and facilities. The temperature and the relative humidity inside the storage cabinet were continuously monitored using a data logger (Digitech datalogger, Jaycar Electronics, Australia), placed next to the samples, over the period of the experiment and ranged between 16-24 °C and 37-73% respectively (storage conditions are given in Appendix 2).

3.2.2 Preliminary investigations

A dusting powder particle (silver/black dual purpose magnetic powder, particle diameter approximately 20-25 µm) was glued to a bare cantilever using epoxy resin (Araldite) and left to dry overnight. Upon contact with the fingermark secretions, the modified cantilever was retracted and the interactions between the powder particle and the secretions were investigated by analysing force-distance curves. Similarly, interactions between secretions and glass surfaces were probed using a modified cantilever with an attached glass sphere (diameter approximately 20-25 µm).

3.2.3 PeakForce quantitative nanomechanical mapping of fingermark droplets

AFM imaging was performed using a Bruker Dimension Icon AFM system in PF QNM mode under ambient conditions. All AFM images with nanomechanical property maps presented in this work were acquired with Bruker probes (type: SNL-A; spring constant 0.35 N/m; tip radius: 2 nm) at a peak force of 2-18 nN. The spring constant of the cantilevers was measured using the thermal tune method. The imaging scan rate was maintained at 2 Hz at a digital resolution of 256 pixels × 256 pixels per image, and the driving frequency of the cantilever was maintained at 2 kHz. Randomly selected 7-10 droplets from different regions of the fingermark, roughly representing the centre, right-hand and left-hand sides of the bottom and upper regions, were imaged per each fresh deposit and the same droplets were monitored over the ageing process. Details of this approach are given in Appendix 2. The raw AFM topography images were then further processed using a first order plane fitting routine using the Bruker Nanoscope Analysis 1.50 software. The absolute adhesion and volume of the sample droplets were determined with roughness and bearing analysis respectively.

3.2.4 Standard Tapping Mode

To observe the areas in between fingermark ridges (furrows), a freshly cleaved mica substrate was first imaged with a Tap300-G AFM probe (Budget Sensors, spring constant: 40 N/m, tip radius: <10 nm, resonance frequency 300 kHz) in standard Tapping Mode using a Bruker Dimension FastScan AFM system. A natural fingermark was then deposited on the mica substrate and the area in between the ridges was imaged. The imaging scan rate was maintained at 1 Hz at a digital resolution of 512 pixels × 512 pixels per image. Imaging was repeated every 15 min over 23 h.

3.3 Results and discussion

In preliminary investigations, efforts were made to study the interactions between fingermark secretions-dust powder particles and fingermark secretions -glass by gluing a dust power particle (magnetic powder) and a glass microsphere to bare cantilevers. It was noted that a considerable amount of secretions was transferred onto the surface of the powder particle and the glass sphere upon the first contact followed by withdrawal of the cantilevers from the secretions. Thus, instead of measuring the interactions between the modified cantilever surfaces and secretions, it was measuring the force required to break the capillary bridge comprised of fingermark secretions. As such, the modified cantilever approach was not further investigated.

3.3.1 Adhesion force

As described in Chapter 1, interactions between the cantilever tip and the sample can be attractive or repulsive in nature. When a sharp cantilever tip (with the tip radius being a few nanometres) is brought into contact with a liquid droplet, a nanoscopic capillary bridge is formed between the tip and the surface of the droplet due to the capillary movement of the liquid. On hydrophilic surfaces under ambient conditions, this capillary bridge is comprised of the liquid itself and water which has condensed on the surface. In the case of fingermark droplets, this capillary bridge is composed of both fingermark secretions and water. The force required to pull-off the cantilever completely from this contact (adhesion, F_{ad}) is the force against all electrostatic attractions (F_{el}), capillary forces (F_{cap}), van der Waals forces (F_{vdW}) and chemical interactions (F_{chem}) between the tip and the sample as given in the following equation.[158, 201-202]

$$F_{ad} = F_{el} + F_{vdW} + F_{cap} + F_{chem}$$

The capillary bridge is the dominant source for tip-sample adhesion in air.[200-201, 203] The dependency of all above-mentioned forces on the chemical nature of the tip and the sample are relatively straightforward except for capillary forces. Several studies have shown that capillary forces are influenced by the surface tension of the liquid (and are thus reliant on the nature of the liquid), relative humidity, contact time, and the contact area between the sample and the tip.[202-205] For a given day of measurements and for a single fingermark droplet, relative humidity and contact time are constant except in regards to the composition of the liquid and contact area. The magnitude of capillary forces can be minimised by reducing the contact area by using a sharp cantilever tip. Nevertheless, the contact area around the tip increases as the tip contacts the droplet at a more oblique angle towards the droplet's edge,[206] resulting in higher capillary force (Figure 3.2). Additionally, the chemical composition within a droplet can be potentially heterogeneous. The adhesion (F_{ad}) therefore provides information about the tip-sample interactions which are strongly related to the chemical composition of both the sample and tip.[203-204]

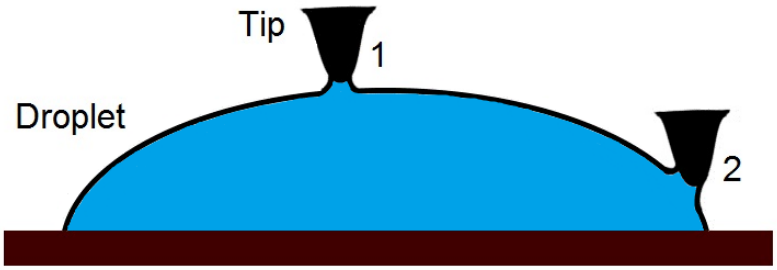

Figure 3.2 Illustration of the capillary bridge formed between the tip and the surface of the droplet. The contact area is larger in contact 2 compared to contact 1. Based on Wang *et al.*[206]

3.3.2 Variation in adhesion of fresh deposits

Since all the AFM probes used in this work were made of silicon (a polar surface), the adhesion offers insights into the hydrophilic-hydrophilic/hydrophobic interactions between the tip and sample surface. Knowledge of interactions that fingermark droplets form with other surfaces (e. g. dust powder particles and nanoparticles) is vital to understand the mechanisms of detection techniques.

Figure 3.3 shows the variation of adhesion within fresh droplets of fingermark deposits from the donor D1F1. The images show 3D AFM topography data of individual droplets overlaid with the respective adhesion maps, in which bright colour areas represent large adhesive forces and the dark colours represent smaller forces. The adhesion of most of the eccrine droplets (7 out of 8) from donor D1F1 was uniform across the droplets with a relatively high magnitude of about 5-17 nN, while natural and sebaceous droplets were approximately 2-7 nN and 0-2 nN respectively. However, only one eccrine droplet from donor D1F1 had an adhesion value at the centre that was smaller than the background (glass surface around the droplet) or the edge of the droplet. This value was approximately -42 nN compared to the background. Adhesion was not uniform in most of the eccrine droplets from both donors D2M1 and D3M2. Some displayed higher adhesion at the edge, compared to the background, while adhesion of the remaining area the droplets was very small (approximately -15 to -35 nN). Some droplets had higher adhesion at the edge compared to the centre (Figure 3.4).

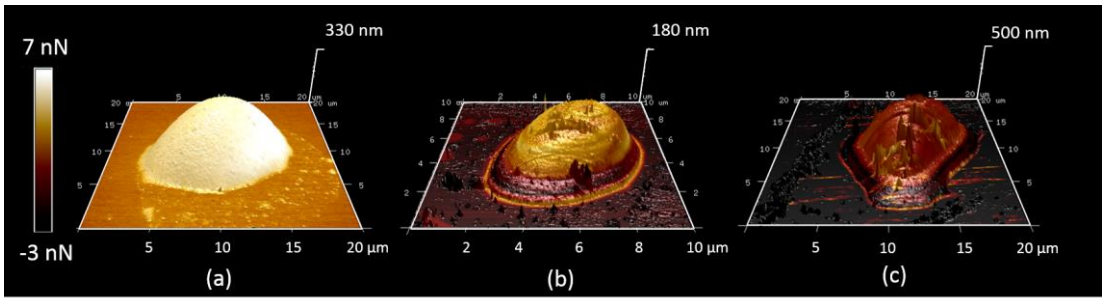

Figure 3.3 Adhesion maps overlaid 3D topographic images of three individual droplets, (a) eccrine, (b) natural, and (c) sebaceous, from the donor D1F1 illustrating the variation in adhesion within fresh droplets of different types of composition. Dark coloured 'bands' like areas are observed within natural and sebaceous droplets while the adhesion map is fairly uniform within the eccrine droplet.

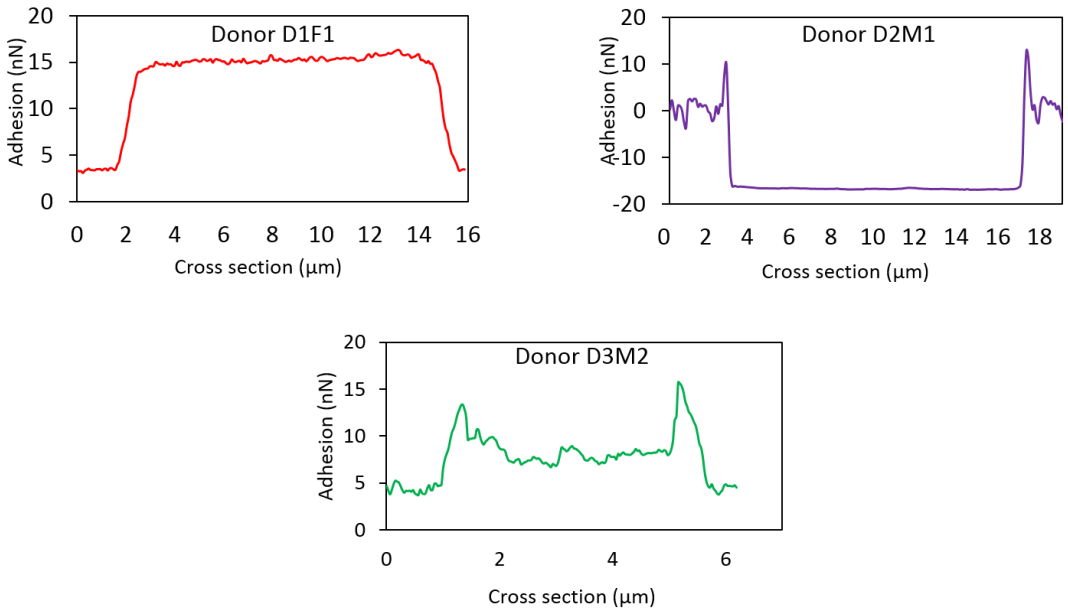

Figure 3.4 Cross sections of adhesion maps of eccrine droplets from three donors showing variation in adhesion observed across the droplets.

At a relative humidity of 65%, an adhesion force of 48 nN was measured between a new AFM probe and a clean glass slide (capillary adhesion of the water layer). Thus, an adhesion that is close to zero or negative as exhibited by some of the eccrine droplets suggests that even though the eccrine sweat is usually in excess of 98% water, the eccrine fingermark droplets might not necessarily have water in abundance (at least near their surface). Thomas and Reynoldson witnessed a lack of systematic dependence of drying rate of fingermark droplets (presumably of a natural deposit) with relative humidity and suggested it may be caused by the low water content of fingermarks.[29] In a chemical investigation using µ-FTIR, Girod *et al.* reported the inconsistent appearance of the large water peak visible at 3150-3600 cm^{-1} and suggested it to be caused by heterogeneous repartition of water in fingermark deposits.[86]

Moreover, as emphasised by Kent, the figure for water content in latent fingermarks (>98%) published in some literature originated from biological data for eccrine sweat production, but has not been measured for actual fingermark deposits.[82] Interestingly, the negative values of adhesion observed in some eccrine droplets propose that these adhesion forces are in fact repulsive forces. As the cantilever tip was a hydrophilic surface, these repulsive forces could be a result of hydrophilic-hydrophobic interactions between the cantilever tip and hydrophobic chemical components of the droplets.

Although the report by Watson and Watson offered insights for the application of SPM to resolve properties of fingermarks down to the nanoscale, some of their observations are not in line with the general understanding of fingermark composition.[193] Submerging fingermark samples in water, is thought to remove water-soluble components of the deposits. Thus, it is surprising that no significant difference in topography or friction or adhesive data was observed during conducting measurements under ambient conditions and *in-situ* in water. The similarity of adhesive forces under these two different conditions was attributed to the presence of contaminants and lipids in the deposit.[193] Yet, this could be a result of the use of contact mode AFM, which is less suited for the investigation of soft samples such as liquid droplets. In Watson and Watson's study, the cantilever tip operated in contact mode may have dragged fingermark secretions along as it moved across the surface, disturbing the spatial integrity of the sample.

3.3.3 Effects of ageing of fingermark droplets

The variation of adhesion in eccrine deposits from donors D1F1 and D2M1 over time is shown in Figure 3.5. It is clear that initially the adhesion increases in most of the droplets (5 out of 8 in D1F1 up to the first week and 7 out of 7 in D2M1 up to the second week) followed by a gradual decrease displayed by all droplets. However, deposits from different donors take different timespans to achieve the maximum adhesion, and the degree of variation is different from droplet to droplet. Although relative humidity contributes to adhesion force, it did not show a significant impact over the variation of adhesion in this study. According to Sedin and Rowlen, the pull-off force at a relative humidity greater than 50% is essentially constant on hydrophilic surfaces.[204] The relative humidity measured in this study was greater than 50% in all the days that measurements were taken with the exception of 42-46% for those taken at 14 days following deposition (see Appendix 2).

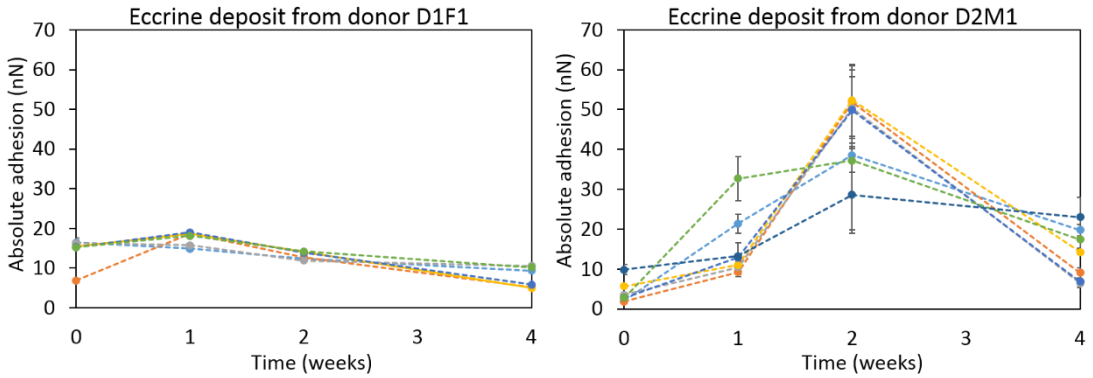

Figure 3.5 Variation of adhesion over time at the middle of eccrine droplets in fingermark deposits from donors D1F1 and D2M1. Each individual line represents variation in adhesion of a single droplet monitored over the period of four weeks and connecting lines are only to aid the reader in following each droplet. The error bars present the standard deviation of the mean adhesion value of individual droplets (extracted using roughness measurements in Bruker Nanoscope Analysis 1.50 software).

There were notable changes in adhesion over time in natural fingermark droplets. In droplets from donor D1F1, the adhesion at the middle decreased after the first week then increased over time. Adhesion at the edge of the droplets followed a similar trend but the magnitude was high compared to the middle of the droplets (Figure 3.6). While adhesion of the natural fingermark droplets from donor D2M1 exhibited the same tendency (Figure 3.7), adhesion of the deposit from the other donor (D3M2) increased after the first week and then decreased over time (Figure 3.8). As per the discussion made on Figure 3.2, it is reasonable to speculate that the stronger adhesion observed at the edge of some droplets are caused by the higher contact area between the tip and the sample. However, stronger adhesion was observed at the edge, especially in aged natural and sebaceous droplets, where they took the form of a thin film rather than hemispheres. Moreover, not all droplets showed stronger adhesion at the edge. These facts provide robust evidence to suggest that the observed stronger adhesion in aged droplets was, in fact, a consequence of chemical transformations occurring within the droplets.

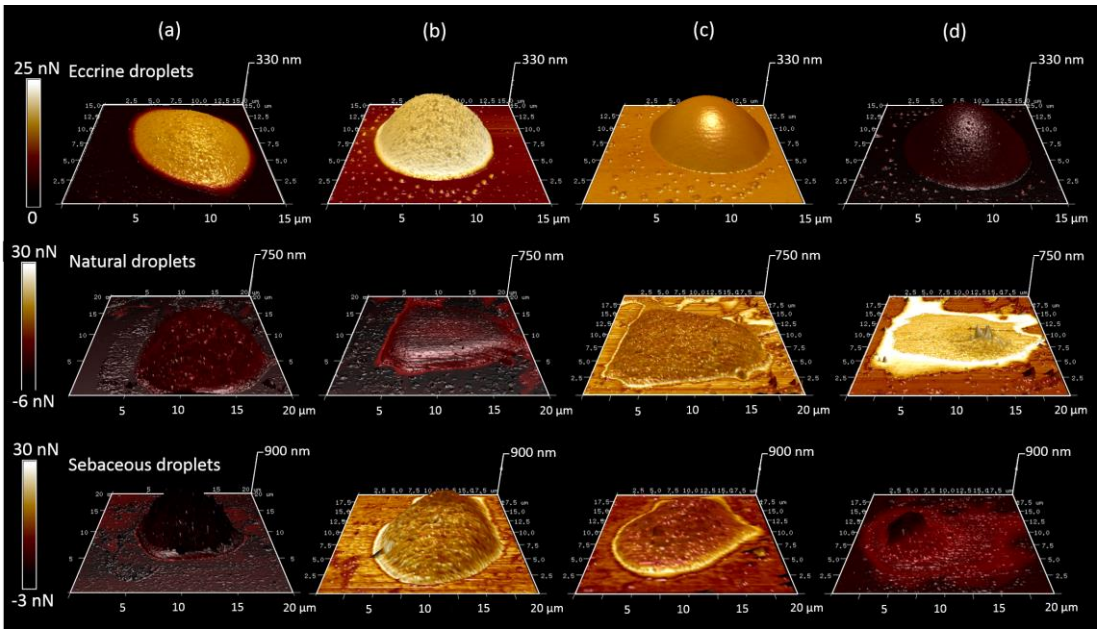

Figure 3.6 Variations in adhesion and topography over time in fingermark droplets from donor D1F1. (a) Fresh, (b) one week old, (c) two week old and (d) four week old. Images (a)-(d) in each type of deposit represent the ageing of the same droplet. The Z axis (height) scale has been set at the same value in all four images in each type of deposit to demonstrate the increase/decrease of height over time.

The height of the droplets of natural fingermark deposits from all three donors diminished with time (Figure 3.6, Figure 3.7, and Figure 3.8), which could be due to the evaporation of volatile constituents from the droplets.[86, 89] Starting from a very low value, the adhesion of sebaceous droplets from donor D1F1 increased significantly after the first week then decreased over time (Figure 3.6). Previous studies into the chemical changes of fingermark deposits over time have reported the breakdown of high molecular weight sebaceous compounds, such as wax esters and triglycerides present in the deposits, to short chain fatty acids[19, 92] that are slightly more hydrophilic. The observed trends in adhesion during the ageing process may be a cumulative result of these chemical transformations and variations in the storage conditions.

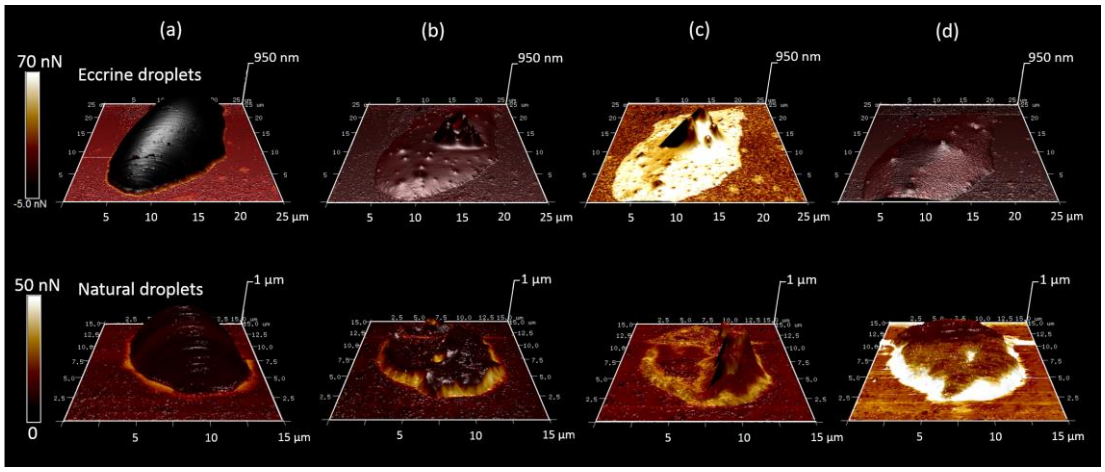

Figure 3.7 Variations in surface adhesion and topography over time in fingermark droplets from donor D2M1. (a) Fresh, (b) one week old, (c) two week old and (d) four week old. Images (a)-(d) in each type of deposit represent the ageing of the same droplet. The Z axis (height) scale has been set at the same value in all four images in each type of deposit to demonstrate the increase/decrease of height over time.

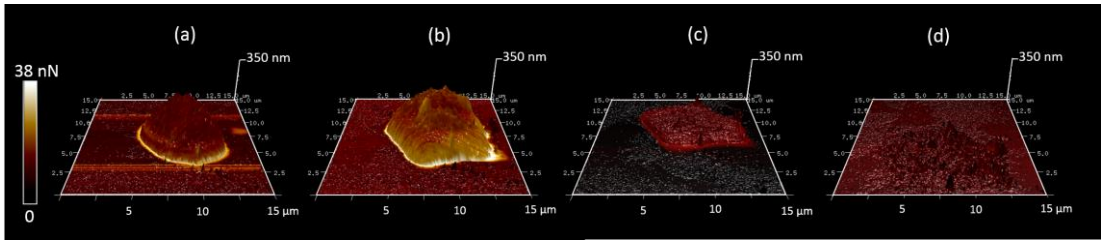

Figure 3.8 Variations in surface adhesion and topography over time in natural fingermark droplets from donor D3M2. (a) Fresh, (b) One week old, (c) Two week old and (d) Four week old. Images (a), (b), (c) and (d) represent the ageing of the same droplet. The Z axis (height) scale has been set at the same value to demonstrate the increase/decrease of height over time.

3.3.4 Topography of fingermark droplets

The height of fingermark droplets was influenced by the donor and the type of the deposit (natural, eccrine or sebaceous). Variation of height was also observed across a deposit (Figure 3.9), which may have been caused by the location of the droplet, as the residue from lower ridge regions is known to have smaller quantities of material.[125]

Surprisingly, both the height and volume of the droplets in the eccrine deposit from donor D1F1 increased after the first week and then remained fairly constant throughout the period of the experiment (see eccrine droplets of Figure 3.6). The escalation in height of eccrine droplets from donor D1F1 could be due to shrinkage of the droplets. This result contradicts observations made by Thomas and Reynoldson where the thickness of the deposit was calculated by using a constant refractive index value across the entire deposit.[29] Conversely, both parameters significantly dropped after the first week in the eccrine deposit from donor D2M1, leaving a residue that appeared to be dried out (see eccrine droplets of Figure 3.7).

Based on these results, providing an average height alone for fingermark droplets is not meaningful due to the inherent variation of fingermark deposits; however, the observations made here may provide support for developing detection techniques of latent fingermarks on non-porous surfaces, which rely on the topographic nature of the deposit. These may include detection techniques that are based on micro- or nanoparticle deposition on the residue[69, 207-208] and optical detection techniques such as Reflected Ultraviolet Imaging System (RUVIS) and side (or oblique) lighting.[209-210]

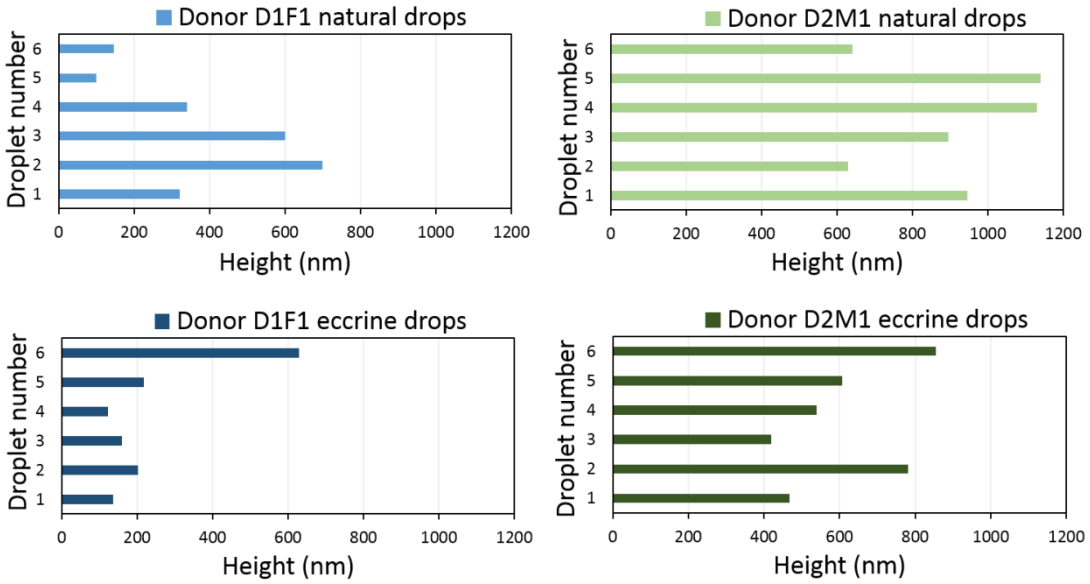

Figure 3.9 Variation in the topography of fresh natural and eccrine fingermark droplets obtained from donors D1F1 and D2M1.

It should be noted here that the topographic images of some of the natural and sebaceous fingermark droplets were distorted in the middle due to the extreme hysteresis of the force curves obtained at those particular pixels.[162] Streaks in the topographic images were observed when a peak force of <5 nN was applied. This effect could be reduced by increasing the force applied on the cantilever >10 nN, but this caused a slight flattening of the droplets, changing their shape. However, even a very small force of 2 nN on aged sebaceous droplets caused deformation. This indicates that the interfacial properties of these droplets dramatically change with time, making their surfaces highly unstable such that they are deformed under tapping by the cantilever tip. Most of the aged eccrine droplets did not display such artefacts during AFM imaging compared to those of natural and sebaceous deposits. They may transform into more solid structures over the ageing process. Comparison of these observations provides further evidence to the fact that the adhesion maps do indeed provide chemically specific information about the sample surface under ambient conditions.

3.3.5 Adhesion in furrows

Another interesting observation was the smaller adhesion value observed at a furrow compared to that measured on a clean glass slide. The areas in-between ridges (furrows) were visible as a clean substrate under the optical microscope attached to AFM. The adhesion between a clean probe and a clean glass slide was initially 48 nN but, after deposition of a natural fingermark on it, the adhesion measured at a furrow was 44 nN 10 min following deposition. This observation suggested presence of a thin layer of chemical components over furrows rendering the area less hydrophilic. Further investigation of this observation using standard Tapping Mode, which allows variations in the physical properties to be captured by phase images, found the freshly cleaved mica surface to be uncontaminated. However, after deposition of a natural fingermark on the mica substrate, propagation of a thin layer of material from the fingermark ridges to the uncontaminated areas of the deposit (furrows) was captured in real-time (Figure 3.10).

This was observed rapidly after deposition (within 10 min) in some parts of the deposit. It has been proposed that this layer is produced by physical contact during deposition,[28] but observations made here suggest that it is instead propagation of a thin film of material across the furrows, starting immediately after deposition and continuing over several hours. The thickness of the layer that was under continuous investigation was 0.2 nm after 2 h, then changed to 1.1 nm and 1.0 nm after 12 h and 23 h respectively following deposition. It was clear that 23 h after deposition, the thin film had propagated across the entire area under investigation (Figure 3.10 d).

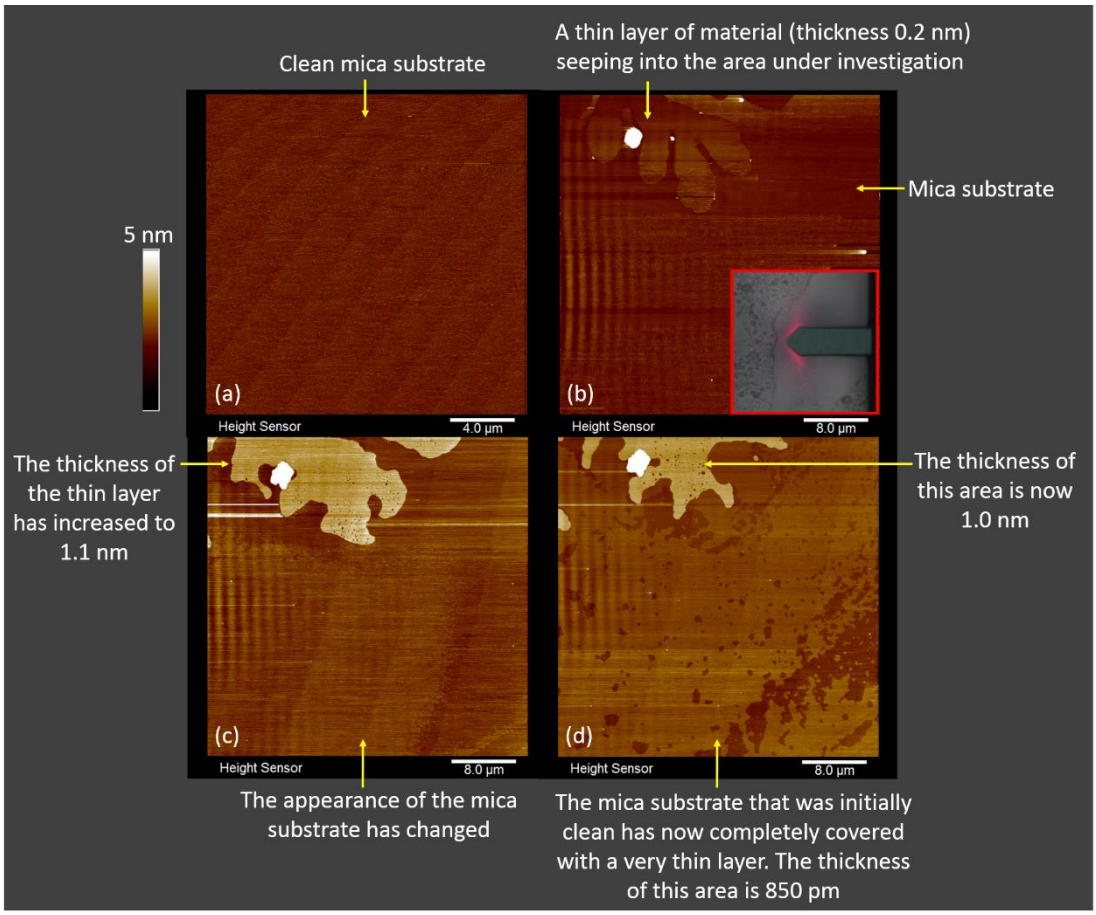

Figure 3.10 Propagation of the thin film of material from the fingermark ridges to furrows captured in real-time by standard Tapping Mode. (a) Clean mica substrate before deposition of fingermark, (b) after 2 h, (c) after 12 h and (d) after 23 h since deposition. The image outlined in red was the area under investigation that appeared to be clean under the optical microscope attached to AFM. The thin film spread to the area under investigation from the top (see the image (b)). Images (c) and (d) show the change in thickness of the film and its deformation.

The drift of developed fingermark ridges on non-porous surfaces over time has been observed on the macroscale by De Alcaraz-Fossoul *et al.* who suggested that this phenomenon can lead to misidentification and misattributions of fingermarks beyond human bias due to dissimilarities produced at the minutiæ level.[147] This observation also supports the findings reported by Muramoto and Sisco, in which the diffusion of lipid molecules in fingermark deposits on non-porous surfaces was observed using time-of-flight secondary ion mass spectrometry.[133] Furthermore, this may explain the observations made by Moret *et al.*, who observed droplets appearing in between fingermark ridges after 24 h since deposition. A similar observation was made in this study under the optical microscope attached to AFM (Figure 3.11). Moret *et al.* assumed the appearance of small droplets in furrows was due to re-deposition of more volatile sebaceous compounds, however, further investigations were recommended.[33]

Recently, electrochemical properties of fingermarks on metallic surfaces were studied by Rosa *et al.* who found that the electrochemical properties were influenced by the reduction of the 'active area' of the metal surface holding the fingermark.[211] Here, the active area is the available surface area not covered by the fingermark deposit.[211] Though the reduction of the surface area was attributed to spreading of the fingermark residue over the substrate, they assumed that spreading is due to evaporation/re-deposition phenomena as suggested by Moret *at. al*.[33] and fingermark ridge drift reported by De Alcaraz-Fossoul *et al*.[147] Observations made in this study, however, strongly suggest that instead of the evaporation/re-deposition phenomena, small droplets appearing in furrows are a consequence of the migration of fingermark components on non-porous surfaces. After the publication of this study, Popov *et al*. reported the same phenomenon by using Tapping Mode AFM on other non-porous surfaces such as Formica and polished silicon.[156] It was reported that the width of the thin film on polished silicon was increased up to 4 µm within the first three weeks and remained constant in the next five weeks.[156]

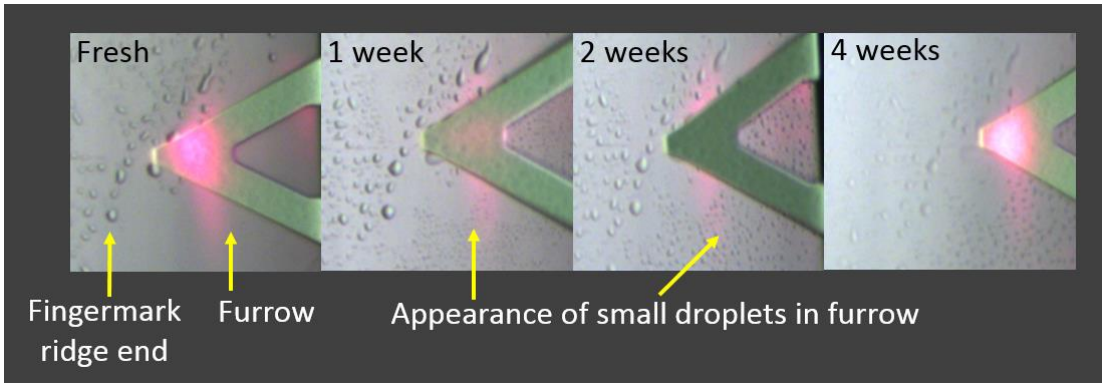

Figure 3.11 Appearance of droplets in between fingermark ridges observed under the optical microscope attached to AFM. The images are from the same area of a sebaceous deposit.

In the study reported by Goddard *et al.*, circular deposits referred to as "spatter" were observed between ridges of an eccrine fingermark on a polished brass surface which was aged for two days in a humid environment at 50 °C.[195] Ageing of eccrine droplets as shown in Figure 3.12 also displays some small structures surrounding the one-week old droplet, which were not present when the droplet was fresh. The diameter of these droplets was approximately 100-400 nm after ageing for one week in the dark while the diameter of the circular droplets observed by Goddard *et al.* was in the range of 5-10 µm. A possible explanation for this discrepancy could be the differences in the storage conditions and the substrates. Even though Goddard *et al.* assumed that the "spatter" is formed during the delivery of the fingermark onto the surface, it could have been caused by the migration of chemical components of the deposit. While Muramoto and Sisco's work demonstrates that

lipid molecules diffuse on non-porous surfaces,[133] it is not clear at this point whether eccrine compounds similarly move on non-porous surfaces.

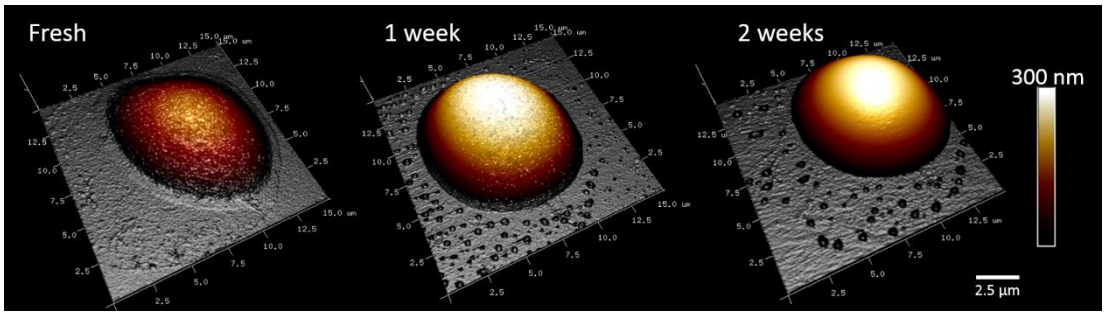

Figure 3.12 Ageing of an eccrine droplet demonstrating the appearance of some small structures surrounding the main droplet after the 1st week. From left to right; 3D topographic images of fresh, one week old and two weeks old droplet. A smear surrounding the fresh droplet is visible which could have formed during transfer of material onto the surface. The Z-axis has been set at the same value (300 nm) for all three images.

This migrating thin layer of material may also contribute to the 'reverse development' (or positive print) and 'empty prints' encountered with some extremely sensitive fingermark detection techniques, e.g. vacuum metal deposition (VMD) and SMD. As described in Chapter 1, these techniques both involve two consecutive depositions of thin films of metal(s) on fingermarks. VMD involves the deposition of thin films of gold followed by zinc on fingermark deposits under vacuum. If the nucleating sites formed by the first gold film are buried at some depth in (i) furrows or (ii) across the entire deposit (including ridges and furrows), the second layer of zinc would not deposit on those areas, resulting in (i) reverse development or (ii) empty prints. The occurrence of reverse development in VMD was discussed by Kent *et al.* who suggested that it is caused by the background substrate absorbing organic constituents from the deposit, leaving a more solid-like inorganic thin residue on the ridges and thus causing development on the ridges.[212] Moreover, Grant *et al.* identified that the type of development (normal or reverse) in VMD was influenced by the surface, where high-density polyethylene displayed the normal development while low-density polyethylene exhibited the reverse development.[213] These disparities could be due to different migration rates of secretions on surfaces with different properties.

Based on the topography of the natural and sebaceous fingermark droplets and the thin film of this study, it can be postulated that the irregular incidence of these phenomena is related to the amount of material deposited. Deposition conditions of incidental contact of fingers with surfaces are subject to high variability, causing some fingermarks to be richer in secretions (greater height of the droplets/ridges).

As a proof-of-concept, it was attempted to measure the physical and chemical properties of droplets and furrows simultaneously by using nanoIR^{TM} (Anasys Instruments, USA) facility located in Monash University, Clayton, Australia. However, aligning the infrared laser was challenging as it should be done on a sample feature hence the infrared laser caused evaporation of the droplets before commencing any measurement. Further efforts could not be carried out due to time constraints.

3.4 Conclusions

For the first time, differences in the adhesion influenced by variations of the distribution of chemical components within latent fingermark droplets were captured by PeakForce quantitative nanomechanical mapping atomic force microscopy. Nanoscale resolution of adhesion and topography suggests that this technique can be effectively employed in detailed investigations of the physical properties of latent fingermark deposits and their variations over time. Furthermore, it was successfully demonstrated that this technique can examine the topography of eccrine deposits, which could not be achieved with other optical microscopy techniques due to the small amount of material in this type of deposits.

While broad trends in physical properties were observed, making firm statements with respect to ageing of droplets was challenging due to following reasons: (i) the chemical composition of the analysed droplets was not accurately known; (ii) limited number of droplets analysed due to limitations of facilities; (iii) inter-donor variation; and (iv) subtle changes in the storage conditions. However, the negative values of adhesion detected in some eccrine droplets suggest that these droplets may consist of non-polar constituents. The distinct differences of adhesion observed within natural fingermark droplets may have been caused by the distribution of compounds within droplets based on their polarity. In addition, relatively high surface interactions displayed by natural droplets, even after four weeks of ageing, is promising for the development of novel fingermark detection techniques. However, chemical imaging of fingermark droplets at the sub-micron or nanoscale is necessary to interpret conflicting physical measurements and identify chemical entities responsible for stronger adhesion.

Nonetheless, this physical investigation has offered indirect but vital insights into the fingermark composition, complex distribution of chemical species within droplets, and a rational explanation for the inconsistent performance of certain fingermark detection techniques. Such knowledge is critical to mitigate these drawbacks and enhance their performance, or for the formulation of advanced novel techniques.

Observed propagation of the thin film from ridges to furrows at the sub-nanometer level, starting immediately after deposition, establishes that on non-porous surfaces, the fingermark deposits are extremely spatially dynamic in nature. This provides robust evidence to prove that the appearance of small droplets in furrows over time is caused by the migration of fingermark components on non-porous surfaces rather than the re-deposition of volatile components as suggested by recent investigations. Although this process initiates at the nanoscale, as the fingermark ages, it influences the spatial integrity of fingermark ridges at the microscale. Since this may have a significant impact on fingermark development, especially with proposed sensitive techniques, further research is necessary to investigate the extent of migration on common non-porous substrates at crime scenes and consequently the reliability of fingermark development with those techniques for personal identification.

Chapter 4: Revealing the spatial distribution of chemical species within latent fingermarks using vibrational spectroscopy

---

Portions of this research have been published in the journal *Analyst:*

Dorakumbura, B. N.; Boseley, R. E.; Becker, T.; Martin D. E.; Richter, A.; Tobin, M. J.; van Bronswijk, W.; Vongsvivut, J.; Hackett, M. J.; Lewis, S.W. Revealing the spatial distribution of chemical species within latent fingermarks using vibrational spectroscopy. *Analyst* **2018**.

DOI: 10.1039/C7AN01615H

Part of this research was undertaken on the infrared spectroscopy beamline at the Australian Synchrotron, part of ANSTO.

4.1 Introduction

As demonstrated in the previous chapter, studying the physical properties of fingermarks can be confusing without the knowledge of the chemical composition, more specifically, the distribution of chemical species across the deposit. Although the previous study strongly indicated that the physical measurements were influenced by the chemical composition, variation of the adhesion across individual droplets as well as negative values of adhesion exhibited by some of the eccrine droplets could not be explicitly explained with the absence of chemical measurements. Four decades ago, Thomas emphasised the importance of knowledge of the spatial distribution of fingermark components to understand and interpret any physical measurements made upon latent fingermark deposits.[26]

Among reported studies into fingermark composition, a few have shown that the distribution of endogenous fingermark components is heterogeneous across the deposit; however, the distribution within individual droplets is not well researched.[14, 23, 108] Research devoted to fingermark detection has emphasised the significance of such information to understanding mechanisms of current techniques and to improve their performance.[61-62] This paucity is mainly because fingermark composition is often characterised by destructive, bulk measurement techniques such as gas chromatography-mass spectrometry (GC-MS) and liquid chromatography-mass spectrometry (LC-MS).[16, 19-20, 90-91] While they have provided important insight into time-course chemical alterations that occur in fingermarks following deposition, bulk methods do not reveal spatial distribution.

In this context, a greater characterisation of the spatial distribution of endogenous chemical species of a fingermark deposit is required. Non-destructive, direct chemical imaging techniques hold great potential in this respect.

4.1.1 Vibrational spectroscopy studies of fingermark composition

Vibrational spectroscopy techniques such as Fourier transform infrared (FTIR) and Raman spectroscopy has become increasingly popular to probe fingermark chemical composition due to their non-destructive nature and the ability to directly image (map) chemical components at the micron scale. While other techniques such as matrix-assisted laser desorption ionisation-mass spectral imaging (MALDI-MSI) are more sensitive and may offer greater chemical specificity,[6, 98] FTIR and Raman provide superior spatial resolution. This is essential to study the distribution of a complex mixture of compounds with different hydrophilic/hydrophobic characteristics, such as fingermark residues. FTIR spectroscopy, in particular, has been used frequently in fingermark research to detect fingermarks on

different substrates, deduce donor traits such as age and gender and to estimate the time since deposition.[14, 22-23, 86, 89, 131, 149, 167]

The first reported study into fingermark composition and imaging using FTIR was by Bartick *et al*., where compositional differences between children's and adults' fingermarks were examined.[131] Following this work, a few studies later found that children's deposits have a higher amount of carboxylic acid salts, proteins, and esters; while adults' deposits are primarily composed of high molecular weight wax esters and fatty acids.[14, 22, 167] Due to the longevity of acid salts in the fingermark residue over time, one study suggested that they should be targeted to detect children's fingermarks instead of targeting the esters and proteins.[22] Ricci *et al.* demonstrated the advantages of using attenuated total reflectance-Fourier transform infrared (ATR-FTIR) spectroscopy for chemical imaging of fingermarks, which revealed chemical and spatial information of primarily sebaceous components.[23] Owing to the non-invasive nature of FTIR, they studied the compositional variation of fingermarks *in-situ* under controlled environmental conditions.[23] It was found that main spectral features such as CH_2 and C=O stretching and CH_2 scissoring modes corresponding to esters and fatty acids were similar, while the relative secreted amount of them varied significantly among various donors.[23] Both protein and lipid material were identified in the spectra extracted with a spatial resolution of approximately 50 μm.[23] By monitoring the same spot over several hours, degradation of esters and urea with increasing temperature was also studied.[23] Antoine *et al*. reported that the three main components of fingermarks, namely skin debris, sebum, and sweat were distinguishable even with light microscopy. Chemical discrimination of them was made based on the amide, ester, and carboxylic acid peaks respectively in the IR spectra.[14]

Studies have also attempted probing the donor characteristics and age estimation of fingermarks using FTIR.[86, 89, 214] Though Hemmila *et al.* identified few spectral regions of IR spectra which were claimed to enable discrimination of subjects in the later stages of puberty from the younger and older age groups,[214] Fritz *et al*. later found no characteristic spectral difference in the lipid composition as a function of donor's age or gender.[89] More recently, Girod *et al*. identified spectral regions 1000-1850 cm^{-1} and 2700-3600 cm^{-1} as the most informative regions for the dating of fingermarks.[86] Based on these conflicting research outcomes it is unclear at the moment whether FTIR is indeed capable of predicting donor characteristics or the age of a deposit.

Although modern globar-sourced FTIR spectrometers can be operated at a spatial resolution as small as 10 µm[140] or even smaller,[215] acquiring quality spectra with high spatial and spectral resolution (<10 µm, 4 cm^{-1}) on thin samples such as fingermarks can be time-consuming.[89] This could be cumbersome when large areas are to be analysed. Fritz *et al.* demonstrated several advantages of using synchrotron sourced FTIR microscopy for the analysis of fingermarks, such as enhanced spatial resolution and signal-to-noise ratio and subsequent reduced spectral acquisition times compared with conventional IR sources.[89]

In contrast to the widespread utility of FTIR, Raman spectroscopy has been little used in the analysis of fingermark composition. However, Raman spectroscopy including surface-enhanced Raman spectroscopy have successfully been applied for chemical imaging of latent fingermark ridge details and to detect contaminants such as illicit drugs and explosive residue,[105, 150, 155, 216] but it has not been used to studying the fundamental chemical characteristics of fingermark deposits until very recently. A proof-of-concept study on dating fingermarks using Raman spectroscopy was contemporaneously published in the final stage of this thesis.[154]

Raman spectroscopy offers better spatial resolution compared to FTIR when operated at wavelengths of visible range. Both FTIR and Raman techniques are complementary to each other. FTIR detects changes in the dipole moment of molecules as they absorb radiation[165] while Raman detects changes in the polarizability of the molecules.[170] Generally, vibrations that are strong in an FTIR spectrum are weak in a Raman spectrum and vice versa.[171, 217] Therefore, they can be used in tandem to gather a more complete spectrum of samples.

4.1.2 Aims

This chapter aimed at studying the relative abundance and distribution of eccrine and sebaceous material in latent fingermarks deposited on non-porous surfaces. Both FTIR microscopy and confocal Raman microscopy were employed to probe the possible heterogeneous distribution of lipids and eccrine material within fingermark droplets and also across the ridges at the sub-micron scale. The findings of this study were used as a guide to interpreting inconclusive observations made in Chapter 3 (AFM study).

4.2 Experimental

4.2.1 Sample deposition

Demographics of the donors and the type of the deposits used are listed in Chapter 2. Donors gently pressed their index fingers down for 10 seconds on the non-porous substrates. Except for aluminium foil, all other substrates were pre-cleaned with ethanol. Zinc selenide (ZnSe) plates and hemispheres (Crystran Ltd., UK), calcium fluoride slides (Crystran Ltd., UK), glass microscope slides (Mikro-Glass, Australia), low-e microscope slides (Kevley Technologies) and commercial aluminium foil (heavy duty catering foil, Confoil, Australia) were used as non-porous substrates for FTIR studies. Glass cover slides (22 mm × 22 mm, Deckgläser, Germany) was used for the Raman study. For time-course experiments using confocal Raman microscopy, a small cross mark was engraved on the glass slide prior to cleaning as a reference mark. Donors were asked to place their fingers centring the engraved mark. At least six randomly selected droplets with different shapes and appearance from four areas of the deposit (top two corners and bottom two corners from the centre of the cross) were analysed.

Two attempts were carried out during the synchrotron-sourced ATR analysis to achieve the smallest possible spatial resolution (Figure 4.1). In the first attempt, a natural fingermark was deposited on a ZnSe plate (0.5 mm thickness), then it was flipped over and placed over the hole of the base window. A small amount of the coupling fluid (n-Hexadecane-d_{34}, 98%, Cambridge isotope laboratories) was applied over the other side and the flat face of a ZnSe hemisphere (radius of curvature 6.5 mm) carefully placed over it. In the second attempt, another natural fingermark was deposited on the face of a ZnSe hemisphere (radius of curvature 7 mm) then it was carefully flipped over and placed over the hole of the interchangeable base window so that the sample was facing down.

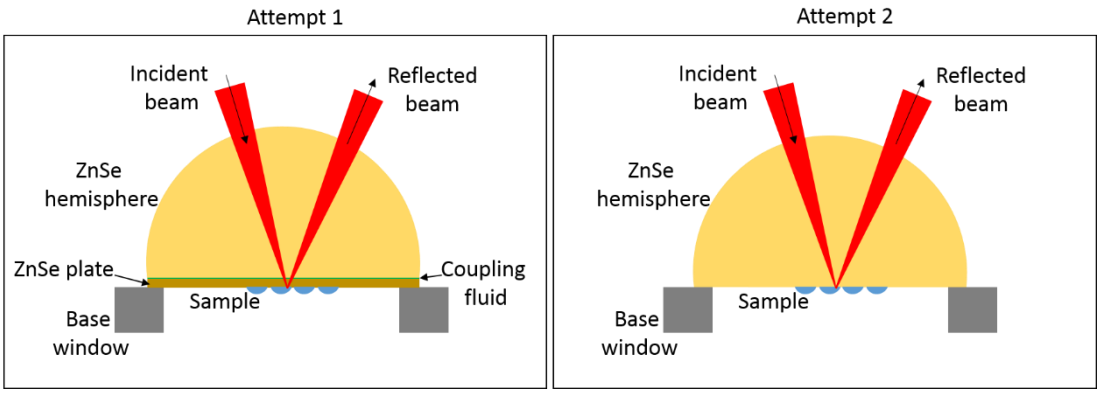

Figure 4.1 Schematic of synchrotron-sourced ATR-IRE experimental setups.

A natural fingermark was simply deposited on a clean ZnSe plate for the transmission mode. Half of the plate/hemisphere was covered with a clean and dust free paper in all cases before deposition to have an uncontaminated background for subsequent analysis.

4.2.2 Benchtop globar-sourced FTIR studies

In the preliminary investigation of potential chemical heterogeneity within droplets, small regions (10 µm × 10 µm) of natural fresh fingermarks deposited on a low-e microscope slide and a zinc selenide slide were analysed in reflection and transmission modes respectively. The FTIR microscope was a Thermo Scientific Nicolet iN10 MX FTIR microscope, coupled to a liquid nitrogen cooled narrow band Mercury Cadmium Telluride (MCT) detector. The sample chamber was purged with dry nitrogen to reduce the contribution of atmospheric water vapour and CO_2. All spectra were acquired with a 4 cm^{-1} spectral resolution and 256 scans.

4.2.3 Synchrotron-sourced FTIR studies

The synchrotron infrared beamline at Australian Synchrotron, Clayton, Victoria consists of a Bruker Vertex V80v FTIR spectrometer, a Bruker Hyperion 2000 microscope with a motorised sample stage (Bruker Optik GmbH, Ettlingen, Germany) and a liquid nitrogen cooled narrow band MCT detector. A 36× (0.5 numerical aperture; NA) was used for both modes of analysis while a matching condenser was used for transmission mode analysis. Both the spectrometer and microscope were continuously purged with dry nitrogen to reduce the spectral contribution of water vapour and CO_2.

The synchrotron beam was focused on the ZnSe substrate, with a beam size of approximately 10 µm diameter (wavelength dependent). The Hyperion microscope utilises pinholes with different sizes (0.25, 0.42, 0.60, and 0.75 mm) to further refine the sampling area from which spectra are recorded. The 0.25 mm pinhole was used in all experiments to obtain the highest possible spatial resolution. In attenuated total reflectance-internal reflection element (ATR-IRE) experiments, the focused synchrotron beam onto the curved face of the hemisphere was further condensed as it transmitted through the hemisphere (refractive index 2.4) which offered a measurement area on the sample of 3 µm diameter. The beam passed straight through the sample in transmission mode thus, offered a 6.9 µm diameter measurement area on the sample.

4.2.4 Confocal Raman imaging

Confocal Raman imaging was performed using a confocal Raman microscope (alpha 300R, WITec, Ulm, Germany) equipped with a frequency doubled Nd: YAG laser (532 nm) and a piezo scanner operated under the following settings: 100× objective, NA 0.9. The spectra were acquired with a thermoelectrically cooled CCD detector placed behind the spectrometer at a spectral resolution of 3 cm^{-1}. The spectrometer and the detector were optimised prior to analysis using the Raman band of a silicon wafer at 520 cm^{-1}. The WITec Control FOUR software was used for data acquisition. Raman images along X-Y and X-Z axes were acquired with 0.1 s integration time per pixel (250 nm × 250 nm) unless stated otherwise. The manufacturer claimed depth resolution was approximately 750 nm.

4.2.5 Data analysis

All raw IR spectra were baseline corrected and analysed using Bruker OPUS v7.2 software.

WITec Project FOUR 4.1 software was used for Raman spectral processing. After performing a smoothing for cosmic ray removal, the background was removed by subtracting a polynomial fit to raw spectra.

4.3 Results and discussion

4.3.1 Benchtop FTIR studies

The primary objective of this study was to image fingermark droplets with the smallest possible spatial resolution to probe differences in the chemical composition. Conventional FTIR spectra acquired over 256 scans with 10 µm spatial resolution displayed a very poor signal-to-noise ratio which demonstrated the need for the much brighter and higher intensity synchrotron source.

4.3.2 Synchrotron-sourced FTIR studies

4.3.2.1 ATR-IRE experiments

The ZnSe hemisphere was utilised as an internal reflection element which condenses the synchrotron beam further by a factor of 2.4 (refractive index of ZnSe), resulting in an improved spatial resolution. The technique of coupling a ZnSe hemisphere with ZnSe plate works similar to traditional ATR-IRE mapping using hemispheres, but the use of an optical coupling fluid of high refractive index allows the beam to travel through the hemisphere, the fluid and finally to the base of the plate where the sample was deposited. Peaks arising due to the deuterated coupling fluid do not interfere with the peaks for typical biological samples. The advantage of this method over the traditional hemispherical technique is that instead of

depositing fingermarks on the base of the hemispheres, requiring several hemispheres for different samples, it permits depositing samples upon a series of interchangeable ZnSe plates, which are comparatively cheaper than hemispheres.

As the path length of the IR beam through the sample is much smaller in ATR-IRE experiments, it resulted in spectra with poor signal-to-noise ratio relative to transmission mode (Figure 4.2). In addition, aligning the IR beam on top of the hemisphere was time-consuming and cumbersome. Due to these reasons, synchrotron-sourced transmission mode was used in further investigations.

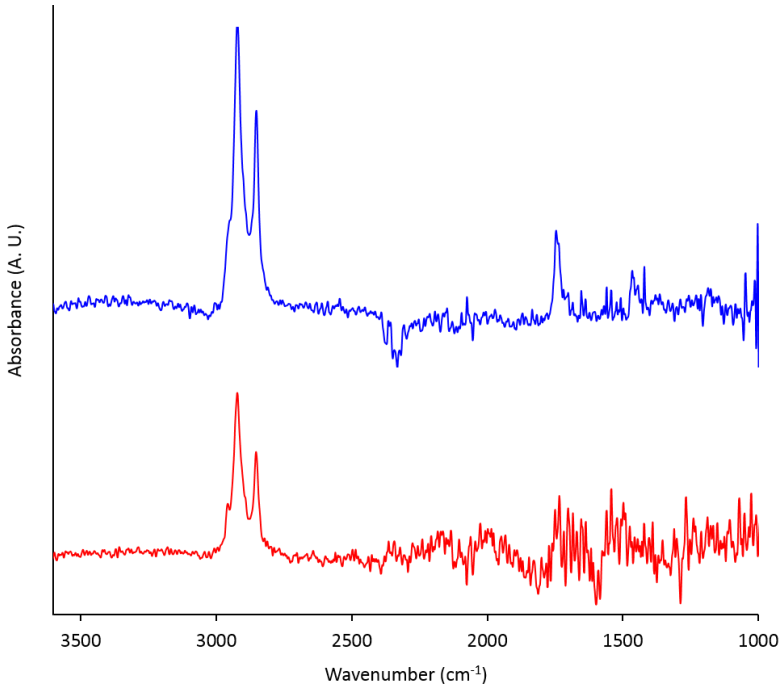

Figure 4.2 Comparison of synchrotron-sourced FTIR spectra of natural fingermarks acquired using transmission (blue) and ATR-IRE (red) modes. Spectra are scaled to the same y-axis. Instrument parameters: 36× objective, 0.25 mm pinhole, 4 cm^{-1} spectral resolution, number of scans 128.

4.3.2.2 Transmission mode experiments

Individual droplets of natural and eccrine fingermark deposits on ZnSe plates were imaged at a 2.5 µm step size using the 0.25 mm pinhole, which offered a 6.9 µm diameter measurement area on the sample. Natural fingermark droplets investigated from both donors D1F1 and D4M3 (11 droplets in total) displayed vibrational bands which are characteristic to lipids only (Figure 4.3, top) and the peak positions were consistent with the literature.[14, 89, 131, 149, 167] The most prominent bands amongst them were C-H stretching bands centred around 2900 cm^{-1}, C=O stretching bands near 1745 cm^{-1} and 1708 cm^{-1}, CH_3 asymmetric bending near 1465 cm^{-1} and CH_3 symmetric bending near 1375 cm^{-1} (see Table 4.1 for band assignment).

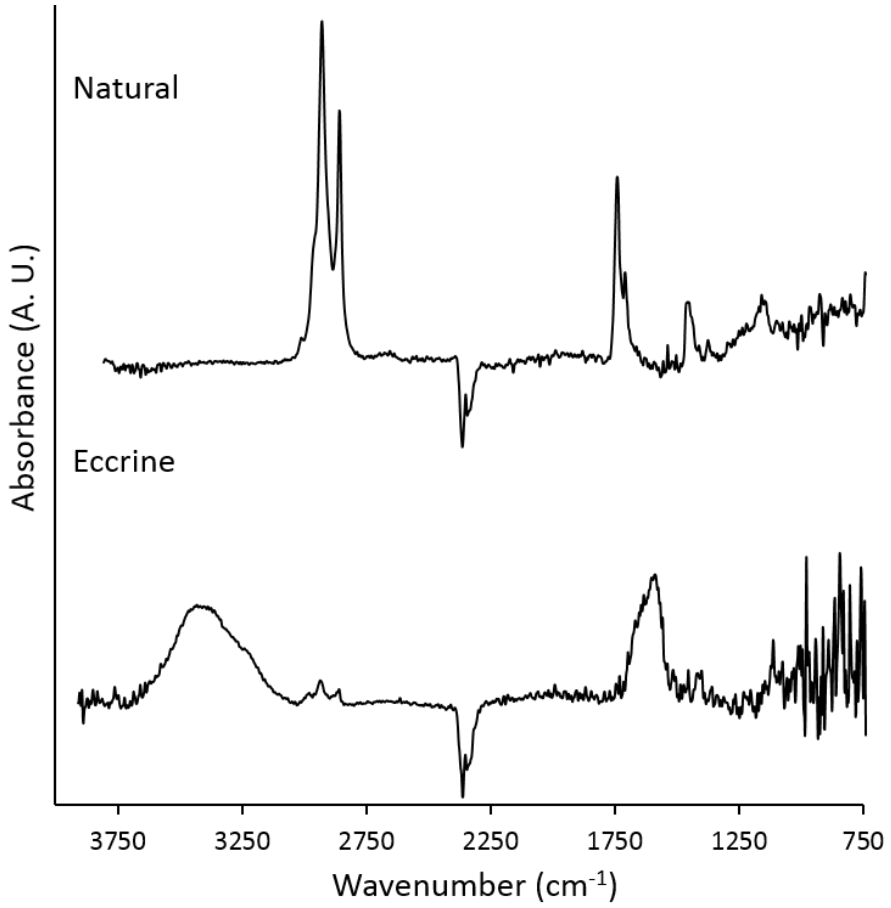

Figure 4.3 Comparison of synchrotron sourced FTIR spectra obtained from a natural deposit (top) and an eccrine deposit (bottom). Spectra are scaled to the same y-axis. Instrument parameters: 36× objective, 0.25 mm pinhole, 4 cm^{-1} spectral resolution, number of scans 128.

Table 4.1 Tentative assignment of FTIR bands observed in glandular secretions of fingermarks.

Wavenumber (cm^{-1})	Band assignment	Putative Chemical Origin	Source
1375	CH_3 symmetric bend	Aliphatic carbon chains	Eccrine and sebaceous
1464	CH_2 symmetric bend	Aliphatic carbon chains	Sebaceous
1540-1700	O-H bend/ N-H bend	Water, lactic acid or urea	Eccrine
1500-1700 (two peaks, 1650 and 1550)	Amide I & Amide II	Protein	Skin Debris
1712	C=O stretch in different environment	Saturated esters	Sebaceous
1745	C=O stretch	Saturated esters	Sebaceous
2854	CH_2 symmetric stretch	Long aliphatic carbon chains	Sebaceous
2927	CH_3 symmetric stretch	Long aliphatic carbon chains	Eccrine and sebaceous
2955	CH_3 asymmetric stretch (sh)	Fatty acids, glycerides and wax esters	Sebaceous
2980	CH_3 stretching	Aliphatic carbon chains	Eccrine
3009	Unsaturated =CH stretch	Squalene, unsaturated fatty acids, glycerides and wax esters	Sebaceous
~3400	O-H stretch	Water	Eccrine

Since some vibrational bands attributed to eccrine secretions were reported in the literature,[86] but not identified in any of the natural droplets in this study, an eccrine deposit obtained from donor D3M2 was imaged with the same instrumental setup. The spectra displayed two broad vibrational bands (Figure 4.3, Eccrine). The broad band from ~3000-3600 cm^{-1} was attributed to O-H stretching. Another prominent band was centred at 1600 cm^{-1} (from 1540-1720 cm^{-1}). Since any other bands were not prominent in this spectrum (Figure 4.3, Eccrine), this band was tentatively attributed to O-H bending. However, this peak is not quite symmetric, as it would be with O-H bending, and since the peak around 3400 cm^{-1} is broad, there could be few underlying components. FTIR spectroscopic bands centred at 1600 and 3400 cm^{-1} have been previously assigned to eccrine components such as urea[23] and lactic acid respectively.[14]

In the µATR-FTIR study reported by Girod *et al*., some IR bands due to eccrine secretions (intense N-H stretching at 3928 cm^{-1}, amide I, II, and III bands) were detected in charged deposits; however, those bands were not consistently observed in all fresh fingermarks.[86] Moreover, they could not detect any eccrine bands using the reflection mode. To further investigate this irregular occurrence of eccrine bands, especially the N-H stretching band, a natural fingermark was deposited on aluminium foil and spectra were acquired using conventional µATR-FTIR on skin debris and secretions. Observed spectral differences of skin debris and glandular secretions are shown in Figure 4.4 Although both N-H and O-H stretching bands are broad and fall in the same wavenumber range, the N-H stretching can be distinguished since it has a sharp peak at the midst of the broad peak due to one conformation of hydrogen bonding having a preferential formation.[166] In fact, other previous studies have reported the N-H stretching band as originating from skin debris rather than skin secretions.[14, 89, 167] Therefore, it was concluded that irrespective to the acquisition mode, possible N-H stretching band around 3300 cm^{-1} is not prominent in the IR spectra of glandular secretions of fingermarks, and cannot be used to discriminate eccrine secretions.

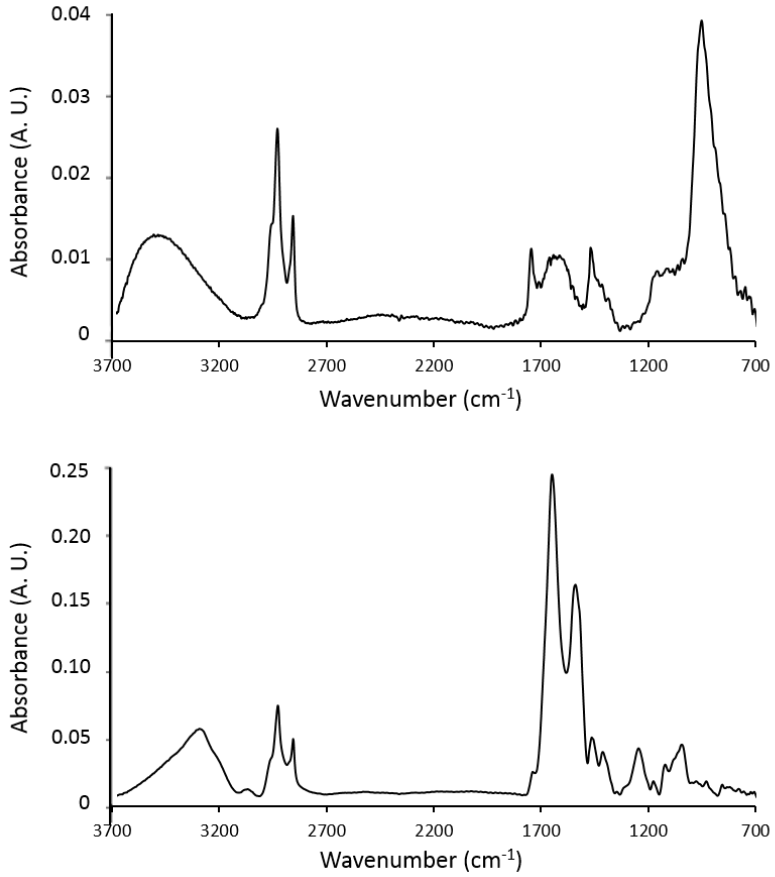

Figure 4.4 Globar-sourced µATR-FTIR spectra acquired with 100 µm × 100 µm aperture on glandular secretions (top) and on skin debris (bottom) of a fingermark deposited on aluminium foil. Number of scans 256 and spectral resolution 4 cm^{-1}.

As discussed above, a possible explanation for discrepancies in the literature is the difference in sampling area/volume used in different investigations and the heterogeneous composition of fingermarks. For example, sampling of large regions of fingermarks at "coarse" spatial resolution (i. e. >5 µm) may result in spectral blending and failure to identify chemical components only found in discrete sub-micron regions of a fingermark. Unfortunately, the time constraints associated with imaging/mapping large regions of a fingermark at high spatial resolution often drive experimental designs incorporating under-sampling of a fingermark, which increases the chance of missing chemical differences observed in micron or sub-micron regions of a deposit. Thus, failure to detect any eccrine bands in natural fingermarks in this study was due to the absence of eccrine material in those droplets and not related to the acquisition mode.

4.3.3 Confocal Raman microscopy studies

4.3.3.1 Raman spectra of proteins and lipids

Aside from the report published contemporaneously at the last stage of this thesis, investigation of fingermark composition using Raman spectroscopy had not been attempted before.[154] Nonetheless, this technique has found its widespread application in chemical imaging of biological samples, even living cells, owing to its non-invasive nature and improved spatial resolution.[218-221] Estimated by the Rayleigh criterion, the confocal Raman microscope utilised in this study has a spatial resolution of approximately 250 nm when operated with the 532 nm laser excitation and 100×, NA 0.9 objective.

The majority of Raman bands in the "fingerprint region" (~500 to ~1700 cm^{-1}) of proteins and lipids derive from CH, CH_2, and CH_3 deformation bands, which are not diagnostic of structural features. However, amide l and lll bands and bands due to S-S bonds and aromatic rings can be used to elucidate structural features of proteins. Diagnostic Raman bands of lipid molecules arise mainly due to the C=O and C=C functional groups. Nonetheless, these diagnostic bands can overlap when proteins and lipids occur in a mixture, especially as a liquid mixture since Raman bands can be broadened in the liquid state.[222] For example, the amide I band at 1652 cm^{-1} can overlap with lipid C=C stretch vibration band at 1660 cm^{-1} and CH_2 deformation band of proteins at 1450 cm^{-1} with that of lipids at 1440 cm^{-1}.

Unlike in FTIR spectra, the vibrational band due to the C=O functional groups in lipids (occurs near 1745 cm^{-1}) is rather weak in Raman spectra,[223] which makes differentiating lipids and proteins in a complex mixture such as fingermarks further challenging. However, different concentrations of proteins and lipids can be revealed indirectly by the spectral

profiles of CH stretching vibration bands in the interval from 2800-3100 cm^{-1}.[224] The highly overlapped band in this region comprises six possible CH stretching bands as listed in Table 4.2.[225] As CH_2 groups are more abundant in lipid molecules than in proteins, they display intense CH_2 stretching bands while these bands are less prominent in proteins (Figure 4.5). Further intuitions can be gathered by examining the peak positions of CH_2 deformation bands of proteins and of lipids near 1440 cm^{-1}.[224] These bands shift in between 1440-1460 cm^{-1} depending on the lipid to protein ratio of the mixture (Figure 4.5).

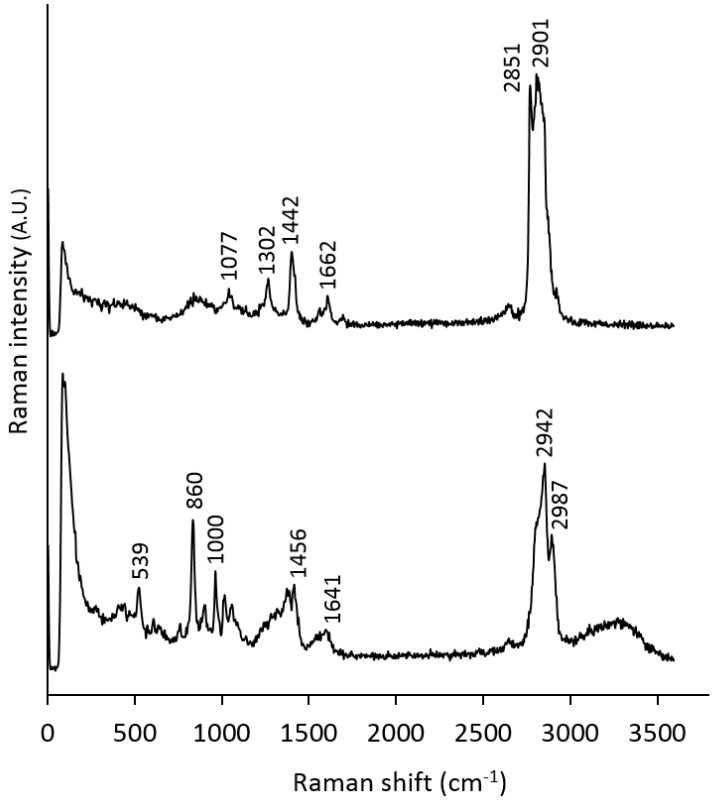

Figure 4.5 Comparison of Raman spectra of sebaceous (top) and eccrine secretions (bottom). Spectra are scaled to the same y-axis.

4.3.3.2 Raman spectra of fresh eccrine fingermark deposits

Compounds of eccrine origin that have been identified in fingermarks include more than 20 amino acids, proteins, salts, lactic acid, uric acid, choline, vitamins and creatinine.[15] Therefore, Raman spectra of eccrine deposits can be generally treated as complex spectra of a mixture of several amino acids/proteins. In the "fingerprint region" of the spectrum, frequently encountered Raman bands are 861, 1000, 1458 and 1652 cm^{-1} (see Table 4.2 for band assignment). The only main band observed in the region from 1700 to 2700 cm^{-1} for natural amino acids and proteins is the thiol S-H stretching observed from 2560 to 2590 cm^{-1};[226] however, this band was not present in any of the spectra. From 2850 to 3000 cm^{-1}, the highly overlapped group of bands make up the most intense bands in

the spectra. Although liquid water is a rather weak Raman scatterer, the broad peak observed around 3330 cm^{-1} was attributed to O-H stretching arising from water and/or lactic acid in the deposit.

Table 4.2 Tentative assignment of Raman bands observed in skin secretions of fingermark deposits.[222, 224-233]

Wavenumber (cm^{-1})	Band assignment	Putative Chemical Origin	Source
539	S-S stretching	Sulphur containing amino acids and proteins	Eccrine
773	Ring breathing	Phenylalanine	Eccrine
861	*para*-substituted ring vibration	Tyrosine	Eccrine
929	C-C_α	Protein backbone	Eccrine
1000	Ring breathing	Phenylalanine	Eccrine
1045	Ring deformation	Phenylalanine	Eccrine
1080	C-C stretching	Aliphatic carbon chains	Sebaceous
1091	O-P-O symmetric stretching	Nucleic acid backbone	Membrane lipids
1127	C-C stretching	Aliphatic carbon chains	Sebaceous
1173	C-C stretching	Aliphatic carbon chains	Sebaceous
1265	=CH deformation	Squalene, unsaturated fatty acids, glycerides and wax esters	Sebaceous
1300	CH_2 twisting	Aliphatic carbon chains	Sebaceous
1300	Amide lll	Amino acids and proteins	Eccrine
1360	CH_2 deformation	Aliphatic carbon chains	Eccrine
1426	Ring stretching	Indole	Eccrine
1440	CH_2 and CH_3 deformation	Aliphatic carbon chains	Sebaceous
1457	CH_2 and CH_3 deformation	Aliphatic carbon chains	Sebaceous
1605	Ring C=C stretching	Histidine	Exogenous
1638	C=C symmetric stretching	Squalene, unsaturated fatty acids, glycerides and wax esters	Sebaceous
1652	Amide l	Amino acids and proteins	Eccrine

1660	C=C symmetric stretching	Squalene, unsaturated fatty acids, glycerides and wax esters	Sebaceous
1719	C=O stretching	Aldehydes	Sebaceous
1745	C=O stretching	Esters	Sebaceous
2725	Aliphatic CH stretching	Amino acids and proteins	Eccrine and sebaceous
2855	CH_2 symmetric stretching	Fatty acids and waxes	Sebaceous
2885	Fermi-resonance CH_2 stretching	Fatty Acids and waxes	Sebaceous
2903	CH_2 asymmetric stretching	Fatty acids and waxes	Sebaceous
2930	Chain-end CH_3 symmetric stretching	Amino acids and proteins	Eccrine and sebaceous
2959	Chain-end CH_3 asymmetric stretching	Amino acids, proteins and aliphatic side-chains	Eccrine and sebaceous
3010	Unsaturated =CH stretching	Squalene, unsaturated fatty acids, glycerides and wax esters	Sebaceous
3330	O-H stretching	Water	Eccrine

As mentioned in Chapter 1, the human friction ridge skin of palms and fingers are free from sebaceous glands. Few medical studies have reported detection of cholesterol (mean 0.04 µg/mL) and free fatty acids (mean 0.04 µg/mL) in minute quantities in "clean eccrine sweat", bulk sampled from the back and the chest areas of the skin.[96-97] Figure 4.6 shows averaged Raman spectra of two components identified in an eccrine droplet where the spectrum at top resembles lipids and the bottom one resembles aqueous components (eccrine material). The composite map in Figure 4.6 (c) along with depth-profile in Figure 4.6 (d) suggests that when lipids occur in minute quantities in eccrine fingermark droplets, they tend to form emulsion droplets of oils in the aqueous matrix. The centre of the droplet in Figure 4.6 (a) is thought to be a small crystal of salt as no Raman bands were observed in that region other than very weak CH stretching bands.

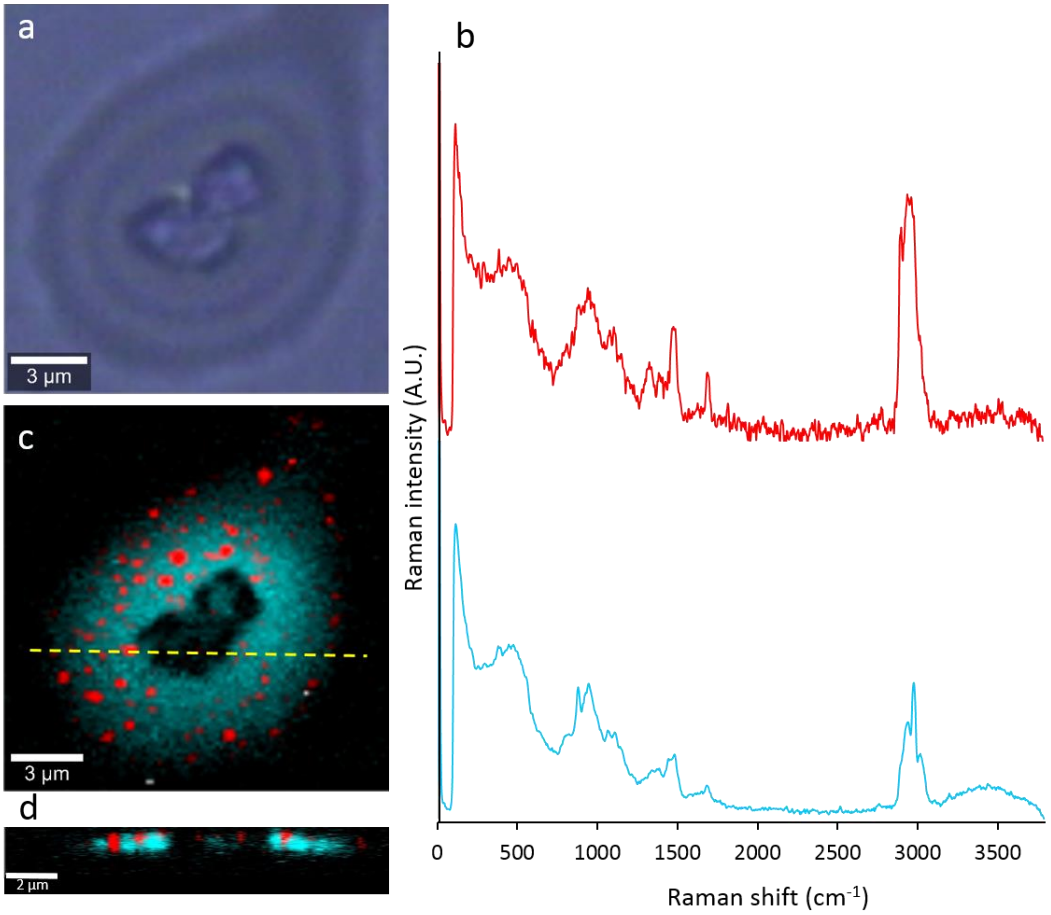

Figure 4.6 Bright-field optical image of a droplet from an eccrine deposit from donor D2M1 (a), averaged Raman spectra of the two components identified in the droplet (b) and its composite distribution map showing the distribution of the two components (c). Depth-profile of the droplet along the yellow colour dashed line (d). X-Z scan range of the depth-profile was 15 µm × 2 µm at a pixel resolution of 100 × 100. Spectra are scaled to the same y-axis.

This result, along with the complete prevalence of lipids in some of the small eccrine droplets (~1-5 µm in diameter), indicates that the occurrence of lipids in eccrine deposits must be taken into account when undertaking method development of fingermark detection techniques and elucidating their mechanisms. Eccrine deposits obtained as outlined in this paper are used in fingermark research[167, 186, 196, 234-235] primarily to understand which type of chemical components of the deposit (amino acids or lipids) react with the reagent. This process has been confusing at times due to the partial understanding of the eccrine deposit. Figure 4.7 shows an eccrine fingermark deposited on paper, developed with a lipid sensitive reagent, Oil red O.[65] This conflicting development can be attributed to the occurrence of lipids in "eccrine deposits".

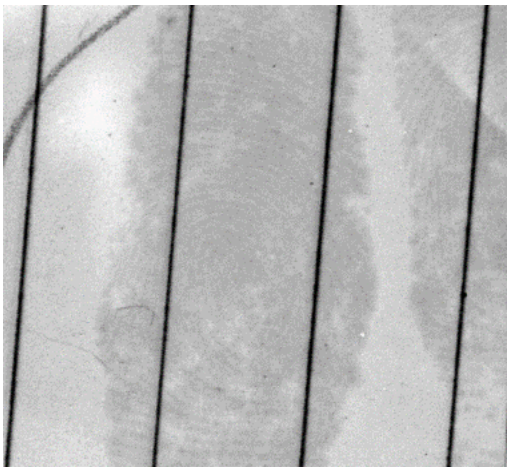

Figure 4.7 An eccrine fingermark on paper developed with Oil Red O (the colour and the contrast of the image were adjusted using Adobe Photoshop CC software to enhance the ridge details). Image courtesy Talia Newland.[236]

Wei *et al*. recently reported a latent fingermark development technique that makes use of the "hydrophobic nature" of the deposit where a hydrophilic dye selectively binds to the bare cellulose membrane, which the fingermark deposit was transferred onto, enhancing the contrast between furrows and ridges.[186] They reported that the technique offered satisfactory results even with eccrine fingermarks, which are thought to be hydrophilic deposits. This contradicts the proposed mechanism of the technique; however, based on our findings, this development is not unexpected.

Ferguson *et al*. investigated peptides and proteins in fingermarks by MALDI-MSI where donors' hands were cleaned with 50% aqueous ethanol solution prior to deposition of eccrine (ungroomed) fingermarks with the intention of removal of any sebaceous material. Yet, they putatively identified some anti-microbial peptides, which are found in sebaceous glands.[98] Current findings of this study do not necessarily suggest that eccrine glands in fingers are the only source of lipids in eccrine deposits. Research findings discussed here including current results of this study suggest that complete removal of sebaceous secretions from fingers is hard to achieve regardless of the use of soap or solvents.

As reported in the previous chapter, very low values (including negative values for adhesion in some eccrine droplets) detected using AFM with hydrophilic cantilever tips were unable to be comprehended, as similar low values were observed on natural and sebaceous droplets. Nevertheless, by employing non-invasive chemical imaging of eccrine droplets at sub-micron scale, this study has now offered a possible explanation to those ambiguous observations.

4.3.3.3 Raman spectra of fresh natural fingermark deposits

The signal-to-noise ratio was improved in the Raman spectra of natural fingermarks compared to eccrine fingermarks as they were loaded with both sebaceous and eccrine material. Figure 4.8 shows an 80 µm × 80 µm area of a natural fingermark deposit imaged during the study from the donor D10M5. Five components were identified in this area by investigating the fingerprint region as well as the high wavenumber region of the Raman spectra.

The distinction between lipid components (iii) and (iv) was based on the spectral dissimilarities in the high wavenumber region. The difference of intensity between both CH_2 symmetric stretching (2855 cm^{-1}) and the Fermi-resonance CH_2 stretching (2886 cm^{-1}) bands of component (iii) was not as large as in component (iv). The peak height ratio, I_{2886}/I_{2850}, is an indication of the intramolecular chain disorder and lateral packing between lipid acyl chains and a lower band intensity ratio indicates a lower hydrocarbon chain order.[225] This ratio was 0.22 and 0.53 for component (iii) and component (iv) respectively, which suggests that the lipids in the blue colour coded region in Figure 4.8 (c) are more crystalline than the lipids in red colour coded regions.

The spectrum of component (i) resembles a mixture of proteins/amino acids due to its distinctive bands at 534, 860, and 1454 cm^{-1}. The spectral differences between components (i) and (ii) were in the fingerprint region. While the band at 1000 cm^{-1} was much intense in component (ii) than in component (i), two additional bands at 451 and 625 cm^{-1} were also observed. As sulphate crystals display a strong band near 988 cm^{-1} and medium intense bands near 459 and 628 cm^{-1}, the magenta colour coded regions in Figure 4.8 (c) were tentatively assigned to sulphate crystals blended within aqueous regions.[237-238] The spectrum of component (v) was attributed to iron oxide,[239] presumably from personal care products. These chemical images thus provide compelling evidence for the heterogeneous distribution of chemical species within individual droplets as well as between droplets.

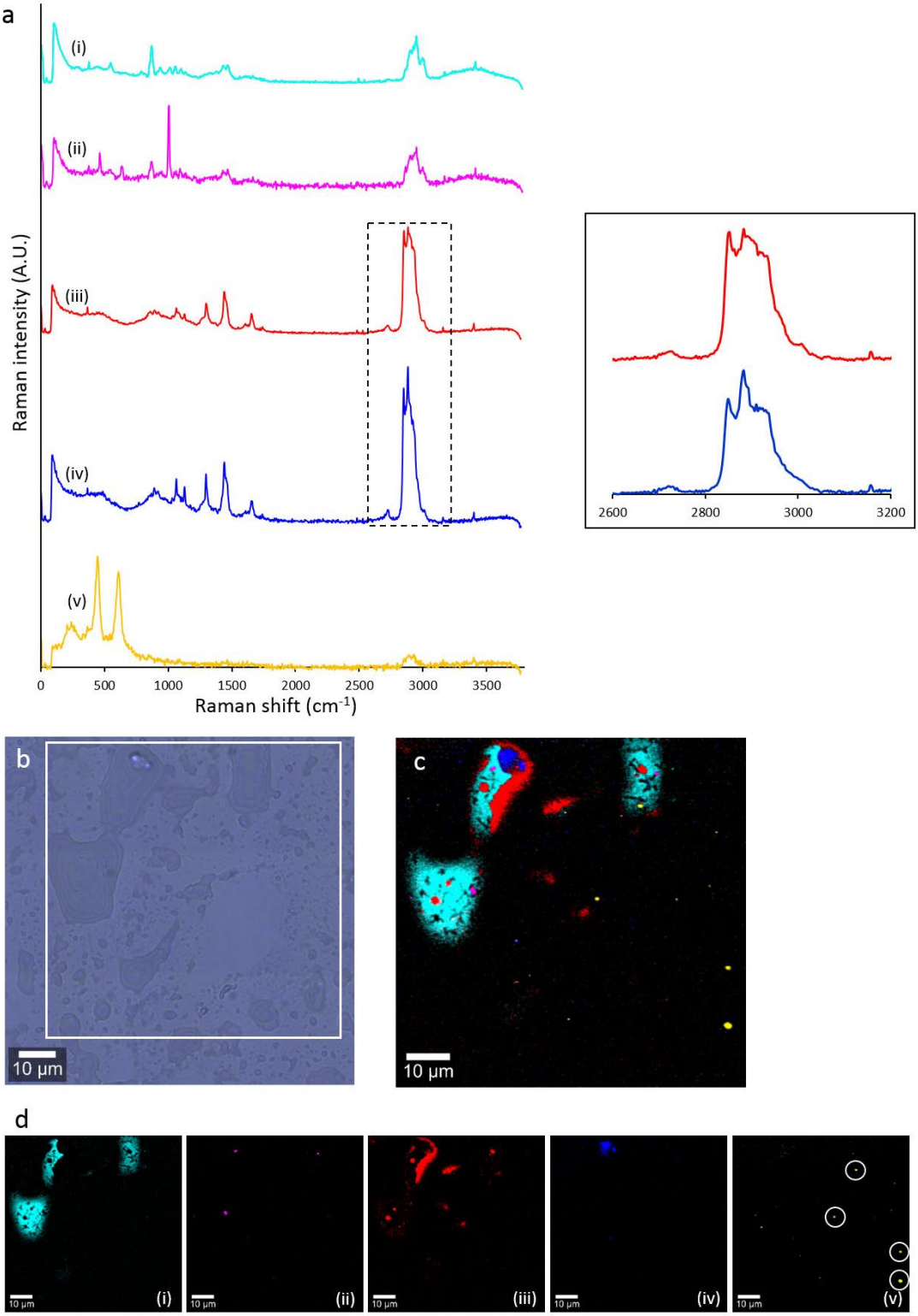

Figure 4.8 Averaged Raman spectra of the five components identified in a natural fingermark deposit from Donor D10M5 (a), bright field optical image of the area investigated (b), the composite distribution map of the five components (c), and their distribution in false colours (d). The high wavenumber region of the component (iii) and (iv) are expanded in the separate box to demonstrate the subtle differences in this region. The spatial distribution of component (v) is circled in (d) to aid the reader.

At the moment, physical developer (PD) is the only technique routinely used in casework to detect fingermarks on wetted porous surfaces regardless of its reagent cost and instability.[61, 71] A detailed investigation into PD was carried out by de la Hunty *et al*. with the intention of identifying chemical targets of the fingermark residue that interact with silver nanoparticles.[61-62] It was suggested that PD may target a defined mixture of eccrine and lipid constituents, both of which must be present in the deposit for silver deposition to occur.[61-62] They also emphasised the need to understand the state in which these targets are present, that is, as a mixture of various compounds or as an emulsion. Although the results are based on non-porous surfaces, they offer insights to this query as they demonstrate the possibility of fingermark droplets to form emulsions depending on the amount of lipid and eccrine secretions in the droplet.

As mentioned earlier, Fritz *et al*. and Girod *et al*. combined FTIR spectroscopy with chemometrics to infer donor traits and time-since deposition.[86, 89] However, due to large uncertainties involved with the data, Fritz *et al.* failed to establish any trends over time with respect to donor traits and time since deposition. Our findings suggest that apart from the inter-donor variation, this large uncertainty is also due to chemical heterogeneity across the deposit. As Girod *et al.* were able to differentiate older fingermarks from newer ones regardless of the substrate and lighting conditions, they recommended further research to validate their fingermark dating models. However, although they acquired 6 spectra replicates per deposit and 4 fingermark specimens per each age, no information was given on how the same area of each deposit was investigated in the time-course study. Due to the observed heterogeneous distribution of chemical components across the deposit in this current study, it is recommended to maintain the spatial specificity of the sample in such future investigations.

Raman imaging was performed further on fingermark droplets with diverse appearances from deposits obtained from donors D1F1, D2M1, D7F3, D8F4, and D9F5. Figure 4.9 shows the distribution of lipids in natural deposits from donors D1F1 and D2M1, demonstrating the pronounced dominance of lipids in natural fingermark deposits. Croxton *et al*. analysed amino acids and fatty acids simultaneously in natural fingermarks deposited on non-porous surfaces by GC-MS and found that the total fatty acids deposited ranged from 0.17-3.37 µg (median 1.77 µg) while the total amino acids deposited ranged from 0.02-0.34 µg (median 0.18 µg) per fingermark.[87] This tenfold increase of fatty acids compared to amino acids further reinforces the results of this present study.

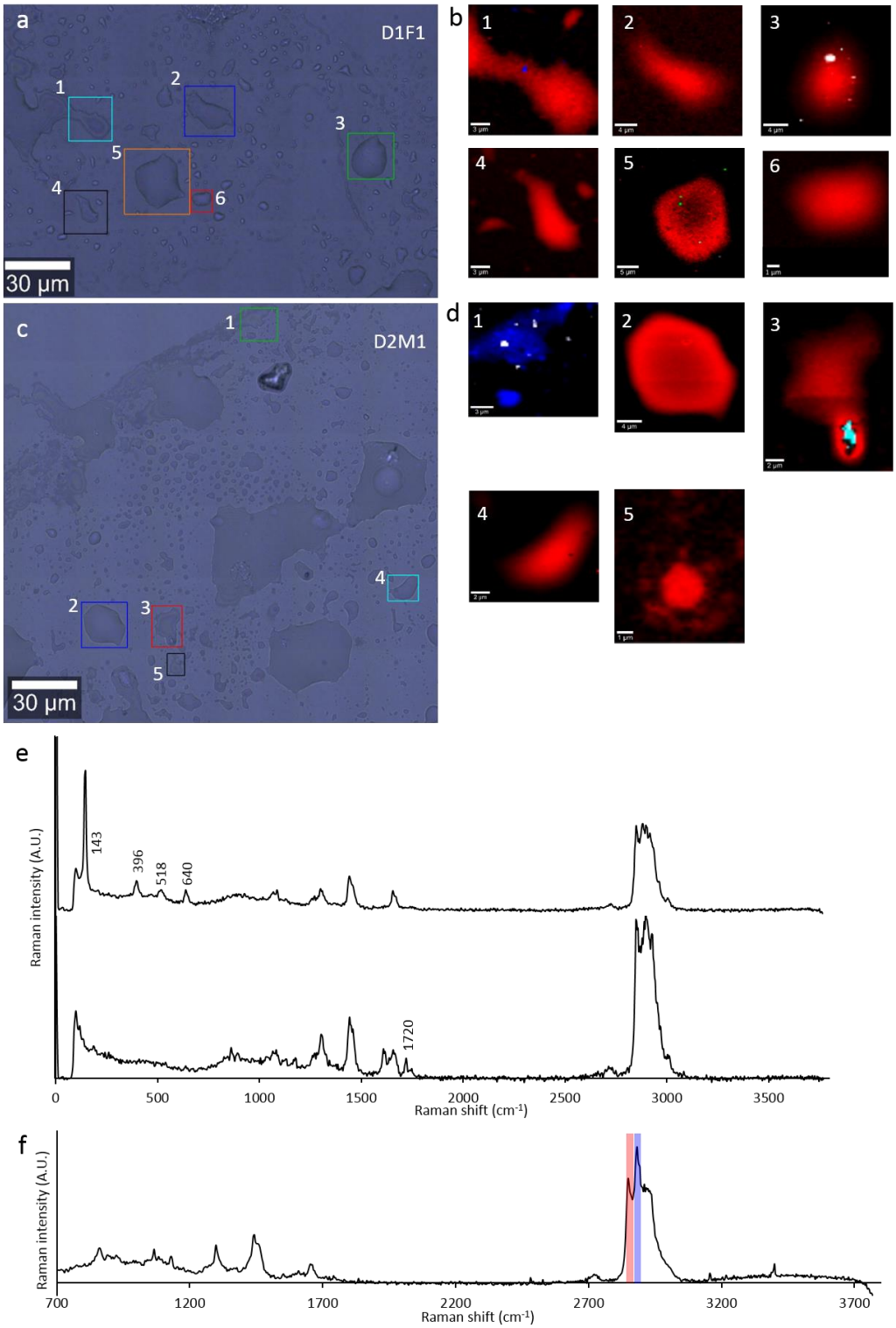

Figure 4.9 Bright-field optical images of natural fingermark deposits from donors D1F1 (a) and D2M1 (c). Coloured squares represent the areas of the deposits that were imaged. Raman images of the droplets showing the distribution of eccrine and sebaceous material and contaminants (b) and (d). Red colour coded regions represent less crystalline lipid components, blue colour; more crystalline lipid components, cyan colour; eccrine material, and yellow colour; ion oxides particles. Raman spectra of white and green colour spots resembled TiO_2 particles (e, top) and another lipid component with a distinct band at 1720 cm^{-1} (e, bottom) respectively. The red and blue colour coded regions in (b) and (d) were generated by integrating over the bands in red (2855 cm^{-1}) and blue (2886 cm^{-1}) rectangles in (f).

Natural fingermark droplets obtained from donors D1F1, D7F3, and D10M5 often displayed a band near 1605 cm^{-1} which was not in the deposit from donor D2M1 (Figure 4.10). This donor has been previously identified as a weak donor against lipid sensitive fingermark reagents by the Forensic and Analytical Chemistry Research Group at Curtin University. Since the band at 1605 cm^{-1} was identified only in lipid droplets or sebaceous areas of the droplets and in the deposits from those who use at least skin moisturisers, it was assumed that the compound responsible for this band is of exogenous origin such as skin moisturisers. Titanium dioxide was also identified in some droplets in almost all donors, which is not surprising as it is a common additive in a range of consumer products, from food items to personal care products (characteristic bands at 143, 396, 518, and 640 cm^{-1}) (Figure 4.9 e, top).

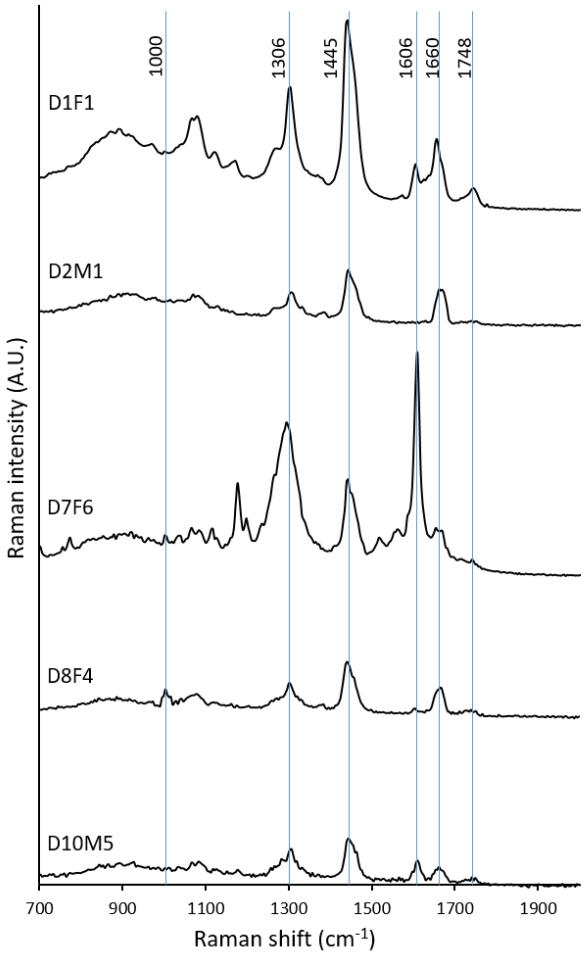

Figure 4.10 Additional Raman bands observed in sebaceous droplets/areas of droplets, presumably from skin moisturisers.

4.3.3.4 Investigation of ageing of fingermarks by confocal Raman microscopy

A preliminary investigation was carried out to probe the potential of confocal Raman microscopy for the analysis of fingermark composition over time. The eccrine fingermark deposit from donor D2M1 was aged under light conditions described in Chapter 2 and the droplets that were imaged at t=0 were re-imaged at t=3 days. As demonstrated in Figure 4.11, the broad O-H stretching band around 3300 cm^{-1} displayed a noticeable reduction in its intensity, probably due to evaporation of water. However, other characteristic bands of amino acids and proteins did not show significant reduction during this period indicating their durability. In addition, the eccrine droplet shown in Figure 4.6 did not show regions of lipids after ageing opposed to the fresh droplet, suggesting volatilisation of lipids. Moreover, it was challenging to detect any Raman signal due to fluorescence from the 3-month old eccrine sweat rich deposit from donor D8F4, although spectral acquisition was successful when the deposit was fresh. Broad fluorescence signal in the Raman spectra caused by samples with high protein content (e.g. biological tissue samples) has been frequently reported in the literature.[240] Hence, this observation may suggest that as water evaporates, the concentration of amino acids and proteins (or their oxidised forms) in droplets increases, causing fluorescence that obscures the Raman signal. On the other hand, these results are somewhat in disagreement with the ageing kinetics of eccrine material reported by Girod *et al*. where all FTIR bands due to eccrine material had completely disappeared after ageing for 9 days.[86]

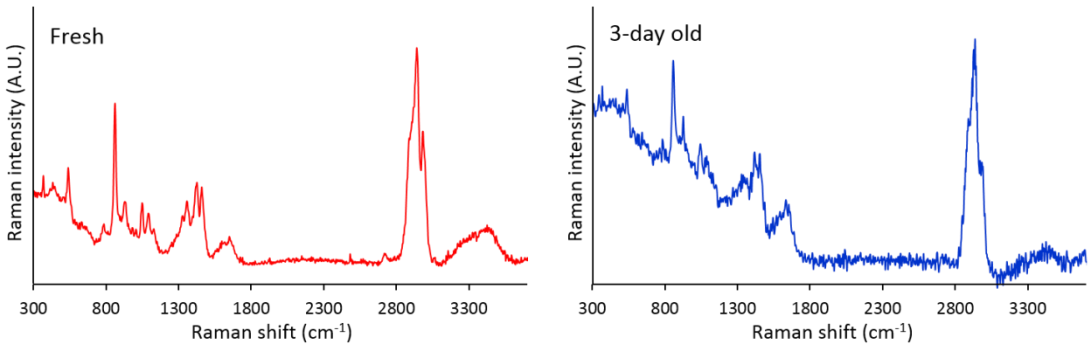

Figure 4.11 Comparison of averaged Raman spectra of the same eccrine fingermark droplet at t=0 and t=3-days.

During the analysis of natural fingermarks over time, it was noticed that when the objective was focused on the surface of the glass slide, relatively less intense peaks were observed at the middle of the droplets compared to the edge. When the objective was moved 1 µm upward from the glass surface, the middle of the droplet had the highest peak intensity. This is because of the attenuation of the laser beam as it travelled through the centre of droplets.

Since the edge of a droplet has less material than the centre, the laser beam is not attenuated, causing high peak intensities. As shown in Figure 4.12, the attenuation of the laser beam may result in misleading spectral information in time-course experiments, although the same droplet was re-analysed over time. FTIR studies have previously shown that the intensity of the C-H stretching bands of fingermarks was reduced over time,[86, 89] but scanning along the X-Y axes in this study showed a reduction of the intensity of this band after ageing for 3 days followed by an increase at 7 days (Figure 4.12, left). Due to these conflicting results, instead of imaging the droplets in the X-Y direction, they were scanned along the X-Z direction (depth-profiling) and the average Raman spectra were obtained (Figure 4.12, right).

The spectra reported at the right of Figure 4.12 clearly show the reduction of the peak intensities as the deposit ages. It should be noted here that spectral acquisition along the X-Z direction was not necessary for eccrine droplets because, according to the topography data reported in Chapter 3, the height of eccrine droplets was in the order or few hundreds of nanometres while many natural droplets reached up to 1 µm or more. The depth resolution of the confocal Raman microscope was approximately 750 nm, thus any droplet with a height less than that will not be affected by beam attenuation.

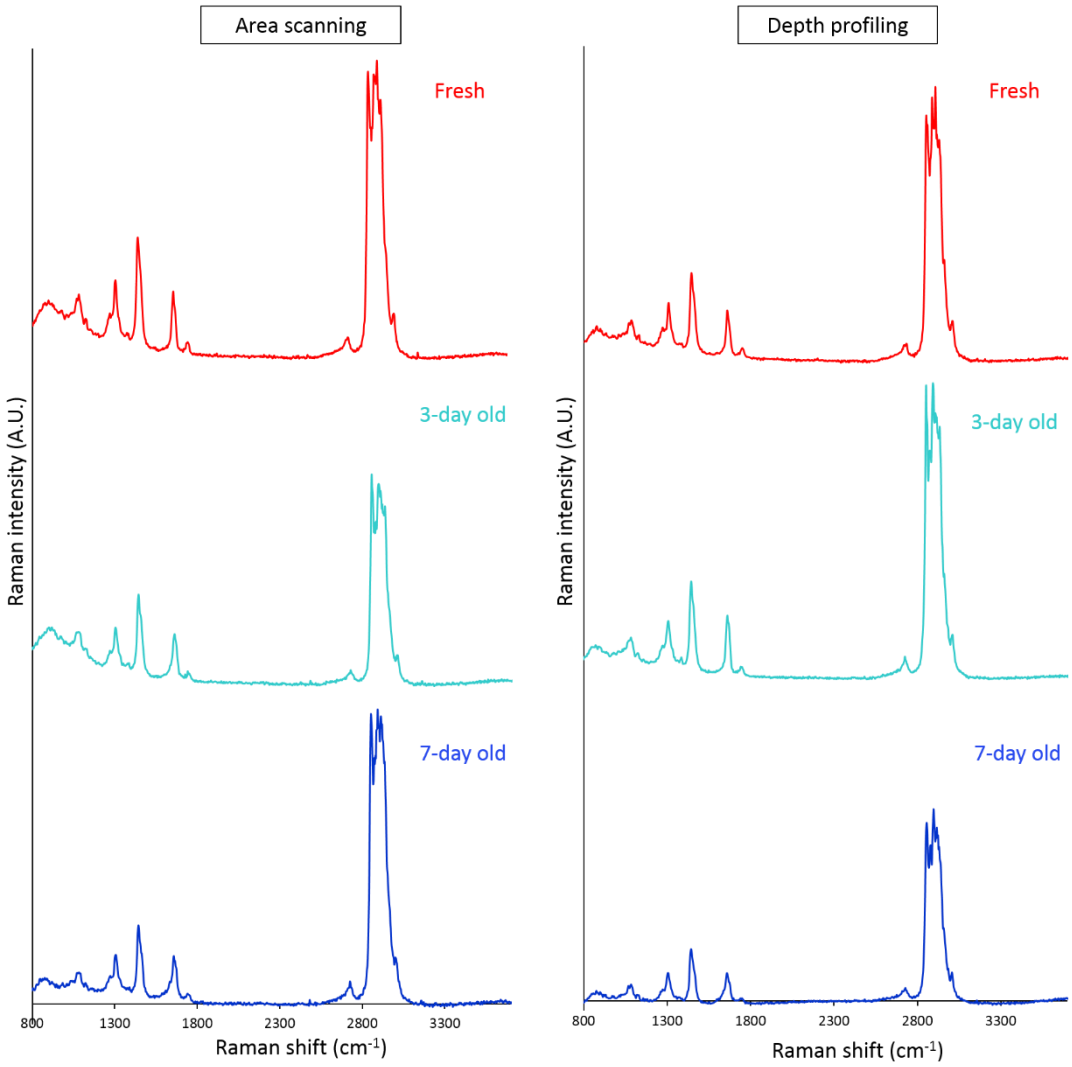

Figure 4.12 Comparison of averaged Raman spectra of the same natural fingermark droplet at t=0, 3, and 7 days acquired by scanning along X-Y (left) and X-Z (right) directions. Spectra in each side (left-hand and right-hand sides) are scaled to the same y-axis.

4.4 Conclusions

The results of this study advance the current understanding of latent fingermark composition and its spatial distribution of chemical components. Specifically, the application of sub-micron spatial resolution confocal Raman microscopy has provided definitive proof that fingermark droplets have a complex chemical composition of hydrophilic and hydrophobic components, and to a first approximation, closely resemble an emulsion. Through extensive analysis of droplets, here for the first time, it was demonstrated that depending on the ratio of eccrine to sebaceous material in droplets, they may exist across a range from totally aqueous (eccrine), lipids in an aqueous matrix, aqueous droplets in a lipid matrix, or totally lipid droplets.

Intriguingly, a prominent presence of lipids across natural deposits were observed, which were previously considered to contain substantially eccrine material. Another key result of this study is the illumination of the necessity for sampling consistency in time-course non-invasive experiments of fingermark composition. Due to the observed chemical variation within a droplet, as well as within a ridge, time-course studies could be substantially confounded if sampling reproducibility is not appropriately controlled.

In a proof-of-concept study, application of confocal Raman microscopy in time-course experiments of fingermarks was successfully demonstrated, emphasising on potential pitfalls and solutions for future applications. Lastly, this study provides the foundation for future research of employing direct chemical/physical imaging on fingermarks at a sub-micron scale to study their chemical and physical properties which is critical to expand and develop current methodologies for fingermark detection.

Chapter 5: Investigations into the sampling methods of fingermark residue for time-course experiments using squalene as a proxy by gas chromatography-mass spectrometry (GC-MS)

5.1 Introduction

Studies aimed at the identification of potential biomarkers for targeted visualisation and age estimation of fingermarks require analysis of the composition over time during the storage of samples under different environmental conditions. While non-destructive analytical techniques such as FTIR and Raman cause little to no sample damage, allowing the analysis of the same sample over time, destructive techniques such as GC-MS and LC-MS demand extraction of the residue into a suitable mixture of solvents. Thus, these techniques require multiple samples so that each sample or a set of samples can be extracted and analysed at pre-determined time intervals. Despite this inconvenience, GC-MS and LC-MS techniques offer more specific and sensitive compound identification compared to vibrational spectroscopy techniques, and are hence better suited to the investigation of the specific compound(s) in fingermark residue. Vibrational bands in the FTIR or Raman spectra only offer information on functional groups of molecules, and one band often represents multiple compounds in complex mixtures such as fingermarks. Although mass spectrometry imaging (MSI) has the advantage of superior specificity, currently it is unclear whether the mass-to-charge ratio (*m/z)* distribution maps truly represent the accurate compound concentration as the ion suppression effects in MSI can cause interference.[16, 241-242] To this end, the use of destructive techniques in time-course experiments of fingermark composition is rather inevitable.

One of the key challenges of investigating fingermark compositional variation over time is the difficulty of obtaining reproducible samples, even from a single donor.[100] Contributing factors include variations in deposition conditions and donor-dependent compositional variation (intra-donor variation). This complication hampers the identification of potential ageing trends of specific compound(s) and obstructs the construction of ageing curves which have been proposed as fingermark dating methodologies.[100-101]

5.1.1 Inter- and intra-donor variation of fingermark composition

As detailed in Chapter 1, section 1.5.2, compositional variation of fingermarks of different donors (inter-donor variation) has been observed in several investigations and as a result, it was proposed that such differences could be probed to discriminate individuals and infer donor traits. Nonetheless, such attempts are not viable if the composition of samples obtained from an individual is subject to significant fluctuation (intra-donor variation), such that it masks variability caused by individuality.[90, 92, 94]

In 1999, Mong *et al.* reported that comparative quantitation of compounds over time is not practical because of the variability of the composition of their subsamples collected from individuals.[90] However, they made this statement by comparing the variability of the chromatograms of initial and aged samples, but not the initial composition of multiple samples. Subsequently, Asano *et al*. investigated the variability of fingermarks collected from three donors in the morning and afternoon on four different days.[94] They observed a little variation of the composition due to different sampling times, while the major contributing factor for compositional variation was the three different subjects (inter-donor).[94] Similar observations for intra-donor variation was made by Archer *et al.* using deposits obtained from one donor over the course of the day.[19] Although analysis of variance (ANOVA) did not identify a significant difference, a boxplot of the relative amount of squalene over time indicated there may be an increase in the amount towards the later sampling period.

In the GC-MS based investigation of fingermark age estimation, Weyermann *et al*. reported that the percentage relative standard deviations (%RSDs) for squalene and cholesterol reached up to 80% for four thumbprints collected from a donor within a day over three non-consecutive days.[100] They investigated different methods of data processing to identify a parameter that could be plotted against time with minimal intra- and inter-donor variation. It was found that instead of using the relative peak area, $RPA_{squalene/internal\ standard}$, the ratio of $RPA_{squalene/cholesterol}$ permitted minimising the intra-donor variability (from 50% to 10%) of the samples obtained from the same day. However, large differences were still detectable between different days (39%).[100] They identified the lack of reproducibility of the results (both inter- and intra-donor) as the key challenge that stands against dating of fingermarks.

Koenig *et al.* reported %RSDs of 47% and 35% for squalene and cholesterol respectively for the traces collected from one donor over a day at three sampling intervals using GC-MS.[93] These %RSDs were increased up to 48% for squalene and 52% for cholesterol for traces collected over a period of two months. Thus, for fingermark dating purposes, it was suggested to use the ratio of peak area of squalene to the sum of the peak areas of cholesterol and myristyl myristate in order to reduce the %RSD of intra-variability. Concerning qualitative intra-donor variability, they identified major lipid compounds such as squalene, fatty acids and cholesterol in all deposits collected over two months; however, some of the wax esters were present only in deposits containing a larger total number of compounds.[93] On the other hand, large qualitative differences were identified for inter-donor variability where, among all the compounds studied, only squalene, cholesterol, and some wax esters were observed in all deposits yet with great quantitative variation. %RSDs for all

compounds increased compared to those of intra-variability, reaching 95% for squalene and 75% for cholesterol.[93]

Following from Koenig's work, Girod and Weyermann later found that donor classification based on "poor" and "rich" lipid donors was affected by the intra-variability to a certain degree.[91] In contrast to Koenig's results, the observed %RSDs for all targeted compounds were more similar between intra- (44-94%) and inter-variability (63-90%), except for larger wax esters. Compared to previous studies, this study employed more donors (n=25) thus, their %RSDs for inter-donor variation were higher than the past studies. Moreover, it was reported that the %RSDs of inter- and intra-variability could be reduced for most of the target lipid compounds by normalising the peak area to the sum of target compounds, excluding squalene.[91] Squalene showed the highest variability in terms of the relative amount (when normalised to the internal standard) was thus excluded from the sum of peak areas.

Recently, a detailed study into the intra-donor variation was carried out by Frick *et al.,* where triplicate samples were collected at a given time over five sampling intervals from five donors over the course of a day.[92] Intra-donor variation over one month was monitored from samples collected in triplicate every 2-3 days from four donors over one month. The relative amounts of free fatty acids varied between triplicate samples as well as samples collected at different time intervals throughout the day. For most donors, no clear trend in fingermark composition was observed during the course of a day. It was suggested that changes in secretion composition might be unnoticeable as the new secretions would become diluted into what was already on the skin surface. Yet, samples from one donor, who did not handle any food or other substances during sampling periods, were found by principal component analysis (PCA) to exhibit a distinct separation based on two sampling times (morning and late afternoon). The increase in relative amounts of compounds towards the late afternoon compared to the early sampling periods was attributed to the gradual accumulation of sebum on the skin surface. Investigation of intra-donor variability over one month found that there was evident variation in the amount of squalene for some donors; however, no clear trend was observed across all donors.[92]

In the same study, Frick *et al.* employed an extensive number of donors (n=106) to study inter-donor variation where it was found that squalene and free fatty acids were the principally responsible compounds for the inter-donor variability.[92] Nevertheless, these differences were not sufficient to enable discrimination of donors within the large donor pool by performing PCA on chromatographic data. Since previously reported studies typically used samples from one donor to study intra-donor variability,[19, 91, 93, 100] they were unable to offer conclusive evidence on whether intra-donor variation occurs to such an extent that it impedes inter-donor discrimination. Based on their results, Frick *et al*. suggested that discrimination of donors based on the fingermark composition is not a viable approach as intra-donor variation can confound such attempts.[92]

As highlighted in this review, intra-donor variation is an inherent issue which poses significant challenges to current lines of fingermark research, especially with time-course studies. Any investigation that involves ageing of fingermarks, therefore, must explore potential strategies to circumvent this issue, yet, within the established research objectives and applicability of results to real-life situations.

5.1.2 Aims

This study was performed as a critical phase of Chapter 6 where the transformation of a major fingermark lipid component; squalene, was investigated over time. For this particular time-course experiment described in the following chapter, deposition of two fingermarks at a given sampling time with approximately similar amounts of squalene was required. This chapter hence depicts efforts made to produce two fingermarks with a minimal variability of the amount of squalene deposited at a given time. Having two samples with similar composition allows analysis of one sample to identify the initial composition and to age the other, such that the initial composition of all aged samples is known. The aged composition can be assessed in relation to the initial composition, enabling identification of trends in the compositional variation of natural fingermarks over time in an evidence-based manner. The amount of squalene (SQ) of fingermark deposits from left and right hands of three donors were investigated under four different sampling methods and the chemical homogeneity between hands was calculated as the percentage difference of squalene between hands.

5.2 Experimental

5.2.1 Chemicals

Squalene (≥98%; Sigma-Aldrich, USA), squalene-d_6 (98%; Toronto Research Chemicals, Canada) and dichloromethane (≥99.9%; Honeywell Inc., USA) were used as received. A stock solution of squalene at a concentration of 10,000 ppm was prepared in dichloromethane (DCM) and diluted to obtain a working solution of 100 ppm. A serial dilution was performed starting with the working solution to create a set of standard solutions at concentrations of 0.1, 0.5, 2.5, 10.0, 25.0, and 50.0 ppm. A standard solution of 20.3 ppm squalene-d_6 was also prepared in DCM. All standard solutions were stored below -18 °C to avoid degradation and solvent evaporation.

5.2.2 Quantification of squalene

Quantitation was performed using the ratio of the peak areas of the analyte and of the deuterated standard. An external calibration curve, plotting ratio against concentration, was obtained by diluting standards in DCM in the concentration range of 0.1-50.0 ppm. Concentrations in the samples were calculated by comparing the peak area ratios of the analyte and their correspondent surrogate standard in the fingermark extracts, to the corresponding ratios in the standard solutions. Calibration curves were acquired at the beginning of each batch of samples.

5.2.3 Sample deposition

5.2.3.1 Method development

Natural and charged fingermarks from donor(s) were deposited on glass coverslips (2.2 cm × 2.2 cm), aluminium foil strips (3 cm × 9 cm) and freshly cleaved mica sheets (2 cm × 2 cm) by following the procedures for sample deposition described in Chapter 2.

5.2.3.1.1 Investigation of sample reproducibility

Four deposition conditions were tested in this study, which are described in Sampling Protocol 1-4. These were based on fingermark sampling procedures previously reported in this field of research and steps that could be adapted to obtain two homogeneous deposits from both hands at a given time. Three donors (D1F1, D6F2, and D5M4) were employed for this study and their demographics are reported in Chapter 2. After rubbing hands together for 10 seconds, donors placed five fingertips from one hand on the matt side of an aluminium strip which was considered as one sample. They were requested to place one fingertip at a time maintaining a constant contact area during deposition as much as possible. Another

sample from the other hand was obtained at the same time and these two samples obtained at a time were considered as one sample set. Deposition time was 10 seconds in all cases. Three sample sets (6 samples) per donor were obtained within the course of a working day (9.00 am-5.00 pm) maintaining at least 30 min gap between each sampling time.

5.2.3.1.2 Sampling Protocol 1

Natural fingermarks from donors were obtained on aluminium foil strips without controlling the deposition pressure (as per the procedures described in Chapter 2 and in the above section).

5.2.3.1.3 Sampling Protocol 2

Aluminium strips were slightly folded, lengthwise down the centre, and unfolded to make a crease to visualise the centreline. One strip was placed on a kitchen scale (increments: 1 g, Soehnle, Germany) where the top surface of the scale was covered with aluminium foil to prevent contamination. Donors were requested to place one fingertip at a time on the aluminium strip while preserving the symmetry of contact area along the centreline. They were also asked to maintain the reading of the scale at 500 ± 100 g during deposition. Following this procedure, two samples of natural fingermarks per sample set were collected. Sample sets were then cut separately along the centreline using a scalpel which was cleaned with DCM before every use. Within a sample set, one piece of the right hand sample was pooled with another piece of the left-hand sample to have three sets of pooled samples (Figure 5.1).

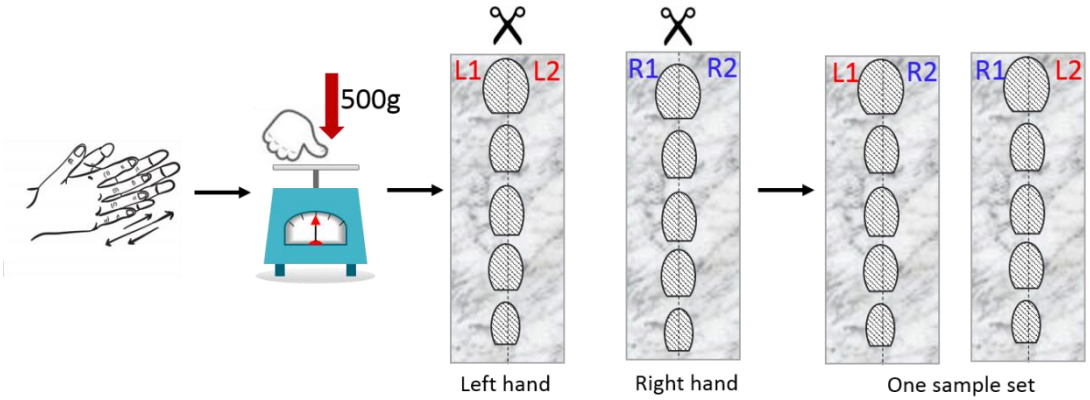

Figure 5.1 Schematic showing the sample deposition procedure for Sampling Protocol 2. Fingermarks were collected on aluminium foil strips by controlling the deposition pressure using a kitchen scale. Then samples from both hands were split along the centreline and pooled (one section of left hand sample was pooled with another section of the right hand sample).

5.2.3.1.4 Sampling Protocol 3

Sebaceous deposits were obtained from donors as described in Chapter 2 and in section 5.2.3.1.1 while maintaining the deposition as above.

5.2.3.1.5 Sampling Protocol 4

Natural fingermarks were obtained from donors as described in Chapter 2 and in section 5.2.3.1.1 while maintaining the deposition pressure as above.

5.2.4 Sample preparation

5.2.4.1 Method development

Aluminium foil strips were rolled and inserted into 4 mL vials pre-rinsed with DCM. Aluminium strips were handled from the edge wearing nitrile gloves to prevent sample loss and contamination. A volume of 0.7 mL of DCM was added to the extraction vials, which were then screw capped using matching caps lined with polytetrafluoroethylene. The vials were wrapped with aluminium foil to avoid exposure to light during sample extraction and placed in a sonicator bath (Soniclean, Australia) which was placed on an orbital shaker (Ratek, Australia) with mild agitation for 10 min. The individual vials were then vortex mixed (Ratek, Australia) for 2 min. Sample extracts were transferred to 2 mL amber colour glass crimp top vials (Agilent Technologies, USA) using glass pasteur pipettes (used as received). The GC vials were sealed with crimp tops after placing a piece of aluminium foil (matt side down) over the vial opening. Sample blanks were prepared using clean substrates bearing no fingermarks.

5.2.4.2 Investigation of sample reproducibility

Each aluminium strip (one sample) was rolled and inserted into separate 4 mL clear glass vials pre-rinsed with DCM. Aluminium strips were handled as described above. A volume of 0.6 mL of DCM was added, followed by 0.1 mL of 20.3 ppm squalene-d_6 standard. Samples were extracted by sonication and vortex mixing as described above and the extracts were transferred to GC vials. Sample blanks were prepared for every batch of samples using aluminium foil strips bearing no fingermarks.

To investigate the extraction efficiency, three 10 µL aliquots of 50.0 ppm squalene standard were deposited (as in three spots) on an aluminium strip and extracted as above. The analysis was carried out in duplicate.

5.2.5 Chemical analysis

Chromatographic analysis was performed using three GC-MS instruments equipped with autosamplers. Method development experiments were carried out using one instrument and the sample reproducibility study was performed on two instruments of similar models. Instrumental details are described in Table 5.1.

Table 5.1 Details of GC-MS instrumentation.

Study	Gas chromatograph	Injector	Column	Mass spectrometer
Method development	Hewlett Packard 6890N series	Gerstel MPS2 autosampler	Phenomenex ZB-5MS (30 m × 0.25 mm ID × 1.00 µm d_f)	Agilent 5973N
Investigation of sample reproducibility	Hewlett Packard 6890 series	Hewlett Packard 6890 series injector	Agilent J&W DB-1MS UI (60m × 0.250 mm ID × 0.25 µm d_f)	Hewlett Packard 5973 MSD

5.2.5.1 Method development

All samples were analysed under the following conditions. 1 µL of sample was injected in splitless mode using an injector maintained at 320 °C with a purge time of 0.75 min. The GC oven program was isothermal at 40 °C for 1 min, then increased from 40 °C to 320 °C at a rate of 20 °C/min and was isothermal at this temperature for another 30 min. Helium was used as a carrier gas at a constant pressure of 8.38 psi. The mass spectrometry detector was operated in electron impact (EI) ionisation mode at 230 °C. The ionisation energy and the electron multiplier voltage were 70 eV and 1505.9 V respectively. A solvent delay of 5 min was applied and analytes were measured in the range of *m/z* 10-580 by a single quadrupole mass spectrometer.

5.2.5.2 Investigation of sample reproducibility

A sample volume of 1 µL was injected in splitless mode using an injector maintained at 300 °C with a purge time of 0.75 min. The GC oven was programmed from 200 °C, held for 2 min, and then ramped to a final temperature of 300 °C at a rate of 2.5 °C/min and held isothermal for 30 min. The carrier gas was helium with a constant pressure of 24.2 psi. The mass spectrometry detector was operated in EI mode at 230 °C. The ionisation energy and the electron multiplier voltage were 70 eV and 1576.6 V respectively. A 9 min solvent delay was applied at the beginning of the chromatographic run, and analytes were measured by scanning in the range *m/z* 30-550 using a single quadrupole mass spectrometer.

5.2.6 Data analysis

The data was processed using MSD ChemStation D.02.00.275 software. Background subtraction was performed for all chromatograms followed by manual integration of the squalene and squalene-d_6 peaks. The squalene peak was identified comparing the retention time against the standards and mass spectra against NIST MS library (NIST 98, Agilent Part No. G1033A). Except in method development, squalene peak area was normalised to that of squalene-d_6 and the amount of squalene per five fingertips was quantified using the calibration curve. The percentage difference of squalene between left and right hands were then calculated using the following formula:

$$\%\ \text{difference of squalene between hands} = \frac{\text{Quantitative difference of SQ between hands}}{\text{Average amount of SQ between both hands}} \times 100$$

5.3 Results and discussion

5.3.1 Method development

5.3.1.1 Sample deposition and preparation

Previous research has shown that fingermarks deposited on non-porous substrates contain less material than those deposited on porous substrates.[16, 100, 116] In addition, it has been demonstrated that charged fingermarks have a significantly higher amount of material compared to natural deposits.[87] Since one of the prime objectives of this thesis was to generate a better understanding of fingermarks which will assist in the detection of aged deposits in real-life cases, it was decided to use natural deposits instead of charged ones as opposed to many previous studies with different objectives.[21, 91-94, 100-101]

As this thesis concerned latent fingermarks on non-porous surfaces, a preliminary study was performed to identify the best suited non-porous substrate for *ex-situ* chromatographic studies of fingermarks. The suitability of four non-porous substrates; glass coverslips, aluminium foil and mica sheets were tested. An ideal substrate for such analytical study would be easy to handle, cause minimal contamination and be representative of real-life crime scenes. While glass and aluminium foil are commonly encountered in such situations, mica is less so. However, mica sheets can be easily peeled off to obtain clean surfaces. On the other hand, glass coverslips and aluminium foil are prone to contamination, requiring possible pre-cleaning procedures.

The use of extraction vials with the narrow opening was preferred as a wide opening leads to rapid solvent evaporation during sample handling. While attempting to insert a glass coverslip bearing fingermarks into an extraction vial with a narrow opening, the substrate had to be broken into small pieces which was cumbersome and caused sample loss. As such, glass coverslips were not used in further investigations. Mica sheets were easier to insert into extraction vials compared to glass coverslips as they could be folded, but sample extracts needed to be filtered through an activated magnesium sulphate column to remove small pieces of mica caused as a result of folding the sheet. Furthermore, a sample blank of mica prepared by following this procedure was analysed by GC-MS which showed no contamination caused by the substrate. Nonetheless, a sample blank of aluminium foil showed a similar outcome. Additionally, aluminium foil was more convenient to handle, and sample extraction was less time-consuming. Hence, aluminium foil was chosen as the most suitable substrate for further chromatographic analysis.

As explained earlier, due to the limitations that arose from using non-porous substrates and natural deposits, investigations were carried out to identify the minimum number of fingermarks (digits) required to provide a reasonable GC-MS signal, at least for squalene. It was found that natural deposits obtained from five fingertips on aluminium foil were sufficient in this regard within a donor population of 3 subjects despite the inter- and intra-donor variability. Total ion chromatograms (TICs) of (i) one charged fingermark on filter paper, (ii) two charged fingermarks on aluminium foil and (iii) five natural fingermarks on aluminium foil are shown in Figure 5.2, illustrating the effect of the type of the deposit, substrate and number of digits per sample on the detector response.

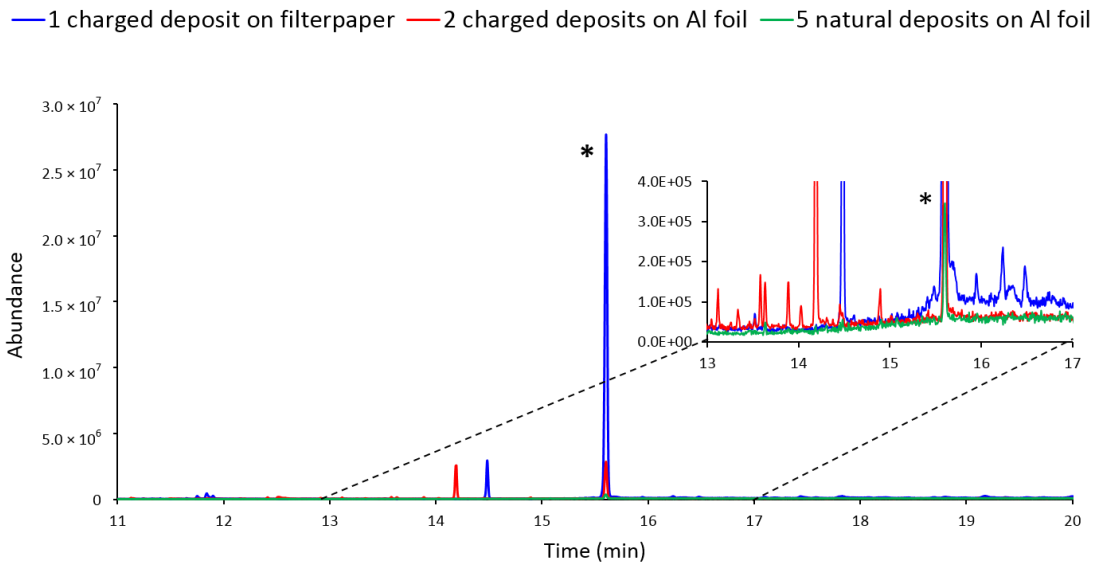

Figure 5.2 Sample TICs showing the effect of type of the deposit, substrate, and number of digits per sample on the detector response. Squalene peak is indicated with an asterisk.

As displayed in Figure 5.2, the number of identifiable peaks in the sample of natural fingermarks deposited on the non-porous substrate is extremely limited and by following the GC-MS method outlined earlier, only squalene was consistently detected in all samples of natural deposits. Although other peaks were detected in some samples, mostly cosmetic residues such as vitamin E and squalane, their intensity was poor. Since this study was intended to identify a suitable sampling method for Chapter 6 which is focused on squalene, detection of squalene only was adequate. As such, squalene was used as a proxy to probe chemical homogeneity between two samples.

The sample extraction procedure was based on the methodology reported by Frick *et al*.[92] Since the samples were not derivatised, this method enabled preparation of a larger number of samples (porous substrates) for the analysis of fatty acids, squalene, cholesterol and some wax esters within a short period of time.[92] In addition, possible contamination in the form of water or plasticisers was avoided by omitting a sample concentration step.[92] As the work reported here and in Chapter 6 involve analysis of a large number of samples, this procedure was chosen in order to minimise the time required for extraction.

5.3.1.2 Chemical analysis

The GC-MS conditions used in method development was previously reported by Frick *et al*.[92] This method allowed detection of squalene within a reasonable chromatographic retention time of 15.60 min.

5.3.2 Investigation of sample reproducibility

5.3.2.1 Sample deposition and preparation

A fingermark sampling method that provides deposits representative of real-life situations should not require any pre-treatment to fingers or strict controls during sample deposition. However, such conditions, for example, washing donors' hands, rubbing hands together, charging fingers with sebum, and control of deposition pressure and time have been frequently used in fingermark research to preserve sample consistency. Most of these studies were related to fingermark detection techniques which required deposition of clear, less distorted deposits to assess their performance. Nonetheless, as discussed in Chapter 1, section 1.7.4, conditions of fingermark sampling employed by various studies greatly vary with little or no explanation as to why certain parameters were chosen.

Two studies reported the use of devices with extreme control measures named "fingerprint sampler"[125] and "Reed-Stanton press rig"[243] for research purposes that offered more reproducible fingermarks without distortion caused by changes in the deposition conditions. However, the reproducibility of deposition was assessed by grading the developed fingermarks (by cyanoacrylate fuming[125] and ink[243]) and hence may not be sensitive to ppm level variations of the composition. Despite the ongoing debate on the application of strict control measures, such applications were generalised based on the established research objectives and limitations with analytical conditions. The objective of having four different sampling methods in this current study was to investigate which method would offer the least variation in the amount of squalene in two fingermark samples deposited at a given time. Sampling Protocol 1 employed natural fingermarks with minimum control over the deposition (deposition pressure was not controlled) which closely resembles deposition events in real-life. Sampling Protocol 2 used rigorous controls over the deposition with the intention of mitigating potential bias due to dominant hand and uneven contact between the fingers and substrates. Charged fingermarks with controlled deposition pressure were used in the Sampling Protocol 3 to investigate if charging fingers really produce homogeneous samples as this method is the most frequently used method in previous literature.[16, 19-21, 91, 93, 100-101] Samples (natural fingermarks) obtained as per Sampling Protocol 4 were reasonably forensically relevant without extreme controls over the deposition. A deposition pressure of 500 ± 100 g exerted by a fingertip was chosen as it has been frequently used in literature.[86, 91, 93, 101, 243-244] Rubbing hands together before deposition has also been frequently performed in previous studies to distribute material evenly between hands,[18-19, 87, 93, 98, 245] yet no study has investigated the extent of uniformity produced.

Variation caused during sample extraction is another factor that contributes to compositional inconsistencies in final sample extracts. A surrogate standard of squalene-d_6 was spiked to extraction vials before sonicating the samples to investigate such variations. For an effective sonication extraction, samples must be in contact with the extracting solvent during sonication,[246] however, the small volume of extracting solvent (0.7 mL in total) was not sufficient to coat the rolled aluminium strip completely inside the vial. Therefore, the sonicator bath was placed on an orbital shaker such that the orbital movement of the bath agitated the vials inside, assisting effective extraction. Samples were further mixed in the vortex mixer to achieve extraction of all five deposits. The openings of the GC vials were covered with aluminium foil to prevent extraction of material from the rubber septa.[247-249]

5.3.2.2 Chemical analysis

Although the GC-MS program reported by Frick *et al*. allowed separation of squalene from the fingermark matrix, squalene and squalene-d_6 were not sufficiently resolved using this method. Thus, a long column of 60 m, instead of a 30 m, was used and the GC oven parameters were changed as reported in the section 5.2.5.2. Squalene and squalene-d_6 were then sufficiently resolved; however, they were not separated at the baseline (Figure 5.3).

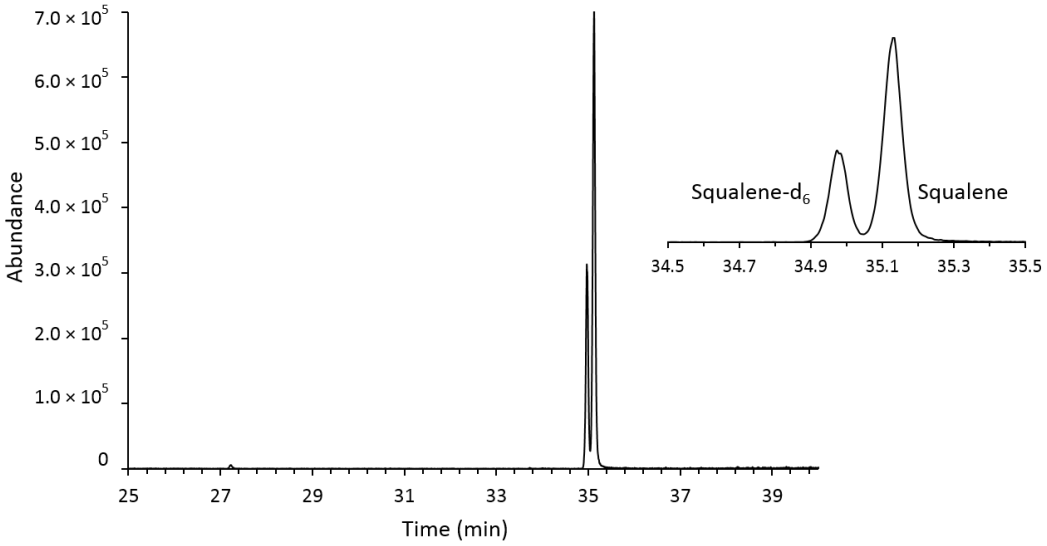

Figure 5.3 Sample TIC illustrating the separation of squalene and squalene-d_6 using the modified GC-MS method.

5.3.2.3 Chemical homogeneity between hands

The average amount of squalene deposited by five fingertips (average between right and left hands) by all three donors in all four deposition conditions are shown in Figure 5.4 (a). In addition, the corresponding percentage differences of the amount of squalene between hands are shown in Figure 5.4 (b).

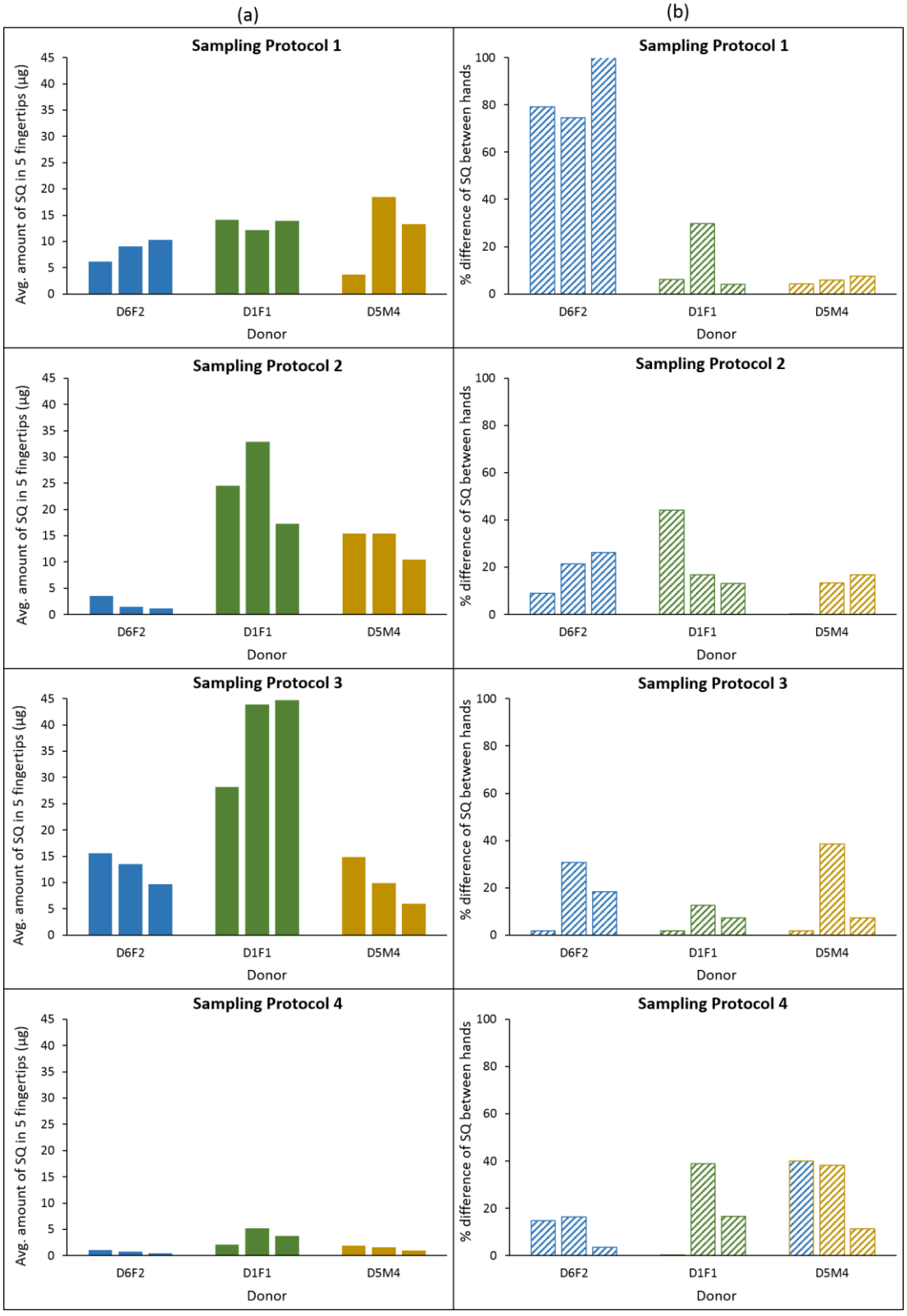

Figure 5.4 Average amount of squalene between right and left hands at a given sampling time in all three donors under four sampling protocols (a). The corresponding percentage difference of squalene between hands (b). From left to right, three coloured bars per each donor represent three sample sets obtained over the course of the day maintaining at least 30 min time interval between consecutive samplings.

The average amount of squalene per five fingertips (averaged between both hands) for Sampling Protocols 1-4 was in the range of 3.70-18.44, 1.20-32.86, 6.00-44.67, and 0.49-5.21 µg respectively. Relatively high amounts were detected in Sampling Protocol 3 where charged deposits were employed in contrast to the other trials, which is consistent with the literature.[87] Samples from donor D1F1 showed the highest amounts, probably due to the regular use of cosmetics in addition to other personal care products. In the study reported by Croxton *et al*. where natural fingermarks were deposited on Mylar® strips, the amount of squalene per sample (4 fingertips per sample) was <300 ng,[87] whereas the results reported in this study are in the range of 0.5-44.7 µg. While the number of digits deposited per sample in their study was less than by only one compared to this study, the discrepancy in the levels of squalene could be largely due to differences in the extraction procedures and substrates.[87] In this current study, a recovery percentage of 113% was achieved for squalene. Although the recovery percentage for derivatised fatty acids was presented in Croxton's previous report,[181] no such data was available for squalene. Therefore, further comparisons could not be made.

While investigating intra-donor variation over the course of a day at five sampling intervals employing charged deposits from five donors, Frick *et al*. observed no clear trend in fingermark lipid composition within the 9.00 am-5.00 pm sampling period.[92] In this present study, a decrease in the amount of squalene in samples obtained between 2.00 pm-4.00 pm from donors D6F2 and D5M4 was observed in Sampling Protocol 3. In the same protocol, in samples from donor D1F1, there was an increase in the first two replicates which were obtained at 10.45 am and 4.30 pm respectively although the squalene level remained almost the same in the third replicate (at 5.00 pm). This could be due to the donor activities that contributed to regain/preserve the squalene concentration during this period. These results, therefore, may indicate that when charged fingermarks are used, the amount of squalene could be influenced by the circadian rhythm of sebaceous glands of the forehead, which reaches a maximal amount of sebum production around mid-day.[250] However, these trends could be masked when total lipid composition is considered because of the further variability of multiple components. Conversely, no such trend was observed when natural fingermarks were used (Sampling Protocols 1, 2, and 4). This is likely to be caused by random contacts between donors' fingers and surfaces which alter the level of squalene in fingertips while charging fingers immediately prior to deposition rules out such variations. In addition, there was no obvious relationship between the amount of squalene and the dominant hand of the donor, which is in agreement with the observations made by Dominick *et al*.[126]

The percentage difference of squalene between two hands at a given sampling time for Sampling Protocol 1-4 was in the range of 4.1-100.3, 0.1-44.0, 1.7-38.5 and 0.2-40.0% and their averages (n=9, 3 replicates per donor x 3 donors) were 34, 18, 13 and 20% respectively. The chemical homogeneity between hands suffered in Sampling Protocol 1, especially in all three replicates from donor D6F2 as seen in Figure 5.4 (b). This means that obtaining two chemically homogeneous samples from both hands across multiple donors would be subject to the highest variability when deposition pressure was not controlled. Averages of the percentage difference between hands in remaining protocols (Sampling Protocol 2, 3, and 4) were relatively close to each other and always less than 20%, though Sampling Protocol 3 showed the lowest variation. As displayed in Figure 5.4 (a), the level of squalene in all replicates of Sampling Protocol 4 was relatively small compared to the other trials, which may have caused further inconsistencies during the manual integration of peak areas due to noisy baselines. These low levels of squalene are likely to be random as Sampling Protocol 2, which had the same approach of sampling, showed relatively higher levels.

Among the four methods tested, sample collection as per Sampling Protocol 2 was tedious compared to Sampling Protocol 4 yet displayed only slight improvement in the average percentage difference (only 2%). Moreover, Sampling Protocol 3 was performed to compare the results of natural deposits against more frequently used charged deposits; however, the use of such deposits counters the set objectives of this work. Based on these results and facts, the deposition method outlined in Sampling Protocol 4 was chosen against other three methods as the most suitable sampling method for the proceeding study described in Chapter 6.

5.4 Conclusions

To date, data interpretation of analytical studies of fingermark composition has been challenging due to significant intra- and inter-donor variation, yet, a systematic study into the degree of variability of subsamples collected as per common sampling methods has not been carried out. This chapter has described investigations into four common fingermark sampling methods within the context of compositional variability between samples obtained from two hands at a time using squalene as a proxy.

In the initial stage of this study, commercially available aluminium foil was found to be a convenient and cost-effective substrate for the chromatographic analysis of squalene in natural fingermarks deposited on non-porous substrates with no concerning level of contamination. The modified extraction procedure without time-consuming derivatisation and sample concentration steps allowed detection of squalene on non-porous substrates with a reasonable detector response and yielded satisfactory recovery. It should be noted here that only squalene was detected in all natural fingermarks deposited on aluminium foil by following this extraction procedure and both GC-MS methods described, thus sample derivatisation or concentration or deposition of more digits per sample may be required if other lipid compounds in natural deposits were to be studied.

Controlling the deposition pressure reduced the average of the percentage difference between both hands by approximately a factor of half compared to uncontrolled deposition (from 37% to approximately 20%), while charging fingers with sebum prior to deposition contributed to yield the lowest difference (13%) amongst all methods. However, as these deposits contained a higher amount of squalene than natural deposits, they may not represent realistic aged composition. Therefore, it was concluded that the method outlined under Sampling Protocol 4 was the most suitable fingermark sampling method for the time-course experiments explained in Chapter 6.

Chapter 6: Analysis of squalene and its transformation by-products in latent fingermarks by ultra-high-pressure liquid chromatography- high-resolution mass spectrometry (UHPLC-HRMS)

6.1 Introduction

As discussed in Chapter 1, degradation of the fingermark residue impairs the effectiveness of most of the current fingermark detection techniques, which has an undesirable impact on forensic investigations. While some studies have been devoted to understanding the mechanism of degradation processes to mitigate those limitations,[61-62, 73, 76, 251] several other studies have focused on developing novel techniques for the detection of aged deposits.[6, 20-21, 25, 190, 252-253] One key approach in this direction is to identify relatively stable compounds in initial composition, or transformation by-products in aged composition, that pose suitable functional groups for targeted visualisation.

In this context, there has been much interest in studying fingermark compositional variation over time using chromatographic techniques on both porous[19, 90, 132] and non-porous substrates.[20-21, 25, 87] An ideal biomarker for targeted visualisation of aged deposits must be readily present in any deposit regardless of the donor characteristics and across a large population. Except for one study,[90] all other chromatographic investigations have identified squalene as the single sebaceous compound detected in abundance in almost every sample, even among an extensively large donor pool.[19, 92-93, 100-101, 132] To this end, investigating squalene and its transformation by-products over time to identify molecular biomarkers as potential targets for fingermark visualisation is a rational approach.

6.1.1 Squalene in human skin secretions

Squalene is an unsaturated triterpene aliphatic hydrocarbon that participates as an intermediate product in the biosynthesis of cholesterol in the human body.[254-255] It is found at significant levels only in sebaceous secretions and accounts for 10-15% of the total sebum lipids.[256-260] The concentration of squalene in skin surface lipids is greater in areas such as the forehead, chest, and back, where there is high sebaceous gland activity.[255] The level of squalene on skin changes in dermal conditions such as psoriasis, atopic dermatitis and acne.[261-262] Research has also found that individuals under caloric restriction display elevated levels of squalene in skin secretions while the total sebum excretion rate was decreased.[122] Therefore, it was postulated that the nutritional status of individuals could be inferred by analysis of skin surface lipids. Although the key role of squalene in sebum has not been recognised yet, it plays multiple functions such as regulation of the immune system and skin microflora.[263-265] Research has also suggested that squalene prevents undesirable lipid peroxidation on the skin by quenching singlet oxygen produced as a result of excitation of photosensitising molecules by UV radiation.[266]

6.1.2 Studies into transformation by-products of squalene

Squalene in skin secretions undergoes decomposition into several oxygenated forms and breakdown products under different stressors such as UV, environmental oxidants, and skin microflora (Figure 6.1).[255] As skin is frequently exposed to direct sunlight, UV irradiation is the main contributor to the oxidation of skin surface lipids.[267-268] This decomposition is facilitated by the presence of six unconjugated double bonds with *trans* geometry and high concentration in skin surface lipids.[259, 268-270] Investigations on human skin have identified squalene monohydroperoxide (SQ-OOH) as a primary oxidation by-product.[266, 268, 270-271] It is believed that the accumulation of SQ-OOH could be responsible for inflammatory skin disorders such as skin cancer and ageing.[266, 269, 272-273] Squalene peroxidation can yield various positional isomers of monohydroperoxide due to the presence of six unsaturated moieties.[268, 270] Nakagawa *et al.* investigated these positional isomers and found that the total concentration of SQ-OOH isomers on forehead skin increased approximately three-fold after 3 h of sunlight exposure, with 6-SQ-OOH, 11-SQ-OOH, and 2-SQ-OOH detected in high concentrations (24, 21, and 17 mol% respectively). Mountfort *et al.* studied the oxidation of squalene in solution with the presence and absence of a photo-oxidiser.[20] They identified squalene hydroperoxides ranging from squalene dihydroperoxide (SQ-$[OOH]_2$) to squalene pentahydroperoxide (SQ-$[OOH]_5$) as a result of further oxidation of SQ-OOH (Figure 6.1). They were able to detect SQ-$[OOH]_4$ and SQ-$[OOH]_5$ even after 20 days in solution in the absence of the photooxidizer, which suggests these compounds could be potential targets for the visualisation of aged fingermarks.[20]

In addition, oxidation of squalene yields a series of isomers of squalene epoxide (SQ-epoxide).[20, 274] In Mountfort's study, both SQ-OOH and SQ-epoxide were identified as readily formed but short-lived species, where SQ-OOH was rapidly oxidised to more highly substituted SQ hydroperoxides.[20] While Luca *et al*. identified four isomers of squalene epoxide, positional isomers were not characterised.[274] They detected trans,trans-farnesal as another oxidation by-product of squalene, noting the difficulty of identification of squalene by-products due to the extreme reactivity and consequent short-lifespans of the intermediates.[274] Photo-oxidation of squalene by exposure to UV irradiation can induce the formation of smaller volatile molecules such as formaldehyde, malonaldehyde, acetaldehyde, and acetone.[269, 275] Oxidation of squalene films under ozone was studied by Petrick and Dubowski where long-chain aldehydes and ketones were detected as surface products while formaldehyde, 4-oxopentanal, glyoxal, and pyruvic acid were recognised as volatile compounds.[276]

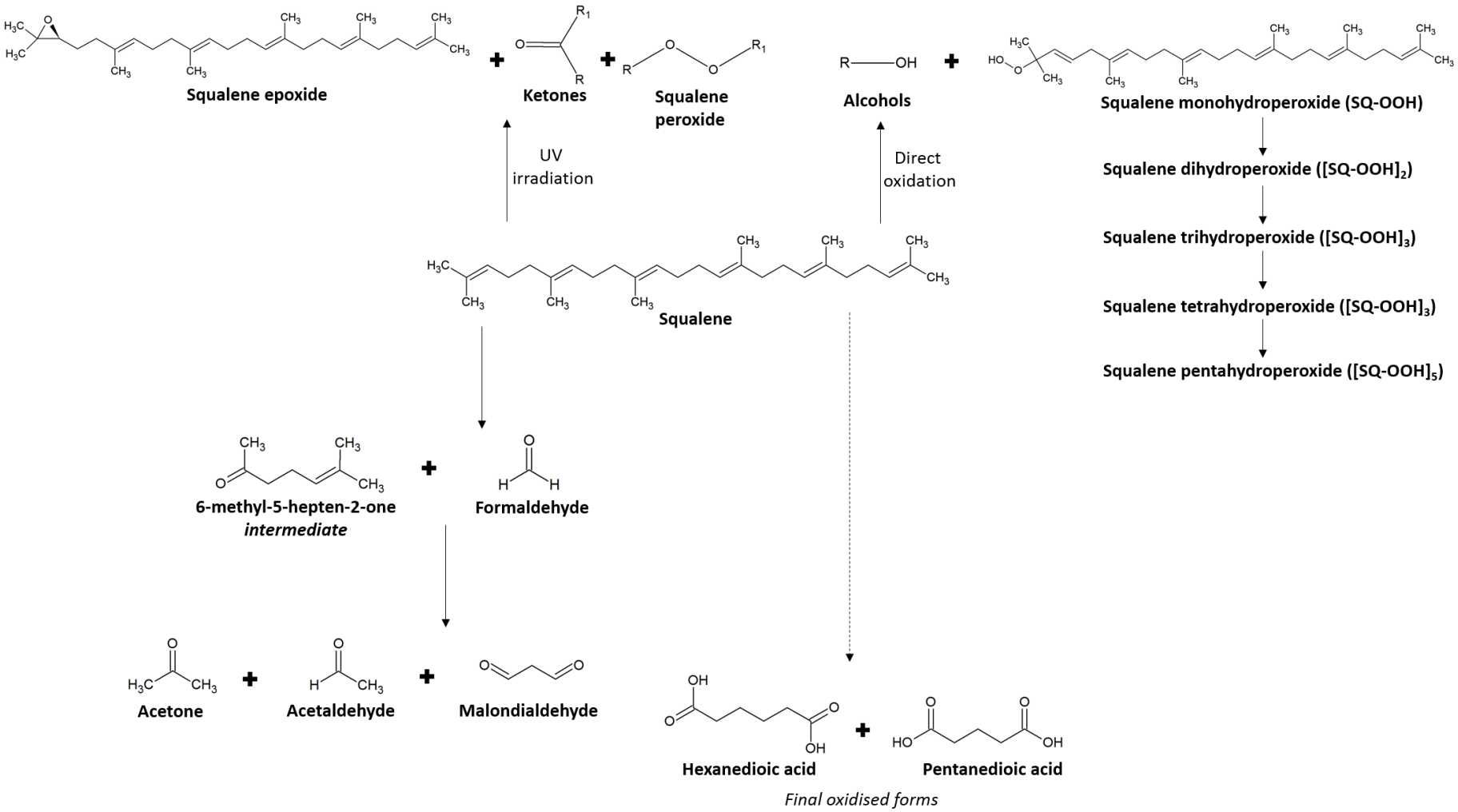

Figure 6.1 Transformation of squalene into various oxygenated derivatives and breakdown products including UV irradiation and direct oxidation. Based on Cadd *et al.*[84]

6.1.3 Transformation of squalene over time in latent fingermarks

Some of these transformation by-products of squalene have been identified in the chromatographic analysis of fingermark residue.[20, 90-91, 101] Mong *et al*. speculated the presence of oxidation by-products of squalene in relatively fresh (1-day old) fingermarks, yet their presence was not confirmed by MS library comparison.[90] One such suggestion was a cyclised product of squalene in the pathway of conversion to a steroid precursor.[90] This product was observed in all samples in which squalene was abundant. Mountfort *et al.* were the first to carry out a preliminary study to identify oxidation by-products of squalene in fingermarks from one donor.[20] Both SQ-OOH and SQ-epoxide were formed within 1 day in samples which were deposited on glass and aged under exposure to light. These products were found to increase in concentration between 1 and 5 days after deposition. However, as SQ depleted from residues, both SQ-OOH and SQ-epoxide were barely detectable in 7-day old samples.[20]

Girod and Weyermann recently identified 6 oxidation by-products of squalene by examining the mass spectra and comparing with the oxidation products described by Petrick and Dubowski.[91, 276] Four of them; 6,10-dimethyl-5,9-undecadien-2-one (geranyl acetone), 5,9,13-trimethyl-tetradeca-4,8,12-triene-al (TTT), 4,8,13,17,21-tetra-methyl-octadeca-4,8,12,16,20-pentaene-al (TOP), and 4,9,13,17-tetramethyl-octadeca-4,8,12,16-tetraeneal (TOT) were detected in all fresh residues deposited by 25 donors on glass microfiber filters. Two products, however, were identified as "possible" oxidation products as no confirmation could be made based on the literature.[91] Centred around their preliminary findings, Girod *et al.* further investigated ageing of these products (TTT, TOP, and TOT) with the intention of constructing ageing models with the use of chemometrics.[101] Six lipid compounds were identified as major influential factors on the results, with four being squalene and related oxidation products (TTT, TOP, and TOT). The three oxidation products alone influenced discrimination of samples based on their age which were deposited on two separate months of a year, highlighting their significance to fingermark chemistry. Although the samples were aged up to about a month, the longevity of the oxidation products was not clearly presented as data interpretation was mainly focused on ageing models, but not necessarily on the durability of individual compounds.[101]

6.1.4 LC-MS analysis of squalene and its transformation by-products

In early studies, oxidation products of skin surface lipids have been indirectly probed by TLC,[277] gas chromatography based techniques,[259, 269, 274-275] and liquid chromatography coupled with chemiluminescence detection (LC-CL).[272-273] In these investigations, the exact origin of the oxidation products was unclear.[273] GC based analysis often required derivatisation of samples to enable detection of polar oxidation products,[259, 269, 274-275] which may induce unintended oxidation.[20] While Girod and Weyermann identified few oxidation by-products of squalene using GC-MS without derivatisation, SQ-hydroperoxides were not identified.[91] Mudiyanselage *et al*. and Mountfort *et al*. successfully demonstrated direct and simultaneous analysis of squalene and its oxidation products by LC in conjunction with UV and MS detection.[20, 268]

HPLC-MS detection gives better selectivity than the conventional HPLC-UV detection as unresolved peaks can be isolated by monitoring only a selected mass-to-charge ratio (*m/z*).[179] In addition, it offers superior sensitivity as the typical mass limit of detection (LOD) is less than 1 pg.[179] The ionisation source and the mass analyser are the key components of any MS system. In liquid chromatography, electrospray ionisation (ESI) and atmospheric pressure chemical ionisation (APCI) are the most frequently used ionisation techniques, as both are soft ionisation techniques.[179] Soft ionisation yields protonated molecular ion in mass spectra since it causes little or no in-source fragmentation.[278] The choice of the ionisation source largely depends on the polarity and the thermal stability of the analytes. While ESI is better suited for polar and ionic molecules, APCI is preferred for poorly functionalised non-polar molecules.[278]

The combination of LC with one mass spectrometer does not provide enough resolution for some complex mixtures, thus more mass spectrometers are coupled to LC which is referred to as LC-MS/MS or LC-tandem mass spectrometry.[179] Traditional tandem mass spectrometers (transmission MS/MS) such as triple quadrupoles (QqQ) physically transmit ions from the first stage mass spectrometer to the second, which causes a loss of ions.[279] This was a significant drawback when multiple stage fragmentation was performed (MS^n).[279] In recent years, ion trapping techniques have emerged as powerful tools of MS/MS analysers, eliminating such problems.[280-281] Quadrupole ion trap (QIT) and Fourier transform ion cyclotron resonance (FT-ICR) mass spectrometers fall under this category.[279] While QIT uses a radio frequency electric field to control ion trapping, FT-ICR uses a combination of magnetic and electric fields.[279] Both QqQ and QIT are not renowned for effective structural elucidation as they are generally operated at unit mass resolution.[282] Patented to Thermo-Fisher Scientific,

Orbitrap™ mass analysers combine QIT with a high-precision ion-trap.[282] Frequencies generated due to oscillation of ions back and forth within an electrostatic field inside the ion-trap is being measured which in turn converted to a mass spectrum by Fourier transformation.[279, 281] Orbitrap™ analysers offer superior resolving power than QIT and quadrupole-time-of-flight (Q-TOF), while maintaining mass accuracy below 2 ppm with internal calibration.[282] Moreover, this hybrid system enables acquisition of MS data using multiple scan modes in a single analytical run.[282] Owing to these strengths, Orbitrap™ mass analysers facilitates unprecedented structural elucidation *via* high-resolution multi-stage fragmentation experiments.[282]

6.1.5 Aims

This chapter describes the development and application of an ultra-high-pressure liquid chromatography-high resolution Orbitrap™ MS (UHPLC-HR Orbitrap™ MS) method for simultaneous and direct analysis of squalene and its transformation by-products formed in fingermarks due to different environmental conditions. Compositional variations of transformation by-products were assessed in relation to the initial concentration of squalene to identify potential targets for visualisation of aged deposits. In addition, some oxidation by-products of cholesterol were tentatively identified.

6.2 Experimental

6.2.1 Chemicals

Squalene (≥98%; Sigma-Aldrich, USA), squalene-d_6 (98%; Toronto Research Chemicals, Canada), acetonitrile (>99.9%; VWR Chemicals, France) and dichloromethane (≥99.9%; Honeywell Inc., USA) were used as received. The ultra-pure water (H_2O) used for laboratory purposes as well as LC mobile phase was purified using an ion exchange system (IBIS Technology, Perth, Australia), followed by Elga Purelab Ultra System (High Wycombe, UK). A set of standard solutions of squalene was prepared in 1:1 v/v acetonitrile (ACN): dichloromethane (DCM) in the concentration range of 0.1-25.0 ppm (0.1, 1.0, 4.5, 12.0, and 25.0 ppm). A standard solution of 20.26 ppm squalene-d_6 was also prepared in the same solvent mixture. All standard solutions were stored in amber glass vials wrapped in aluminium foil below -18 °C to avoid degradation and solvent evaporation.

6.2.2 Sample deposition

6.2.2.1 Monitoring degradation of squalene over time (without knowing the initial composition)

Natural fingermarks were obtained from three donors (D1F1, D2M1, and D12F6) on aluminium foil strips following the procedure outlined under Sampling Protocol 1 in section 5.2.3.1.2, Chapter 5 (uncontrolled deposition pressure). Samples obtained from both hands at a given time were considered as duplicate samples. A maximum of three sample sets were collected from each donor within the course of a working day (9.00 am-5.00 pm). This procedure was repeated throughout a week.

To investigate the influence of the fingermark matrix over the degradation process, three 10 µL aliquots of 50.0 ppm squalene standard were deposited as three separate spots on an aluminium strip. Eight strips were prepared in a similar fashion.

6.2.2.2 Investigation of transformation of squalene (with known initial composition)

The procedure for sample deposition was chosen as per the experimental results described in Chapter 5. Natural fingermarks from three donors (D1F1, D2M1, and D11M6) were obtained on aluminium foil strips while controlling deposition pressure as per the procedure outlined under Sampling Protocol 4, section 5.2.3.1.5, Chapter 5. After rubbing hands together, two samples from both hands were obtained (one set of samples) and three such sets were obtained from each donor per storage condition. This procedure was repeated over two consecutive weeks to obtain nine sample sets from each donor (54 samples in total, 18 samples × 3 donors). A time interval of at least 30 min was maintained in between each sampling time. Demographics of the donors are detailed in Chapter 2. Recent use of cosmetics, personal care products (moisturisers, hair care products and hand and body lotions) and nutritional supplements of donors were recorded at each sampling time.

6.2.3 Sample storage

All samples, except those that were extracted within 5 h following deposition (t=0 samples), were stored under three different storage conditions: light, dark and underwater in dark. Details of these conditions are listed in Chapter 2.

6.2.4 Sample preparation

Squalene standard spots deposited on aluminium foil strips were extracted using three solvent combinations: 100% ACN, 100% DCM, and 1:1 v/v ACN:DCM. Two different sizes of extraction vials; 1.75 mL (Thermo Fisher Scientific, Australia) and 4 mL (Grace Davison Discovery Sciences, Australia) glass screw-top vials were then tested to obtain optimal extraction efficiency.

Aluminium strips were rolled and inserted into extraction vials pre-rinsed with DCM. 0.7 mL of extraction solvent was added, and vials were screw capped using matching caps lined with polytetrafluoroethylene. Vials were wrapped in aluminium foil to avoid exposure to light during sample extraction. Samples were extracted by sonication and vortex mixing as outlined in Chapter 5. The extracts were transferred to 2 mL amber autosampler vials (Agilent Technologies, USA) and sealed with matching polytetrafluoroethylene/silicon bonded screw caps. Sample blanks were prepared for every batch of samples using aluminium foil strips bearing no deposits.

6.2.4.1 Monitoring degradation of squalene over time (without knowing the initial composition)

One sample set (duplicates) per donor was extracted on the same day of deposition (t=0 samples) and others were aged under the pre-determined storage conditions. The analysis time intervals were t=1 and t=5 days. After ageing, they were extracted and analysed in duplicate. Aluminium strips bearing standard spots of squalene were aged up to 1 day under the same storage conditions and analysed in duplicate. The extraction procedure was same as mentioned in the above section.

6.2.4.2 Investigation of transformation of squalene (with known initial composition)

One sample of a given set (a sample from one hand) was extracted within 5 h since deposition and the remaining sample (sample from the other hand) was extracted after ageing under a selected storage condition (light or dark or underwater) up to the desired time interval (1 or 5 or 7 days). Aluminium strips were rolled and inserted into 4 mL clear glass vials. Samples aged underwater were air dried on paper towels in dark for 5-10 min before inserting into extraction vials. Then 0.6 mL of 1:1 v/v ACN:DCM was added followed by 0.1 mL of the 20.3 ppm squalene-d_6 surrogate standard. Samples were extracted by sonication and vortex mixing as mentioned in Chapter 5. The extracts were transferred to amber autosampler vials and sealed. Sample blanks were prepared for every batch.

6.2.5 Chemical analysis

Chromatographic analysis was performed using a Dionex Thermofisher Ultimate 3000 UHPLC system coupled to a Q-Exactive Focus Thermo-Fisher Orbitrap mass spectrometer via an APCI (eV+) ion source. The chromatography and mass spectrometry parameters were adapted from the work reported by Mountfort *et al.*[20] to accommodate the use of different equipment. The UHPLC system was equipped with a solvent degasser unit, a quaternary pump, and a 100 well-plate autosampler. The injection volume was 5-10 µL. An Acquity C18 column (Waters USA, 2.1 × 100 mm, 1.7 µm particle size) was used for the separation of compounds. A mobile-phase gradient was employed as follows: 1:1 v/v ACN:H_2O for 10 min, then increased to 100% ACN up to 20 min and held at this up to 25 min, and then re-equilibrated for 5 min at the initial conditions. A flow rate of 0.4 mL/min was maintained throughout the chromatographic run. MS conditions are listed in Table 6.1.

Table 6.1 APCI (+) and MS tuning parameters used for the detection of squalene and its transformation by-products.

APCI-Orbitrap MS parameters	Setting
Vaporization temperature	375 °C
Spray voltage	5 kV
Sheath gas flow rate	30 (arbitrary units)
Aux/sweep gas flow rate	5/0 (arbitrary units)
Discharge current	4.5 µA
Capillary temperature	237.5 °C
RF lenses	70 V
AGC target 10^6	MS Scan
AGC target $5e^4$	MS/MS
Max injection time	auto
Dynamic exclusion	auto
Collision Energy	30 eV
MS acquisition mode	Full scan (70-1000 amu @70K resolution) + ddHRMS^2 (@17.5K resolution) in "discovery mode" Full scan (150-600 amu @70K resolution) + ddHRMS^2 (@17.5K resolution) with inclusion list

6.2.6 Data analysis

Identification and quantification of squalene and potential transformation by-products were performed using Thermo Xcalibur QualBrowser 4.0.27.13 and TraceFinder 4.2 software. For the identification of unknown transformation by-products, the *m/z* ratio of potential peaks was identified using the "ion map" function in Xcalibur, which plots retention time vs *m/z* vs peak intensities (Figure 6.2). In addition to this, the *m/z* values corresponding to the most intense hundred peaks were also extracted from the chromatographic traces and evaluated. The *m/z* ratio of positively identified peaks was used as the base peak *m/z* to confirm the presence of the particular compound with a mass tolerance of 5 ppm and a mass precision of 4 decimal places. Measured masses of the positive peaks were then used to generate molecular formulas where measured mass and the isotope pattern were compared against the theoretical mass of the predicted compound (with a relative error <5 ppm) and the simulated isotope pattern. When possible, MS^2 spectra were also used to confirm the structure of the newly identified transformation by-products. Absolute quantification of squalene was performed as per the procedure outlined in Chapter 5, section 5.2.2, using the software package TraceFinder 4.2. Relative quantification of by-products was performed by normalising the peak area of the by-product to that of the deuterated standard.

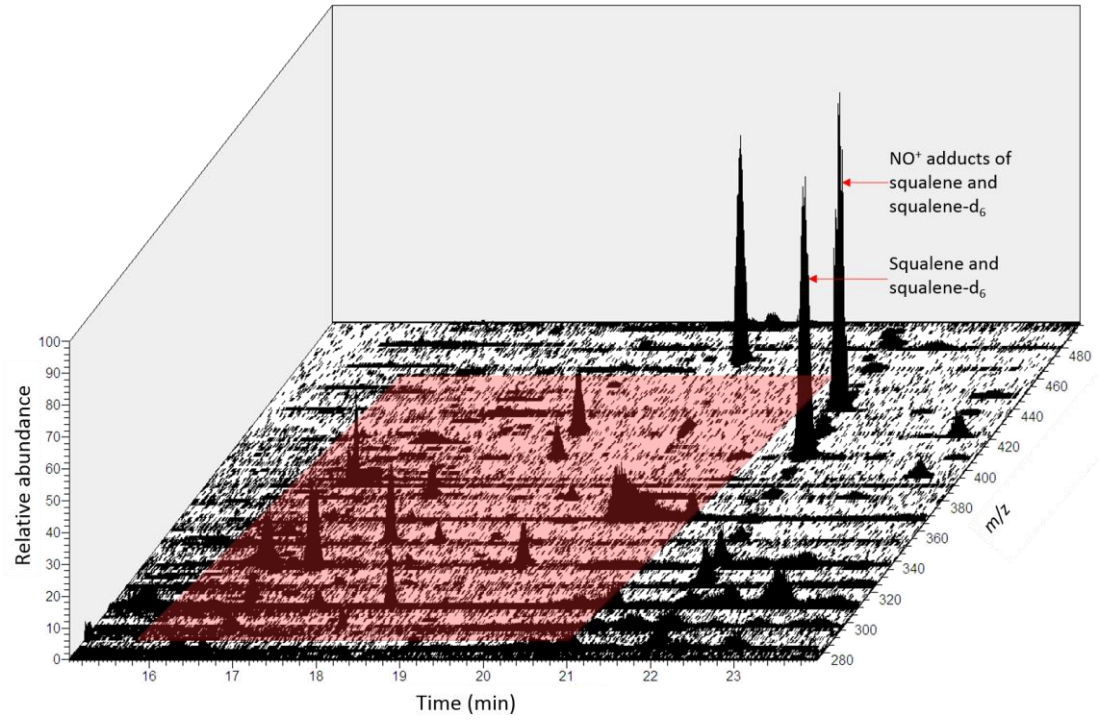

Figure 6.2 A sample ion map showing squalene, squalene-d_6 and the degradation by-products (in the red shaded area) identified in the study.

6.3 Results and discussion

6.3.1 Preliminary considerations

The extraction procedure and the conditions for the chromatographic separation reported by Mountfort *et al.* were used as a starting point for this study.[20] In the initial stage, suitability of ACN, DCM, and 1:1 v/v ACN:DCM as the extraction solvent was investigated. Extraction was initially carried out with 0.7 mL of the extraction solvent in 1.75 mL vials. The recovery of squalene using ACN and DCM was 56% and 104% respectively. Although Mountfort *et al*. used ACN for their sample extraction (150 µL), in the present study, it was observed that squalene was immiscible in ACN. Despite the improved recovery of squalene with DCM, 100% DCM caused peak fronting. This is due to disturbance caused to the mobile phase equilibrium in the column as the mobile phase composition was ACN/H_2O.[283] The third solvent combination of 1:1 v/v ACN:DCM yielded a recovery of only 26%. Nonetheless, when the same solvent combination was used in a 4 mL extraction vial, a recovery of 113% was achieved. These results suggest that the correct size of the extraction vial was important to achieve optimal extraction. The aluminium foil was tightly packed inside the small 1.75 mL vial, which impeded proper contact between the solvent and the sample leading to incomplete extraction.

6.3.2 Degradation of squalene over time

6.3.2.1 Without knowing the initial composition

Although previous chromatographic studies have detected squalene in abundance in fresh fingermarks, they have used charged deposits except for Croxton and co-workers.[87] While Mountfort *et al*. investigated oxidation by-products in aged fingermarks for the identification of potential biomarkers, results of this study may not represent real-life aged samples due to the use of charged deposits. To this end, this study, for the first time, investigated the transformation of squalene in natural fingermarks deposited on non-porous surfaces.

Figure 6.3 demonstrates the compositional variation of squalene in duplicate samples obtained from both hands and squalene standard spots deposited on aluminium foil which were aged under different storage conditions. It should be noted here that the luminosity of the office environment used to store the fingermark samples in this study was not measured. Hence, the “light condition” discussed in this chapter resembles an office space which was exposed to fluorescent bulbs for more than 8 h of the day and natural light during the daytime. Although degradation of squalene in fingermarks aged under light condition followed the same trend as the standard spots, the fate of squalene was not clear in other

storage conditions. The average amounts of squalene in final extracts (0.7 mL) of samples aged under dark and dark underwater conditions from both donors D1F1 and D2M1 increased after 1 day while the standard spots displayed a reduction. As squalene is highly sensitive to photo- and air-oxidation, this result could due to following reasons; (i) There could be reactions taking place within the residue that contribute to generation of squalene with time;[90] or (ii) the aged samples initially had high amounts of squalene hence the reduction over time was not prominent against the "initial composition" (a different sample set with a different amount of squalene).

As discussed in Chapter 5, the intra-donor variability is a key issue in fingermark research which may have predominantly contributed to these results.[92-93, 100] This practical difficulty of comparative quantitation of fingermark components over time using destructive techniques has been highlighted in previous studies,[19, 90, 100] yet the approach undertaken here has been widely employed throughout fingermark research due to limitations of other techniques.[19-21, 90, 93] While these studies have greatly contributed to current understanding of fingermark composition, this approach may have confounded the recognition of potential trends in the degradation of fingermark components. As such, the work reported in Chapter 5 was carried out to identify strategies to produce two samples with a similar composition of squalene, such that the initial concentrations of squalene in all aged samples are known within a reasonable level of certainty.

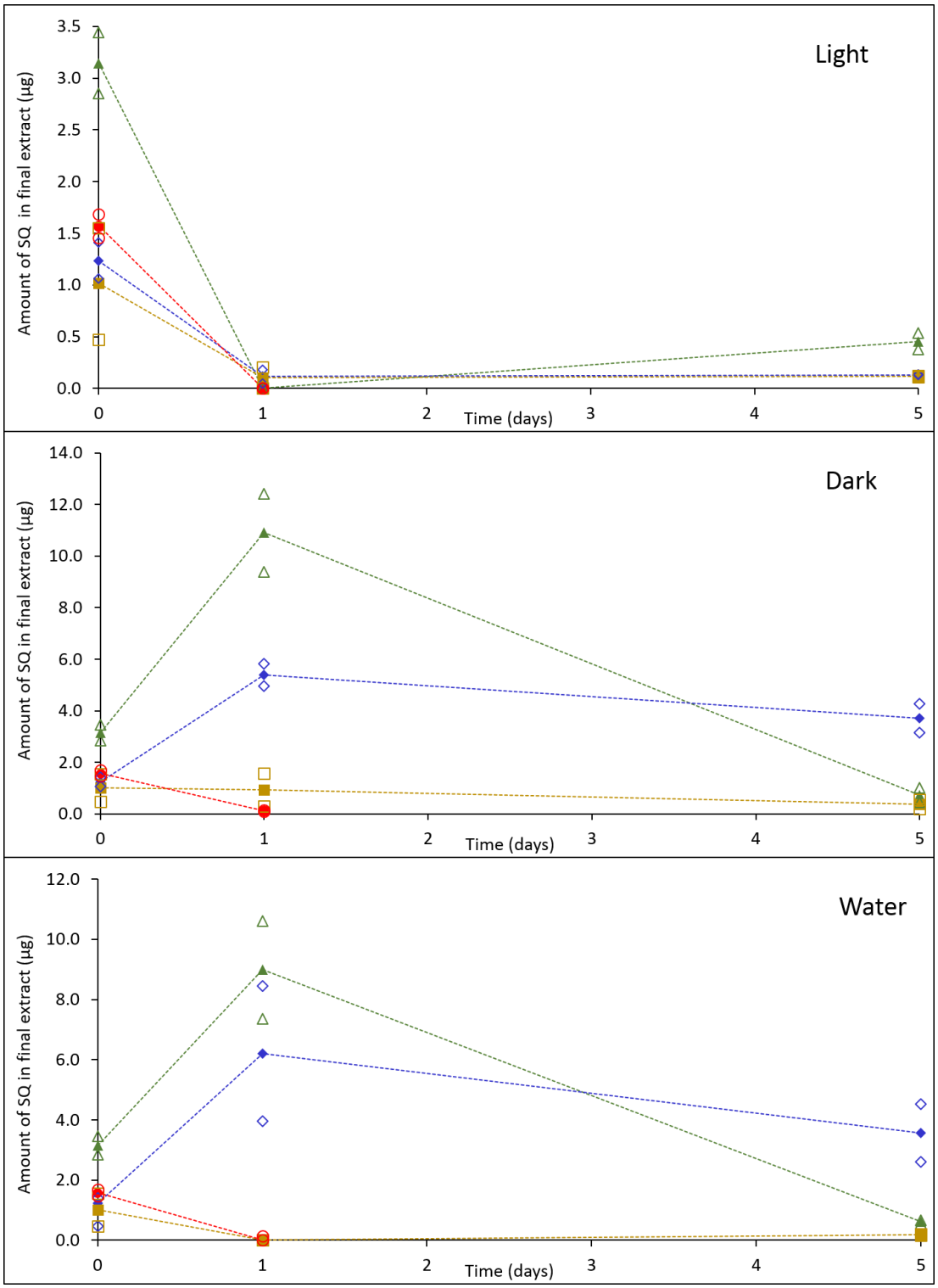

Figure 6.3 Degradation of squalene over time (1, 5, and 7 days) in fingermarks and in standard spots deposited on aluminium foil. Absolute values of duplicate samples are presented in bullets which are not filled, and the average values are presented in filled bullets. Data for donor D1F1 is in green, D2M1 in blue, D12F6 in brown, and standard spots in red. The connecting lines are only to assist visualisation of possible trends of degradation and do not represent the continuous variation of the same sample over time.

6.3.2.2 Investigation of degradation of squalene with known initial composition

As shown in Figure 6.4, squalene was detected in all samples that were analysed for initial composition and was within a range of 0.20-11.32 µg/5 fingertips. It should be noted here that, according to the results of Sampling Protocol 4 in Chapter 5, the homogeneity of samples obtained from both hands at a time with respect to the amount of squalene is subjected to a percentage difference of approximately 20%. This means that each initial composition and the corresponding initial composition of the aged sample can be different from each other by approximately 20%. Presumably, largely due to this variability, the fate of squalene after ageing for 1 day under light conditions was not conclusive. Only the donor D2M1 showed a 22% reduction from the initial amount of squalene while donors D1F1 and D11M6 showed a 66% and 102% increase respectively. However, a clear reduction in the amount of squalene in 5-day and 7-day old samples from all donors was visible in Figure 6.4.

In contrast to the standard spots mentioned in the previous section where squalene was not detected or tentatively detected (LOD 0.09 µg/mL, limit of quantification, LOQ 0.30 µg/mL) in 1-day old samples under any storage condition, squalene was still detectable in aged fingermarks, especially t=1 and 5-day old samples stored under dark and underwater. Research into the oxidation of olive oil has found that the degradation of squalene is delayed by the presence of α-tocopherol (an antioxidant molecule found in vitamin E).[284-285] Since α-tocopherol is a common ingredient in cosmetics,[286] this may retard the degradation of squalene in fingermarks of those who use such products. Moreover, γ-tocopherol; another antioxidant molecule of Vitamin E[287] not present in cosmetic formulations, has been detected in fingermarks.[91] This suggests that these antioxidant molecules of either exogenous or endogenous origin may contribute to slow the degradation of squalene in fingermarks. Hence, the longevity of squalene in samples from donor D1F1 is possibly due to regular use of cosmetics and hand cream enriched with vitamin E. This result demonstrates the influence of the fingermark matrix over the degradation process.

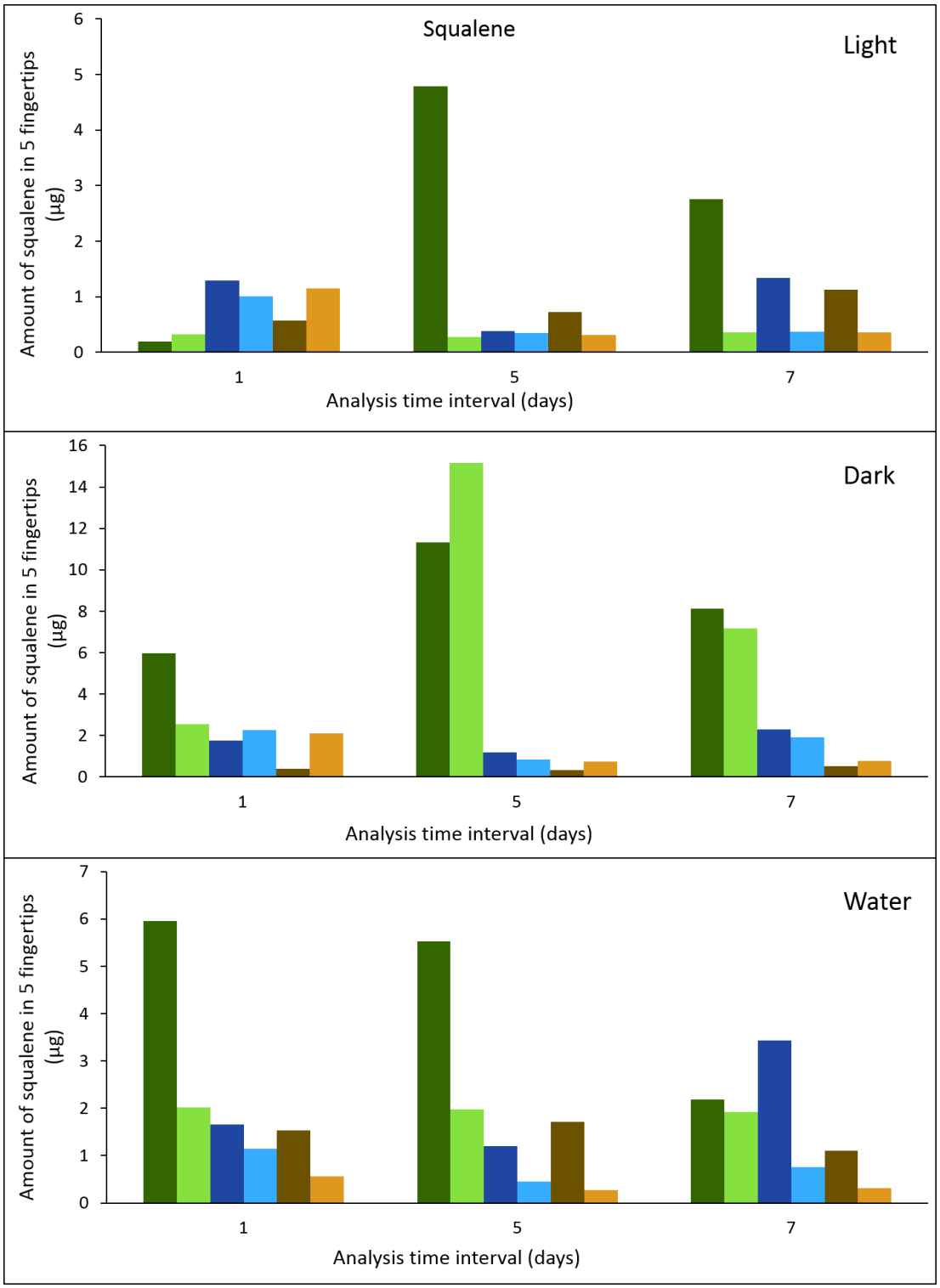

Figure 6.4 Degradation of squalene over time (1, 5, and 7 days) in fingermarks in relation to their initial composition. Data for donor D1F1 is presented in green, D2M1 in blue and D11M6 in brown. Each darker colour bar represents initial composition and lighter colour bar represents corresponding aged composition.

In Mountfort's study, oxidation of squalene was faster in fingermarks than in standard solutions (*in vitro*) because of approximately 100-fold higher starting concentration of squalene in solution. Based on the preliminary findings of this study, the amount of squalene deposited on foil strips (approximately 1.5 µg) was chosen to be comparable to natural fingermarks on the same substrate. Hence, the faster degradation rate of standard spots may be also due to differences in the morphology of fingermarks and spots. Fingermarks are comprised of small droplets of material while standard spots were not. As demonstrated in Chapter 4, depending on the lipid-to-eccrine material ratio within droplets, lipids may co-exist in aqueous droplets as an emulsion. The observed slower degradation rate of squalene in fingermarks consequently could be a result of this complex spatial distribution of material within droplets.

The degradation rate of squalene in the dark was much slower than that under light conditions. All three donors showed a greater than 69% reduction of the initial amount of squalene after ageing for 7 days under the light, while two of three donors exhibited a lower than 17% reduction after ageing for the same period under dark. In the study reported by Archer *et al*. where charged fingermarks were deposited on filter paper, squalene was detectable in some samples even after 33 days when they were stored in dark.[19] Bearing in mind the number of digits deposited per sample in their study (1.5 digits), the greater longevity of squalene in Archer's study can be attributed to the effect of substrate porosity and the type of the deposits (charged vs natural) analysed.

To the best of this author's knowledge, transformation kinetics of squalene underwater in fingermarks has not been explored before. In forensic investigations, wetted surfaces are known to be challenging surfaces on which to develop fingermarks.[288] Studies have found the small particle reagent (SPR) technique to be more effective (if the articles are developed without leaving them air-dry) among other popular techniques applied on non-porous surfaces.[288-290] This technique involves a surfactant and a suspension material where the enhancement is achieved upon the interactions formed between fatty components of the residue and hydrophobic tails of the surfactant.[290-292] To this end, investigation of the degradation of lipid molecules underwater is of high significance.

Squalene degraded in all samples when they were stored underwater. The percentage reduction of squalene from the initial concentration for donors D1F1, D2M1, and D11M6 were 66%, 31%, and 63% for t=1-day samples; 64%, 62%, and 84% for t=5-day samples; and 12%, 78%, and 71% for t=7-day samples respectively. In a comparison of percentage reduction of t=7-day samples aged underwater to that under dark conditions, relatively higher percentages are observed for underwater conditions. As water baths containing samples were covered with foil to avoid exposure to light, this result suggests that water has accelerated the degradation process. This could be due to the removal of water-soluble eccrine material from the fingermark droplets which increased the surface area of lipids to interact with dissolved oxygen. It was previously thought that hydrophobic fingermark lipid compounds are preserved under aquatic environments compared to dry conditions,[62] thus it could be assumed that they could be targeted for the visualisation of fingermarks on items recovered from aquatic environments. However, according to the results of this study, aquatic conditions are indirectly detrimental to the major hydrophobic lipid compound in fingermarks; squalene.

6.3.2.3 Identification of transformation by-products

A range of products was identified in the mass spectra including oxidation by-products of SQ and cholesterol. Identification based on fragment ions of SQ and most of its oxidation products was performed as per results reported by Mountfort *et al*.[20] The relative quantification of SQ-OOH and SQ-epoxide was based on the fragment ions at *m/z* 425.3780 and *m/z* 427.3938, respectively. As both products have a common fragment ion at *m/z* 409.3832, it was not used for quantification. The presence of 4,9,13,17-tetramethyl-octadeca-4,8,12,16-tetraeneal (TOT) was confirmed based on the ozonolysis mechanism of SQ proposed by Petrick and Dobowski,[276] and detection of this compound in fingermarks using GC-MS by Girod and Weyermann.[91] Positive identification of cholesterol in the sample extracts was confirmed through the following: (i) the mass accuracy of the observed parent ion *m/z* 369.3519 was less than 3 ppm from the theoretical mass-to-charge ratio of cholesterol ($[(M+H)-H_2O]^+$ correct elemental formula $C_{27}H_{45}$, *m/z* 369.3516), (ii) comparison of MS/MS spectra against NIST msms library (80% match), and (iii) comparison of the isotopes distribution of the observed parent ion against the simulated HRMS spectra of $C_{27}H_{45}$ (Appendix 3). Cholesterol oxidation products were identified based on the study reported by Raith *et al*. where five cholesterol oxidation products were identified in meat by liquid chromatography-atmospheric chemical ionisation/mass spectrometry (LC-APCI/MS).[293] Target products (TPs) detected only in samples from donor

D1F1 that did not show any correlation to the available amount of SQ were not further assigned, assuming that they were of exogenous origin or not derived from SQ. Compound eluted at 17.55 min were attributed to $(M+H)^+$ fragment of $C_{19}H_{34}O_4$ based on previous HRMS studies.[294-295] Table 6.2 shows fragment ions in the mass spectra used for target product identification and the ion map in Figure 6.2 shows all the degradation products detected.

Table 6.2 Compound identification based on fragment ions in the mass spectra under the established UHLPC-APCI/HR Orbitrap™ MS.

***m/z* of fragment ion**	**Retention time (min)**	**Fragment ion (target product)**	**Molecular formula of the fragment**	***m/z* error (ppm)**	**Tentative assignment/ comment**
207.1017	20.29		$C_{12}H_{15}O_3$	<1.3	Only in D1F1
257.2476	16.61		$C_{16}H_{33}O_2$	<1.6	Only in D1F1
312.3263	17.54		$C_{20}H_{42}ON$	<1.9	Not prominent in aged samples
313.3103	18.36		$C_{20}H_{41}O_2$	<1.5	Only in D1F1
317.2841	16.66	$[M+H]^+$	$C_{22}H_{37}O$	<1.9	TOT
327.2534	17.55	$[M+H]^+$	$C_{19}H_{35}O_4$	<1.7	$C_{19}H_{34}O_4$
355.2845	17.77-20.18		$C_{21}H_{39}O_4$	<1.7	Only in D1F1
367.3360	17.85	$[(M+H)-2H_2O]^+$	$C_{27}H_{43}$	<1.5	Cholesterol oxidation products
369.3519	20.33	$[(M+H)-H_2O]^+$	$C_{27}H_{45}$	<2.5	Cholesterol
385.3468	18.85	$[M+H]^+$	$C_{27}H_{45}O$	<1.1	Cholesterol oxidation products
409.3832	18.99	$[(M+H)-H_2O_2]^+$	$C_{30}H_{49}$	<1.7	SQ-OOH
		$[(M+H)-H_2O]^+$			SQ-epoxide
411.3988	21.95	$[M+H]^+$	$C_{30}H_{51}$	<0.8	SQ
417.4665	21.85	$[M+H]^+$	$C_{30}H_{45}D_6$	<0.93	SQ-d_6
425.3780	18.99	$[(M+H)-H_2O]^+$	$C_{30}H_{49}O$	<1.1	SQ-OOH
427.3938	18.99	$[M+H]^+$	$C_{30}H_{51}O$	<1.35	SQ-epoxide
473.3991	20.27		$C_{29}H_{51}O_3N_3$	<1.2	Not a by-product of SQ

Cholesterol oxidation products (Figure 6.5); 25-hydroxycholesterol, 5,6α-epoxycholesterol, and 7β-hydroxycholesterol have the same monoisotopic mass of 402.3498 Da ($C_{27}H_{46}O_2$), thus they cannot be distinguished based on the $[(M+H)-H_2O]^+$ (*m/z* 385.3604) fragment or the $[(M+H)-2H_2O]^+$ (*m/z* 367.3498) fragment.[293] In addition, the $[(M+H)-2H_2O]^+$ fragment of cholestane-3β-5α-6β-triol ($C_{27}H_{48}O_3$, monoisotopic mass 420.3604 Da) has the same *m/z* ratio; 385.3604 which is isobaric to the aforementioned compounds.[293] Collision-induced dissociation in tandem mass spectrometry only yields fragments due to loss of water which are nonspecific for characterisation.[293] As a result, APCI/MS is not capable of structure elucidation of these compounds, which in turn demands LC based separation.[293] Such LC separation was not initially planned and authentic standards of these compounds were not analysed as it was beyond the established objectives of the current study. Therefore, fragment ions of *m/z* 367.3498 and *m/z* 385.3604 were collectively attributed to oxidation by-products of cholesterol with no further assigning to individual compounds.

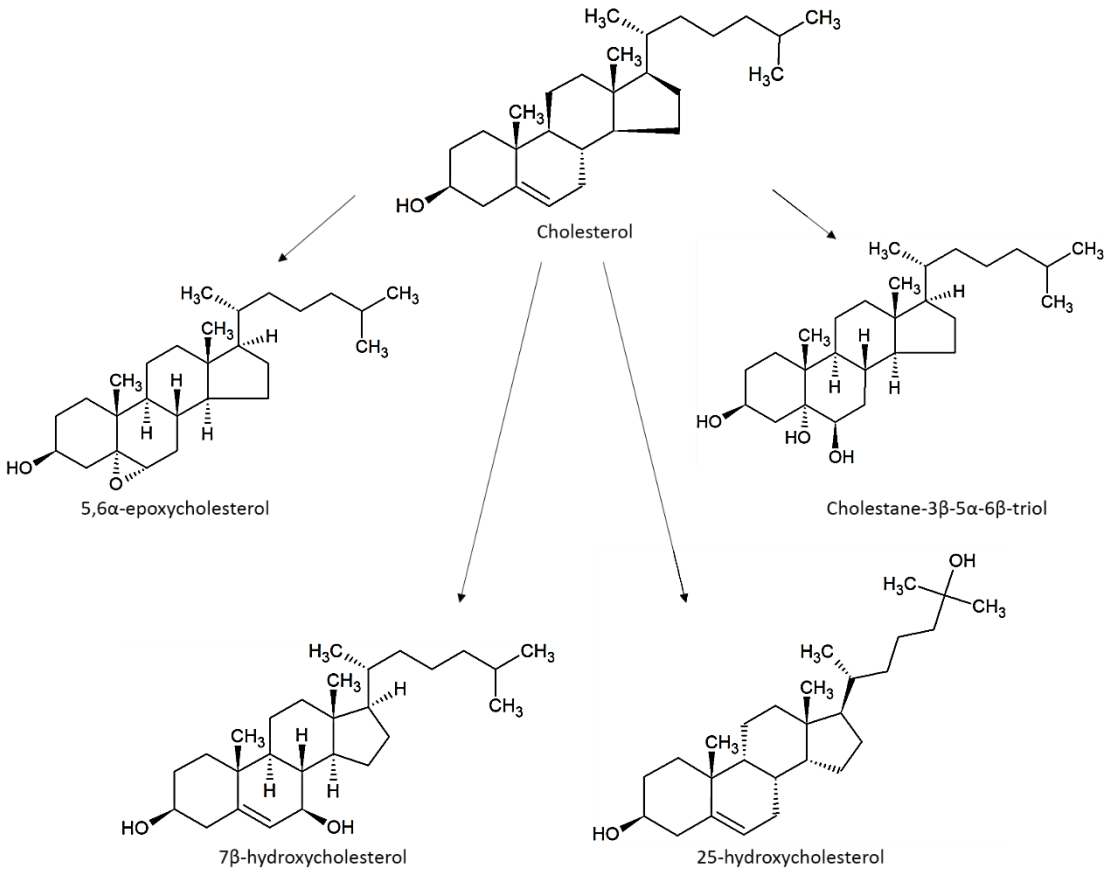

Figure 6.5 Some oxygenated forms of cholesterol based on Raith *et al.*[293]

6.3.2.4 Potential trends of transformation by-products over time

Figure 6.6 shows the relative quantity of SQ-OOH in both fresh and aged (t=1, 5, and 7-day) samples to demonstrate the formation/degradation of the by-product. It also shows the relative amount of SQ present at a given aged sample (t=1, 5, and 7-day), which enables comparison of the extent of transformation in relation to the availability of SQ in the system. Although Mountfort *et al.* observed an increase in the amount of SQ-OOH between 1 and 5 days of ageing under the light, this product was hardly detected in all samples aged under the light. SQ-OOH was detected in very small amounts in some of the fresh samples mostly from donor D1F1.

SQ-OOH was detected in some of the samples (t=5 and 7-day) aged under dark and water, presumably due to retardation of photo-oxidation in those environments. Mountfort *et al.* were unable to detect SQ-OOH only when SQ was no longer available for oxidation. Intriguingly, in this study, SQ-OOH was undetectable in all samples aged under light although SQ was still available for oxidation (at least in small quantities). Moreover, further oxidised forms of SQ-OOH (i. e. SQ-$[OOH]_n$) were not detected which suggests that SQ-OOH is extremely short-lived and may transform to oxidised products other than SQ-$[OOH]_n$.[274]

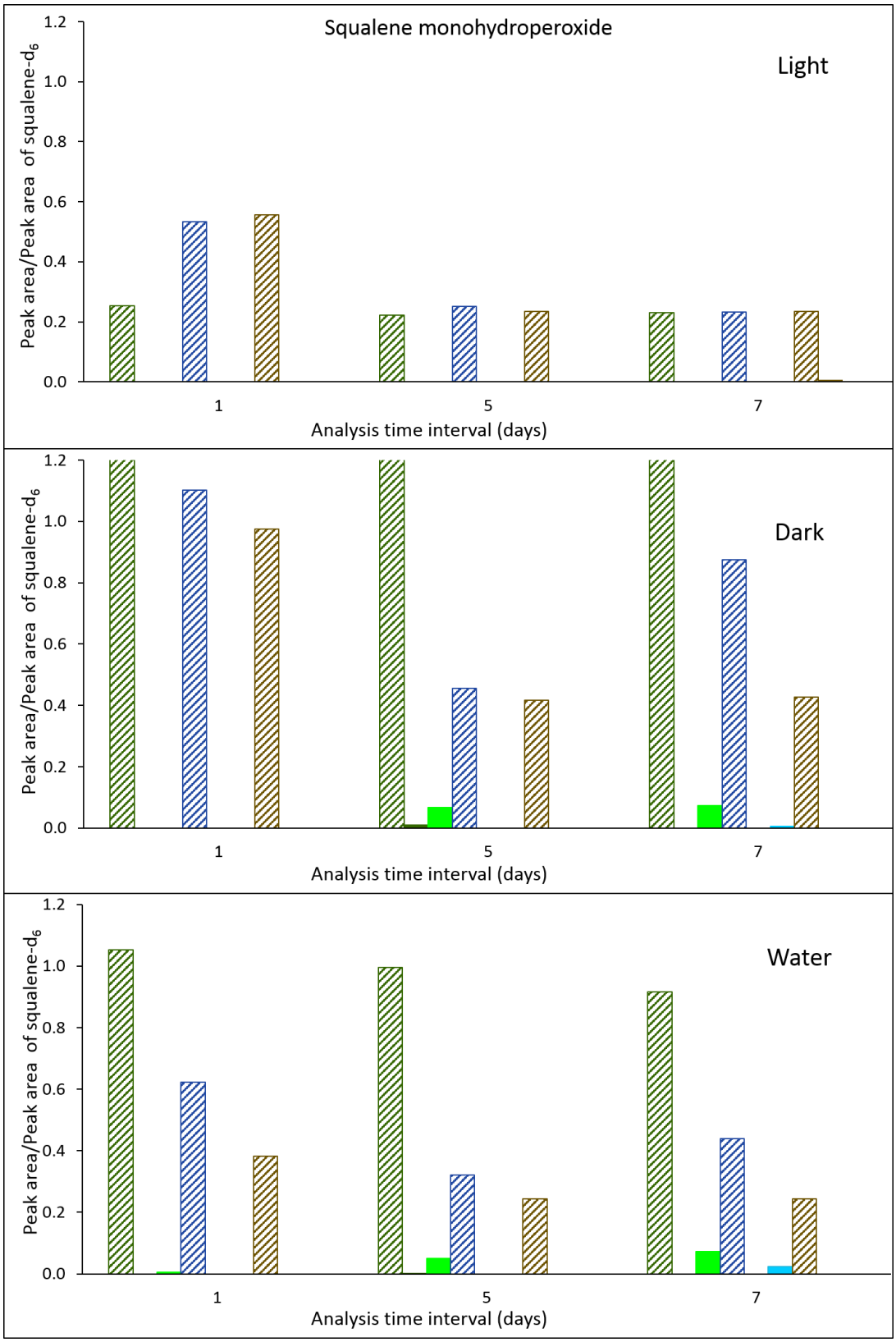

Figure 6.6 From left to right, relative amounts of squalene in aged samples (patterned filled bars), SQ-OOH in fresh samples (t=0, dark coloured green, blue, and brown bars), and SQ-OOH in aged samples (t=t, brighter coloured green, blue, and brown bars) of fingermarks from donor D1F1 (green), D2M1 (blue) and D11M6 (brown). Except patterned bars, most of the other bars are not visible as SQ-OOH was not detected in these samples. Y-axis of the graphs is not set to illustrate the maximum value of the data set.

Figure 6.7 shows the transformation of SQ → SQ-epoxide in samples aged under different storage conditions. Unlike SQ-OOH, SQ-epoxide was detected in all fresh samples and a general increasing trend was observed against the initial concentration in samples aged in the dark across all analysis time intervals. However, under light conditions, SQ-epoxide concentration increased only up to 1 day and then reduced markedly in t=5 and t=7-day samples. Since SQ was more depleted underwater than under dark, SQ-epoxide was also more depleted underwater. Highest amounts of SQ-epoxide in t=7-day samples were observed in samples from donor D1F1 due to considerable amounts of SQ available at those time intervals. In addition, although Mouzdahir *et al*. observed a rapid oxidation of SQ under aerobic conditions in seawater caused by the presence of hydroperoxysterols (e.g. SQ-2-ol and SQ-epoxide), such a trend was not observed in this study, presumably due to competing behaviours of both hydroperoxysterols and the antioxidant vitamin E.[296]

4,9,13,17-tetramethyl-octadeca-4,8,12,16-tetraenol (TOT) was also identified in all fresh samples (Figure 6.8), which is in agreement with Girod and Weyermann's study.[91] A similar trend as with SQ-epoxide was noticed for TOT in the samples stored under the light. While TOT was decreased from its initial amount in t=7-day samples stored in the dark, it was still rising in t=7-day samples stored underwater. Since squalene was more degraded underwater than in dark, the increasing TOT level underwater suggests that TOT is relatively stable and accumulates under water.

Some of the products detected with fragment ions such as *m/z* 207.1017, 257.2476, 312.3263, 313.3103, 355.2845, 359.3156, and 473.3991 were present only in fresh and/or aged samples of donor D1F1. As SQ was present in fresh samples from all three donors, these products were regarded as not deriving from SQ (Figure 6.9).

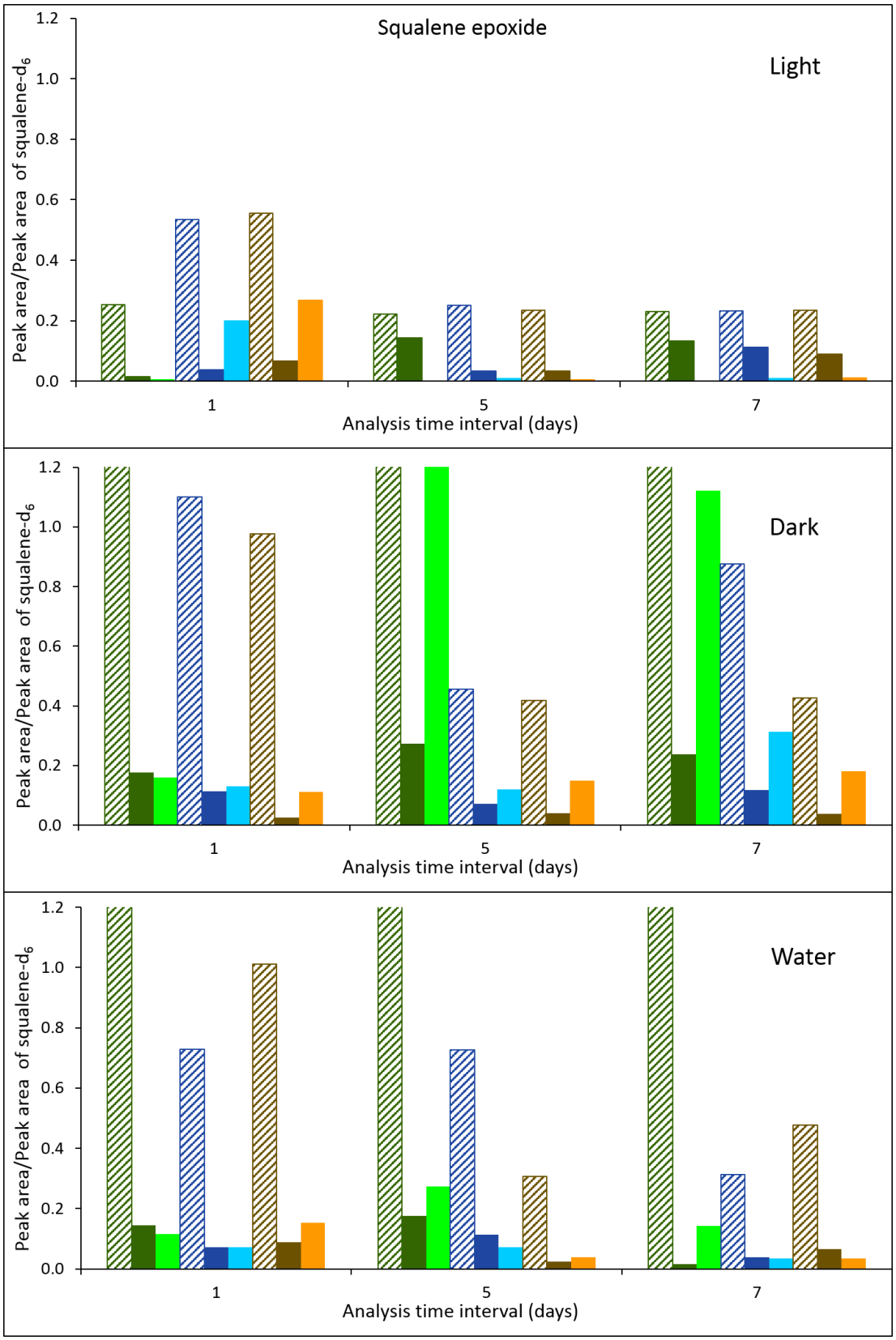

Figure 6.7 From left to right, relative amounts of squalene in aged samples (patterned filled bars), SQ-epoxide in fresh samples (t=0, dark coloured green, blue and brown bars) and SQ-epoxide in aged samples (t=t, brighter coloured green blue and brown bars) of fingermarks from donor D1F1 (green), D2M1 (blue) and D11M6 (brown). Y-axis of the graphs is not set to illustrate the maximum value of the data set.

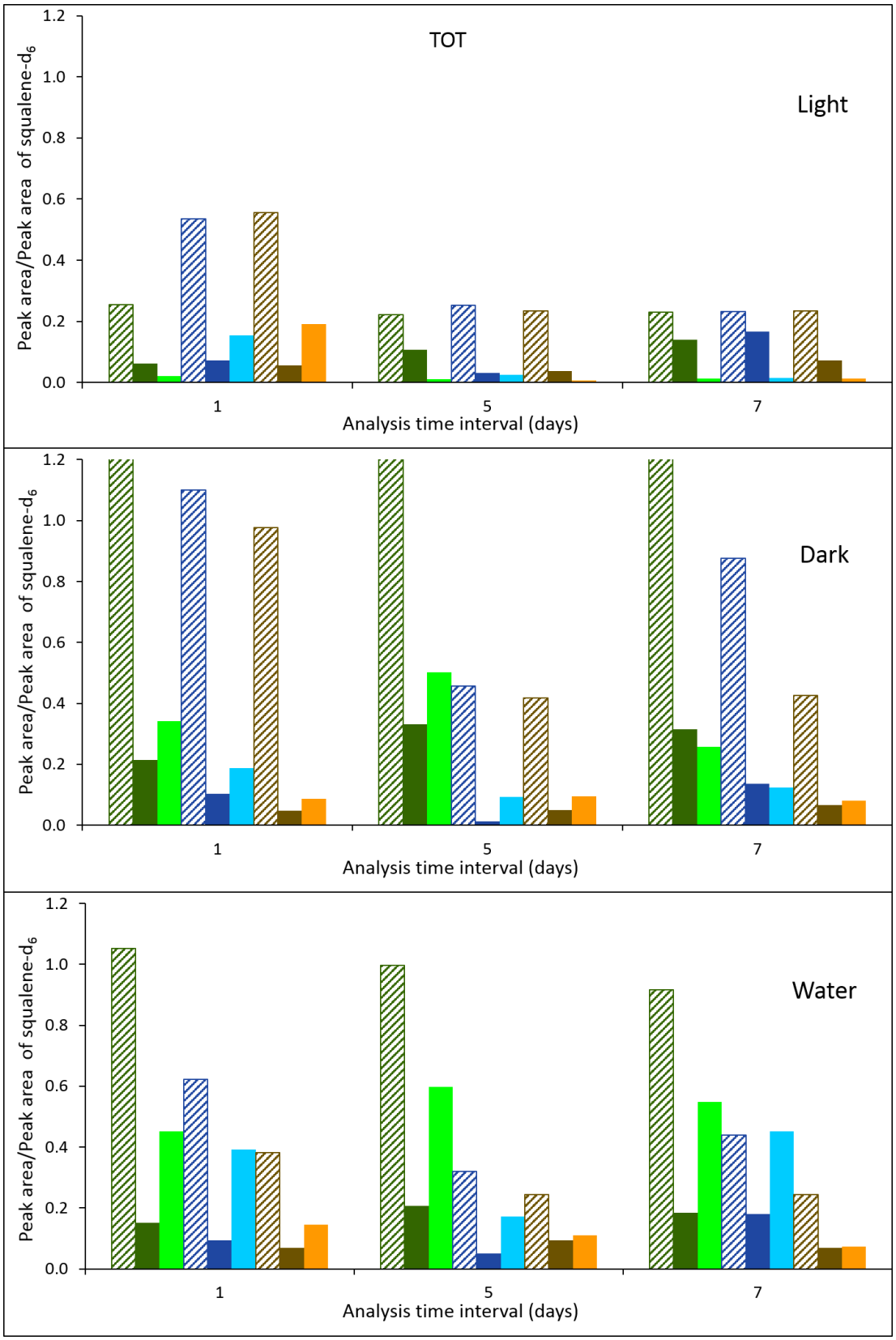

Figure 6.8 From left to right, relative amounts of SQ in aged samples (patterned filled bars), TOT in fresh samples (t=0, dark coloured green, blue and brown bars) and TOT in aged samples (t=t, brighter coloured green blue and brown bars) of fingermarks from donor D1F1 (green), D2M1 (blue) and D11M6 (brown). Y-axis of the graphs is not set to illustrate the maximum value of the data set.

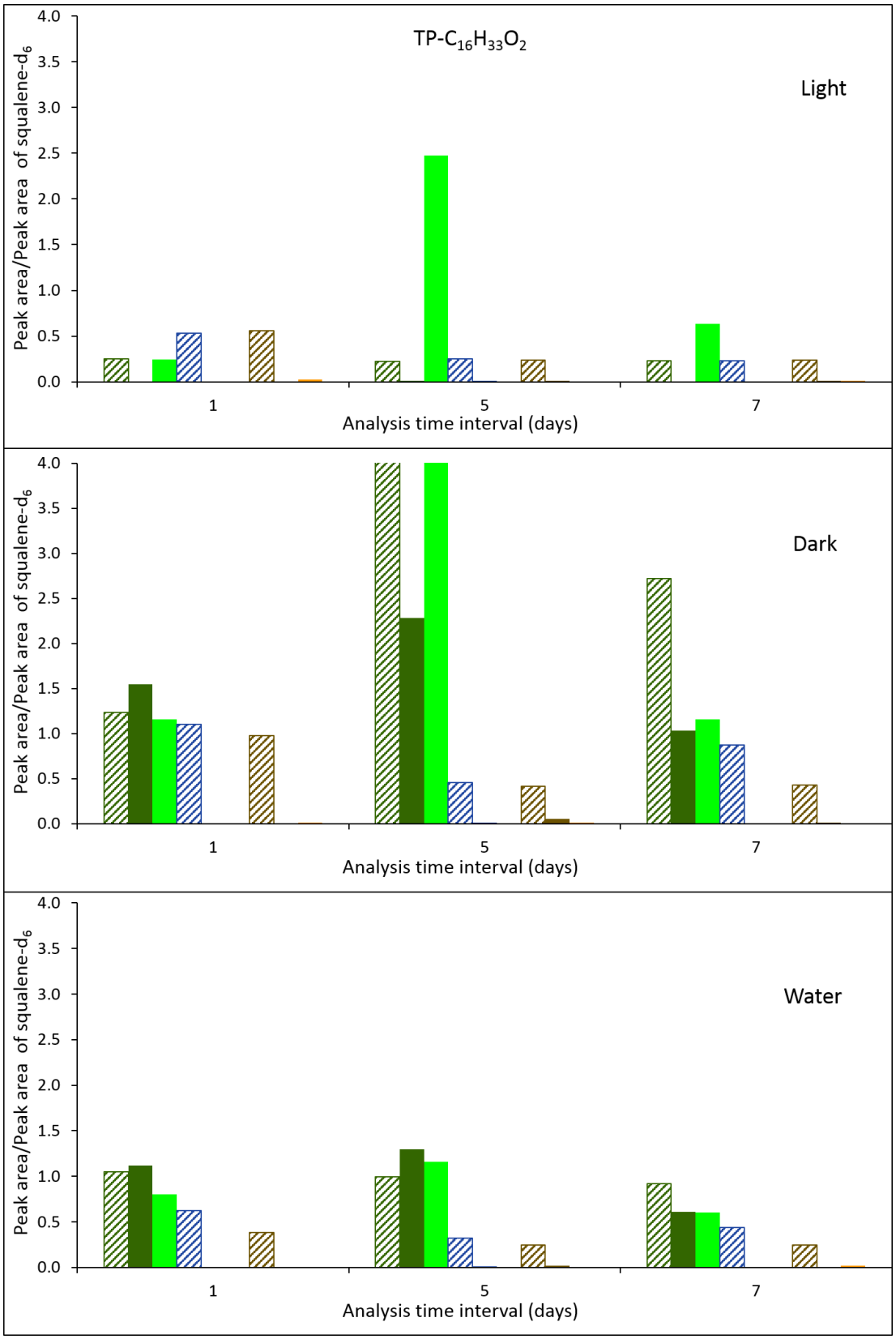

Figure 6.9 Compositional variation of the fragment ion $C_{16}H_{33}O_2$ (filled bars) in relation to the availability of SQ in the aged samples (patterned filled bars). The relative amount of the ion in fresh samples are in dark colour green, blue and brown bars and t=t samples are in brighter colour green blue and brown bars. Samples from donor D1F1 are shown in green, D2M1 in blue and D11M6 in brown. Y-axis of the graphs is not set to illustrate the maximum value of the data set.

While cholesterol was identified in samples based on the fragment at *m/z* 369.3519, the corresponding peak was not sufficiently resolved for relative quantification. However, the peak at *m/z* 367.3360 (exact mass *m/z* 367.3359 Da), which was tentatively attributed to cholesterol oxidation products by HRMS analysis, was sufficiently resolved to enable further investigations (Appendix 3). Cholesterol oxidation products were identified in all fresh samples, with a slow increasing trend with increasing sample age (Figure 6.10). Interestingly, this was seen with all storage conditions across all analysis time intervals. Cholesterol is another lipid compound that has been identified frequently in fingermark composition, but in relatively low quantities compared to SQ.[19, 91-93, 100] It was reported that cholesterol in fingermarks degraded at a much slower pace than SQ in a dark environment with no air flow.[100] This relatively high longevity of cholesterol could be the reason why the amount of cholesterol oxidation products were still increasing after 7 days of ageing. Since both SQ-OOH and SQ-epoxide were unable to be detected after ageing for 7 days under light, cholesterol oxidation products could be promising biomarkers for visualisation of aged fingermarks.

Investigations carried out on physical developer (PD) have found that among main lipid classes found in fingermarks, only spots of cholesterol produced significant silver deposition upon treatment with PD.[297] Due to the fact that cholesterol degrades over time while PD performs effectively on aged deposits, de la Hunty *et al*. proposed that PD's reactivity towards fingermarks may not be entirely attributed to the presence of cholesterol.[62] Based on the results of this current study and the research findings and suggestions discussed above, it could be postulated that PD targets both cholesterol and its oxidation by-products. However, since this study was based on non-porous surfaces, further investigations using porous surfaces are required to establish this hypothesis. As emphasised by Cadd *et al.* in their recent review on the ageing of fingermark composition, cholesterol decomposition products in fingermarks have never been explored before.[84] In light of this, the oxidation products of cholesterol are potentially of great significance.

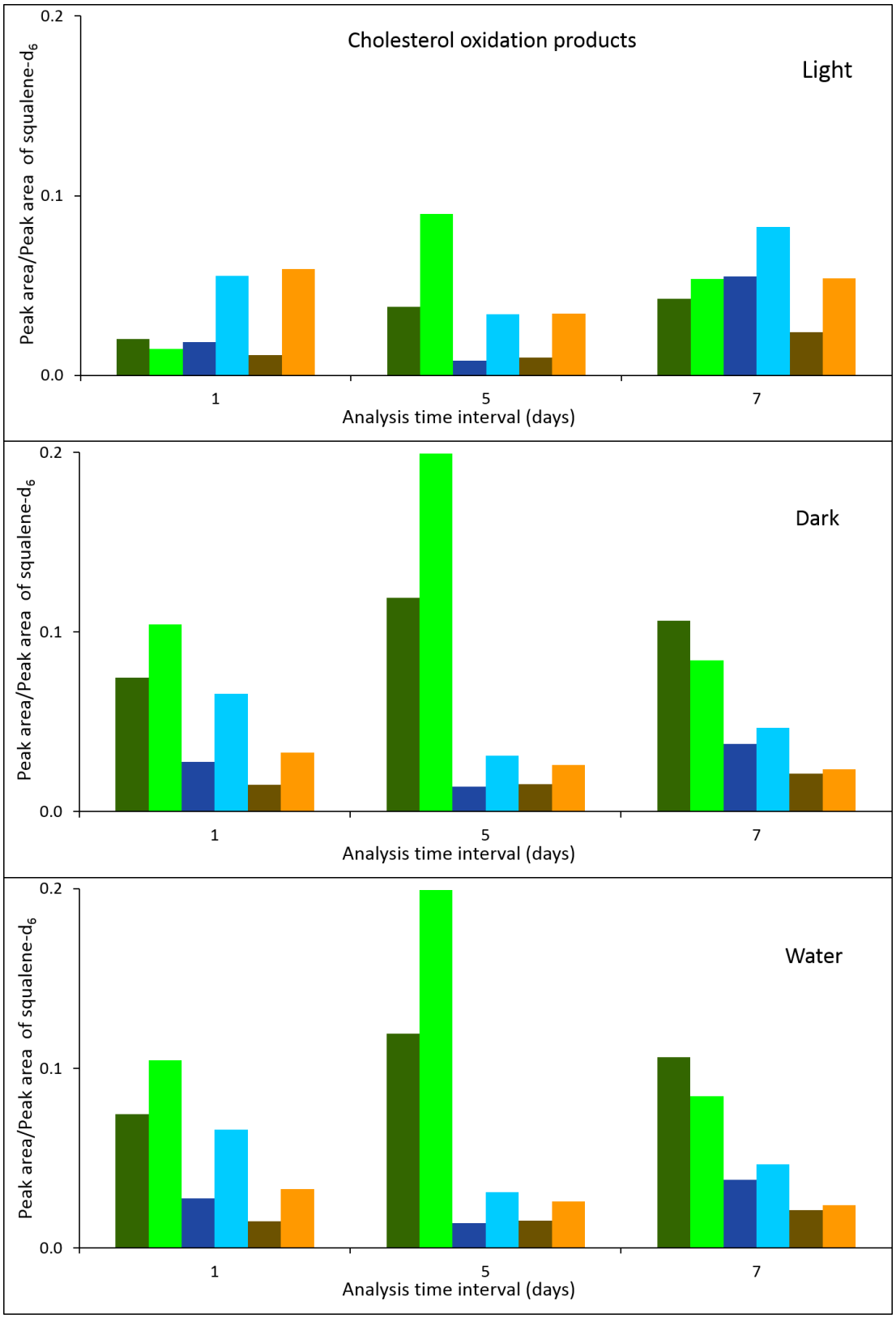

Figure 6.10 Compositional variation of cholesterol oxidation products in fresh samples (t=0, dark coloured green, blue and brown bars) and in aged samples (t=t, brighter coloured green, blue, and brown bars) of fingermarks from donor D1F1 (green), D2M1 (blue) and D11M6 (brown).

As displayed in Figure 6.11, oxidation of SQ into various products in the APCI ion source was observed. Base peaks of fragment ions used for the identification of oxidation by-products were seen at two retention times, one being the retention time of SQ (21.95 min). However, this did not interfere with the analysis since this oxidation occurred post-column (i.e. in the ion source) rather than pre-column and therefore they are chromatographically separated. One practical difficulty faced during this study was the random incidence of carryover of residual SQ. In this particular analysis sequence, a carryover was detected in blanks which were run after the standards. As the observed peak had the same retention time of SQ, it was identified as autosampler carryover.[298] Highly hydrophobic compounds such as SQ are known to absorb/trap in the flow path of the autosampler via ionic interaction with metallic surfaces and hydrophobic interaction with plastic materials due to their tendency to form charged species.[298] Throughout this study, the injector needle and the injection port was thoroughly washed with ACN with 10 rinsing cycles before and after each injection. Nevertheless, a small carryover of SQ (c.a. 0.4 ppm) was still detected in the sample blank. The same set of standards and sample blank were run on a different day using the same instrumental conditions by injecting the sample blank after each standard, no carryover was detected. Consequently, the carryover could not be quantified and was not subtracted from the samples.

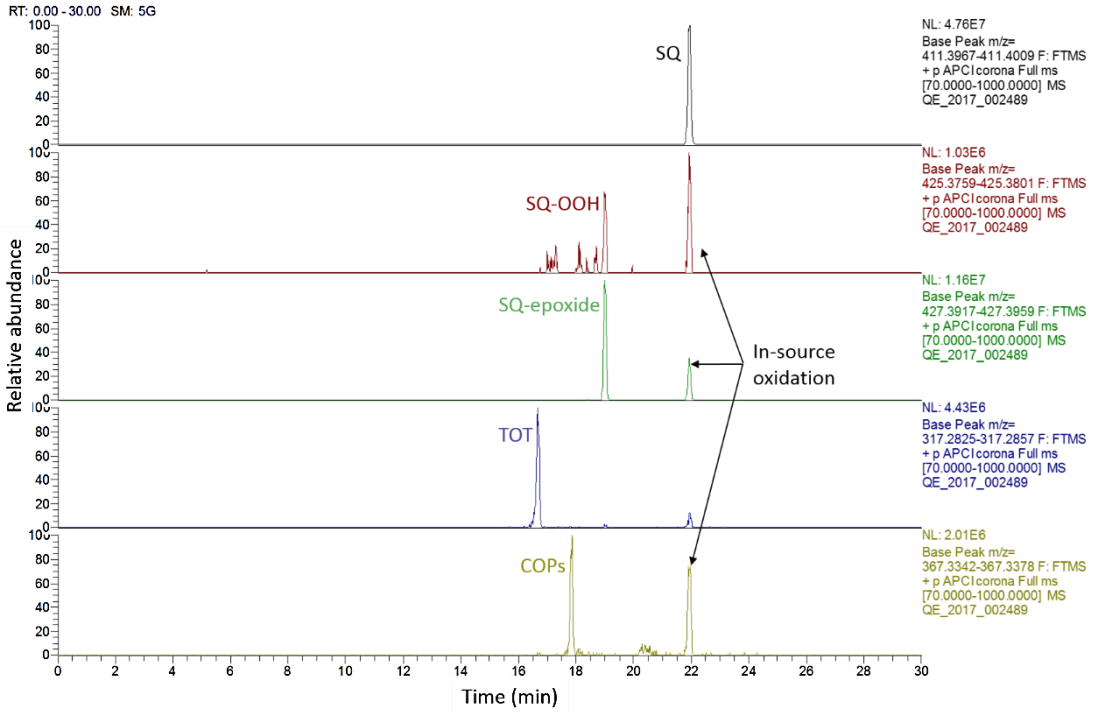

Figure 6.11 Oxidation of SQ into other oxidation products in the MS source.

Mountfort *et al.* suggested that oxidation by-products of SQ such as SQ-$[OOH]_4$ and SQ-$[OOH]_5$ could make suitable targets for novel fingermark detection techniques due to their durability in solution.[20] Nakagawa *et al*. further proposed that isomers of SQ-OOH such as 6-SQ-OOH, 11-SQ-OOH, and 2-SQ-OOH may present such targets.[270] Nonetheless, results of this study propose that none of these products would be present in fingermark deposits recovered from real-life situations due to their short lifetime or non-existence in such matrices.

However, the results suggest that SQ-epoxide and oxidation by-products of cholesterol may offer suitable functionalities with sufficient longevity that could be targeted by novel techniques for visualisation of aged deposits. Oil red O and Nile red are lipid stains that are currently being used to detect fingermarks where dye molecules interact with the labile fraction of lipids (non-polar or less polar) such as fatty acids and triglycerides.[65] Upon exposure to air, fatty acids and triglycerides oxidise rapidly hence, these techniques offer unreliable performance on aged deposits.[65] To this end, probing more polar robust fraction of fingermark lipids would be advantageous.[65] Biochemical imaging of polar lipids by staining with a luminescent rhenium complex was successfully demonstrated recently.[299] Since SQ-epoxide and the oxidation products of cholesterol identified in this study are polar biomolecules,[300] perhaps these novel staining methods could be adapted as innovative techniques for visualisation of aged fingermarks.

6.4 Conclusions

Transformation of squalene over time in fingermarks deposited on non-porous surfaces was studied under different storage conditions by ultra-high-pressure liquid chromatography-high resolution Orbitrap™ mass spectrometry. Complications of assessing fingermark compositional variation using multiple samples with varying initial compositions were demonstrated and an alternate approach was proposed which successfully identified trends of degradation of squalene over time.

A rapid oxidation of squalene was observed in all storage conditions while some of its oxidation by-products were relatively stable under dark and aquatic environments. Though individual identification was not carried out, some oxidation by-products of cholesterol were collectively identified that displayed prolonged persistence under any storage condition tested. These oxidation by-products, therefore, hold great potential as biomarkers for targeted visualisation of aged deposits and should be further explored. In addition, the significance of using natural deposits in time-course studies of fingermark composition was

demonstrated, as otherwise research outcomes may be overstated and inefficacious.

The results discussed in this chapter illuminate key areas of fingermark research; investigating compositional variation over time while addressing issues arising due to intra-donor variation and underwater fingermark chemistry, which have not been explored in detail previously. While the inherent difficulties associated with fingermark research may never be eliminated, the investigation of strategies to evade them within a realistic context may result in significant improvements in current detection capabilities.

Chapter 7: Conclusions and future work

The aim of this dissertation was to investigate the fundamental properties of latent fingermarks on non-porous surfaces in relation to their detection and ageing processes by employing advanced analytical instrumentation. The significance of this thesis was the combining of both the chemical and physical characteristics of fingermarks to generate a comprehensive knowledge of those aspects. The results have provided compelling evidence for the heterogeneous and dynamic nature of the deposit on non-porous surfaces, which has a direct influence on understanding mechanisms of current detection techniques and formulating more rational and novel ones.

7.1 Physical properties of fingermarks

Chapter 3 discussed the potential of a novel imaging mode of atomic force microscopy for the simultaneous acquisition of topography profiles and adhesion of fingermark droplets at the nanoscale. Results prove the technique can successfully examine the topography of fingermark deposits, including the ones with less material such as eccrine sweat-rich deposits. The observed variation in adhesion across individual droplets indicated potential chemical heterogeneity within droplets that had not been experimentally proven before.

Investigation of the physical properties revealed that the topography of eccrine-rich and sebum-rich droplets change differently over time, where some eccrine droplets increased their height and the sebaceous ones decreased. Some natural droplets exhibited long-lasting adhesion during the storage under dark conditions up to a month. There were, however, some inconclusive observations, such as negative adhesion values exhibited by some eccrine droplets, which could not be explained without the distribution of chemical species within droplets as well as across the deposits.

Another key finding of this study was the observed propagation of a thin film of material from fingermark ridges to furrows at the sub-nanometer scale, starting immediately after deposition, which indicated the dynamic nature of the deposit on non-porous surfaces. Along with other research published concurrently supporting this phenomenon, further research is highly recommended to investigate the impact of the migration of fingermark components on non-porous surfaces over the interpretation of ridge details for personal identification. Considering the topography of fingermark droplets and the thin film, a rational explanation was provided for the occasional occurrence of empty prints and reverse development in some detection techniques that involve deposition of nanoparticles on fingermarks.

Application of this technique to monitor ageing of other physical properties of fingermarks on non-porous surfaces, such as charge distribution and electrical conductivity, is recommended as it offers non-invasive imaging of soft samples with facilities to maintain sampling consistency in time-course experiments.

7.2 Spatial distribution of chemical species of fingermarks

The high-resolution chemical imaging of latent fingermark droplets on non-porous surfaces using vibrational spectroscopy provided definitive proof for the complex distribution of eccrine and lipid components within fingermark droplets. Results show that depending on the ratio of eccrine to sebaceous material in droplets, they may exist across a range of formations, from totally aqueous (eccrine), or lipids in an aqueous matrix, or aqueous droplets in a lipid matrix, or totally lipid droplets. Considerable presence of lipids identified in “eccrine deposits” offered a rational explanation for the inconclusive observations made in the physical investigations demonstrating the significance of combining both lines of research. The abundance of lipids observed in natural fingermarks showed they are more hydrophobic in composition and do not contain water as abundantly as thought previously.

The necessity for a consistent sampling of the fingermark residue in non-invasive, time-course experiments was another key opinion that was emphasised in this study. Ongoing research into the compositional variation of fingermarks can be benefited from non-invasive techniques, as the destructive analysis has been confronted by challenges with obtaining reproducible samples even from a single donor. However, failure to maintain sampling reproducibility would considerably confound the outcomes of such non-invasive studies due to the observed heterogeneous distribution of the chemical composition.

Since the confocal Raman microscopy was successfully employed in monitoring the compositional variation of fingermarks, the technique is recommended for future investigations, especially into the water-soluble fraction as spectra were rich in information than the FTIR spectra.

7.3 *Ex-situ* time-course experiments of fingermark components

The compositional variation of a major fingermark lipid component; squalene, was probed through the chromatographic studies outlined in chapters 5 and 6 with the intention of identifying potential biomarkers for targeted visualisation of aged deposits. By following the approach undertaken by previous studies in this context, it was found that quantitative comparison of the compositional variation over time was less likely to produce realistic research outcomes as a result of variation in the initial composition of the samples. Chapter 5 thus explored strategies to obtain two fingermark samples which are reproducible in terms of the amount of squalene deposited, which enabled analysis of one sample to identify the initial composition of every sample along the ageing curve.

It was found that rubbing hands together followed by deposition of natural fingermarks on non-porous substrates with controlled deposition pressure yielded a percentage difference of the amount of squalene between two hands of approximately 20%. Charging fingers with sebum followed by controlled deposition showed the lowest variability (13%); however, as these fingermarks are less typical to those left behind by incidental contact at crime scenes, such deposits were not further employed. Rubbing hands together has been frequently practised throughout fingermark research to evenly distribute secretions between fingers and hands, which enabled collection of multiple samples for replicate analysis or for a side-by-side comparison of detection techniques. As the greatest variation between hands (approximately 37%) was induced by the uncontrolled deposition, using squalene as a proxy, it can be predicted that such a sampling protocol is likely to cause more variability among replicate analysis of fingermark composition. Deposition of natural fingermarks by controlling the deposition pressure was hence chosen as the most appropriate sampling protocol for the subsequent investigation.

It should be noted that using the GC-MS methods described in Chapter 5, only squalene was consistently detected across all the samples from both lipid-rich and -poor donors with a satisfactory detector response. The methods require further improvements if other classes of compounds are to be investigated in natural fingermarks deposited on non-porous surfaces. Sample derivatisation and concentration are possible approaches that could be explored. Alternatively, the method based on liquid chromatography described in Chapter 6 could be used, which offered better sensitivity.

Chapter 6 probed the transformation by-products of squalene formed in natural deposits during the storage under light, dark, and aquatic conditions with a more rational approach to data interpretation. Ultra-high-pressure liquid chromatography-high-resolution mass spectrometry permitted direct and simultaneous detection of squalene and its transformation by-products without the need for sample derivatisation, which can cause induced oxidation of lipids.

This study emphasised the significance of employing natural deposits in investigations intended for identifying suitable biomarkers in aged composition, as some previously reported by-products in the aged composition of charged deposits were no longer detected in natural ones. Moreover, the influence of storage conditions over the degradation of squalene was illustrated. In particular, the degradation kinetics of squalene in fingermarks aged under aquatic conditions were not available before.

Although this study was intended to investigate the degradation of squalene, other lipid compounds such as cholesterol and its oxidation by-products were tentatively identified by high-resolution mass spectrometry. The oxidation by-products of cholesterol were not individually identified due to isobaric elution of them under the chromatographic conditions utilised; however, their compositional variation was monitored collectively by using one common fragment ion in the mass spectra. It was found that the oxidation by-products of cholesterol were still detectable after ageing up to 7 days under all storage conditions tested. Further research is recommended for the separation and identification of oxidation by-products of cholesterol in fingermarks during the storage under a range of environmental conditions, especially where detection of fingermarks is challenging.

Overall, this dissertation has provided compelling evidence for the heterogeneous and dynamic nature of fingermark deposits on non-porous surfaces. It has also demonstrated that natural fingermark composition is not largely water as previously thought but, sebum-rich. An evidence-based approach for the investigation of fingermark compositional variation over time using chromatography was suggested to overcome the complications caused by intra-donor variation. Using this approach, lipid molecular biomarkers were identified in aged deposits which may be used for the development of rational techniques for visualisation of aged fingermarks in future.

References

1. Thompson, W.; Black, J.; Jain, A.; Kadane, J. *Forensic Science Assessments: A Quality and Gap Analysis- Latent Fingerprint Examination*; American Association for the Advancement of Science: 2017.

2. Galton, F. *Finger Prints*. Macmillan and Company: 1892.

3. Jain, A. K.; Prabhakar, S.; Pankanti, S. On the similarity of identical twin fingerprints. *Pattern Recognition* **2002,** *35* (11), 2653-2663.

4. Gaensslen, R. E.; Ramotowski, R.; Lee, H. C. *Advances in fingerprint technology*. CRC press: 2001.

5. Bleay, S.; Sears, V.; Bandey, H.; Gibson, A.; Bowman, V.; Downham, R.; Fitzgerald, L.; Ciuksza, T.; Ramadani, J.; Selway, C. Fingerprint Source Book. *Home Office Center for Applied Science Technology (CAST)* **2012**.

6. Wolstenholme, R., Bradshaw, R., Clench, M., Francese, S. Study of latent fingermarks by matrix-assisted laser desorption/ionisation mass spectrometry imaging of endogenous lipids. *Rapid Communications in Mass Spectrometry* **2009,** *23* (19), 3031-3039.

7. Emerson, B., Jennifer, G., Lay, J., Durham, B. Laser Desorption/Ionization Time-of-Flight Mass Spectrometry of Triacylglycerols and Other Components in Fingermark Samples. *Journal of Forensic Sciences* **2011,** *56* (2), 381-389.

8. Champod, C.; Lennard, C. J.; Margot, P.; Stoilovic, M. *Fingerprints and other ridge skin impressions*. CRC press: 2004.

9. Saferstein, R. *Criminalistics: An Introduction to Forensic Science*. 9th ed.; USA: Prentice Hall Career & Technology Englewood Cliffs, New Jersey: 2007.

10. Bramble, S. K.; Brennan, J. S. FINGERPRINTS (DACTYLOSCOPY) | Chemistry of Print Residue. In *Encyclopedia of Forensic Sciences*, Siegel, J. A., Ed. Elsevier: Oxford, 2000; pp 862-869.

11. Frick, A.; Fritz, P.; Lewis, S. Chemistry of Print Residue. In *Encyclopedia of Forensic Sciences*, 2 ed.; Elsevier Ltd.: Australia: Academic Press, 2013; Vol. 4, pp 92-97.

12. Lee, H. C.; Gaensslen, R. E. Methods of Latent Fingerprint Development. In *Advances in Fingerprint Technology*, Lee, H. C.; Gaensslen, R. E., Eds. CRC Press: Boca Raton, 2001.

13. Kent, T. Visualization or development of crime scene fingerprints. In *Encyclopedia of Forensic Sciences*, 2nd ed.; Siegel, J. A.; Saukko, P. J., Eds. Oxford : Elsevier: Oxford, 2013; pp 117-129.

14. Antoine, K. M.; Mortazavi, S.; Miller, A. D.; Miller, L. M. Chemical differences are observed in children's versus adults' latent fingerprints as a function of time. *Journal of Forensic Sciences* **2010,** *55* (2), 513-518.

15. Girod, A.; Ramotowski, R.; Weyermann, C. Composition of fingermark residue: A qualitative and quantitative review. *Forensic Science International* **2012,** *223* (1), 10-24.

16. Frick, A. A. Chemical investigations into the lipid fraction of latent fingermark residue. PhD Thesis, Curtin University, 2015.

17. Ramotowski, R. S. Composition of Latent Print Residue. In *Advances in Fingerprint Technology*, 2nd ed.; CRC Press: 2001.

18. Fritz, P. Chemical studies into the amino acids present in latent fingermarks. PhD Thesis, Curtin University: Perth, 2015.

19. Archer, N. E.; Charles, Y.; Elliott, J. A.; Jickells, S. Changes in the lipid composition of latent fingerprint residue with time after deposition on a surface. *Forensic Science International* **2005,** *154* (2), 224-239.

20. Mountfort, K. A.; Bronstein, H.; Archer, N.; Jickells, S. M. Identification of Oxidation Products of Squalene in Solution and in Latent Fingerprints by ESI-MS and LC/APCI-MS. *Analytical Chemistry* **2007,** *79* (7), 2650-2657.

21. Pleik, S.; Spengler, B.; Schäfer, T.; Urbach, D.; Luhn, S.; Kirsch, D. Fatty Acid Structure and Degradation Analysis in Fingerprint Residues. *Journal of The American Society for Mass Spectrometry* **2016,** *27* (9), 1565-1574.

22. Williams, D. K.; Brown, C. J.; Bruker, J. Characterization of children's latent fingerprint residues by infrared microspectroscopy: Forensic implications. *Forensic Science International* **2011,** *206* (1), 161-165.

23. Ricci, C.; Phiriyavityopas, P.; Curum, N.; Chan, K. A.; Jickells, S.; Kazarian, S. G. Chemical imaging of latent fingerprint residues. *Applied Spectroscopy* **2007,** *61* (5), 514-522.

24. van Helmond, W.; Kuijpers, C.-J.; van Diejen, E.; Spiering, J.; Maagdelijn, B.; de Puit, M. Amino Acid Profiling from Fingerprints, Novel Methodology Using UPLC-MS. *Analytical Methods* **2017**.

25. De Paoli, G., Lewis Sr, S., Schuette, E., Lewis, L., Connatser, R., Farkas, T. Photo-and Thermal-Degradation Studies of Select Eccrine Fingerprint Constituents. *Journal of Forensic Sciences* **2010,** *55* (4), 962-969.

26. Thomas, G. The physics of fingerprints and their detection. *Journal of Physics E: Scientific Instruments* **1978,** *11* (8), 722-731.

27. Thomas, G. The Resistivity of Fingerprint Material. *Journal of the Forensic Science Society* **1975,** *15* (2), 133-135.

28. Thomas, G. A fingerprint thin film. *Thin Solid Films* **1974,** *24* (2), S52-S54.

29. Thomas, G.; Reynoldson, T. Some observations on fingerprint deposits. *Journal of Physics D: Applied Physics* **1975,** *8* (6), 724.

30. Baniuk, K. Determination of age of fingerprints. *Forensic Science International* **1990,** *46* (1), 133-137.

31. Barros, R. M.; Faria, B. E.; Kuckelhaus, S. A. Morphometry of latent palmprints as a function of time. *Science & Justice* **2013,** *53* (4), 402-408.

32. Popa, G.; Potorac, R.; Preda, N. Method for fingerprints age determination. *Romanian Journal of Legal Medicine* **2010,** *18* (2), 149-154.

33. Moret, S.; Spindler, X.; Lennard, C.; Roux, C. Microscopic examination of fingermark residues: Opportunities for fundamental studies. *Forensic Science International* **2015,** *255*, 28-37.

34. Maceo, A. V. Anatomy and physiology of adult friction ridge skin. In *The Fingerprint Sourcebook*, U.S. Department. of Justice, Office of Justice Programs, National Institute of Justice: 2011.

35. Freinkel, R. K.; Woodley, D. T. *The biology of the skin*. CRC Press: 2001.

36. Madhero88; Komorniczak, M. Skin layers. In *(https://commons.wikimedia.org/wiki/File:Skin_layers.svg), "Skin layers", https://creativecommons.org/licenses/by-sa/3.0/legalcode*, layers, S., Ed. Wikipedia: 2012; Vol. 1.81 MB, p Layers of the skin.

37. Houck, M. M. An investigation into the foundational principles of forensic science. PhD Thesis, Curtin University, 2010.

38. Locard, E. *L'enquête criminelle et les méthodes scientifiques*. E. Flammarion: 1920.

39. Haan, P. V.-D. Physics and fingerprints. *Contemporary Physics* **2006,** *47* (4), 209-230.

40. Jain, A. K. In *On the uniqueness of fingerprints*, NAS Sackler Forensic Science Colloquium, Washington, DC, 2005.

41. Han, Y.; Ryu, C.; Moon, J.; Kim, H.; Choi, H. In *A study on evaluating the uniqueness of fingerprints using statistical analysis*, International Conference on Information Security and Cryptology, Springer: 2004; pp 467-477.

42. Zhu, Y.; Dass, S. C.; Jain, A. K. Statistical models for assessing the individuality of fingerprints. *IEEE Transactions on Information Forensics and Security* **2007,** *2* (3), 391-401.

43. Wertheim, K.; Maceo, A. The critical stage of friction ridge and pattern formation. *Journal of Forensic Identification* **2002,** *52* (1), 35.

44. National Academy of Sciences. *DNA Technology in Forensic Science*. National Research Council: Washington, DC, 1992.

45. National Academy of Sciences. *Evaluation of Forensic DNA Evidence*. National Research Council: Washington, DC, 1995.

46. Ashbaugh, D. R. *Quantitative-qualitative friction ridge analysis: an introduction to basic and advanced ridgeology*. CRC press: 1999.

47. Lee, H. C.; Gaensslen, R. Methods of latent fingerprint development. In *Advances in Fingerprint Technology*, 2001; Vol. 2, pp 105-176.

48. Kent, T. Sequential treatment and enhancement. In *Encyclopedia of Forensic Sciences*, 2nd ed.; Siegel, J. A.; Saukko, P. J., Eds. Oxford : Elsevier: Oxford, 2013; pp 101-110.

49. Odén, S.; von Hofsten, B. Detection of fingerprints by the ninhydrin reaction. *Nature* **1954,** *173* (4401), 449.

50. Pounds, C. A. Developments in fingerprint visualisation. In *Forensic Science Progress*, Springer: 1988; pp 91-119.

51. Pounds, A. C.; Grigg, R.; Mongkolaussavaratana, T. The use of 1, 8-diazafluoren-9-one (DFO) for the fluorescent detection of latent fingerprints on paper. A preliminary evaluation. *Journal of Forensic Science* **1990,** *35* (1), 169-175.

52. Ramotowski, R.; Cantu, A.; Joullié, M.; Petrovskaia, O. 1, 2-Indanediones: a preliminary evaluation of a new class of amino acid visualizing compounds. *Fingerprint Whorld* **1997,** *23* (90), 131-140.

53. Hauze, D. B.; Petrovskaia, O.; Taylor, B.; Joullié, M. M.; Ramotowski, R.; Cantu, A. 1, 2-Indanediones: new reagents for visualizing the amino acid components of latent prints. *Journal of Forensic Science* **1998,** *43* (4), 744-747.

54. Jelly, R.; Patton, E. L.; Lennard, C.; Lewis, S. W. The detection of latent fingermarks on porous surfaces using amino acid sensitive reagents: A review. *Analytica Chimica Acta* **2009,** *652* (1), 128-142.

55. Frick, A. A.; Fritz, P.; Lewis, S. W. Chemical methods for the detection of latent fingermarks. In *Forensic Chemistry: Fundamentals and Applications*, Siegel, J. A., Ed. Chichester, West Sussex Hoboken, NJ John Wiley and Sons: 2015; pp 354-399.

56. Spindler, X.; Shimmon, R.; Roux, C.; Lennard, C. The effect of zinc chloride, humidity and the substrate on the reaction of 1, 2-indanedione–zinc with amino acids in latent fingermark secretions. *Forensic science international* **2011,** *212* (1-3), 150-157.

57. Salama, J.; Aumeer-Donovan, S.; Lennard, C.; Roux, C. Evaluation of the Fingermark Reagent oil red O as a Possible Replacement for Physical Developer. *Journal of Forensic Identification* **2008,** *58* (2), 203.

58. Frick, A. A.; Busetti, F.; Cross, A.; Lewis, S. W. Aqueous Nile blue: a simple, versatile and safe reagent for the detection of latent fingermarks. *Chem. Commun.* **2014,** *50* (25), 3341-3343.

59. Cain, A. The use of Nile blue in the examination of lipoids. *Journal of Cell Science* **1947,** *3* (3), 383-392.

60. Dunnigan, M. The use of Nile blue sulphate in the histochemical identification of phospholipids. *Stain Technology* **1968,** *43* (5), 249-256.

61. de la Hunty, M.; Moret, S.; Chadwick, S.; Lennard, C.; Spindler, X.; Roux, C. Understanding physical developer (PD): Part I–Is PD targeting lipids? *Forensic Science International* **2015,** *257*, 481-487.

62. de la Hunty, M.; Moret, S.; Chadwick, S.; Lennard, C.; Spindler, X.; Roux, C. Understanding Physical Developer (PD): Part II–Is PD targeting eccrine constituents? *Forensic Science International* **2015,** *257*, 488-495.

63. Houlgrave, S.; Ramotowski, R. Comparison of different physical developer working solutions-Part II: Reliability studies. *Journal of Forensic Identification* **2011,** *61* (6), 640.

64. Champod, C.; Lennard, C.; Margot, P.; Stoilovic, M. Fingerprint Detection Techniques. In *Fingerprints and Other Ridge Skin Impressions*, CRC Press: 2004.

65. Ramotowski, R. S. Lipid Reagents. In *Lee and Gaensslen's Advances in Fingerprint Technology*, 3rd ed.; CRC Press: 2012; pp 83-96.

66. Lennard, C. Fingerprint detection: future prospects. *Australian Journal of Forensic Sciences* **2007,** *39* (2), 73-80.

67. Becue, A.; Scoundrianos, A.; Moret, S. Detection of fingermarks by colloidal gold (MMD/SMD)–beyond the pH 3 limit. *Forensic Science International* **2012,** *219* (1), 39-49.

68. Bécue, A.; Cantú, A. A. *Fingermark detection using nanoparticles*. CRC Press LLC: 2012.

69. Stauffer, E.; Becue, A.; Singh, K. V.; Thampi, K. R.; Champod, C.; Margot, P. Single-metal deposition (SMD) as a latent fingermark enhancement technique: an alternative to multimetal deposition (MMD). *Forensic Science International* **2007,** *168* (1), e5-e9.

70. Newland, T. G.; Moret, S.; Bécue, A.; Lewis, S. W. Further investigations into the single metal deposition (SMD II) technique for the detection of latent fingermarks. *Forensic Science International* **2016,** *268*, 62-72.

71. Bleay, S.; Sears, V.; Bandey, H.; Gibson, A.; Bowman, V.; Downham, R.; Fitzgerald, L.; Ciuksza, T.; Ramadani, J.; Selway, C. Finger mark development techniques within scope of ISO 17025. In *Fingerprint Source Book,* , Home Office Centre for Applied Science and Technology (CAST): 2012; Vol. 1, pp 105-177.

72. Sodhi, G.; Kaur, J. Powder method for detecting latent fingerprints: a review. *Forensic Science International* **2001,** *120* (3), 172-176.

73. Wargacki, S. P.; Lewis, L. A.; Dadmun, M. D. Understanding the chemistry of the development of latent fingerprints by superglue fuming. *Journal of Forensic Sciences* **2007,** *52* (5), 1057-1062.

74. Lewis, L. A.; Smithwick, R.; Devault, G. L.; Bolinger, B.; Lewis, S. Processes involved in the development of latent fingerprints using the cyanoacrylate fuming method. *Journal of Forensic Science* **2001,** *46* (2), 241-246.

75. Chesher, B. K.; Stone, J. M.; Rowe, W. F. Use of the Omniprint™ 1000 alternate light source to produce fluorescence in cyanoacrylate-developed latent fingerprints stained with biological stains and commercial fabric dyes. *Forensic Science International* **1992,** *57* (2), 163-168.

76. Wargacki, S. P.; Lewis, L. A.; Dadmun, M. D. Enhancing the quality of aged latent fingerprints developed by superglue fuming: loss and replenishment of initiator. *Journal of Forensic Sciences* **2008,** *53* (5), 1138-1144.

77. Jones, N.; Stoilovic, M.; Lennard, C.; Roux, C. Vacuum metal deposition: factors affecting normal and reverse development of latent fingerprints on polyethylene substrates. *Forensic Science International* **2001,** *115* (1), 73-88.

78. Jones, N.; Mansour, D.; Stoilovic, M.; Lennard, C.; Roux, C. The influence of polymer type, print donor and age on the quality of fingerprints developed on plastic substrates using vacuum metal deposition. *Forensic Science International* **2001,** *124* (2), 167-177.

79. Jaber, N.; Lesniewski, A.; Gabizon, H.; Shenawi, S.; Mandler, D.; Almog, J. Visualization of latent fingermarks by nanotechnology: reversed development on paper—a remedy to the variation in sweat composition. *Angewandte Chemie International Edition* **2012,** *51* (49), 12224-12227.

80. Wiesner, S.; Springer, E.; Sasson, Y.; Almog, J. Chemical development of latent fingerprints: 1, 2-indanedione has come of age. *Journal of Forensic Science* **2001,** *46* (5), 1082-1084.

81. Frick, A. A.; Fritz, P.; Lewis, S. W.; Van Bronswijk, W. A Modified Oil Red O Formulation for the Detection of Latent Fingermarks on Porous Substrates. *Journal of Forensic Identification* **2012,** *62* (6), 623.

82. Kent, T. Water content of latent fingerprints–Dispelling the myth. *Forensic Science International* **2016**.

83. Goode, G.; Morris, J. *Latent fingerprints: a review of their origin, composition and methods for detection*; Atomic Weapons Research Establishment: 1983.

84. Cadd, S.; Islam, M.; Manson, P.; Bleay, S. Fingerprint composition and aging: A literature review. *Science & Justice* **2015,** *55* (4), 219-238.

85. Yamashita, B.; French, M. Latent Print Development. In *The Fingerprint Sourcebook*, McRoberts, A.; McRoberts, D., Eds. National Institute of Justice: Washington, 2011.

86. Girod, A.; Xiao, L.; Reedy, B.; Roux, C.; Weyermann, C. Fingermark initial composition and aging using Fourier transform infrared microscopy (μ-FTIR). *Forensic Science International* **2015,** *254*, 185-196.

87. Croxton, R. S.; Baron, M. G.; Butler, D.; Kent, T.; Sears, V. G. Variation in amino acid and lipid composition of latent fingerprints. *Forensic Science International* **2010,** *199* (1), 93-102.

88. Drapel, V.; Becue, A.; Champod, C.; Margot, P. Identification of promising antigenic components in latent fingermark residues. *Forensic Science International* **2009,** *184* (1), 47-53.

89. Fritz, P., Bronswjik, W., Lepkova, K., Lewis, S., Martin, D., Puskar, L. Infrared microscopy studies of the chemical composition of latent fingermark residues. *Microchemical Journal* **2013,** *111*, 40-46.

90. Mong, G. M.; Petersen, C.; Clauss, T. *Advanced fingerprint analysis project fingerprint constituents*; Pacific Northwest National Lab., Richland, WA (US): 1999.

91. Girod, A.; Weyermann, C. Lipid composition of fingermark residue and donor classification using GC/MS. *Forensic Science International* **2014,** *238*, 68-82.

92. Frick, A.; Chidlow, G.; Lewis, S.; Van Bronswijk, W. Investigations into the initial composition of latent fingermark lipids by gas chromatography–mass spectrometry. *Forensic Science International* **2015,** *254*, 133-147.

93. Koenig, A.; Girod, A.; Weyermann, C. Identification of Wax Esters in Latent Print Residues by Gas Chromatography-Mass Spectrometry and Their Potential Use as Aging Parameters. *Journal of Forensic Identification* **2011,** *61* (6), 606-631.

94. Asano, K. G.; Bayne, C. K.; Horsman, K. M.; Buchanan, M. V. Chemical composition of fingerprints for gender determination. *Journal of Forensic Science* **2002,** *47* (4), 1-3.

95. Puit, M.; Ismail, M.; Xu, X. LCMS Analysis of Fingerprints, the Amino Acid Profile of 20 Donors. *Journal of Forensic Sciences* **2014,** *59* (2), 364-370.

96. Boysen, T. C.; Yanagawa, S.; Sato, F.; Sato, K. A modified anaerobic method of sweat collection. *Journal of Applied Physiology* **1984,** *56* (5), 1302-1307.

97. Takemura, T.; Wertz, P.; Sato, K. Free fatty acids and sterols in human eccrine sweat. *British Journal of Dermatology* **1989,** *120* (1), 43-47.

98. Ferguson, L. S.; Wulfert, F.; Wolstenholme, R.; Fonville, J. M.; Clench, M. R.; Carolan, V. A.; Francese, S. Direct detection of peptides and small proteins in fingermarks and determination of sex by MALDI mass spectrometry profiling. *Analyst* **2012,** *137* (20), 4686-4692.

99. Sugase, S.; Tsuda, T. Determination of lactic acid, uric acid, xanthine and tyrosine in human sweat by HPLC, and the concentration variation of lactic acid in it after the intake of wine. *Bunseki Kagaku* **2002,** *51* (6), 429-435.

100. Weyermann, C.; Roux, C.; Champod, C. Initial results on the composition of fingerprints and its evolution as a function of time by GC/MS analysis. *Journal of Forensic Sciences* **2011,** *56* (1), 102-108.

101. Girod, A.; Spyratou, A.; Holmes, D.; Weyermann, C. Aging of target lipid parameters in fingermark residue using GC/MS: effects of influence factors and perspectives for dating purposes. *Science & Justice* **2016,** *56* (3), 165-180.

102. Bright, J.-A.; Petricevic, S. F. Recovery of trace DNA and its application to DNA profiling of shoe insoles. *Forensic Science International* **2004,** *145* (1), 7-12.

103. Swensson, O.; Langbein, L.; McMillan, J.; Stevens, H.; Leigh, I.; McLean, W.; Lane, E.; Eady, R. Specialized keratin expression pattern in human ridged skin as an adaptation to high physical stress. *British Journal of Dermatology* **1998,** *139* (5), 767-775.

104. Hartzell-Baguley, B.; Hipp, R. E.; Morgan, N. R.; Morgan, S. L. Chemical composition of latent fingerprints by gas chromatography–mass spectrometry. An experiment for an instrumental analysis course. *J. Chem. Educ* **2007,** *84* (4), 689.

105. Day, J. S.; Edwards, H. G.; Dobrowski, S. A.; Voice, A. M. The detection of drugs of abuse in fingerprints using Raman spectroscopy I: latent fingerprints. *Spectrochimica Acta Part A: Molecular and Biomolecular Spectroscopy* **2004,** *60* (3), 563-568.

106. Malka, I.; Petrushansky, A.; Rosenwaks, S.; Bar, I. Detection of explosives and latent fingerprint residues utilizing laser pointer–based Raman spectroscopy. *Applied Physics B* **2013,** *113* (4), 511-518.

107. Tripathi, A.; Emmons, E. D.; Wilcox, P. G.; Guicheteau, J. A.; Emge, D. K.; Christesen, S. D.; Fountain III, A. W. Semi-automated detection of trace explosives in fingerprints on strongly interfering surfaces with Raman chemical imaging. *Applied Spectroscopy* **2011,** *65* (6), 611-619.

108. Chen, T.; Schultz, Z. D.; Levin, I. W. Infrared spectroscopic imaging of latent fingerprints and associated forensic evidence. *Analyst* **2009,** *134* (9), 1902-1904.

109. Benton, M.; Chua, M.; Gu, F.; Rowell, F.; Ma, J. Environmental nicotine contamination in latent fingermarks from smoker contacts and passive smoking. *Forensic Science International* **2010,** *200* (1), 28-34.

110. Jones, N. E.; Davies, L. M.; Russell, C. A.; Brennan, J. S.; Bramble, S. K. A systematic approach to latent fingerprint sample preparation for comparative chemical studies. *Journal of Forensic Identification* **2001,** *51* (5), 504.

111. Buchanan, M. V.; Asano, K.; Bohanon, A. *Chemical characterization of fingerprints from adults and children*; Oak Ridge National Lab., TN (United States): 1996.

112. Thody, A. J.; Shuster, S. Control and function of sebaceous glands. *Physiological Reviews* **1989,** *69* (2), 383-416.

113. Rony, H. R.; Zakon, S. J. Effect of androgen on the sebaceous glands of human skin. *Archives of Dermatology and Syphilology* **1943,** *48* (6), 601-604.

114. Yamamoto, A.; Ito, M. Sebaceous gland activity and urinary androgen levels in children. *Journal of Dermatological Science* **1992,** *4* (2), 98-104.

115. Ramasastry, P.; Downing, D. T.; Pochi, P. E.; Strauss, J. S. Chemical composition of human skin surface lipids from birth to puberty. *Journal of Investigative Dermatology* **1970,** *54* (2), 139-144.

116. Cuthbertson, F. *The chemistry of fingerprints*; United Kingdom Atomic Energy Authority, Atomic Weapons Research Establishment (AWRE): 1969.

117. Huynh, C.; Brunelle, E.; Halámková, L.; Agudelo, J.; Halámek, J. Forensic identification of gender from fingerprints. *Analytical Chemistry* **2015,** *87* (22), 11531-11536.

118. Johnson, H. L.; Maibach, H. I. Drug excretion in human eccrine sweat. *Journal of Investigative Dermatology* **1971,** *56* (3), 182-188.

119. Czarnowski, D.; Langfort, J.; Pilis, W.; Gorski, J. Effect of a low-carbohydrate diet on plasma and sweat ammonia concentrations during prolonged nonexhausting exercise. *European Journal of Applied Physiology and Occupational Physiology* **1995,** *70* (1), 70-74.

120. Smith, R. N.; Braue, A.; Varigos, G. A.; Mann, N. J. The effect of a low glycemic load diet on acne vulgaris and the fatty acid composition of skin surface triglycerides. *Journal of Dermatological Science* **2008,** *50* (1), 41-52.

121. Kim, J.; Ko, Y.; Park, Y.-K.; Kim, N.-I.; Ha, W.-K.; Cho, Y. Dietary effect of lactoferrin-enriched fermented milk on skin surface lipid and clinical improvement of acne vulgaris. *Nutrition* **2010,** *26* (9), 902-909.

122. Downing, D. T.; Strauss, J. S.; Pochi, P. E. Changes in skin surface lipid composition induced by severe caloric restriction in man. *The American Journal of Clinical Nutrition* **1972,** *25* (4), 365-367.

123. Pochi, P. E.; Downing, D. T.; Strauss, J. S. Sebaceous Gland Response in Man to Prolonged Total Caloric Deprivation** From the Departments of Dermatology and Biochemistry, Boston University School of Medicine and the Evans Memorial Department of Clinical Research. University Hospital. Boston University Medical Center, Boston, Massachusetts 02118. *Journal of Investigative Dermatology* **1970,** *55* (5), 303-309.

124. Jasuja, O. P.; Toofany, M.; Singh, G.; Sodhi, G. Dynamics of latent fingerprints: The effect of physical factors on quality of ninhydrin developed prints—A preliminary study. *Science & Justice* **2009,** *49* (1), 8-11.

125. Fieldhouse, S. Consistency and reproducibility in fingermark deposition. *Forensic Science International* **2011,** *207* (1), 96-100.

126. Dominick, A. J.; Welch, L. A.; Daéid, N. N.; Bleay, S. M. Is there a relationship between fingerprint donation and DNA shedding? *Journal of Forensic Identification* **2009,** *59* (2), 133.

127. Azoury, M.; Cohen, D.; Himberg, K.; Qvintus-Leino, P.; Saari, T.; Almog, J. Fingerprint Detection on Counterfeit US $ Banknotes: The Importance of Preliminary Paper Examination. *Journal of Forensic Science* **2004,** *49* (5), JFS2003424-2.

128. Bobev, K. Fingerprints and factors affecting their condition. *Journal of Forensic Identification* **1995,** *45* (2), 176-83.

129. IFRG. Guidelines for the assessment of fingermark detection techniques *Journal of Forensic Identification* **2014,** *64* (2), 174-197.

130. Almog, J.; Azoury, M.; Elmaliah, Y.; Berenstein, L.; Zaban, A. Fingerprint's Third Dimension: The Depth and Shape of Fingerprints Penetration into Paper—Cross Section Examination by Fluorescence Microscopy. *Journal of Forensic Science* **2004,** *49* (5), JFS2004009-5.

131. Bartick, E.; Schwartz, R.; Bhargava, R.; Schaeberle, M.; Fernandez, D.; Levin, I. In *Spectrochemical analysis and hyperspectral imaging of latent fingerprints*, 16th Meeting of the International Association of Forensic Sciences, 2002; pp 61-64.

132. Frick, A.; Chidlow, G.; Goodpaster, J.; Lewis, S.; van Bronswijk, W. Monitoring compositional changes of the lipid fraction of fingermark residues deposited on paper during storage. *Forensic Chemistry* **2016,** *2*, 29-36.

133. Muramoto, S.; Sisco, E. Strategies for Potential Age Dating of Fingerprints through the Diffusion of Sebum Molecules on a Nonporous Surface Analyzed Using Time-of-Flight Secondary Ion Mass Spectrometry. *Analytical Chemistry* **2015,** *87* (16), 8035-8038.

134. Barnett, P. D.; Berger, R. A. The Effects of Temperature and Humidity on the Permanency of Latent Fingerprints. *Journal of the Forensic Science Society* **1976,** *16* (3), 249-254.

135. Alcaraz-Fossoul, D.; Mestres Patris, C.; Barrot Feixat, C.; McGarr, L.; Brandelli, D.; Stow, K.; Gené Badia, M. Latent fingermark aging patterns (part I): minutiae count as one indicator of degradation. *Journal of Forensic Sciences* **2016,** *61* (2), 322-333.

136. Alcaraz-Fossoul, D.; Barrot Feixat, C.; Tasker, J.; McGarr, L.; Stow, K.; Carreras-Marin, C.; Turbany Oset, J.; Gené Badia, M. Latent fingermark aging patterns (part II): color contrast between ridges and furrows as one indicator of degradation. *Journal of Forensic Sciences* **2016,** *61* (4), 947-958.

137. Alcaraz-Fossoul, D.; Barrot Feixat, C.; Carreras-Marin, C.; Tasker, J.; Zapico, S. C.; Gené Badia, M. Latent Fingermark Aging Patterns (Part III): Discontinuity Index as One Indicator of Degradation. *Journal of Forensic Sciences* **2017**.

138. van Dam, A.; Schwarz, J. C.; de Vos, J.; Siebes, M.; Sijen, T.; van Leeuwen, T. G.; Aalders, M. C.; Lambrechts, S. A. Oxidation Monitoring by Fluorescence Spectroscopy Reveals the Age of Fingermarks. *Angewandte Chemie International Edition* **2014**.

139. Wertheim, K. Fingerprint age determination: is there any hope? *Journal of Forensic Identification* **2003,** *53* (1), 42.

140. Johnston, A.; Rogers, K. The Effect of Moderate Temperatures on Latent Fingerprint Chemistry. *Applied Spectroscopy* **2017,** *71* (9), 2102-2110.

141. Scruton, B.; Blott, B. A high resolution probe for scanning electrostatic potential profiles across surfaces. *Journal of Physics E: Scientific Instruments* **1973,** *6* (5), 472.

142. Scruton, B.; Robins, B.; Blott, B. The deposition of fingerprint films. *Journal of Physics D: Applied Physics* **1975,** *8* (6), 714.

143. Merkel, R.; Dittmann, J. In *Resolution and size of measured area influences on the short- and long-term aging of latent fingerprint traces using the binary pixel feature and a high-resolution non-invasive chromatic white light (CWL) sensor*, Image and Signal Processing and Analysis (ISPA), 2011 7th International Symposium on, IEEE: 2011; pp 644-649.

144. Merkel, R.; Gruhn, S.; Dittmann, J.; Vielhauer, C.; Bräutigam, A. On non-invasive 2D and 3D Chromatic White Light image sensors for age determination of latent fingerprints. *Forensic Science International* **2012,** *222* (1), 52-70.

145. Merkel, R.; Dittmann, J.; Vielhauer, C. In *Approximation of a mathematical aging function for latent fingerprint traces based on first experiments using a chromatic white light (CWL) sensor and the binary pixel aging feature*, Communications and Multimedia Security, Springer: 2011; pp 59-71.

146. Merkel, R.; Dittmann, J.; Vielhauer, C. In *How contact pressure, contact time, smearing and oil/skin lotion influence the aging of latent fingerprint traces: First results for the binary pixel feature using a CWL sensor*, Information Forensics and Security (WIFS), 2011 IEEE International Workshop on, IEEE: 2011; pp 1-6.

147. De Alcaraz-Fossoul, J.; Roberts, K. A.; Feixat, C. B.; Hogrebe, G. G.; Badia, M. G. Fingermark ridge drift. *Forensic Science International* **2016,** *258*, 26-31.

148. Hazarika, P.; Russell, D. A. Advances in fingerprint analysis. *Angewandte Chemie International Edition* **2012,** *51* (15), 3524-3531.

149. Crane, N. J.; Bartick, E. G.; Perlman, R. S.; Huffman, S. Infrared spectroscopic imaging for noninvasive detection of latent fingerprints. *Journal of Forensic Sciences* **2007,** *52* (1), 48-53.

150. Connatser, R. M.; Prokes, S. M.; Glembocki, O. J.; Schuler, R. L.; Gardner, C. W.; Lewis, S. A.; Lewis, L. A. Toward Surface-Enhanced Raman Imaging of Latent Fingerprints. *Journal of Forensic Sciences* **2010,** *55* (6), 1462-1470.

151. Widjaja, E. Latent fingerprints analysis using tape-lift, Raman microscopy, and multivariate data analysis methods. *Analyst* **2009,** *134* (4), 769-775.

152. Ifa, D. R.; Manicke, N. E.; Dill, A. L.; Cooks, R. G. Latent fingerprint chemical imaging by mass spectrometry. *Science* **2008,** *321* (5890), 805-805.

153. Cuthbertson, F.; Morris, J. R. *The chemistry of fingerprints*; Atomic Weapons Research Establishment: Aldermaston.: 1972.

154. Andersson, P. O.; Lejon, C.; Mikaelsson, T.; Landström, L. Towards Fingermark Dating: A Raman Spectroscopy Proof-of-Concept Study. *ChemistryOpen*.

155. Day, J. S.; Edwards, H. G.; Dobrowski, S. A.; Voice, A. M. The detection of drugs of abuse in fingerprints using Raman spectroscopy II: cyanoacrylate-fumed fingerprints. *Spectrochimica Acta Part A: Molecular and Biomolecular Spectroscopy* **2004,** *60* (8), 1725-1730.

156. Popov, K. T.; Sears, V. G.; Jones, B. J. Migration of latent fingermarks on non-porous surfaces: Observation technique and nanoscale variations. *Forensic Science International* **2017,** *275*, 44-56.

157. Smith, F. Microscopic interferometry. *Modern Methods of Microscopy* **1955**, 76.

158. Butt, H.-J.; Cappella, B.; Kappl, M. Force measurements with the atomic force microscope: Technique, interpretation and applications. *Surface Science Reports* **2005,** *59* (1), 1-152.

159. *A practical guide to scanning probe microscopy*; Veeco Instruments Inc.: 2005.

160. Voigtländer, B. *Scanning Probe Microscopy*. Springer: 2016.

161. B. Pittenger, N. E., C. Su. *Quantitative Mechanical Property Mapping at the Nanoscale with PeakForce QNM*; Bruker application note Bruker Corporation: 2012.

162. Barker, E. C.; Goh, C. Y.; Jones, F.; Mocerino, M.; Skelton, B. W.; Becker, T.; Ogden, M. I. Investigating hydrogel formation using in situ variable-temperature scanning probe microscopy. *Chemical Science* **2015,** *6* (11), 6133-6138.

163. Pittenger, B. Advances in AFM Nanomechanics. Bruker Nano Surfaces Division: 2013.

164. Wilson, A. S.; Edwards, H. G.; Farwell, D. W.; Janaway, R. C. Fourier transform Raman spectroscopy: evaluation as a non-destructive technique for studying the degradation of human hair from archaeological and forensic environments. *Journal of Raman Spectroscopy* **1999,** *30* (5), 367-373.

165. Stuart, B. Infrared spectroscopy. In *Kirk-Othmer Encyclopedia of Chemical Technology*, Wiley Online Library: 2005.

166. Smith, B. C. *Infrared spectral interpretation: a systematic approach*. CRC press: 1998.

167. Williams, D. K.; Schwartz, R. L.; Bartick, E. G. Analysis of latent fingerprint deposits by infrared microspectroscopy. *Applied Spectroscopy* **2004,** *58* (3), 313-316.

168. Infrared Microscopy. In *Handbook of Microscopy Set*, Amelinckx, S.; van Dyck, D.; van Landuyt, J.; van Tendeloo, G., Eds. Wiley-VCH Verlag GmbH: 2008; pp 97-115.

169. Smith, B. C. *Fundamentals of Fourier transform infrared spectroscopy*. CRC press: 2011.

170. Nafie, L. A. Theory of Raman Scattering. In *Handbook of Raman Spectroscopy*, Lewis, I. R.; Edwards, H. G. M., Eds. CRC Press: 2001.

171. Byrne, H. J.; Sockalingum, G. D.; Stone, N. Raman Microscopy: Complement or Competitor? *Biomedical Applications of Synchrotron Infrared Microspectroscopy* **2010,** *11*, 105-142.

172. Dieing, T.; Hollricher, O.; Toporski, J. *Confocal raman microscopy*. Springer Science & Business Media: 2011; Vol. 158.

173. Rintoul, L.; Fredericks, P.; Coates, J. Vibrational Spectroscopy. In *Analytical Instrumentation Handbook*, 3rd ed.; Cazes, J., Ed. CRC Press: 2004; pp 163-164.

174. Darke, D.; Wilson, J. *The analysis of the free fatty acid component of fingerprints*; Atomic Energy Research Establishment: Harwell1977.

175. Haahti, E.; Horning, E.; Castren, O. Microanalysis of» Sebum «and Sebum-Like Materials by Temperature Programmed Gas Chromatography. *Scandinavian Journal of Clinical and Laboratory Investigation* **1962,** *14* (4), 368-372.

176. Plank, C.; Lorbeer, E. Simultaneous determination of glycerol, and mono-, di-and triglycerides in vegetable oil methyl esters by capillary gas chromatography. *Journal of Chromatography A* **1995,** *697* (1-2), 461-468.

177. Bailey, M. J.; Bright, N. J.; Croxton, R. S.; Francese, S.; Ferguson, L. S.; Hinder, S.; Jickells, S.; Jones, B. J.; Jones, B. N.; Kazarian, S. G. Chemical characterization of latent fingerprints by matrix-assisted laser desorption ionization, time-of-flight secondary ion mass spectrometry, mega electron volt secondary mass spectrometry, gas chromatography/mass spectrometry, X-ray photoelectron spectroscopy, and attenuated total reflection Fourier transform infrared spectroscopic imaging: an intercomparison. *Analytical Chemistry* **2012,** *84* (20), 8514-8523.

178. Michalski, S.; Shaler, R.; Dorman, F. L. The evaluation of fatty acid ratios in latent fingermarks by gas chromatography/mass spectrometry (GC/MS) analysis. *Journal of Forensic Sciences* **2013,** *58* (s1).

179. Skoog, D. A.; West, D. M.; Holler, F. J.; Crouch, S. *Fundamentals of analytical chemistry*. Nelson Education: 2013.

180. Camera, E.; Ludovici, M.; Galante, M.; Sinagra, J.-L.; Picardo, M. Comprehensive analysis of the major lipid classes in sebum by rapid resolution high-performance liquid chromatography and electrospray mass spectrometry. *Journal of Lipid Research* **2010,** *51* (11), 3377-3388.

181. Croxton, R. S.; Baron, M. G.; Butler, D.; Kent, T.; Sears, V. G. Development of a GC-MS Method for the Simultaneous Analysis of Latent Fingerprint Components. *Journal of Forensic Sciences* **2006,** *51* (6), 1329-1333.

182. Xiong, X.; Yin, Y.; Huang, Y.; Wang, Y.; Wen, Q.; Mu, Y.; Shu, X.; Zhan, Z.; Zhou, Y.; Qiu, G. Methods of amino acid analysis. In *Nutritional and Physiological Functions of Amino Acids in Pigs*, Blachier, F.; Wu, G.; Yin, Y., Eds. Springer: 2013; pp 217-229.

183. Petritis, K.; Chaimbault, P.; Elfakir, C.; Dreux, M. Ion-pair reversed-phase liquid chromatography for determination of polar underivatized amino acids using perfluorinated carboxylic acids as ion pairing agent. *Journal of Chromatography A* **1999,** *833* (2), 147-155.

184. Gómez-Ariza, J.; Villegas-Portero, M.; Bernal-Daza, V. Characterization and analysis of amino acids in orange juice by HPLC–MS/MS for authenticity assessment. *Analytica Chimica Acta* **2005,** *540* (1), 221-230.

185. Almog J, Cantu AA, Champod C (2014). Guidelines for the assessment of fingermark detection techniques, IFRG version1.

186. Wei, Q.; Li, X.; Du, X.; Zhang, X.; Zhang, M. Universal and one-step visualization of latent fingermarks on various surfaces using hydrophilic cellulose membrane and dye aqueous solution. *Science China Chemistry* **2017**, 1-8.

187. Hong, S.; Kim, M.; Yu, S. Latent Fingermark Development on Thermal Paper using 1, 2-Indanedione/Zinc and Polyvinylpyrrolidone. *Journal of Forensic Sciences* **2017**.

188. Hong, S.; Hong, I.; Han, A.; Seo, J. Y.; Namgung, J. A new method of artificial latent fingerprint creation using artificial sweat and inkjet printer. *Forensic Science International* **2015,** *257*, 403-408.

189. Schwarz, L. An amino acid model for latent fingerprints on porous surfaces. *Journal of Forensic Sciences* **2009,** *54* (6), 1323-1326.

190. Spindler, X.; Hofstetter, O.; McDonagh, A. M.; Roux, C.; Lennard, C. Enhancement of latent fingermarks on non-porous surfaces using anti-l-amino acid antibodies conjugated to gold nanoparticles. *Chem. Commun.* **2011,** *47* (19), 5602-5604.

191. Lee, J.; Lee, C. W.; Kim, J.-M. A Magnetically Responsive Polydiacetylene Precursor for Latent Fingerprint Analysis. *ACS Applied Materials & Interfaces* **2016**.

192. Moret, S.; Bécue, A.; Champod, C. Nanoparticles for fingermark detection: an insight into the reaction mechanism. *Nanotechnology* **2014,** *25* (42), 425502.

193. Watson, G. S.; Watson, J. A. In *Potential applications of scanning probe microscopy in forensic science*, Journal of Physics: Conference Series, IOP Publishing: 2007; p 1251.

194. Jones, B.; Downham, R.; Sears, V. Effect of substrate surface topography on forensic development of latent fingerprints with iron oxide powder suspension. *Surface and Interface Analysis* **2010,** *42* (5), 438-442.

195. Goddard, A. J.; Hillman, A. R.; Bond, J. W. High resolution imaging of latent fingerprints by localized corrosion on brass surfaces. *Journal of Forensic Sciences* **2010,** *55* (1), 58-65.

196. Dorakumbura, B. N.; Becker, T.; Lewis, S. W. Nanomechanical mapping of latent fingermarks: A preliminary investigation into the changes in surface interactions and topography over time. *Forensic Science International* **2016,** *267*, 16-24.

197. *Introduction to Bruker's ScanAsyst and PeakForce Tapping AFM Technology*; Bruker Corporation: 2011.

198. Walczyk, W.; Schönherr, H. Dimensions and the Profile of Surface Nanobubbles: Tip–Nanobubble Interactions and Nanobubble Deformation in Atomic Force Microscopy. *Langmuir* **2014,** *30* (40), 11955-11965.

199. Zhao, B.; Wang, X.; Song, Y.; Hu, J.; Lü, J.; Zhou, X.; Tai, R.; Zhang, X.; Zhang, L. Stiffness and evolution of interfacial micropancakes revealed by AFM quantitative nanomechanical imaging. *Physical Chemistry Chemical Physics* **2015,** *17* (20), 13598-13605.

200. Connell, S.; Allen, S.; Roberts, C.; Davies, J.; Davies, M.; Tendler, S.; Williams, P. Investigating the interfacial properties of single-liquid nanodroplets by Atomic Force Microscopy. *Langmuir* **2002,** *18* (5), 1719-1728.

201. Wei, Z.; Zhao, Y.-P. Growth of liquid bridge in AFM. *Journal of Physics D: Applied Physics* **2007,** *40* (14), 4368.

202. Thundat, T.; Zheng, X.-Y.; Chen, G.; Warmack, R. Role of relative humidity in atomic force microscopy imaging. *Surface Science* **1993,** *294* (1), L939-L943.

203. van der Werf, K. O.; Putman, C. A.; de Grooth, B. G.; Greve, J. Adhesion force imaging in air and liquid by adhesion mode atomic force microscopy. *Applied Physics Letters* **1994,** *65* (9), 1195-1197.

204. Sedin, D. L.; Rowlen, K. L. Adhesion forces measured by atomic force microscopy in humid air. *Analytical Chemistry* **2000,** *72* (10), 2183-2189.

205. Israelachvili, J. N. *Intermolecular and surface forces: revised third edition*. Academic press: 2011.

206. Wang, Y.; Wang, H.; Bi, S.; Guo, B. Nano-Wilhelmy investigation of dynamic wetting properties of AFM tips through tip-nanobubble interaction. *Scientific Reports* **2016,** *6*, 30021.

207. Becue, A.; Scoundrianos, A.; Champod, C.; Margot, P. Fingermark detection based on the in situ growth of luminescent nanoparticles—Towards a new generation of multimetal deposition. *Forensic Science International* **2008,** *179* (1), 39-43.

208. Choi, M. J.; McDonagh, A. M.; Maynard, P.; Roux, C. Metal-containing nanoparticles and nano-structured particles in fingermark detection. *Forensic Science International* **2008,** *179* (2), 87-97.

209. Cantú, A. A. The Physical Principles of the Reflected Ultraviolet Imaging Systems. *Journal of Forensic Identification* **2014,** *64* (2), 123.

210. Lennard, C. Fingerprint detection: current capabilities. *Australian Journal of Forensic Sciences* **2007,** *39* (2), 55-71.

211. Rosa, R.; Giovanardi, R.; Bozza, A.; Veronesi, P.; Leonelli, C. Electrochemical impedance spectroscopy: A deeper and quantitative insight into the fingermarks physical modifications over time. *Forensic Science International* **2017,** *273*, 144-152.

212. Kent, T.; Thomas, G.; Reynoldson, T.; East, H. A vacuum coating technique for the development of latent fingerprints on polythene. *Journal of the Forensic Science Society* **1976,** *16* (2), 93-101.

213. Grant, H.; Springer, E.; Ziv, Z. In *Vacuum metal deposition inhibition on polythene bags*, Proceedings of the International Symposium on Fingerprint Detection and Identification, Ne'urim, Israel, Ne'urim, Israel, 1996; pp 203-215.

214. Hemmila, A.; McGill, J.; Ritter, D. Fourier Transform Infrared Reflectance Spectra of Latent Fingerprints: A Biometric Gauge for the Age of an Individual*. *Journal of Forensic Sciences* **2008,** *53* (2), 369-376.

215. Chan, K.; Kazarian, S.; Mavraki, A.; Williams, D. Fourier transform infrared imaging of human hair with a high spatial resolution without the use of a synchrotron. *Applied Spectroscopy* **2005,** *59* (2), 149-155.

216. Song, W.; Mao, Z.; Liu, X.; Lu, Y.; Li, Z.; Zhao, B.; Lu, L. Detection of protein deposition within latent fingerprints by surface-enhanced Raman spectroscopy imaging. *Nanoscale* **2012,** *4* (7), 2333-2338.

217. Socrates, G. *Infrared and Raman characteristic group frequencies: tables and charts*. John Wiley & Sons: 2004.

218. Freudiger, C. W.; Min, W.; Saar, B. G.; Lu, S.; Holtom, G. R.; He, C.; Tsai, J. C.; Kang, J. X.; Xie, X. S. Label-free biomedical imaging with high sensitivity by stimulated Raman scattering microscopy. *Science* **2008,** *322* (5909), 1857-1861.

219. Hamada, K.; Fujita, K.; Smith, N. I.; Kobayashi, M.; Inouye, Y.; Kawata, S. Raman microscopy for dynamic molecular imaging of living cells. *Journal of Biomedical Optics* **2008,** *13* (4), 044027-044027-4.

220. Nan, X.; Cheng, J.-X.; Xie, X. S. Vibrational imaging of lipid droplets in live fibroblast cells with coherent anti-Stokes Raman scattering microscopy. *Journal of Lipid Research* **2003,** *44* (11), 2202-2208.

221. Caspers, P.; Lucassen, G.; Wolthuis, R.; Bruining, H.; Puppels, G. In vitro and in vivo Raman spectroscopy of human skin. *Biospectroscopy-New York-* **1998,** *4*, S31-S40.

222. De Gelder, J.; De Gussem, K.; Vandenabeele, P.; Moens, L. Reference database of Raman spectra of biological molecules. *Journal of Raman Spectroscopy* **2007,** *38* (9), 1133-1147.

223. Lin-Vien, D.; Colthup, N. B.; Fateley, W. G.; Grasselli, J. G. *The handbook of infrared and Raman characteristic frequencies of organic molecules*. Elsevier: 1991.

224. Krafft, C.; Knetschke, T.; Funk, R. H.; Salzer, R. Identification of organelles and vesicles in single cells by Raman microspectroscopic mapping. *Vibrational Spectroscopy* **2005,** *38* (1), 85-93.

225. Borchman, D.; Tang, D.; Yappert, M. C. Lipid composition, membrane structure relationships in lens and muscle sarcoplasmic reticulum membranes. *Biospectroscopy* **1999,** *5* (3), 151-167.

226. Jenkins, A. L.; Larsen, R. A.; Williams, T. B. Characterization of amino acids using Raman spectroscopy. *Spectrochimica Acta Part A: Molecular and Biomolecular Spectroscopy* **2005,** *61* (7), 1585-1594.

227. Krafft, C.; Knetschke, T.; Siegner, A.; Funk, R. H.; Salzer, R. Mapping of single cells by near infrared Raman microspectroscopy. *Vibrational Spectroscopy* **2003,** *32* (1), 75-83.

228. Matthäus, C.; Chernenko, T.; Newmark, J. A.; Warner, C. M.; Diem, M. Label-free detection of mitochondrial distribution in cells by nonresonant Raman microspectroscopy. *Biophysical Journal* **2007,** *93* (2), 668-673.

229. Barry, B.; Edwards, H.; Williams, A. Fourier transform Raman and infrared vibrational study of human skin: assignment of spectral bands. *Journal of Raman Spectroscopy* **1992,** *23* (11), 641-645.

230. Langlais, M.; Tajmir-Riahi, H. A.; Savoie, R. Raman spectroscopic study of the effects of Ca2+, Mg2+, Zn2+, and Cd2+ ions on calf thymus DNA: binding sites and conformational changes. *Biopolymers* **1990,** *30* (7-8), 743-752.

231. Neault, J.; Naoui, M.; Manfait, M.; Tajmir-Riahi, H. Aspirin-DNA interaction studied by FTIR and laser Raman difference spectroscopy. *FEBS Letters* **1996,** *382* (1-2), 26-30.

232. Das, R. S.; Agrawal, Y. Raman spectroscopy: recent advancements, techniques and applications. *Vibrational Spectroscopy* **2011,** *57* (2), 163-176.

233. Zhu, G.; Zhu, X.; Fan, Q.; Wan, X. Raman spectra of amino acids and their aqueous solutions. *Spectrochimica Acta Part A: Molecular and Biomolecular Spectroscopy* **2011,** *78* (3), 1187-1195.

234. Xu, C.; Zhou, R.; He, W.; Wu, L.; Wu, P.; Hou, X. Fast imaging of eccrine latent fingerprints with nontoxic Mn-doped ZnS QDs. *Analytical Chemistry* **2014,** *86* (7), 3279-3283.

235. Li, Y.; Xu, C.; Shu, C.; Hou, X.; Wu, P. Simultaneous extraction of level 2 and level 3 characteristics from latent fingerprints imaged with quantum dots for improved fingerprint analysis. *Chinese Chemical Letters* **2017**.

236. Newland, T. Detection of Latent Fingermarks Using Gold Nanoparticles. Curtin University: 2015.

237. Kloprogge, J. T.; Wharton, D.; Hickey, L.; Frost, R. L. Infrared and Raman study of interlayer anions CO32–, NO3–, SO42–and ClO4–in Mg/Al-hydrotalcite. *American Mineralogist* **2002,** *87* (5-6), 623-629.

238. Periasamy, A.; Muruganand, S.; Palaniswamy, M. Vibrational studies of Na2SO4, K2SO4, NaHSO4 and KHSO4 crystals. *Rasayan Journal of Chemistry* **2009,** *2* (4), 981-989.

239. De Faria, D.; Venâncio Silva, S.; De Oliveira, M. Raman microspectroscopy of some iron oxides and oxyhydroxides. *Journal of Raman Spectroscopy* **1997,** *28* (11), 873-878.

240. Rygula, A.; Majzner, K.; Marzec, K. M.; Kaczor, A.; Pilarczyk, M.; Baranska, M. Raman spectroscopy of proteins: a review. *Journal of Raman Spectroscopy* **2013,** *44* (8), 1061-1076.

241. Frick, A.; Berryman, D.; Lewis, S. Mass spectral imaging: a powerful new tool for the study of latent fingermark chemistry. *Identification Canada* **2011,** *34* (3), 84-96.

242. Blanksby, S. J.; Mitchell, T. W. Advances in mass spectrometry for lipidomics. *Annual Review of Analytical Chemistry* **2010,** *3*, 433-465.

243. Reed, H.; Stanton, A.; Wheat, J.; Kelley, J.; Davis, L.; Rao, W.; Smith, A.; Owen, D.; Francese, S. The Reed-Stanton press rig for the generation of reproducible fingermarks: Towards a standardised methodology for fingermark research. *Science & Justice* **2016,** *56* (1), 9-17.

244. Trapecar, M.; Balazic, J. Fingerprint recovery from human skin surfaces. *Science & Justice* **2007,** *47* (3), 136-140.

245. Cadd, S.; Mota, L.; Werkman, D.; Islam, M.; Zuidberg, M.; De Puit, M. Extraction of fatty compounds from fingerprints for GCMS analysis. *Analytical Methods* **2015,** *7* (3), 1123-1132.

246. Snyder, L. R.; Kirkland, J. J.; Glajch, J. L. *Practical HPLC method development*. John Wiley & Sons: 2012.

247. Smith, E. D.; Sorrells, K. E. A quantitative comparison of gas chromatograph septum bleed. *Journal of Chromatographic Science* **1971,** *9* (1), 15-17.

248. Olsavicky, V. A comparison of high-temperature septa for gas chromatography. *Journal of Chromatographic Science* **1978,** *16* (5), 197-200.

249. Pattinson, S. J.; Wilkins, J. P. Investigation by gas chromatography-mass spectrometry of potential contamination incurred by the use of crimp-cap vial closures. *Analyst* **1989,** *114* (4), 429-434.

250. Verschoore, M.; Poncet, M.; Krebs, B.; Ortonne, J.-P. Circadian variations in the number of actively secreting sebaceous follicles and androgen circadian rhythms. *Chronobiology International* **1993,** *10* (5), 349-359.

251. Czekanski, P.; Fasola, M.; Allison, J. A mechanistic model for the superglue fuming of latent fingerprints. *Journal of Forensic Sciences* **2006,** *51* (6), 1323-1328.

252. Richmond-Aylor, A.; Bell, S.; Callery, P.; Morris, K. Thermal Degradation Analysis of Amino Acids in Fingerprint Residue by Pyrolysis GC–MS to Develop New Latent Fingerprint Developing Reagents*. *Journal of Forensic Sciences* **2007,** *52* (2), 380-382.

253. Ma, R.; Shimmon, R.; McDonagh, A.; Maynard, P.; Lennard, C.; Roux, C. Fingermark detection on non-porous and semi-porous surfaces using YVO 4: Er, Yb luminescent upconverting particles. *Forensic Science International* **2012,** *217* (1), e23-e26.

254. Langdon, R. G.; Bloch, K. The utilization of squalene in the biosynthesis of cholesterol. *Journal of Biological Chemistry* **1953,** *200* (1), 135-144.

255. Camera, E.; Ottaviani, M.; Picardo, M. Squalene chemistry and biology. In *Lipids and Skin Health*, Springer: 2015; pp 185-198.

256. Kellum, R. E. Human sebaceous gland lipids: Analysis by thin-layer chromatography. *Archives of Dermatology* **1967,** *95* (2), 218-220.

257. Downing, D. T.; Strauss, J. S.; Pochi, P. E. Variability in the chemical composition of human skin surface lipids. *Journal of Investigative Dermatology* **1969,** *53* (5), 322-327.

258. Greene, R. S.; Downing, D. T.; Pochi, P. E.; Strauss, J. S. Anatomical variation in the amount and composition of human skin surface lipid. *Journal of Investigative Dermatology* **1970,** *54* (3), 240-247.

259. Picardo, M.; Zompetta, C.; De Luca, C.; Cirone, M.; Faggioni, A.; Nazzaro-Porro, M.; Passi, S.; Prota, G. Role of skin surface lipids in UV-induced epidermal cell changes. *Archives of Dermatological Research* **1991,** *283* (3), 191-197.

260. Nicolaides, N. Skin lipids: their biochemical uniqueness. *Science* **1974,** *186* (4158), 19-26.

261. Passi, S.; Picardo, M.; Morrone, A.; De Luca, C.; Ippolito, F. Skin surface lipids in HIV sero-positive and HIV sero-negative patients affected with seborrheic dermatitis. *Journal of Dermatological Science* **1991,** *2* (2), 84-91.

262. Zouboulis, C. Die Talgdrüse. *Der Hautarzt* **2010,** *61* (6), 467-477.

263. Sobel, H. Squalene in Sebum and Sebum-Like Materials** From the Department of Laboratories, Beth Israel Hospital, New York, New York. *Journal of Investigative Dermatology* **1949,** *13* (6), 333-338.

264. Ahn, Y. K.; Kim, J. H. Effects of squalene on the immune responses in mice (II): Cellular and non-specific immune response and antitumor activity of squalene. *Archives of Pharmacal Research* **1992,** *15* (1), 20-29.

265. Nowicki, R.; Barańska-Rybak, W. Shark liver oil as a supporting therapy in atopic dermatitis. *Polski merkuriusz lekarski: organ Polskiego Towarzystwa Lekarskiego* **2007,** *22* (130), 312-313.

266. Kohno, Y.; Egawa, Y.; Itoh, S.; Nagaoka, S.-i.; Takahashi, M.; Mukai, K. Kinetic study of quenching reaction of singlet oxygen and scavenging reaction of free radical by squalene in n-butanol. *Biochimica et Biophysica Acta (BBA)-Lipids and Lipid Metabolism* **1995,** *1256* (1), 52-56.

267. Thiele, J. Oxidative targets in the stratum corneum. *Skin Pharmacology and Physiology* **2001,** *14* (Suppl. 1), 87-91.

268. Mudiyanselage, S. E.; Elsner, P.; Thiele, J. J.; Hamburger, M. Ultraviolet A induces generation of squalene monohydroperoxide isomers in human sebum and skin surface lipids in vitro and in vivo. *Journal of Investigative Dermatology* **2003,** *120* (6), 915-922.

269. Dennis, K. J.; Shibamoto, T. Production of Malonaldehyde from Squalene, A Major Skin Surface Lipid, During UV-Irradiation. *Photochemistry and Photobiology* **1989,** *49* (5), 711-716.

270. Nakagawa, K.; Ibusuki, D.; Suzuki, Y.; Yamashita, S.; Higuchi, O.; Oikawa, S.; Miyazawa, T. Ion-trap tandem mass spectrometric analysis of squalene monohydroperoxide isomers in sunlight-exposed human skin. *Journal of Lipid Research* **2007,** *48* (12), 2779-2787.

271. Ohsawa, K.; Watanabe, T.; Matsukawa, R.; Yoshimura, Y.; Imaeda, K. The possible role of squalene and its peroxide of the sebum in the occurrence of sunburn and protection from the damage caused by UV irradiation. *The Journal of Toxicological Sciences* **1984,** *9* (2), 151-159.

272. Kohno, Y.; Sakamoto, O.; Tomita, K.; Horii, I.; Miyazawa, T. Determination of human skin surface lipid peroxides by chemiluminescence-HPLC. *Journal of Japan Oil Chemists' Society* **1991,** *40* (9), 715-718.

273. Chiba, K.; Sone, T.; Kawakami, K.; Onoue, M. Skin roughness and wrinkle formation induced by repeated application of squalenemonohydroperoxide to the hairless mouse. *Experimental Dermatology* **1999,** *8* (6), 471-479.

274. Luca, C.; Picardo, M.; Brcathnach, A.; Passi, S. Lipoperoxidase activity of Pityrosporum: characterisation of by-products and possible rôle in pityriasis versicolor. *Experimental Dermatology* **1996,** *5* (1), 49-56.

275. Yeo, H.; Shibamoto, T. Formation of formaldehyde and malonaldehyde by photooxidation of squalene. *Lipids* **1992,** *27* (1), 50-53.

276. Petrick, L.; Dubowski, Y. Heterogeneous oxidation of squalene film by ozone under various indoor conditions. *Indoor Air* **2009,** *19* (5), 381-391.

277. Nazzaro-Porro, M.; Passi, S.; Picardo, M.; Mercantini, R.; Breathnach, A. S. Lipoxygenase activity of Pityrosporum in vitro and in vivo. *Journal of Investigative Dermatology* **1986,** *87* (1), 108-112.

278. Christian, G. D. *Analytical Chemistry* 6th ed.; Hoboken, N.J. : Wiley: Hoboken, N.J., 2004.

279. Noble, D. MS/MS flexes its muscles. *Analytical Chemistry* **1995,** *67* (7), 265A-269A.

280. Makarov, A. Electrostatic axially harmonic orbital trapping: a high-performance technique of mass analysis. *Analytical Chemistry* **2000,** *72* (6), 1156-1162.

281. Eliuk, S.; Makarov, A. Evolution of orbitrap mass spectrometry instrumentation. **2015**.

282. Busetti, F.; Swann, L. Liquid Chromatography-Mass Spectrometry In *Encyclopedia of Forensic Sciences*, Saukko, P. J.; Houck, M. M., Eds. Academic Press: Waltham, 2013; pp 590-595.

283. Gheshlaghi, R.; Scharer, J.; Moo-Young, M.; Douglas, P. Application of statistical design for the optimization of amino acid separation by reverse-phase HPLC. *Analytical Biochemistry* **2008,** *383* (1), 93-102.

284. Rastrelli, L.; Passi, S.; Ippolito, F.; Vacca, G.; De Simone, F. Rate of degradation of α-tocopherol, squalene, phenolics, and polyunsaturated fatty acids in olive oil during different storage conditions. *Journal of Agricultural and Food Chemistry* **2002,** *50* (20), 5566-5570.

285. Hrncirik, K.; Fritsche, S. Relation between the endogenous antioxidant system and the quality of extra virgin olive oil under accelerated storage conditions. *Journal of Agricultural and Food Chemistry* **2005,** *53* (6), 2103-2110.

286. Thiele, J. J.; Hsieh, S. N.; Ekanayake-Mudiyanselage, S. Vitamin E: critical review of its current use in cosmetic and clinical dermatology. *Dermatologic Surgery* **2005,** *31* (s1), 805-813.

287. Dietrich, M.; Traber, M. G.; Jacques, P. F.; Cross, C. E.; Hu, Y.; Block, G. Does γ-tocopherol play a role in the primary prevention of heart disease and cancer? A review. *Journal of the American College of Nutrition* **2006,** *25* (4), 292-299.

288. Daéid, N. N.; Carter, S.; Laing, K. Comparison of vacuum metal deposition and powder suspension for recovery of fingerprints on wetted nonporous surfaces. *Journal of Forensic Identification* **2008,** *58* (5), 600.

289. Trapecar, M. Fingerprint recovery from wet transparent foil. *Egyptian Journal of Forensic Sciences* **2012,** *2* (4), 126-130.

290. Rohatgi, R.; Kapoor, A. K. Development of latent fingerprints on wet non-porous surfaces with SPR based on basic fuchsin dye. *Egyptian Journal of Forensic Science* **2016,** *6*.

291. Bumbrah, G. S. Small particle reagent (SPR) method for detection of latent fingermarks: A review. *Egyptian Journal of Forensic Sciences* **2016,** *6* (4), 328-332.

292. Cuce, P.; Polimeni, G.; Lazzaro, A. P.; Fulvio, G. D. Small particle reagents technique can help to point out wet latent finger prints. *Forensic Science International (Suppl)* **2004,** *146*.

293. Raith, K.; Brenner, C.; Farwanah, H.; Müller, G.; Eder, K.; Neubert, R. H. A new LC/APCI-MS method for the determination of cholesterol oxidation products in food. *Journal of Chromatography A* **2005,** *1067* (1), 207-211.

294. Newton, S.; Carter, C. F.; Pearson, C. M.; de C Alves, L.; Lange, H.; Thansandote, P.; Ley, S. V. Accelerating spirocyclic polyketide synthesis using flow chemistry. *Angewandte Chemie International Edition* **2014,** *53* (19), 4915-4920.

295. Hori, S.; Murai, M.; Takai, K. Rhenium-Catalyzed anti-Markovnikov Addition Reaction of Methanetricarboxylates to Unactivated Terminal Acetylenes. *Journal of the American Chemical Society* **2015,** *137* (4), 1452-1457.

296. Mouzdahir, A.; Bakkas, S.; Rontani, J.-F. Aerobic and anaerobic abiotic oxidation of squalene in the presence of hydroperoxides. *Chemosphere* **2001,** *44* (4), 771-777.

297. Anon. What is the oldest fingerprint that you have developed? In *Fingerprint Development and Imaging Update*, Home Office Police Scientific Development Branch. Publication No. 26/2003: 2003.

298. Hughes, N. C.; Wong, E. Y.; Fan, J.; Bajaj, N. Determination of carryover and contamination for mass spectrometry-based chromatographic assays. *The American Association of Pharmaceutical Scientists Journal* **2007,** *9* (3), E353-E360.

299. Bader, C.; Carter, E.; Safitri, A.; Simpson, P.; Wright, P.; Stagni, S.; Massi, M.; Lay, P.; Brooks, D.; Plush, S. Unprecedented staining of polar lipids by a luminescent rhenium complex revealed by FTIR microspectroscopy in adipocytes. *Molecular BioSystems* **2016,** *12* (7), 2064-2068.

300. Schmarr, H.-G.; Gross, H. B.; Shibamoto, T. Analysis of polar cholesterol oxidation products: evaluation of a new method involving transesterification, solid phase extraction, and gas chromatography. *Journal of Agricultural and Food Chemistry* **1996,** *44* (2), 512-517.

Every reasonable effort has been made to acknowledge the owners of copyright material. I would be pleased to hear from any copyright owner who has been omitted or incorrectly acknowledged.

Appendices

Appendix 1: Donor participation forms

Curtin University

Department of Chemistry

GPO Box U1987 Perth Western Australia 6845

Telephone +61 8 9266 2484
Facsimile +61 8 9266 2300
Email s.lewis@curtin.edu.au
Web
chemistry.curtin.edu.au/staff/swl.cfm

Participant Information Sheet

My name is Buddhika Dorakumbura. I am currently conducting a research project as part of my PhD at Curtin University under the supervision of Professor Simon Lewis.

Purpose of Research
I am investigating how the properties of latent fingermarks change as they age using a combination of chemical and physical measurement techniques. This constitutes part of an on-going program of research at Curtin into latent fingermarks, the outcomes from which will provide a basis for improvements to existing detection techniques and the development of new methods.

How You Can Help
This research depends upon a large collection of sample latent fingermarks to analyse. I am requesting you allow the research team to collect a sample of your fingermarks for this research. The fingermarks will be collected on a variety of surfaces including paper and polished metal plates. Information concerning your age, gender and history of recent activity at the time of sample collection will also be collected.

Consent to Participate
Your involvement in the research is entirely voluntary. You have the right to withdraw at any stage without it affecting your rights or my responsibilities. When you have signed the consent form we will assume that you have agreed to participate and allow us to use your data in this research.

Confidentiality
The fingermarks you provide will be allocated a number and kept separate from your personal details. It will not be possible for the impression to be associated with you by any outside person. In adherence to Curtin University policy, the impression and separate information will be kept in a locked cabinet within the Chemistry Department at Curtin for at least five years, before a decision is made as to whether it should be destroyed.

Further Information
This study has been approved by the Curtin University Human Research Ethics Committee (Approval Number RDSE-02-15). If needed, verification of approval can be obtained either by writing to the Curtin University Human Research Ethics Committee, c/-Office of Research and Development, Curtin University of Technology, GPO Box U1987, Perth, 6845 or by telephoning 9266 2784. If you would like further information about the study, please feel free to contact us by e mail (b.dorakumbura@postgrad.curtin.edu.au or s.lewis@curtin.edu.au) or by phone (Buddhika Dorakumbura 0449908837,_Professor Simon Lewis on 9266 2484).

Thank you very much for your involvement in this research.

Your participation is greatly appreciated.

Appendix 1.1 Information sheet provided to fingermark donors.

Curtin University

Department of Chemistry

GPO Box U1987
Perth Western Australia 6845

Telephone +61 8 9266 2484
Facsimile +61 8 9266 2300
Email s.lewis@curtin.edu.au
Web chemistry.curtin.edu.au/staff/swl.cfm

CONSENT FORM

- I understand the purpose and procedures of the study.
- I understand that the procedure itself may not benefit me.
- I understand that our involvement is voluntary and we can withdraw at any time.
- I understand that no personal identifying information like names and addresses will be used in any published materials.
- I understand that all information will be securely stored at Curtin for at least 5 years before a decision is made as to whether it should be destroyed.
- I have been given the opportunity to ask questions about this research.
- I agree to participate in the study outlined to me.

Name: _____

Signature: _____

Date: _____

Curtin University is a trademark of Curtin University of Technology.

CRICOS Provider Code 00301J (WA), 02637B (NSW)

Appendix 1.2 Consent form filled out by fingermark donors.

Appendix 2: Storage conditions during the AFM investigation

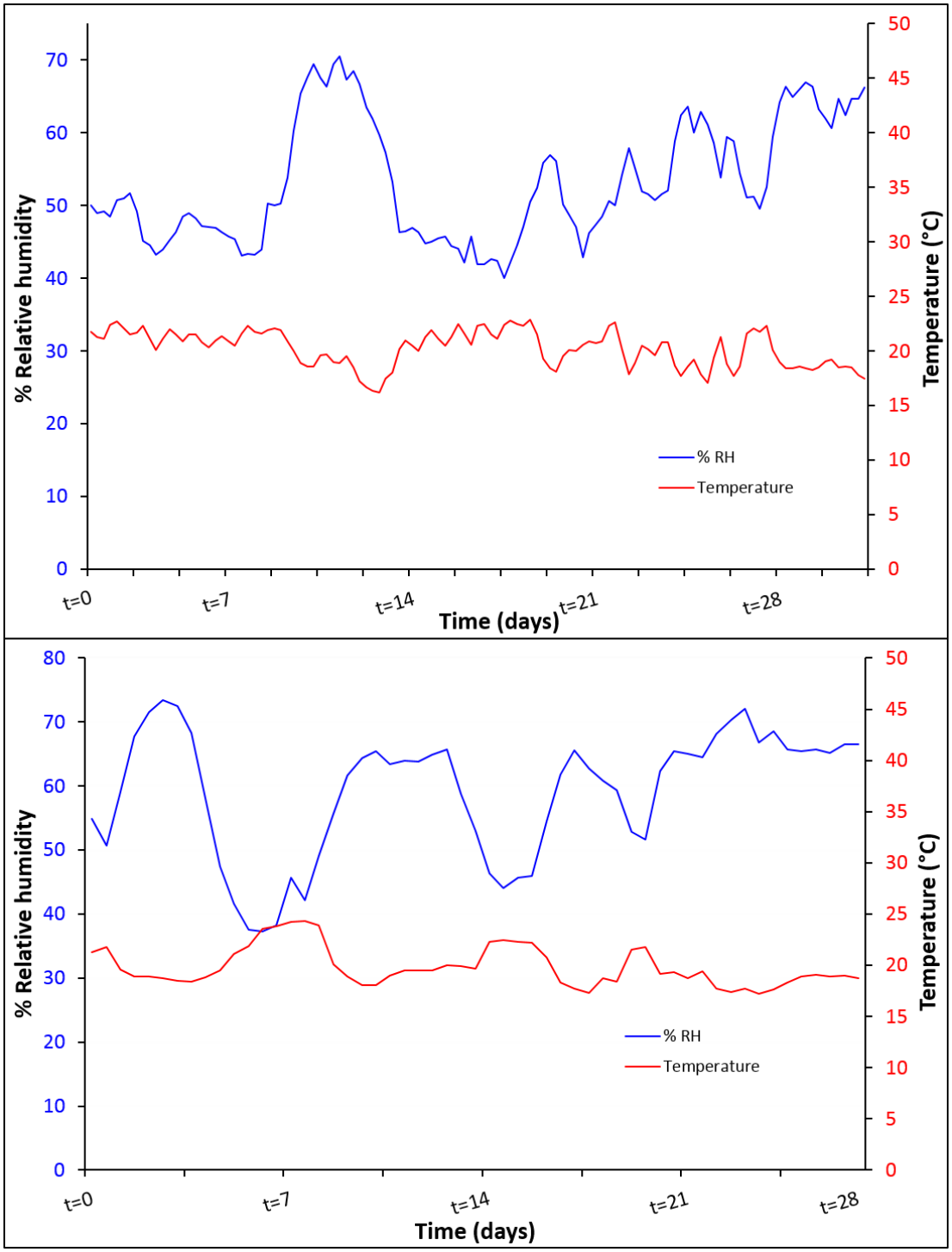

Appendix 2.1 Storage conditions during the experiment with samples obtained from donor D1F1 (top) and donors D2M1 and D3M3 (bottom).

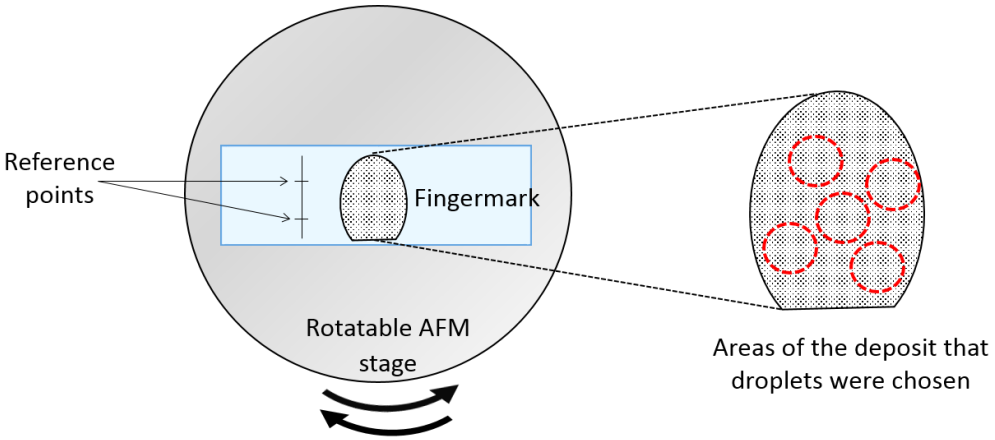

Appendix 2.2 Experimental setup illustrating the approach for relocating the same droplet in each day of measurements.

A line was engraved on the glass slide with very little pressure, adjacent to the fingermark deposit, and two crosses were marked on it in the same manner. The x-y coordinates of the first reference point were adjusted to zero by aligning the centre of it with the cross at the centre of the optical window. The x-y coordinates of the other reference point were obtained by moving the AFM stage to the centre of the second cross. Once a fingermark droplet was selected for mapping, the x-y coordinates of its position were noted down and the optical view of the area under investigation was captured as an image. On the next day of measurements, the x-y coordinates of the first reference point were set to zero and the AFM stage was moved to the x-y coordinates of the second reference point. Then the AFM stage was rotated until the centre of the second reference point is aligned with the centre cross of the optical window. This step was repeated until both reference points were aligned with the centre cross of the optical window at the corresponding coordinates. Once this alignment is achieved, the desired droplet could be found by moving the stage to its coordinates and confirmation by the captured images.

Appendix 3: Confirmation of the presence of cholesterol and its oxidation products in samples

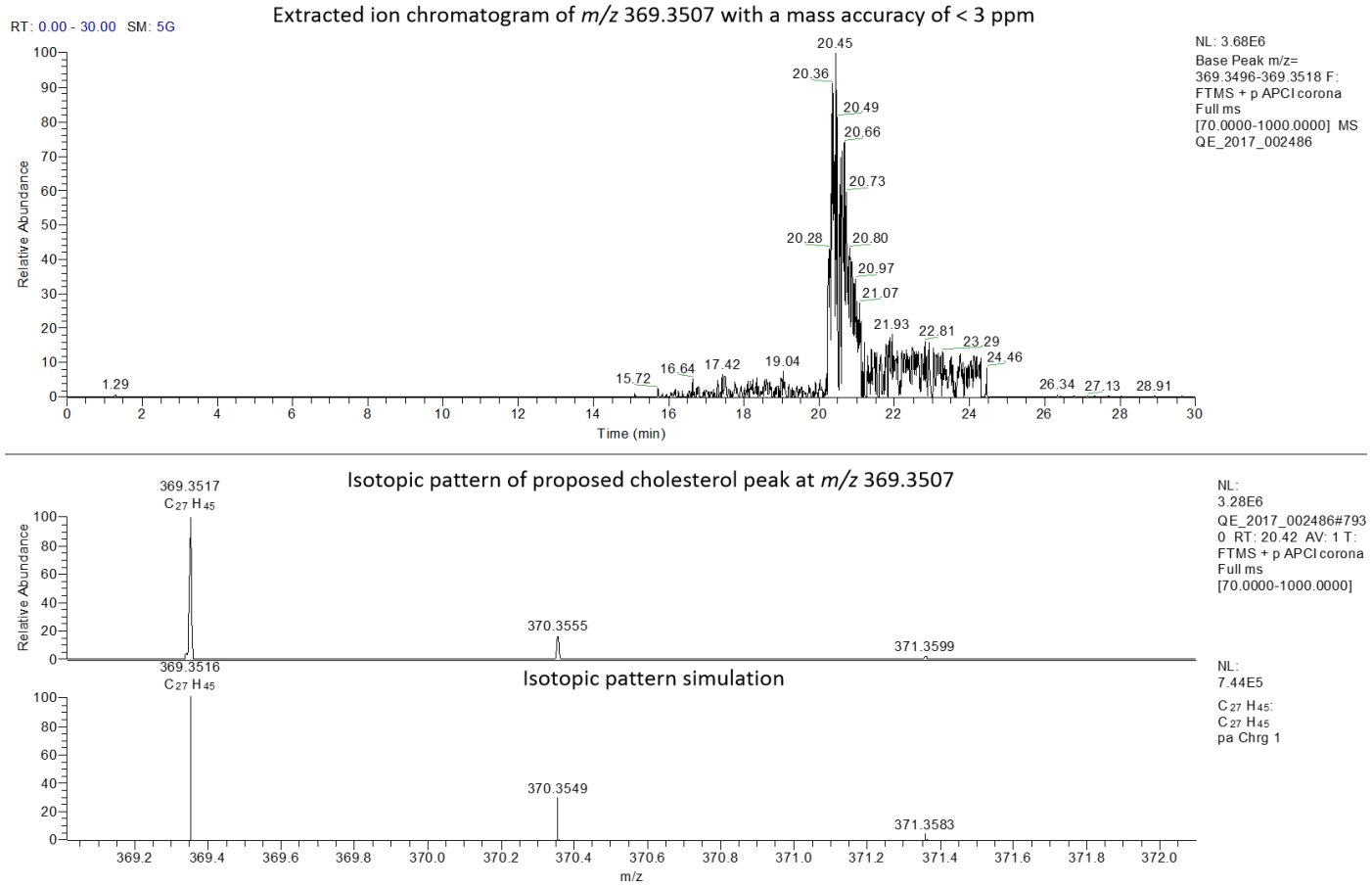

Appendix 3.1 Extracted ion chromatogram of m/z 369.3507 and isotopic pattern comparison between peak proposed to be cholesterol and simulation using Xcalibur software.

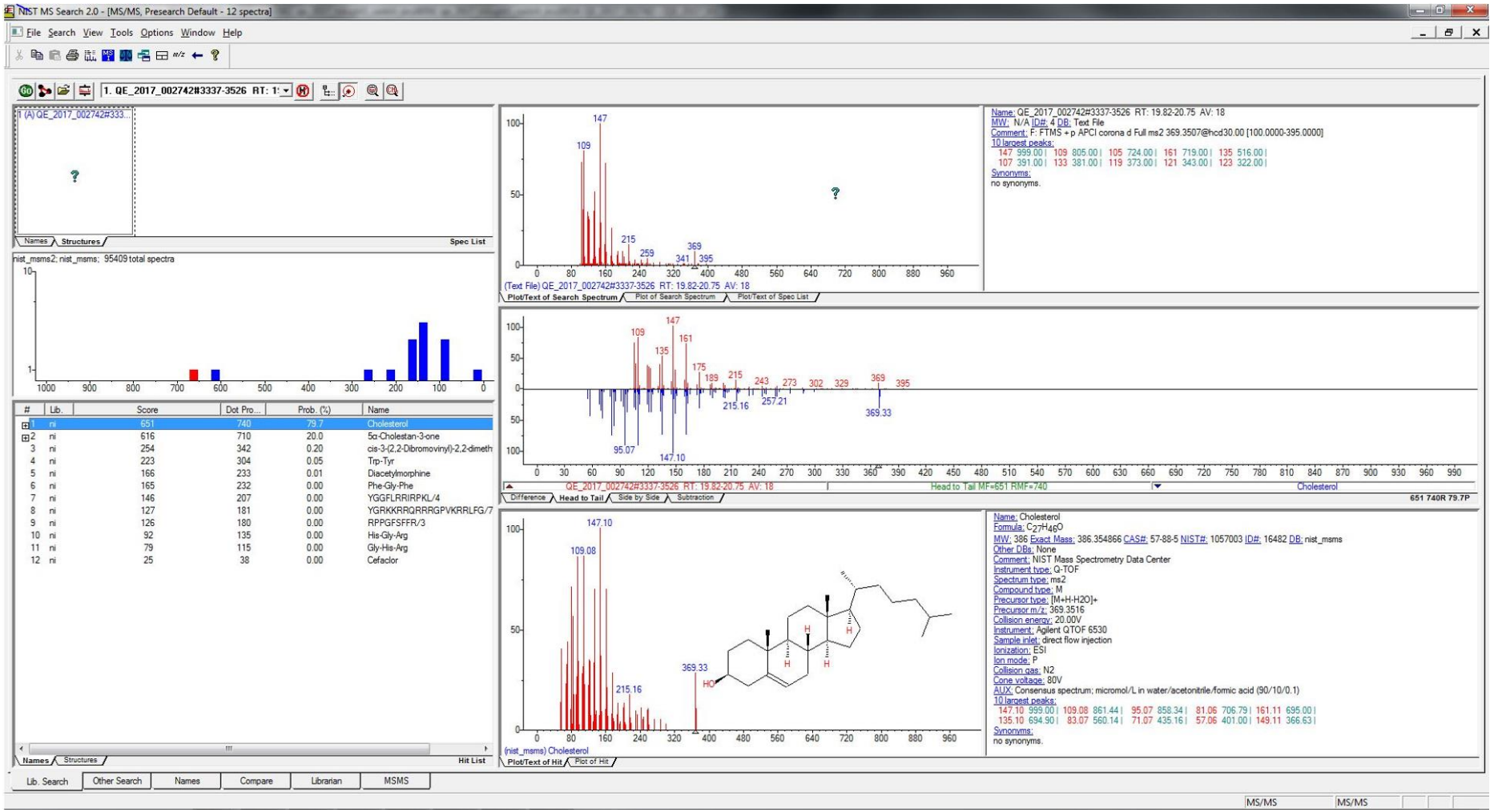

Appendix 3.2 NIST MS/MS library comparison of the proposed cholesterol peak at *m/z* 369.3507.

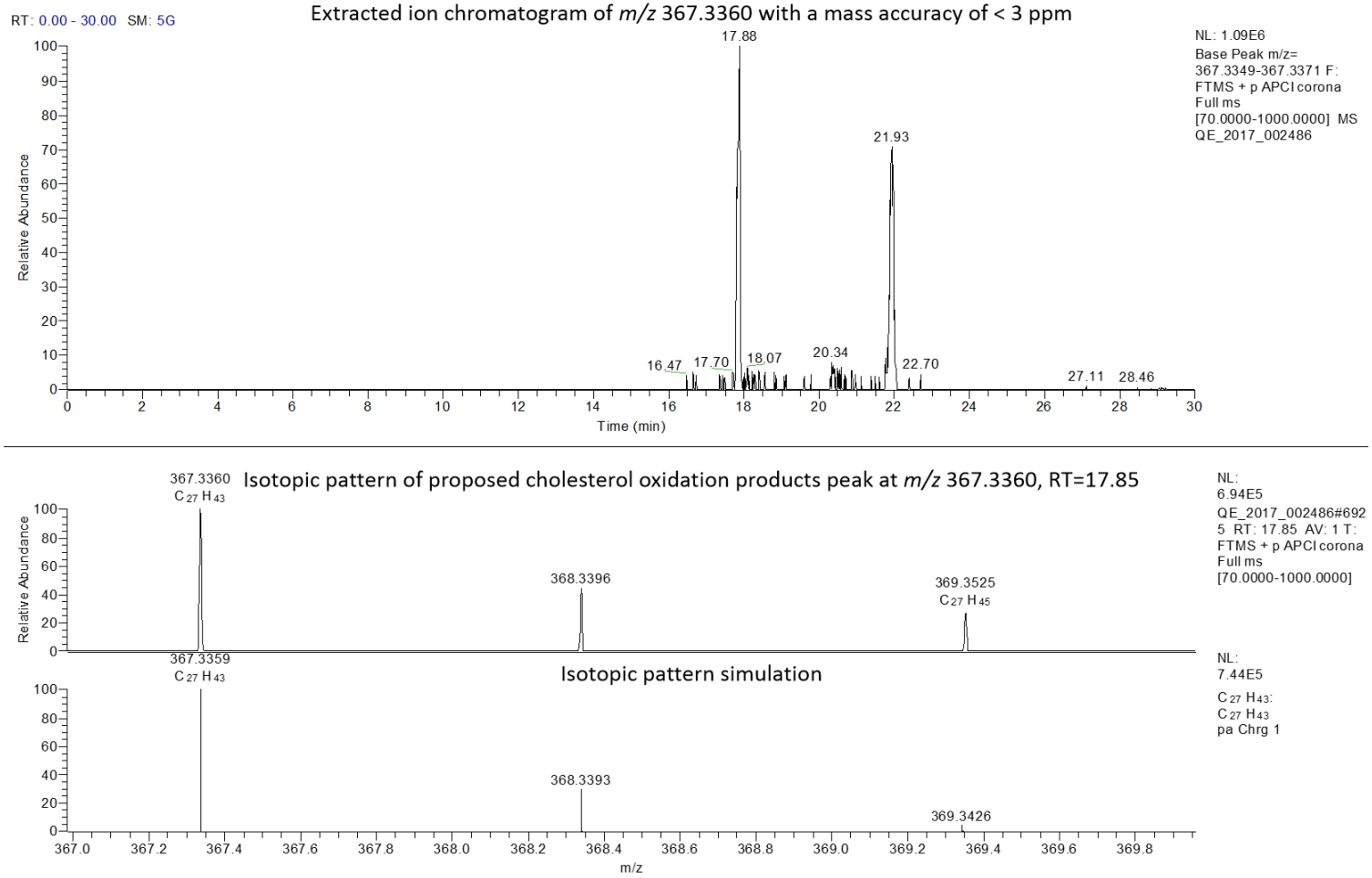

Appendix 3. 3 Extracted ion chromatogram of *m/z* 367.3360 and isotopic pattern comparison between peak proposed to be cholesterol oxidation products and simulation using Xcalibur software.